

Forensic Testing of a Double Tee Bridge

Final Report
December 2014

Paul Barr
Associate Professor
Utah State University
Logan UT 84332

Marv W. Halling
Professor
Utah State University
Logan UT 84332

Christopher S. Pettigrew, P.E.
Utah State University
Logan UT 84332

External Project Manager
Dave Petty
Utah Department of Transportation

In cooperation with
Rutgers, The State University of New Jersey
And
State of Utah
Department of Transportation
And
U.S. Department of Transportation
Federal Highway Administration

Disclaimer Statement

The contents of this report reflect the views of the authors, who are responsible for the facts and the accuracy of the information presented herein. This document is disseminated under the sponsorship of the Department of Transportation, University Transportation Centers Program, in the interest of information exchange. The U.S. Government assumes no liability for the contents or use thereof.

TECHNICAL REPORT STANDARD TITLE PAGE

1. Report No. CAIT-UTC-044	2. Government Accession No.	3. Recipient's Catalog No.	
4. Title and Subtitle Forensic Testing of a Double Tee Bridge		5. Report Date December 2014	
		6. Performing Organization Code CAIT/Utah State University	
7. Author(s) Paul J. Barr, Marv W. Halling, and Christopher S. Pettigrew		8. Performing Organization Report No. CAIT-UTC-044	
9. Performing Organization, Name and Address Utah State University 4110 Old Main Hill Logan, UT 84332		10. Work Unit No.	
		11. Contract or Grant No. DTRT12-G-UTC16	
12. Sponsoring Agency Name and Address Center for Advanced Infrastructure and Transportation Rutgers, The State University of New Jersey 100 Brett Road Piscataway, NJ 08854		13. Type of Report and Period Covered Final Report 11/08/13 - 12/18/2014	
		14. Sponsoring Agency Code	
15. Supplementary Notes U.S Department of Transportation/Research and Innovative Technology Administration 1200 New Jersey Avenue, SE Washington, DC 20590-0001			
16. Abstract <p>This report describes an investigation to quantify the behavior of precast, prestressed concrete double-tee bridge girders made with lightweight concrete. As part of the investigation, three bridge girders were salvaged from a decommissioned bridge in Coalville, Utah. Each girder was subjected to a cracking test to determine the residual prestress force after approximately forty-eight years of service life. Once the prestress losses were quantified, a flexural capacity test was performed on each girder, as well as shear capacity tests performed at various distances from the support. The measured losses and capacities were compared to estimated values calculated according to procedures in the AASHTO LRFD Specifications. It was concluded that the AASHTO LRFD procedures for calculating prestress losses were accurate and the calculated shear capacities were conservative. However, the calculated flexural capacities were not conservative, which is believed to be a result of deck deterioration. In addition to the physical tests, a nonlinear finite-element analysis (FEA) was conducted using ANSYS that was found to replicate the experimental behavior, failure mechanism, and magnitude.</p>			
17. Key Words Prestressed concrete, lightweight, flexure, shear, punching, capacity, forensic		18. Distributional Statement	
19. Security Classification Unclassified	20. Security Classification (of this page) Unclassified	21. No. of Pages 240	22. Price

CONTENTS

	Page
LIST OF TABLES	iii
LIST OF FIGURES	iv
LIST OF EQUATIONS	viii
 CHAPTER	
1. INTRODUCTION	1
2. LITERATURE REVIEW	2
2.1 Full-Scale Test of Prestressed Double-Tee Beam (Grace et al. 2003)	3
2.2 Lightweight Concrete Reduces Weight and Increases Span Length of Pretensioned Concrete Bridge Girders (Meyer and Kahn 2002)	4
2.3 Prestress Losses in High Performance Lightweight Concrete Pretensioned Bridge Girders (Kahn and Lopez 2005)	7
2.4 Structural Performance of Precast/Prestressed Bridge Double-Tee Girders Made of High-Strength Concrete, Welded Wire Reinforcement, and 18-mm-Diameter Strands (Maguire et al. 2012)	10
2.5 Evaluation of Effective Prestress Force in 28-Year-Old Prestressed Concrete Bridge Beams (Pessiki et al. 1996)	12
2.6 Testing of Five 30-Year-Old Prestressed Concrete Beams (Lundqvist and Riihimaki 2010)	13
2.7 Static Behavior of 40 Year-Old Prestressed Concrete Bridge Girders Strengthened with Various FRP Systems (Rosenboom et al. 2006)	15
2.8 Testing of Two 50-Year-Old Precast Post-Tensioned Concrete Bridge Girders (Eder et al. 2005)	18
2.9 NCHRP Report 733 High-Performance/High-Strength Lightweight Concrete for Bridge Girders and Decks (Cousins et al. 2013)	22
3. EXPERIMENTAL TESTING OF THE ICY SPRINGS BRIDGE GIRDERS	25
3.1 Bridge Description	25
3.2 Girder Dimensions	28
3.3 Girder Reinforcement	28
3.4 Experimental Testing	31
3.4.1 Crack Testing	33
3.4.2 Flexural Capacity Testing	55
3.4.3 Shear Capacity Testing	59
3.4.4 Punching Shear Capacity Testing	74

4. ANALYSIS OF THE ICY SPRINGS BRIDGE GIRDERS	83
4.1 Material Properties	83
4.1.1 Concrete.....	83
4.1.2 Prestressing Strands.....	90
4.1.3 Mild Steel	91
4.2 AASHTO LRFD Bridge Design Specifications Analysis and Comparison.....	92
4.2.1 Prestressing Losses	92
4.2.2 Moment Design	96
4.2.3 Shear Design.....	102
4.2.4 Punching Shear Design.....	111
4.2.5 Camber.....	112
5. FINITE ELEMENT MODELING	114
5.1 Volumes	114
5.2 Materials.....	115
5.3 Tables	115
5.4 Real Constants.....	116
5.5 Element Types.....	116
5.6 Element Size and Boundary Conditions.....	118
5.7 Executing an Analysis	118
5.8 ANSYS Models.....	119
5.8.1 Flexural Models.....	120
5.8.2 Shear Models	125
5.8.3 Punching Shear Models	133
6. CONCLUSIONS	135
REFERENCES.....	139
APPENDICES	141
APPENDIX A. GIRDER PHYSICAL PROPERTIES	142
APPENDIX B. TESTED DATA	148
APPENDIX C. AASHTO CALCULATIONS	165
APPENDIX D. ANSYS INPUT FILES & FIGURES.....	207

LIST OF TABLES

Table		Page
3.1	Measured camber	28
3.2	Effective prestress for each girder	55
3.3	Flexural capacity testing results	59
3.4	Shear test setup by girder	59
3.5	Shear capacity test results	73
3.6	Punching shear capacity results	82
4.1	Calculated prestressing loss summary	96
4.2	Calculated moment capacity summary	99
4.3	Calculated maximum deflection summary	101
4.4	Simplified method analysis results	106
4.5	Calculated shear capacity summary	110
4.6	Calculated punching shear capacity summary	111
4.7	Calculated camber comparison	112
5.1	ANSYS material numbers	115
5.2	Flexural modeling summary	125
5.3	Shear modeling summary	132
5.4	Punching shear modeling summary	134
B.1	Tested concrete material properties	163
B.2	Tested prestressing strand capacity	163

LIST OF FIGURES

Figure		Page
3.1	Original bridge prior to demolition.....	25
3.2	New Icy Springs Bridge.....	27
3.3	Original bridge dimensions.....	27
3.4	Original bridge cross section A-A	27
3.5	Prestressing strand layout side view	29
3.6	Prestressing strand layout at ends of girders.....	30
3.7	Prestressing strand layout at midspan of girders.....	30
3.8	End of middle girder with shear steel exposed	30
3.9	Girder removal cross-sections.....	32
3.10	Reaction frame with Girder #1 ready for crack test.....	32
3.11	Flexural instrumentation plan view	34
3.12	Flexural instrumentation side view	47
3.13	Flexural instrumentation end view.....	50
3.14	Typical concrete leveling pads.....	51
3.15	Strain gages and marked cracks on Girder #1.....	52
3.16	Girder #1 cracking load test data	52
3.17	Girder #1 after flexural failure.....	56
3.18	Girder #1 moment vs. deflection at midspan	58
3.19	Girder #1 strain distribution at midspan	58
3.20	2d _v setup of Girder #1	61
3.21	Shear instrumentation plan view.....	61
3.22	Shear instrumentation side view	61
3.23	Shear instrumentation end view	61

3.24	2d _v shear failure of Girder #1.....	63
3.25	3d _v shear failure of Girder #2.....	65
3.26	Girder #1 2d _v shear vs. deflection plot.....	69
3.27	Girder #3 4d _v shear vs. deflection plot.....	70
3.28	Girder #1 2d _v moment vs. deflection plot.....	71
3.29	Girder #3 4d _v moment vs. deflection plot.....	72
3.30	Girder #3 2d _v failure	73
3.31	Girder #1 west side deck deterioration	74
3.32	Typical punching shear test setup.....	75
3.33	Punching shear instrumentation side view.....	77
3.34	Punching shear instrumentation end view	79
3.35	Punching shear test #13 load vs. deflection.....	81
3.36	Tire contact area plate embedded in deck.....	81
3.37	Typical punching shear failure.....	81
4.1	Concrete cylinder test setup.....	88
4.2	Concrete cylinder after failure	88
4.3	Concrete aggregate	89
4.4	Prestressing strand test setup	90
4.5	Mild steel stress vs. deflection curve.....	91
4.6	Mild steel specimen following test	91
4.7	Strut and tie model.....	106
5.1	SOLID45 & SOLID65 geometric shapes (ANSYS, Inc. 2009)	117
5.2	LINK8 geometric shape (ANSYS, Inc. 2009).....	117
5.3	Girder #1 flexural finite element model.....	120
5.4	Girder #1 flexural model load vs. deflection	121

5.5	Girder #1 tested vs. modeled flexural cracking	124
5.6	Girder #1 flexural moment vs. deflection comparison	125
5.7	Girder #1 2d _v finite element model.....	129
5.8	Girder #1 2d _v shear vs. deflection comparison (flexural concrete properties).....	130
5.9	Girder #1 2d _v shear vs. deflection comparison (modified concrete properties).....	131
5.10	Girder #1 2d _v crack comparison	131
5.11	Punching shear 3D view	133
B.1	Girder #1 cracking load test data	149
B.2	Girder #2 cracking load test data	149
B.3	Girder #3 cracking load test data	150
B.4	Girder #1 moment vs. deflection at midspan north side	153
B.5	Girder #1 strain distribution at midspan south side	153
B.6	Girder #2 moment vs. deflection at midspan north side	154
B.7	Girder #2 strain distribution at midspan north side.....	154
B.8	Girder #3 moment vs. deflection at midspan north side	155
B.9	Girder #3 strain distribution at midspan south side	155
B.10	2d _v test of Girder #1 shear vs. deflection	156
B.11	2d _v test of Girder #1 moment vs. deflection	156
B.12	2d _v test of Girder #3 shear vs. deflection	157
B.13	2d _v test of Girder #3 moment vs. deflection	157
B.14	3d _v test of Girder #1 shear vs. deflection	157
B.15	3d _v test of Girder #1 moment vs. deflection	158
B.16	3d _v test of Girder #2 shear vs. deflection	158
B.17	3d _v test of Girder #2 moment vs. deflection	159
B.18	4d _v test of Girder #3 shear vs. deflection.....	159

B.19	4d _v test of Girder #3 moment vs. deflection	160
B.20	Punching shear test #7 Girder #2 west side load vs. deflection	160
B.21	Punching shear test #8 Girder #2 west side load vs. deflection	160
B.22	Punching shear test #9 Girder #2 west side load vs. deflection	160
B.23	Punching shear test #10 Girder #1 east side load vs. deflection	161
B.24	Punching shear test #11 Girder #1 east side load vs. deflection	161
B.25	Punching shear test #12 Girder #1 east side load vs. deflection	162
B.26	Punching shear test #13 Girder #1 east side load vs. deflection	162
D.1	Girder #1 modeled flexural load vs deflection.....	222
D.2	Girder #2 modeled flexural load vs deflection.....	222
D.3	Girder #3 modeled flexural load vs deflection.....	223
D.4	Girder #1 modeled 2d _v load vs deflection.....	223
D.5	Girder #2 modeled 3d _v load vs deflection.....	224
D.6	Girder #3 modeled 4d _v load vs deflection.....	224
D.7	Girder #1 flexural comparison to FEM.....	225
D.8	Girder #2 flexural comparison to FEM.....	225
D.9	Girder #3 flexural comparison to FEM.....	226
D.10	Girder #1 2d _v comparison to FEM.....	226
D.11	Girder #2 3d _v comparison to FEM.....	227
D.12	Girder #3 4d _v comparison to FEM.....	227

LIST OF EQUATIONS

Equation	Page
(2.1).....	5
(2.2).....	5
(2.3).....	6
(2.4).....	14
(2.5).....	21
(3.1).....	53
(3.2).....	54
(3.3).....	54
(3.4).....	54
(4.1).....	89
(4.2).....	90
(4.3).....	93
(4.4).....	93
(4.5).....	94
(4.6).....	95
(4.7).....	95
(4.8).....	95
(4.9).....	95
(4.10).....	95
(4.11).....	95
(4.12).....	95
(4.13).....	95
(4.14).....	95

(4.15).....	95
(4.16).....	97
(4.17).....	98
(4.18).....	98
(4.19).....	98
(4.20).....	99
(4.21).....	99
(4.22).....	100
(4.23).....	100
(4.24).....	101
(4.25).....	102
(4.26).....	102
(4.27).....	103
(4.28).....	103
(4.29).....	104
(4.30).....	104
(4.31).....	104
(4.32).....	105
(4.33).....	105
(4.34).....	105
(4.35).....	105
(4.36).....	105
(4.37).....	107
(4.38).....	107
(4.39).....	107

(4.40).....	108
(4.41).....	108
(4.42).....	108
(4.43).....	109
(4.44).....	109
(4.45).....	109
(4.46).....	109
(4.47).....	109
(4.48).....	111
(5.1).....	119
(5.2).....	120

CHAPTER 1

INTRODUCTION

This research is focused on the flexural, shear, and punching shear capacity of prestressed lightweight concrete double-tee bridge girders. Three girders were salvaged from the Icy Springs Bridge in Coalville, Utah and lab tested for residual prestressing, flexural and shear capacity, and punching shear capacity. The residual prestress testing was performed using two point loads oriented six or seven feet apart over each double-tee stem to produce a constant moment region and to induce the cracking moment. The ultimate capacity testing was accomplished by applying the load at various locations along the length of the girders to induce flexure, flexure-shear, and shear type failures. The results from the lab testing were compared to the 2012 AASHTO LRFD Bridge Design Specifications (AASHTO 2012) and finite element models using the computer program ANSYS. Comparisons with the AASHTO LRFD Bridge Design Specification were performed to verify the specifications are valid for lightweight concrete double-tee members. The finite element modeling was performed to accurately represent the girder behavior experienced in the lab. The material properties from the calibrated finite element model were compared to the lab tested material properties to find the differences between modeled and actual values.

CHAPTER 2

LITERATURE REVIEW

Prestressed concrete double-tee beams have been utilized and tested in building construction for many years. However, the use of prestressed concrete double-tee girders has not been as common in bridge construction, where the use of prestressed I-shaped girders, bulb-tees, and box girders is more common (Svirsky, 2014). The research presented in this paper is for prestressed lightweight concrete double-tee girders salvaged from a bridge that was in service for 48 years.

High strength concrete is normally preferable in prestressed concrete girder construction due to the higher allowable loads, reduced cross-sectional area, and the ability to span longer distances with minimal cracking of the concrete. Conversely, lightweight concrete is used to reduce the dead load of a concrete structure. In most cases, the higher cost of the lightweight concrete is offset by a reduction in size of structural elements. Lightweight concrete has been used for bridge decks, girders, and piers. However, there has been limited research performed on double-tee bridge girders constructed of lightweight concrete. Multiple tests were conducted on three girders for this research to determine the prestressing losses, ultimate capacities for flexural, shear-flexure, and shear failures, as well as the ultimate punching shear capacity of the concrete deck.

The following sections summarize past research conducted that is considered relevant to the research presented in this paper. The past research includes the testing and analysis of girders fabricated in a lab and girders salvaged from bridge replacement projects. Citations of the past papers reviewed are included in the sub-headings.

2.1 Full-Scale Test of Prestressed Double-Tee Beam (Grace et al. 2003)

Advanced fiber-reinforced polymer (FRP) materials are used worldwide in the construction of small and large structures. However, there are few prestressed concrete bridges constructed using carbon fiber-reinforced polymer (CFRP) tendons as the only flexural reinforcement. This research tested a full-scale prestressed double-tee beam to evaluate the design and construction procedures used for twelve double-tee beams to be constructed for the Bridge Street Bridge in Southfield, Missouri.

The beam used in the testing was constructed at a precast fabrication plant using a concrete mixture that developed a cylinder strength of 53.8 MPa at the time the beam was tested. Thirty strain gages were embedded in the concrete to measure strain distributions along the depth of the cross sections at midspan and quarter spans. Seven vibrating wire strain gages were installed in each of the two webs at opposite ends of the beam to measure transfer length. A load cell was also installed between the fabricator's stressing jack at the live end and the anchorage and was used to measure the pretensioning forces with a read-out device. The beam was post-tensioned with load cells measuring the post-tensioning forces.

The beam had a test span of 20.4 m and was simply supported at both ends using roller supports. The test beam was loaded along two lines orthogonal to its longitudinal centerline to create a 3653 mm-wide constant moment region symmetrical about its midspan. Along each line, load was applied at two bearing points that were coincident with the beam's webs. Load was applied using a series of hydraulic jacks with load and extension capability sufficient to induce flexural failure. All loads applied to the beam during the tests were monitored using load cells. Beam deflections at midspan and quarter-span locations were monitored using two displacement transducers at each location attached to the underside of the two webs. In addition to the applied

loads and deflections, output from the concrete strain gages installed for measuring strain distribution at midspan and the two quarter-span sections was monitored during the flexural test.

The results of this test provided the design and research team with adequate information to proceed with the development of the design approach and construction documents for the Bridge Street Bridge. The combined internal and external prestressing induced the desired compressive strains in the cross section, which balanced the tensile strains induced by the applied load to prevent service load cracking in the beam. The ultimate flexural capacity of the double-tee beam was approximately 3.4 times the service moment and the cracking moment was about 1.2 times the service moment. The tested flexural strength was approximately 1.6 times the calculated capacity. The beam webs experienced significant cracking prior to the failure load. The failure of the double-tee beam was preceded by the crushing of the concrete topping, followed by the rupture of the internal prestressing tendons. None of the post-tensioning strands ruptured.

2.2 Lightweight Concrete Reduces Weight and Increases Span Length of Pretensioned Concrete Bridge Girders (Meyer and Kahn 2002)

The Georgia Department of Transportation (DOT) requires a “super-load permit” when the gross vehicle weight (GVW) is greater than 150 kips (68,200 kg). This special permit requires the hauler to adhere to additional restrictions that may include stopping before every bridge, proceeding over the bridge at a speed less than 5 miles per hour, and having escorts lead and follow the truck along the route. In some cases, there may not be an acceptable alternate route for the truck. The slow rate of speed also has the potential to disrupt normal traffic. The Georgia DOT would like to avoid issuing super-load permits, but it would like to take advantage of the benefits of HPC in pretensioned girders.

The purpose of this research was to determine whether high strength lightweight concrete (HSLWC) could be used to fabricate pretensioned concrete bridge girders for a simple span

length of 150 feet (45.7 m), a girder spacing of 7 feet (2.13 m), and a GVW of 150 kips (68,200 kg) or less. Standard AASHTO I-girders Types II through V and Standard and Modified AASHTO-PCI bulb tees BT-54, BT-63, and BT-72 were considered. The concrete strengths for the girders were 8, 10, and 12 ksi (55, 69, and 83 MPa). The strength of the 7-inch (178 mm) normal weight composite concrete deck was 3.5 ksi (24 MPa). The HSLWC in this study assumed the use of regionally available expanded slate lightweight aggregate (LWA). The use of slate LWA was thought to produce concrete compressive strengths of 12 ksi (83 MPa). Prestressing strands were 0.6 in (15 mm) diameter, 270 ksi (1862 MPa) low relaxation strands spaced at 2 inches (51 mm) on center.

All girder designs were based on the 16th Edition of the AASHTO Standard Specifications for Highway Bridges and used the Georgia DOT bridge design computer program with modifications by the authors to enable the use of HSLWC. It was assumed that prestress losses would be the same as for normal strength concrete. Ongoing research indicates that for normal weight and lightweight HPC, the creep and shrinkage losses are less than for normal strength concretes. This is significant because deflection was a major concern in the designs for this study.

The modulus of elasticity for HSLWC made using slate LWA at the time of release (E_{ci}) and at 28 days (E_c) were preliminarily determined using the ACI and AASHTO equation for modulus of elasticity:

$$E = w_c^{1.5} 33 \sqrt{f'_c} \quad (2.1)$$

When used with HSLWC, Eq. 2.1 was found to over predict the modulus of elasticity.

The following equation from Morales was then used:

$$E = (40,000 \sqrt{f'_c} + 1,000,000) \left(\frac{w_c}{145} \right)^{1.5} \quad (2.2)$$

However, when Eq. 2.2 was compared to the experimental results for HSLWC strengths below 10 ksi (69 MPa) it was found the calculated values were lower. The calculated values were higher than the experimental results for HSLWC strengths above 10 ksi (69 MPa). The following equation was derived from the Morales equation based on a “best fit” analysis of experimental data from the 13 slate mixes:

$$E = (33,000\sqrt{f'_c} + 4,000,000)(w_c/242)^{0.9} \quad (2.3)$$

The unit weights of the HSLWC averaged 119 lb/ft³ (1906 kg/m³), 124 lb/ft³ (1986 kg/m³), and 128 lb/ft³ (2051 kg/m³) for 8 ksi (55 MPa), 10 ksi (69 MPa), and 12 ksi (83 MPa) concrete, respectively.

The Georgia DOT computer program was used to find the maximum span length for each girder type. The variables were the concrete strength and concrete unit weight. The design of the HSLWC was compared with the design of high strength normal weight concrete (HSNWC) assuming unit weight of 150 lb/ft³ (2403 kg/m³) for the HSNWC. The modulus of elasticity for the HSNWC was calculated using Eq. 2.1.

The analysis resulted in span lengths of AASHTO Type II through V girder sections using 8 ksi (55 MPa) HSLWC being extended by up to 4 percent [7 ft (2.13 m) for 140 ft (42.7 m) spans]. The most significant length increases resulted from the use of the lightest concrete unit weight. The use of HSLWC provided the most significant benefit for girders with lengths over 105 ft (32 m).

Standard bulb-tee sections reacted similar to AASHTO I-girder sections. HSLWC with a strength of 8 ksi (55 MPa) provided a length increase up to 3 percent [3 ft (0.91 m) for 110 ft (33.5 m) girders]. The bulb-tee sections exhibited a consistent benefit from using concrete strengths up to 12 ksi (83 MPa). Based on the efficiency of the bulb-tee sections, there was not

an observed plateau within the strength range investigated for the constant 7 ft (2.13 m) girder spacing.

Modified bulb-tee sections behaved similarly to the standard bulb-tee sections with the largest percent increase in length using 8 ksi (55 MPa) HSLWC at about 3 percent [4 ft (1.22 m) for a 146 ft (44.5 m) girders].

The research concluded the use of HSLWC has the potential to increase the length of simple span AASHTO I-girders by up to 4 percent and the length of AASHTO-PCI bulb-tee girders by up to 3 percent. For spans between 125 ft and 155 ft (38.1 m and 47.2 m), the use of HSLWC can reduce the gross vehicle weight to less than 150 kips (68,200 kg) so a super-load permit would not be required for transportation of the long span girders. The same span range using normal weight concrete would require a super-load permit. The use of HSLWC provides no appreciable benefit to AASHTO Type II and III sections. The modified bulb-tee can be extended by 10 ft (3.1 m) over a standard bulb-tee using either HSLWC or HSNWC at strengths of 8, 10, or 12 ksi (55, 69, or 83 MPa). For girders over 105 ft (32 m) in length, both standard and modified AASHTO-PCI bulb-tee sections provide longer spans at less weight than standard AASHTO I-girder sections.

2.3 Prestress Losses in High Performance Lightweight Concrete Pretensioned Bridge Girders (Kahn and Lopez 2005)

The purpose of this research was to determine the time-dependent behavior of high performance lightweight concrete (HPLC) and to examine how long-term behavior affects the prestress losses in high strength precast, prestressed concrete bridge girders made using expanded slate lightweight aggregate. Previous research from Section 2.2 concluded HPLC permits easier and more economical transportation of long-span precast bridge girders as a result of the reduced weight. The long-term properties of HPLC need to be determined to safely implement HPLC for bridge construction, including their effect on prestress losses.

The following factors influence prestress losses: friction from post-tensioning operations; movement of the prestressing steel at the end anchorage; elastic shortening at transfer; effect of the connection of the prestressed member to other structural members; and time-dependent losses due to steel relaxation and creep and shrinkage of the concrete. Each loss factor is dependent on the structural design, material properties of concrete and steel, prestressing method (pre-tensioned or post-tensioned), concrete age at stressing, and the method of prestress computation.

Three AASHTO Type II girders with lengths of 39, 39, and 43 ft (11.9, 11.9, and 13.1 m) were cast from Grade 2 - 8 ksi (55 MPa) and Grade 3 - 10 ksi (69 MPa) HPLC mixes each for a total of six girders. Each girder was reinforced with ten 0.6 inch (15 mm) diameter, 270 ksi (1860 MPa), seven-wire, low relaxation strands. Eight strands were located in the bottom flange and two strands in the top flange. The strands were stressed to 75 percent of their ultimate strength, 202.5 ksi (1400 MPa). Shear reinforcement in the girders was No. 4 (13 mm), Grade 60 bars (428 MPa). The deck was 11.5 in. (292 mm) thick and 19 in. (483 mm) wide with an average 56-day concrete compressive strength of 5380 psi (37.1 MPa). External demountable mechanical (DEMEC) gage points and internal vibrating wire strain gages (VWSG) were used to measure long-term deformations at the girder midspans. The girders were tested for shear capacity and strand transfer and development length. The results were compared with the results of normal weight HPC Type II girders previously studied.

Samples of the concrete used to construct the test girders were taken to determine the concrete material properties. The following tests were performed; compressive strength, chord modulus of elasticity, modulus of rupture, chloride permeability, creep and shrinkage, and coefficient of thermal expansion.

DEMEC gage points were embedded in the creep and shrinkage specimens at a spacing of 10 in. (254 mm) on opposite sides of the longitudinal section. Four DEMEC gage readings were taken from each specimen and averaged for determining strain. Creep was measured on 26

specimens stored at 50 percent relative humidity and 73°F (22.8°C) temperature for a period of 620 days. All creep and shrinkage specimens were accelerated cured. One half of the specimens were loaded to 40 percent of the initial compressive strength with the other half loaded to 60 percent. Some specimens in each group were loaded 16 hours after casting and the rest loaded 24 hours after. Shrinkage measurements started at 82°F (27.8°C) and after three hours they reached thermal equilibrium at the standard conditions of 73°F (22.8°C). Creep results were obtained by subtracting the shrinkage value from the combined creep-plus-shrinkage measurement and by dividing the creep strain by the applied stress. Ninety percent of the 620-day values of creep and shrinkage were reached after approximately 250 days of loading and drying.

Vibrating wire strain gage data from the Type II AASHTO girders was used for the actual prestress computations. Measurements started before stress transfer and finished 100 days later when the girders were tested. The readings from the vibrating wire strain gages were corrected for temperature changes to obtain “load related” strains.

The creep and shrinkage data from the HPLC cylinders were used to estimate prestress losses in the bridge girders. These experimental losses were compared with four models: the AASHTO refined and the AASHTO lump sum methods from the AASHTO LRFD Specifications, the ACI 209 method, and the PCI method. Steel relaxation was not measured separately. All four methods overestimated the projected measured losses for Grade 3 HPLC girders. The AASHTO refined and ACI 209 methods overestimated losses of Grade 2 HPLC girders, but the AASHTO lump sum and PCI methods underestimated the total losses of Grade 2 HPLC girders.

Grade 2 HPLC had a 56-day strength of 9350 psi (64.5 MPa), a unit weight of 116 lb/ft³ (1855 kg/m³), a 620-day specific creep of 0.51 $\mu\epsilon$ /psi and a 620-day shrinkage of 820 $\mu\epsilon$. Grade 3 HPLC had a 56-day strength of 10,580 psi (73.0 MPa), a unit weight of 118 lb/ft³ (1890 kg/m³), a 620-day specific creep of 0.37 $\mu\epsilon$ /psi and a 620-day shrinkage of 610 $\mu\epsilon$. Grade 3 HPLC had a

specific creep similar to that of a normal weight HPC of the same grade, but with less cement paste content.

2.4 Structural Performance of Precast/Prestressed Bridge Double-Tee Girders Made of High-Strength Concrete, Welded Wire Reinforcement, and 18-mm-Diameter Strands (Maguire et al. 2012)

The research conducted for this paper focuses on the development of high-strength precast prestressed double-tee girders for bridge construction. Double-tee sections are used to simplify girder production and erection and to maximize span-to-depth ratio, which improves construction economy and speed. Two full-scale 15.24-m long, 1.21-m wide, and 0.5-m deep single-tee girders were fabricated by a precast producer and tested at the University of Nebraska structural laboratory.

18-mm diameter seven-wire Grade 1860 strands are becoming more commonly used by precast concrete producers. Therefore, 18-mm diameter seven-wire Grade 1860 strands in a 51-mm by 51-mm grid were used in the fabrication of the girders for this study. The girders were also constructed using the nonproprietary University of Nebraska high-strength concrete (NUHSC), a self-consolidating concrete with very high early and final strength. The low content of coarse aggregate and small maximum coarse aggregates used in NUHSC reduces aggregate interlock and makes the shear capacity of the concrete a concern. Also, the self-consolidating properties of NUHSC prevent surface roughening of the top flange and results in a smooth surface, which makes the interface shear capacity between the girder and the deck less than ideal. There has been limited research into the transfer and development lengths of 18-mm diameter strands when a spacing of 51-mm by 51-mm is used. A total of six tests were conducted for each specimen to determine the flexural and shear capacities, to evaluate the interface shear transfer between the precast girders and the cast-in-place deck, and to compare the transfer and development length of 18-mm diameter strands in NUHSC to predicted values.

The 2008 AASHTO LRFD Bridge Design Specification was used to design the girders and the girders were fabricated by Coreslab Structures, Inc. in Omaha, Nebraska. The girders were instrumented with 16 detachable mechanical (DEMEC) strain gages at each end to determine transfer length. The strain gages were placed approximately 100 mm apart and were located along the top flange centerline. Surface strain readings were taken immediately prior to release, 30 minutes after release, and 14-days after release.

Each girder underwent three tests in the lab. In the first test the load was placed at the AASHTO LRFD-prescribed development length to verify code prediction. The second test was a midspan flexural testing to failure. The last test was a shear test with the load being placed 1,676-mm from the support. A string potentiometer (S-POT) was used to measure deflection directly under the loading points for each test. Linear potentiometers (L-POTs) measured strand end-slip nearest to the load for all tests. Electrical resistance strain gages (ERSGs) were oriented horizontally and located 6.5-mm vertically from the interface and 13-mm apart to monitor the difference in strain between the cast-in-place deck and the precast girder.

The research conducted concluded the transfer length of harped 18-mm diameter prestressing strands tensioned to $0.6 f_{pu}$ at 51-mm by 51-mm spacing in 83-MPa concrete is significantly shorter than that predicted using ACI 318-08 and AASHTO LRFD Bridge Design specifications. Second, the development length of harped strands in the same configuration is conservatively predicted by the AASHTO LRFD Bridge Design Specifications. Third, the flexure and shear capacities predicted using the AASHTO LRFD Bridge Design Specifications are applicable to the proposed double-tee girders compare very well to the actual flexure and shear capacities predicted using measured material properties. Fourth, the interface between the NUHSC double-tee and the cast-in-place deck does not contribute to the horizontal shear resistance and should be considered a smooth surface unless appropriate interface roughening is

achieved. Lastly, the proposed double-tee girders can result in a span-to-depth ratio of 33 while being economical to fabricate and erect.

2.5 Evaluation of Effective Prestress Force in 28-Year-Old Prestressed Concrete Bridge Beams (Pessiki et al. 1996)

To evaluate the load rating of an existing bridge constructed using prestressed concrete bridge beams an assumption must be made concerning the existing effective prestress force. This assumption is difficult to make because the effective prestress force is influenced by several time-dependent variables such as relaxation of the prestressing strands and the shrinkage and creep of the concrete. This paper presents the findings of an experimental study completed at the Center for Advanced Technology for Large Structural Systems (ATLSS) at Lehigh University to determine the effective prestress force in two prestressed concrete I-beams after approximately 28-years of service. The two beams tested were Pennsylvania Department of Transportation (PennDOT) 24 x 60 in. (610 x 1524 mm) prestressed concrete I-beams with a span of 89 ft (27.1 m) and overall length of 90 ft 5 in. (27.6 m).

Each specimen was loaded to obtain the decompression load in the bottom fiber of each beam using three independent techniques; visual observation, strain gages, and displacement transducers. Once the decompression loads were determined the beams were loaded to failure. The beams were tested without the concrete deck, which was removed during the demolition of the bridge. A point load was applied to the mid-point of the beam using a 5000 kip (22.2 MN) capacity universal testing machine. Each beam was tested in three separate phases. First, the load was applied to create and locate a series of flexural cracks to instrument with strain gages and displacement transducers. This phase is also known as the Cracking Test. Second, the decompression load in each beam was determined based on strain and displacement measurements of crack openings for the cracks identified and instrumented in the first phase.

Phase 2 is known as the Decompression Load Test. Third, each beam was loaded to failure in the Ultimate Strength Test.

After an analysis of the obtained data, the following conclusions were made;

1. A visual inspection of each beam in the laboratory revealed members that were in excellent physical condition with no indication that cracking had occurred in service and testing seemed to confirm that each beam had remained uncracked while in service.
2. An average prestress loss of 18 percent was determined for the two specimens. Predicted prestress losses of 29, 32, and 33 percent were computed by the Modified Bureau of Public Roads, Lehigh, and AASHTO methods, respectively. The average experimental determined prestress is approximately 60 percent of that predicted by each of the three design code procedures.
3. The use of strain gages seemed to produce the most repeatable and reliable results in determining the decompression load in each beam. It is suggested that a minimum of three to five cracks be instrumented to account for the scatter that was observed.
4. Determining the decompression load by visually observing crack reopening will generally provide unconservative results. The minimum load at which crack opening was visually observed was 110 kips (489 kN), which corresponds to a prestress loss of approximately 3 percent. The overestimation of the decompression load results in lower than actual prestress losses and unconservative predictions of flexural capacity.

2.6 Testing of Five 30-Year-Old Prestressed Concrete Beams (Lundqvist and Riihimaki 2010)

When the Olkiluoto nuclear power plant in Finland was constructed in the mid-1970's several prestressed concrete beams were fabricated to monitor the prestress-losses. This monitoring was performed by testing one of these beam approximately every three years. However, the test results were deemed unreliable and the entire testing program was cancelled.

Five of the remaining beams were tested as part of this study and the prestress losses obtained from the tests were compared with several different models for predicting creep and shrinkage of the concrete and relaxation of the prestressing steel. Two of the beams were manufactured in 1975 and three were manufactured in 1977. All beams are 9 ft 10 in. (3 m) long and have a square cross section of 19.7 in. x 19.7 in. (0.5 m x 0.5 m). For the 1975 beams Vorspann System Losinger (VSL) type 19, 0.5-in. diameter (13 mm) strand was used. The 1977 beams used Birkenmaier, Brandestini, and Ros system V (BBRV) type R 238, seventy-two 0.24-in. diameter strands. The initial tensioning forces in the 1975 and 1977 beams were 550 kips (2.4 MN) and 567 kip (2.5 MN), respectively. The beams were stored inside the containment building of the nuclear reactor at approximately 90°F (32°C) and 21% relative humidity (RH).

For testing, the beams were simply supported and subjected to a single point load at midspan. The beams were loaded in deflection control with increments of 3.9×10^{-4} in. (0.01 mm) per second until flexural cracks appeared at the bottom of the beam. The initial crack was marked and the beam unloaded and reloaded until the crack reopened. One linear variable displacement transducer (LVDT) was mounted across the crack to determine the decompression load. The decompression load was determined by intersecting the tangents of the two slopes of the load vs. crack width diagram. Because the stress at the bottom of the beam is zero at the decompression load, the remaining tendon force can be calculated using Navier's formula:

$$0 = \frac{P_{eff}}{A_c} - \frac{M}{S} \quad (2.4)$$

where,

P_{eff} = remaining tendon force

A_c = cross-sectional area of beam

M = bending moment applied from testing machine

S = section modulus of the beam

The European Committee for Concrete (CEB)/International Federation for Prestressing (FIP) model code 1990 and 1999, ACI 209, Model B3, GL2000, and the PCI Committee on Prestress Losses model codes were used to calculate creep and shrinkage of the concrete. The PCI model was used to calculate the relaxation in the tendons. The CEB/FIP model code was used despite the model being valid for concrete subjected to mean RH between 40% and 100%. The creep and shrinkage models are empirical and each model is based on data from shrinkage and creep tests. A final creep coefficient/shrinkage strain is calculated from different parameters such as compressive strength, water-cement ratio, and ambient RH. The development of strain over a certain period of time is described by a time function calculated from concrete age, age at loading, and the volume-to-surface ratio of the structure. Most of the data regarding the beams were available. However, the modulus of elasticity and compressive strength of the concrete was missing and these values were estimated.

This study concluded the prestress losses in the beams are relatively high compared with results from similar tests found in literature, which is most likely due to the ambient climate in which the beams were stored. An almost constant temperature of 90°F (32°C) and low RH increases both the creep and shrinkage strains in the concrete. Model B3 was the most accurate of the prediction models and agreed well with the tested prestress losses. Most of the prediction models underestimated the measured prestress losses. The ambient climate may be one explanation for the differences between the prediction models and the measured values.

2.7 Static Behavior of 40 Year-Old Prestressed Concrete Bridge Girders Strengthened with Various FRP Systems (Rosenboom et al. 2006)

This research was aimed at investigating the static behavior of five 40-year old, 9.14 m long prestressed bridge girders strengthened with various Carbon Fiber Reinforced Polymer

(CFRP) systems. The girders were tested at the Constructed Facilities Laboratory (CFL) at North Carolina State University (NCSU). One specimen was tested as a control specimen, while the other four specimens were strengthened with near surface mounted (NSM) CFRP bars, strips, and externally bonded CFRP strips and sheets. All specimens were C-channel type prestressed concrete bridge girders taken from the same bridge constructed in 1961 in Cartaret County, North Carolina.

According to core samples taken from the girders, the average compression strength of the concrete ranged from 48 MPa to 74 MPa. Each girder had ten 1725 MPa seven-wire stress relieved prestressing strands (five in each web) and a 125 mm deck with minimal reinforcing. The camber at midspan due to prestressing and self-weight was 40 mm. Two Externally Bonded (EB) and two Near-Surface Mounted (NSM) CFRP were applied to the two webs in each strengthened specimen. All were designed to achieve a 30 percent increase in strength. The first EB system used one 50 mm wide Sika CarboDur strip per web bonded with SikaDur 30 adhesive. The second EB system used two and a half 50 mm wide plies of VSL V-Wrap C-200 sheets per web bonded using VSL saturant. The first NSM system used one 10 mm Aslan 200 CFRP bar by Hughes Brothers bonded using SikaDur 30 adhesive per web. The second NSM system used two 2 mm x 16 mm Aslan 500 strips by Hughes Brothers bonded together prior to strengthening and bonded to the concrete using SikaDur 30 adhesive per web. The two EB systems included 150 mm wide U-wraps at 900 mm spacing along the length of the girder to control the debonding mechanism.

The girders were tested using a 490 kN hydraulic actuator mounted to a steel frame placed at the midspan of the girder. To simulate loading on an actual bridge, a set of truck tires filled with silicone rubber filler were used to apply the load from the actuator. The foot-print of the two tires was approximately 250 mm x 500 mm per AASHTO. The girders were instrumented with a set of string potentiometers placed at midspan, quarter span, and at the ends

to measure the deformation in the neoprene pads. A combination of PI gages and strain gages were used to measure the compressive strain in the top concrete surface. PI gages were placed at the level of the lowest prestressing strands to measure the crack width. Six strain gages were applied to the CFRP reinforcement. The specimens were loaded to 20 kN and unloaded, then reloaded to failure at a rate of 2.5 mm/min. The effective prestressing force was determined by this loading scenario and the reopening of the flexural cracks. The effective prestressing per strand ranged between 67 kN and 80 kN. The loading rate was increased to 5 mm/min after yielding of the prestressing strands. Cracking of the control specimen occurred at a load of 61.5 kN. Yielding of the prestressing strands took place at a load of 115 kN and the specimen failed due to concrete crushing at a load of 148 kN. Both NSM CFRP systems cracked at a load of 55 kN and failed near a load of 180 kN. The EB CFRP systems cracked at a load of 57 kN. The EB CFRP strips failed at 176 kN, while the EB CFRP sheets failed at 163 kN.

A nonlinear finite element model using the ANACAP computer program was used to analyze the control specimen and the NSM CFRP bars and to compare the modeled results with the results found in the lab.

Based on the results of this study, the following conclusions were formulated:

1. The ultimate strength of prestressed concrete member can be substantially increased using CFRP strengthening systems. The ultimate load carrying capacity of aged prestressed girders tested increased by as much as 23 percent compared with the control specimen.
2. Since negligible differences were observed among the various techniques at the service load level, serviceability could not be used as a criterion to compare the efficiency of various CFRP strengthening techniques for prestressed concrete members.

3. The U-wraps enhanced the behavior of the strengthened prestressed girders and delayed delamination of externally bonded CFRP strips and sheets.
4. Using both NSM and EB CFRP systems reduced the crack width at ultimate by 20 percent to 40 percent compared with the control specimen.
5. The most cost-effective systems are those which utilize NSM strengthening. EB CFRP strips are the least cost effective system compared with other techniques.
6. A nonlinear finite element analysis can accurately predict the behavior of the aged unstrengthened and strengthened prestressed concrete girders.

2.8 Testing of Two 50-Year-Old Precast Post-Tensioned Concrete Bridge Girders (Eder et al. 2005)

Although precast, prestressed concrete girders have been used for more than 50 years, there is relatively little experimental data available on the performance of older girders. Data on the performance of older girders are needed to aid management agencies in the decision-making policies regarding older structures. The Hamilton County, Ohio Engineer replaced the decks of several bridges with 50-year old post-tensioned, precast concrete I-girders in 2001. On some of the bridges, the girders were significantly cracked or showed other signs of deterioration and were replaced. The girders for the remaining bridges were left in-place and new fiber reinforced polymer (FRP) decking was installed. From the original drawing of the girders, it was found that 1-1/8 in. (29 mm) diameter bars were used to post-tension each girder and that two of these bars were harped. The drawing did not make clear the exact arrangement of the bars, their initial tension, and the method of harping. Furthermore, the material properties and whether the bridge was intended to be a composite structure was not indicated. The investigation of two of the girders were undertaken to provide experimental verification of the performance of precast, prestressed concrete girders constructed using older construction methods. The testing was

performed to determine the cracking strength, ultimate strength, stiffness, mode of failure, post-tensioning force, composite action, and correlation to similar in-service girders.

The girders had an in-service span length of 45 ft (13.7 m) measured from center-to-center of bearings. Part of the original deck slab and abutment were left on the girder for ease of removal from the bridge. The deck was 7.75 in. (197 mm) thick and overlapped the top flange by 1 in. (25 mm) on each side. The girders were post-tensioned using four 1-1/8 in. (29 mm) diameter bars. The girders were demolished following the testing to reveal that the bars were anchored to the end of the girder by nuts and steel bearing plates. The bars were enclosed in flexible steel conduits, which prevented bonding of the bars to the concrete. The top two bars were bent at 4.5 ft (1.37 m) on either side of midspan to create the harped profile. Shear reinforcing was comprised of No. 4 (13 mm) stirrups spaced at 9 in. (230 mm) along the entire length of the girder. The stirrups extended up into the deck slab concrete.

Six concrete cores were extracted from the web of an untested girder from the same bridge. The concrete contained aggregate with a maximum size of 2 in. (51 mm) and the measured compressive strength was approximately 9.8 ksi (68 MPa). The splitting tensile strength was measured at 800 psi (6.3 MPa). Three samples of the straightest section of post-tensioning bar were extracted and machined into standard round tensile specimens [1/2 in. diameter x 4 in. long (13 mm x 102 mm)] to test their tensile strength properties. The bar was found to have a 0.2 percent offset yield strength of 100 ksi (700 MPa), a tensile strength of 144 ksi (1000 MPa), an elastic modulus of 25,300 ksi (175 GPa), and a percentage of elongation of 16.9 percent.

A span of 42 ft (12.8 m) was chosen for the testing based on damage to the base plate during the removal process. Two elastomeric bearing pads 9 in. x 18 in. x 3 in. (230 mm x 460 mm x 76 mm) in dimension were used at each end. A steel spreader beam was used to distribute a single point load from a single hydraulic load cylinder to two point loads spaced 5 ft (1.52 m)

on either side of the girder midspan. This created a 10 ft (3.0 m) long zone of constant moment over the center of the girder. Five clip surface strain gages were installed on each girder at midspan. One gage was placed just below the mid-height of the cross section and the other four gages were placed at 8 in. and 20 in. (203 mm and 508 mm) above and below it. Wire potentiometers were placed at midspan and quarter points to measure deflections. A load cell attached to the load cylinder measured the total applied load. The girders were loaded in deflection control using 0.01 in. (0.25 mm) deflection increments. Once a crack was visible, the girder was unloaded and an additional clip strain gage was installed across the crack. This gage was used to determine the initial prestressing force in the bars based on the measured concrete strains. The girder was then loaded continuously to ultimate capacity.

Both girder tests were identical to each other within a few percentage points. The applied cracking load for both girders was 90 kips (400 kN). This load corresponds to a midspan cracking moment due to applied load and a total cracking moment (applied load plus dead load) at midspan of 720 kip-ft and 828 kip-ft (976 kN-m and 1123 kN-m), respectively. The cracking moment in this test can now be used to evaluate similar girders still in service. The ultimate load capacity for Girder 1 was 156 kips (693 kN) and 151 kips (670 kN) for Girder 2, a difference of only 3 percent. The corresponding moments at midspan due to the maximum applied load were 1248 kip-ft and 1208 kip-ft (1690 kN-m and 1640 kN-m), and the total moments (applied load plus dead load) at midspan were 1356 kip-ft and 1316 kip-ft (1839 kN-m and 1784 kN-m). The maximum applied moment in both cases was approximately 15 percent below the calculated theoretical moment capacity assuming a fully composite deck slab. If it is assumed the slab is ineffective in carrying the moment, the theoretical capacity is recalculated and drops to 1300 kip-ft (1765 kN-m), which compares favorably with the measured values of 1356 kip-ft and 1316 kip-ft (1839 kN-m and 1784 kN-m). The total post-tensioning force, P , was found by solving the following equation:

$$0 = \frac{P}{A_g} + \frac{Pec}{I_g} - \frac{(M_{applied} - M_g)c}{I_g} \quad (2.5)$$

where,

A_g = gross cross-sectional area

e = eccentricity of tensioning bars

c = distance from neutral axis to clip gauge

I_g = gross moment of inertia

$M_{applied}$ = applied moment

M_g = moment due to self-weight of girder

The post-tensioning force per bar was calculated to be 50 kips (223 kN) with a corresponding stress of 50 ksi (414 MPa). The effective strain in the bars was 0.002 for an elastic modulus of 25,300 ksi (200 GPa). The post-tensioning was calculated at approximately 1 in. (25 mm). Post-tensioning losses could not be determined because the information on the original stress applied to the bars was not available. The total force in the bar at nominal load was calculated to be 140 ksi (960 MPa), which is approximately equal to the ultimate tensile strength of the bar.

The following conclusions were made as a result of this investigation:

1. The girders failed at an average total moment 21 percent below the theoretical value based on composite action with the deck. Since the deck slab separated during testing, the theoretical nominal moment capacity is recalculated and is in excellent agreement with the tested values.
2. Because the deck slab was severely damaged, the initial stiffness data indicates the slab was not effective in carrying the load for these girders. The stirrups, however, suggest that the deck was intended to act compositely with the girder.

3. The structural performance, even after 50 years of service, has not been compromised based on the measured ultimate strength of the tested girders.
4. The tested cracking strength of the girders indicated the girders still in service have sufficient strength to carry the service design truck loads without cracking.
5. Given that the post-tensioning bars had a yield strength of 100 ksi (700 MPa), it is a good assumption that an initial effective stress of 80 ksi (560 MPa) for the post-tensioning bars was used. This results in an estimated long-term loss of 37 percent.

2.9 NCHRP Report 733 High-Performance/High-Strength Lightweight Concrete for Bridge Girders and Decks (Cousins et al. 2013)

This research focused on developing recommended changes to the AASHTO LRFD Bridge Design Specifications (2010) and the AASHTO LRFD Bridge Construction Specifications (2010) with respect to high-strength lightweight concrete girders and high-performance lightweight concrete decks. The concrete used in this research had a density less than 125 lb/ft³. The research objectives were to identify and evaluate key design parameters for lightweight concretes, to propose relevant changes to the AASHTO LRFD Bridge Design Specification and the AASHTO LRFD Bridge Construction Specification, and to perform design examples to investigate the effect of the proposed changes on design practice. The results of the analyses performed during the research are;

1. The AASHTO LRFD equation for modulus of elasticity with $K_1 = 1.0$ is appropriate for lightweight aggregates. Predictions of modulus can be improved by calibrating the K_1 value for each aggregate type.
2. The average splitting tensile strength of the lightweight concrete mixtures was $0.25\sqrt{f'_c}$ which exceeded $\sqrt{f'_c}/4.7$.
3. On average, the modulus of rupture of the lightweight concrete was $0.31\sqrt{f'_c}$, with a lower bound of $0.26\sqrt{f'_c}$.

4. The AASHTO model for shrinkage generally predicted the shrinkage of lightweight concrete better than ACI 209 or CEB MC90.
5. The AASHTO model for creep generally predicted the creep coefficients of the lightweight girder mixtures better than ACI 209 or CEB MC90. The creep coefficients of the deck concrete mixtures were considerably higher than predicted by the AASHTO model and were better predicted by the ACI 209 model.
6. Based on a reliability analysis, normal weight and lightweight concrete should have the same shear strength reduction factor for interface shear.
7. The factor, λ_v , has an insignificant effect on the calculated shear strength of prestressed girders when using the AASHTO sectional or simplified shear design approach.
8. The bias of measured shear strength to calculated shear strength for normal weight and lightweight prestressed girders is approximately the same.
9. Modification of the $\sqrt{f'_c}$ term in shear calculations for lightweight concrete is not necessary.
10. The ϕ factor for shear design of sand lightweight concrete of 0.85 is appropriate.
11. The current AASHTO refined method for calculating prestress losses is appropriate for lightweight girders with lightweight decks.
12. The majority of the difference between calculated and measured prestress loss occurs during the time between release and deck placement. The AASHTO method consistently predicts higher losses than were measured during this period.
13. Of the three creep and shrinkage models allowed by AASHTO (AASHTO, ACI 209, CEB MC90), the AASHTO model results in estimates of prestress loss closest to those measured and is appropriate for use with lightweight prestressed concrete girders.
14. For identical configurations, the lightweight girder and deck design example required 10% fewer strands than the normal weight example.

15. The current strength reduction factor for a shear of 0.70 for lightweight girder results in almost twice the amount of shear reinforcement required for the normal weight example.
16. A change in the strength reduction factor to 0.85 will result in required amounts of shear reinforcement similar to that required for normal weight girders.

CHAPTER 3

EXPERIMENTAL TESTING OF THE ICY SPRINGS BRIDGE GIRDERS

3.1 Bridge Description

The Icy Springs Bridge crosses the Weber River in Coalville, Utah and was originally constructed in 1965 as a 15.54 m (51 ft 0 in.) single span bridge using three double-tee girders. The original bridge was replaced in November 2013 with a 24.38 m (80 ft 0 in.) single span bridge using prestressed concrete decked bulb-tee girders. Figure 3.1 shows the original bridge just prior to demolition. Figure 3.2 shows the replacement bridge in January 2014. Unfortunately, the construction documents for the original bridge are unavailable. As a result, measurements in the field were made to determine span length and other bridge parameters. Additional measurements of the girders were taken following transportation of the girders to the lab. The plan dimensions of the original bridge and the cross-sectional dimensions of the double-



Figure 3.1 Original bridge prior to demolition

tee girders are included as Figures 3.3 & 3.4, respectively.



Figure 3.2 New Icy Springs Bridge

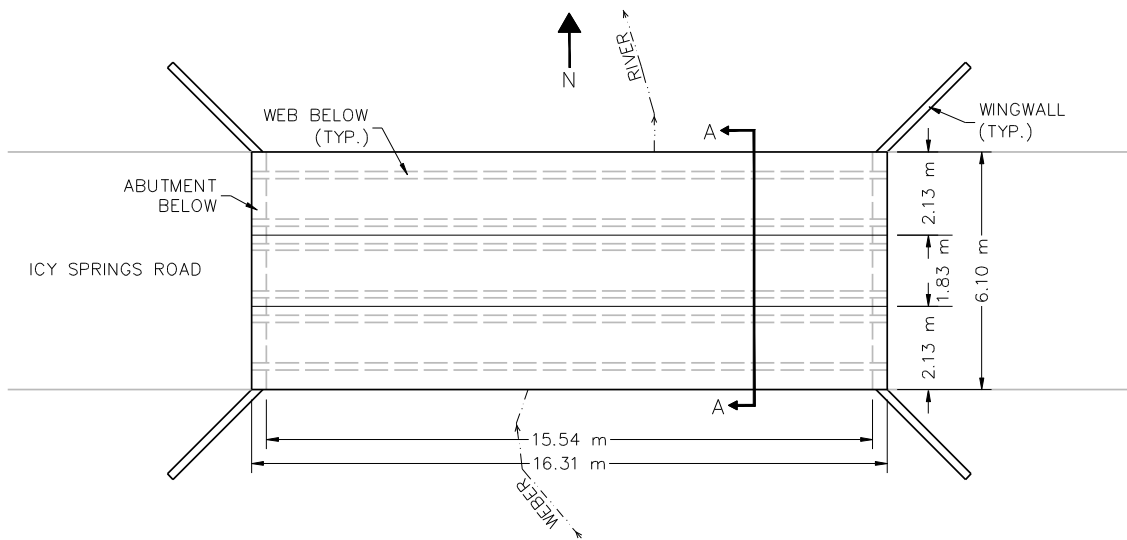


Figure 3.3 Original bridge dimensions

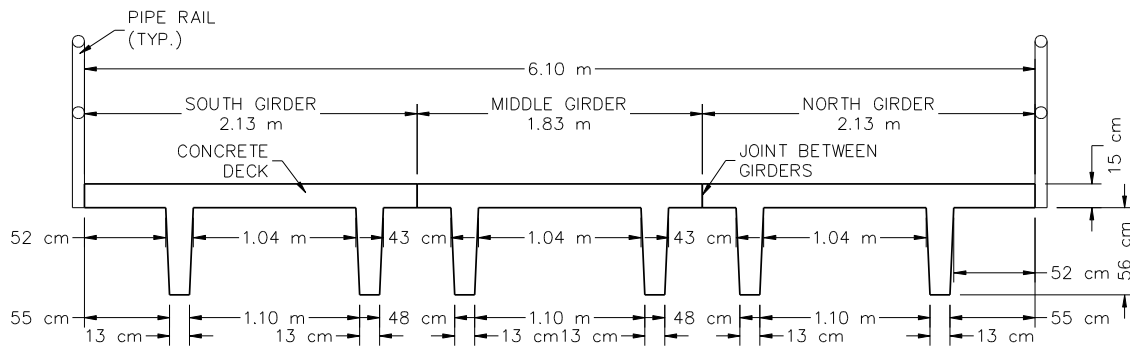


Figure 3.4 Original bridge cross section A-A

3.2 Girder Dimensions

All three double-tee girders had the same length of 16.31 m (53 ft 6 in.). The standard double-tee section that most closely matches the original Icy Springs Bridge girders is the 8LDT24 girder (Wilden 2010). The north and south girders were both 2.13 m (7 ft 0 in.) wide and had the same cross-sectional dimensions, but were mirrored from each other. The middle girder was 1.83 m (6 ft 0 in.) wide. The flanges of all three girders were 15 cm (6 in.) thick. The webs were all 56 cm (22 in.) tall and tapered from 18 cm (7 in.) wide where the webs met the flange to 13 cm (5 in.) wide at the bottom of the webs. The webs for all girders were spaced 1.22 m (4 ft 0 in.) apart center-to-center. The webs for the middle girder were centered about the centerline of the girder. The centerline of the outside webs for the north and south girders were located 61 cm (2 ft 0 in.) from the outside edge of the flange. The measured camber, after the girders were separated and taken to the lab, at the midspans is summarized in Table 3.1. The

Table 3.1 Measured camber
calculated camber is discussed and compared with the measured values in Chapter 4.

Girder Location	Girder #	Measured Camber		
		North Web Camber (cm/in.)	South Web Camber (cm/in.)	Average Camber (cm/in.)
Middle	1	13.82 / 5.44	13.84 / 5.45	13.83 / 5.45
North	2	9.3 / 3.66	10.97 / 4.32	10.13 / 3.99
South	3	11.84 / 4.66	10.11 / 3.98	10.97 / 4.32

3.3 Girder Reinforcement

Each web of the double-tee girders was designed with sixteen 11 mm (7/16 in.) seven-wire prestressing strands. Four of these strands were arranged in a single vertical pattern near the bottom of the web and ran horizontal the entire length of the girder. The remaining twelve

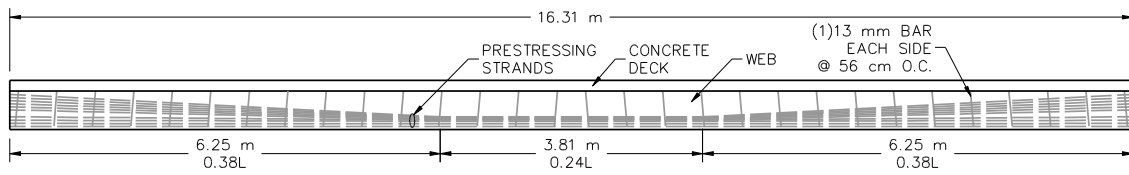


Figure 3.5 Prestressing strand layout side view

strands were configured in horizontal pairs of six rows and harped down toward the midspan of the girders. The harped strands ran horizontal near the midspan of the girders for 3.81 m (12 ft 6 in.) or 0.24L, as shown in Figure 3.5 thru Figure 3.7. The deck was reinforced with one mat of 13 mm (No. 4) bars at 25 cm (10 in.) on center longitudinally and two mats of 13 mm (No. 4) bars at 10 cm (4 in.) on center transverse. No joint between the deck and the web existed, as the deck concrete was cast monolithically with the web. Shear reinforcement was configured with one 13

mm (No. 4) bar oriented approximately 5-degrees from vertical on each side of the web spaced approximately 56 cm (22 in.) apart and extending from the ends of the girders to the midspan.

Figure 3.8 shows one end of Girder #1 with the shear steel exposed.

After transportation to the lab, the ends of all girders had sustained some damage as a result of the removal from the abutments. However, the webs of the girders beyond where girders were attached to the abutments were not damaged. The flanges of the girders exhibited some reduction in the original section as a result of heavy truck traffic utilizing the bridge. Sections of the flanges were removed on the outsides of the webs near the ends of the girders to accommodate the lifting cables during removal. The middle girder was clearly in the most deteriorated state as a result of traffic using the girder while traveling in both directions across the bridge. The condition of the girders is further discussed in Chapter 4 for the comparisons of the

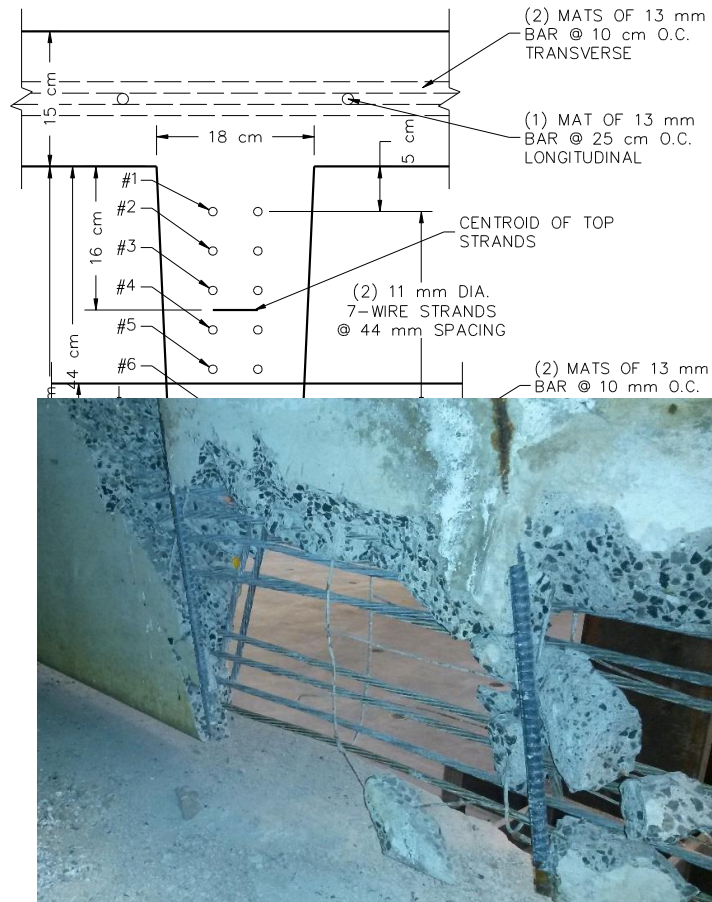


Figure 3.8 End of middle girder with shear steel exposed

measured and calculated capacities. Physical properties of the girders are included in Appendix A.

3.4 Experimental Testing

The experimental testing for this research was performed at the Systems, Materials, and Structural Health Lab (SMASH Lab) on the Utah State University (USU) campus located at 1500 Canyon Road, Logan, Utah. The SMASH Lab contains a strong floor, a reaction frame, various hydraulic rams, and a Vishay 5000 data acquisition system. The strong floor was designed and constructed as a heavily reinforced 0.914 m (3 ft 0 in.) thick concrete slab with vertical conduits spaced in a grid pattern 0.914 m (3 ft 0 in.) apart to allow the flexibility of a reaction frame to be positioned at various locations. The reaction frame is comprised of two steel columns with a steel spreader beam spanning between the columns. The spreader beam is bolted to the columns and the columns are attached to a base plate that can be bolted to the strong floor using threaded rods. The elevation of the spreader beam may be adjusted from approximately 1.52 m (5 ft 0 in.) above the strong floor to approximately 3.04 m (10 ft 0 in.). A single or multiple hydraulic rams can be positioned anywhere along the spreader beam to apply a downward load on a test specimen. Two 222 kN (500 kip) hydraulic rams were used to apply the static loading for these experiments. The Vishay data acquisition system is capable of continuously monitoring and recording data from various sensors, such as load cells, string potentiometers, and strain gages.

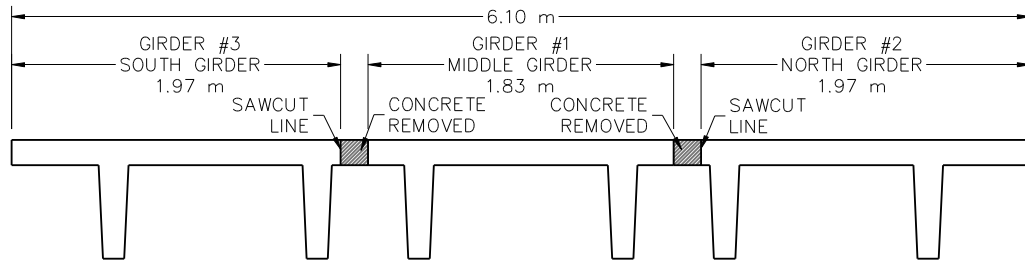


Figure 3.9 Girder removal cross-sections

For the purposes of this study, the girders were numbered in the order in which they were tested. Therefore, the middle girder is Girder #1, the north girder is Girder #2, and the south girder is Girder #3. Prior to the removal of the girders from the abutments, the decks of Girder #2 and Girder #3 were cut by the contractor to ensure a clean removal as shown in Figure 3.9. The

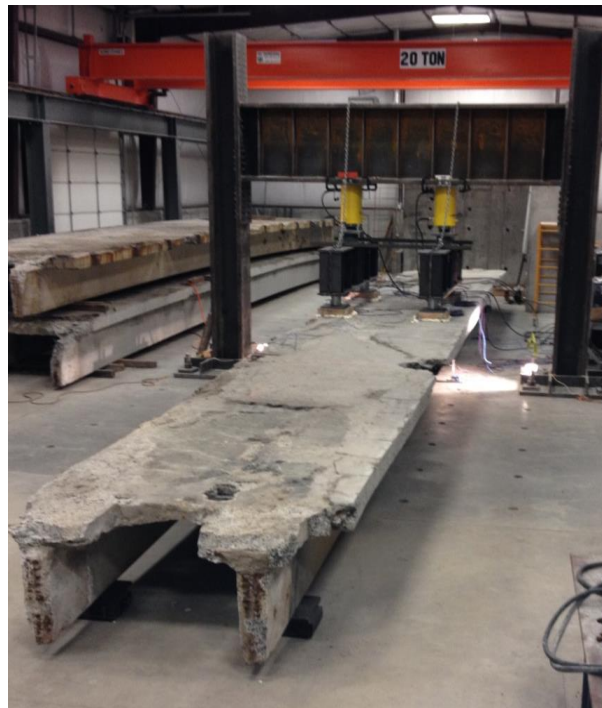


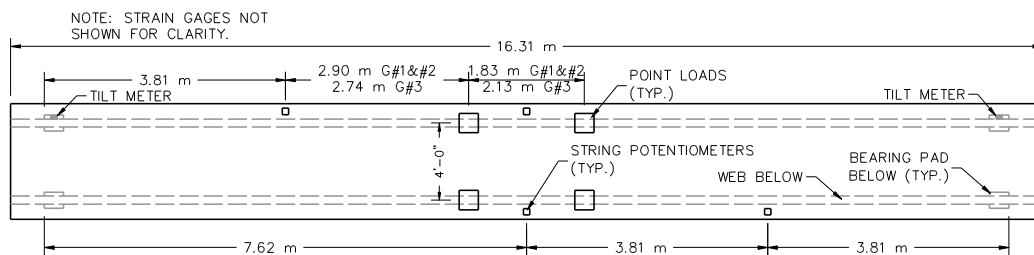
Figure 3.10 Reaction frame with Girder #1 ready for crack test

resulting cross-sectional dimensions of the girders were not modified for testing. Figure 3.10 shows Girder #1 under the reaction frame being prepared for a crack test. Note the damage to the end of the girder and damaged deck.

3.4.1 Crack Testing

Since the ends of two of the girders were damaged during the bridge demolition, all

Figure 3.11 Flexural instrumentation plan view



girders were tested at a simply supported length of 14.94 m (49 ft 0 in.) rather than the overall

length of the girders of 16.31 m (53 ft 6 in.). The girders were supported on four elastomeric

bearing pads that were placed between 305 mm x 305 mm x 25 mm (12 in. x 12 in. x 1 in.) steel

plates. When slight adjustments were needed for clearance, additional steel plates were added to

raise the girders above the strong floor. The girders were loaded with two point loads situated

over each web as shown in Figures 3.11 through 3.14. Dimensions not shown with units in the

figures are assigned the unit of centimeters (cm). The point loads were spaced 1.83 m (6 ft 0 in.)

apart for Girder #1 and Girder #2 and spaced 2.13 m (7 ft 0 in.) apart for Girder #3 to create a

constant moment region between the point loads. Four square concrete pads 30.5 cm x 30.5 cm

(12 in. x 12 in.) were cast directly on the deck above the webs of the girders at the same elevation

to provide a level surface to place the spreader beams and load cells. Two of the leveling pads

used on Girder #1 are shown in Figure 3.14. Two 305 mm x 305 mm x 25 mm (12 in. x 12 in. x

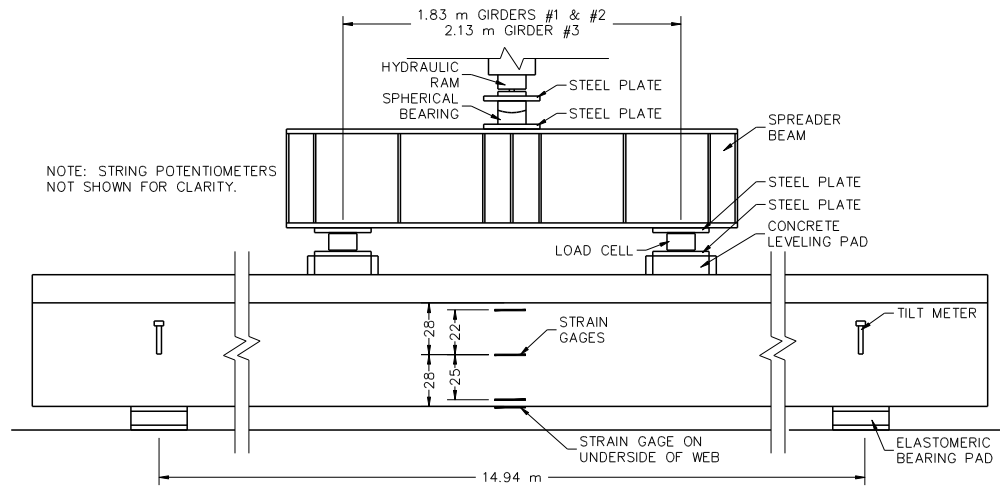


Figure 3.12 Flexural instrumentation side view

1 in.) steel plates were then placed on each concrete pad with the load cells being located between

the plates. Two 2.44 m (8 ft) long steel wide flange spreader beams were then situated on the

load cells running parallel to the webs and were used to divide the forces from the hydraulic rams.

The top flanges of the two spreader beams were braced laterally to each other using two lengths

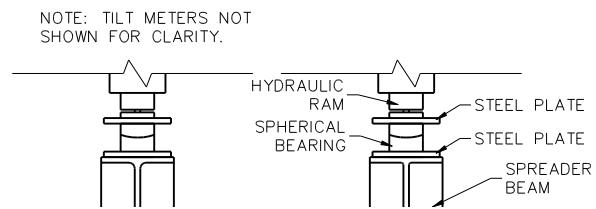


Figure 3.13 Flexural instrumentation end view

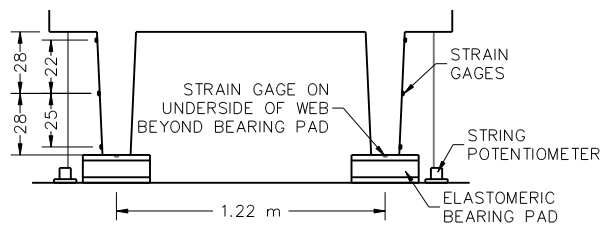




Figure 3.14 Typical concrete leveling pads

of 5 cm x 5 cm (2 in. x 2 in.) angle iron and C-clamps. Chains were attached to the ends of the

spreader beams and routed over the reaction frame to prevent the spreader beams from shifting and falling off the deck of the girders in the event of a sudden failure.

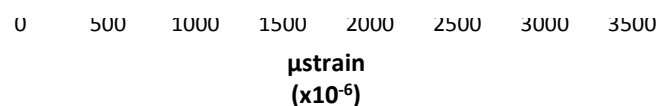
For the initial crack test, all girders were instrumented with two string potentiometers at midspan (one on each side of the girder), one string potentiometer at each quarter-point of the girder (one on each side of the girder), three strain gages on each side of the girder at the midspan, and one 1779 kN (400 kip) load cell at each point load. Figure 3.15 shows one side of Girder #1 with the strain gages and chain for the string potentiometer. Girder #3 was additionally instrumented with a tilt meter at each end to measure the angle of rotation at the ends of the girder during the tests.

The external load on the girders was monotonically increased until cracks were noticeable in the bottom portions of the webs. The cracks were marked and the girders unloaded. Once the load was removed and the cracks closed, an additional strain gage was placed on the bottom of each web where there was an observed crack that extended through the web nearest the midspan of the girders. The girders were then loaded and unloaded numerous times to a



Figure 3.15 Strain gages and marked cracks on Girder #1

Figure 3.16 Girder #1 cracking load test data



magnitude equal to 125 percent of the previously observed cracking load. During the loading and unloading, data from the various sensors was recorded. This data was used to determine the cracking load and moment. In all cases, the magnitude of the applied load did not exceed that which would result in permanent damage to the girders.

Following the test, a load vs. strain plot for each girder was created to determine the magnitude of the applied load when the crack opened. The load vs. strain plot of the Girder #1 crack test is shown in Figure 3.16. As shown in the plot, nonlinear strain behavior was observed. The steeper straight line is the pre-cracking girder stiffness and the straight line beyond the nonlinear section is the post-cracking girder stiffness. The extension of these two lines has been shown to be the location of the decompression load. The decompression load is the magnitude of the external load that causes zero stress at the bottom of the girder.

Equation 3.1 is used to calculate the stress at the bottom of a prestressed concrete girder subjected to an external load. Since the girders are not composite, C and I in the last term of the equation are taken as C_g and I_g , respectively.

$$\sigma = -\frac{P}{A_g} - \frac{Pe_{pg}C_g}{I_g} + \frac{M_{sw}C_g}{I_g} + \frac{M_{xt}C}{I} \quad (3.1)$$

where,

σ = stress at the bottom of the girder

P = effective prestressing force

A_g = total cross-sectional area of girder and deck (gross)

e_{pg} = eccentricity of the prestressing force from the centroid of the girder (gross)

C_g = distance from the girder neutral axis to the bottom of the girder (gross)

I_g = gross moment of inertia

M_{sw} = moment at crack location due to girder self-weight

M_{xt} = moment caused by decompression load at crack

C = distance from girder neutral axis to bottom of the girder (effective)

I = composite moment of inertia

At the decompression load of a girder the stress, σ , is zero and Equation 3.1 can be solved for the effective prestressing force, P , as shown in Equation 3.2. The effective prestressing force, P , is the total effective prestressing force in the girder, not the prestressing force in each strand.

$$P = \frac{(M_{sw} + M_{xt})C_g}{\frac{1}{A_g} + \frac{e_{pg}C_g}{I_g}} \quad (3.2)$$

Once the total effective prestressing force is determined, the total effective prestress is calculated using Equation 3.3 and the effective prestress strain is calculated using Equation 3.4.

$$\sigma_{ps} = \frac{P}{A_{ps}} \quad (3.3)$$

where,

σ_{ps} = effective stress in the prestressing strands

A_{ps} = total cross-sectional area of the prestressing strands

$$\epsilon_{ps} = \frac{\sigma_{ps}}{E_{ps}} \quad (3.4)$$

where,

ϵ_{ps} = effective strain in prestressing strands

E_{ps} = modulus of elasticity of prestressing strands

The values of effective prestressing calculated for each of the girders compared very well with each other, with a difference of 5% or less for all values between girders. Full calculations for the effective prestressing for each girder are included in Appendix B with Table 3.2 summarizing the calculated values. Further discussion of the jacking stress and effective

Table 3.2 Effective prestress for each girder

Girder #	Cracking Load, F (kN/kips)	M_{xt} (kN-m/kip-ft)	P (kN/kips)	σ_{ps} (MPa/ksi)	ϵ_{ps}
1	114.59 / 25.76	375.45 / 276.92	1448.69 / 325.68	610.19 / 88.50	0.003105
2	114.46 / 25.73	375.04 / 276.62	1523.73 / 342.55	641.8 / 93.08	0.003266
3	118.08 / 26.55	377.89 / 278.72	1530.65 / 344.10	644.71 / 93.51	0.003281

prestress is included in Section 4.2.1.

The slight differences noticed in the prestressing force and prestressing stress between Girder #1 and Girders #2 & #3 could be attributed to the wider decks of Girders #2 & #3 and the higher initial load from the self-weight of the girders.

3.4.2 Flexural Capacity Testing

Following the crack test of each girder, the specimens were loaded using the same support and loading conditions with the same instrumentation as the crack test until failure of the girder occurred. The girders were monotonically loaded through failure with data from the various sensors being sampled at 10 Hz. All sensors were zeroed and calibrated prior to the commencement of testing. A small load was applied to the load cells using the hydraulic rams before the full test to ensure the readings from the load cells were congruous with what was expected. The string pots were calibrated by matching the voltage output from the data collection system with various known distances to develop the linear relationship. The strain gages were



Figure 3.17 Girder #1 after flexural failure

shunt calibrated, where the resistance in the wire from the data collection system to the strain gage is subtracted out to increase the accuracy of the reading from the actual strain gage.

All three girders were loaded to flexural failure, which occurred as a result of a failure in the concrete compression block in the deck. Figure 3.17 shows the failure of the deck and web of Girder #1. During the loading, several vertical cracks and some horizontal cracks formed on each of the webs between the applied point loads. The maximum loads achieved in Girders #1, #2, and #3 were 403.5 kN (90.7 kips), 443.9 kN (99.8 kips), 484.9 kN (109 kips), respectively. A plot of the moment vs. midspan deflection of Girder #1 is shown in Figure 3.18. The moment vs. midspan deflection plots for the other two girders are included in Appendix B.

The strain gages were attached at various elevations along the web at midspan. As the loading increased, a few of them sustained damage during the ultimate flexural test. Some of the

data at the higher applied loads was lost, but enough data was recovered to create strain distribution plots for each girder. The strain distribution plot of Girder #1 is shown in Figure 3.19 with strain distribution plots for the other two girders being located in Appendix B.

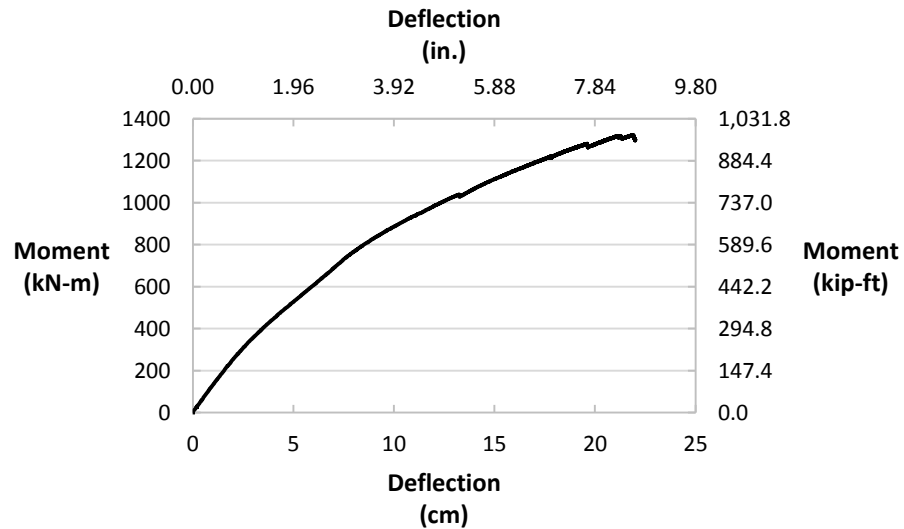


Figure 3.18 Girder #1 moment vs. deflection at midspan

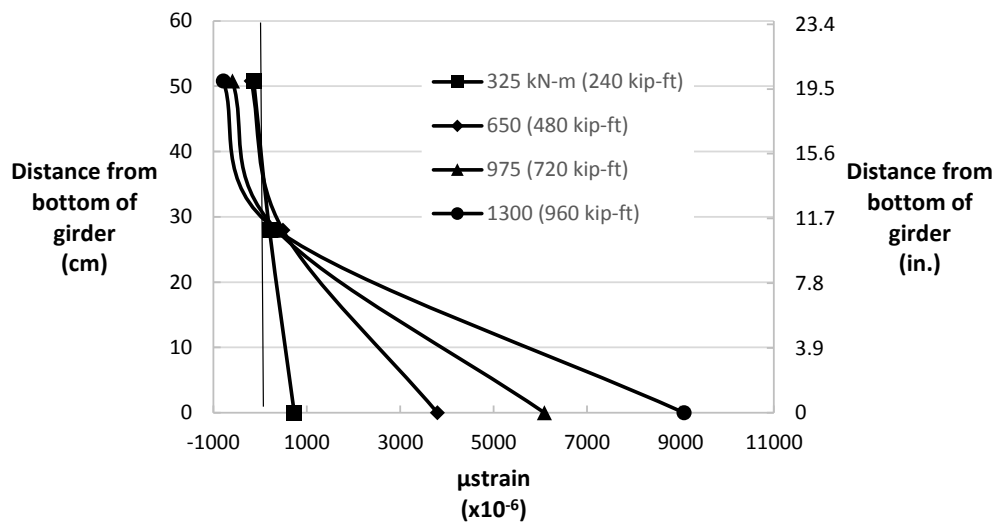


Figure 3.19 Girder #1 strain distribution at midspan

The strain distribution for each of the girders is nonlinear, which is a result of the concrete cracking near the bottom of the webs and the neutral axis of the section shifting upward towards the deck. Plane sections remain plane at lower applied moments and become nonlinear after cracking occurs. Positive strain, indicating tension, was observed near the bottom of each of

the girders throughout the tests. Negative strain, indicating compression, was observed along the web near the deck of Girder #1 as the load was increased beyond the cracking load. The negative strain in the web indicates the bottom of the compression block had moved up in the web. The strain distribution plots show the plane sections remaining plane through the linearly elastic region of the loading. When cracking occurs, the neutral axis moves upward in the cross-section. The moments shown in the plots are the applied moments in the constant moment regions between the point loads. Table 3.3 shows the results of the flexural capacity testing. The maximum moments compared well with each other with an average of 906 kN-m (1,228 kip-ft)

Table 3.3 Flexural capacity testing results and a range of $\pm 7.1\%$. Girder #1 had the most deteriorated deck, therefore the lowest flexural capacity.

Girder #	Max. Applied Load (kN/kips)	Span (m/ft)	Load Spacing (m/ft)	Max. Applied Moment, M_{xt} (kN-m/kip-ft)	Self-Weight Moment, M_{sw} (kN-m/kip-ft)	Total Moment (kN-m/kip-ft)	Max. Deflection (cm/in)
1	403.5 / 90.7	160.8 / 49.0	19.7 / 6.0	719.2 / 975.0	117.7 / 159.6	836.9 / 1134.6	25.6 / 10.07
2	443.9 / 99.8	160.8 / 49.0	19.7 / 6.0	791.3 / 1072.9	123.3 / 167.1	914.6 / 1240.0	24.3 / 9.57
3	484.4 / 108.9	160.8 / 49.0	23 / 7.0	843.4 / 1143.5	123.3 / 167.1	966.7 / 1310.6	27.1 / 10.65

3.4.3 Shear Capacity Testing

Following each of the flexural capacity tests, the girder was split where the flexural failure occurred and a shear test was performed on each the remaining sections of end of the girder. The shear testing was based on the distance from the center of the compression block to the centroid of the prestressing strands, d_v , at the midspan of the girders. A preliminary value for

Table 3.4 Shear test setup by girder

Girder #	West End	East End
1	$3d_v$	$2d_v$
2	$3d_v$	$4d_v$
3	$2d_v$	$4d_v$

d_v of 53.4 cm (21.0 in.) was calculated using assumed values as shown in the calculations in Appendix A. For the purposes of the shear testing, a value of 53.3 cm (21 in.) was used. For comparison, the value of d_v calculated at midspan after using the tested values of the concrete, prestressing strands, and mild steel as outlined in Section 4.1 was 53.6 cm (21.1 in.) and 53.9 cm (21.2 in.) for Girder #1 and Girders #2 & #3, respectively. Shear tests were performed by placing

the load a distance of $2d_v$, $3d_v$, and $4d_v$ from the support. Table 3.4 summarizes the type of shear test setup used on each girder. Figures 3.20 through 3.23 show the shear test configurations.

Again, dimensions not shown with units in the figures are assigned the units of centimeters (cm).

The $2d_v$ tests were designed to determine the capacity of the girders with the loads primarily in shear. The $3d_v$ and $4d_v$ tests were designed to determine the capacity of the girders in both shear

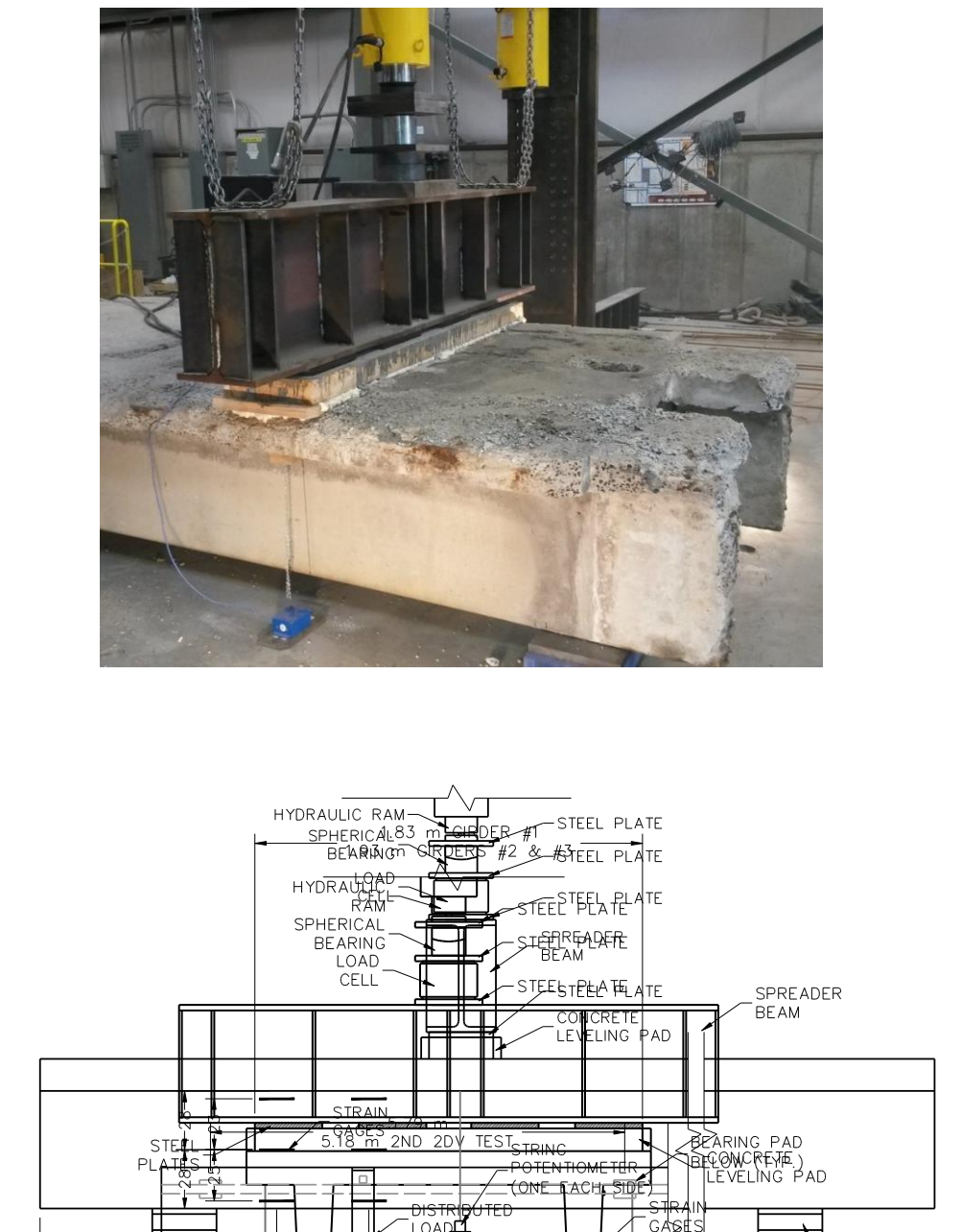


Figure 3.23 Shear instrumentation end view

and flexure.

The girders were loaded monotonically through failure using a continuous concrete leveling pad across the entire width of the girder and by placing a steel spreader beam on the leveling pad to create the uniformly distributed load. A 5338 kN (1,200 kip) load cell was used to measure the total force experienced by the girders. String potentiometers were placed directly under the externally applied load on both sides of the girders. Strain gages were installed for the first $2d_v$ test and the first $3d_v$ test as shown in Figure 3.22. Chains were positioned over the reaction frame and attached to the lifting hooks on the spreader beam to prevent the spreader beam from falling during the testing.

The maximum load and the maximum shear force applied at failure of the girders decreased as the distance from the applied force to the supports increased, as expected. The maximum shear force experienced by the girders was 1298.7 kN (292.0 kips), 1036.9 kN (233.1 kips), and 891.4 kN (200.4 kips) for the $2d_v$, $3d_v$, and $4d_v$ tests, respectively. At failure, the $2d_v$



Figure 3.24 $2d_v$ shear failure of Girder #1

tests exhibited a failure plane roughly 45 degrees from horizontal, indicating a mainly shear



Figure 3.25 $3d_v$ shear failure of Girder #2

failure, as shown in Figure 3.24. The $3d_v$ and $4d_v$ tests failed at more shallow angles than 45

degrees, which is a result of a flexure-shear failure as shown in Figure 3.25. All girders failed in

a fast, brittle manner when the maximum shear load was achieved. Based on visual inspections

following failure, it was determined the shear reinforcing was not particularly effective in

preventing the shear cracks from continuing through the webs of the girders as the shear

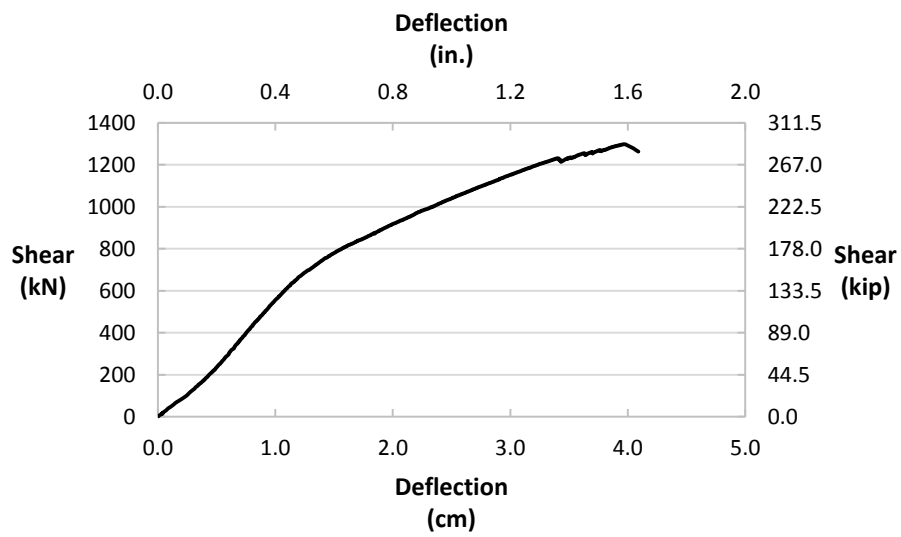


Figure 3.26 Girder #1 $2d_v$ shear vs. deflection plot

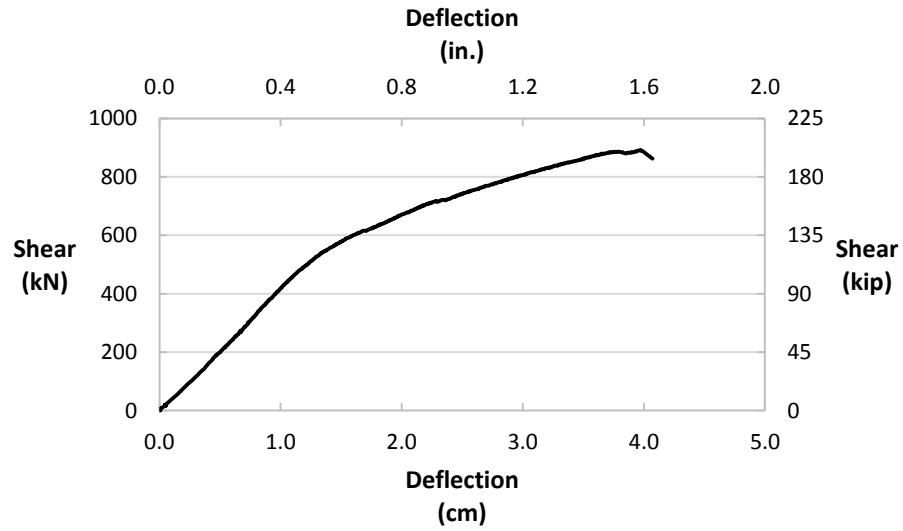


Figure 3.27 Girder #3 $4d_v$ shear vs. deflection plot

reinforcement did not yield or deform significantly. Possible explanations for this are the shear

reinforcing was not wrapped around the prestressing strands, as is currently common practice to produce the required development length, and the shear reinforcing was oriented at a slight angle in the direction of the expected shear plane. Shear vs. deflection plots for the Girder #1 $2d_v$ and Girder #3 $4d_v$ tests are shown in Figures 3.26 and 3.27, respectively. The plots clearly show an

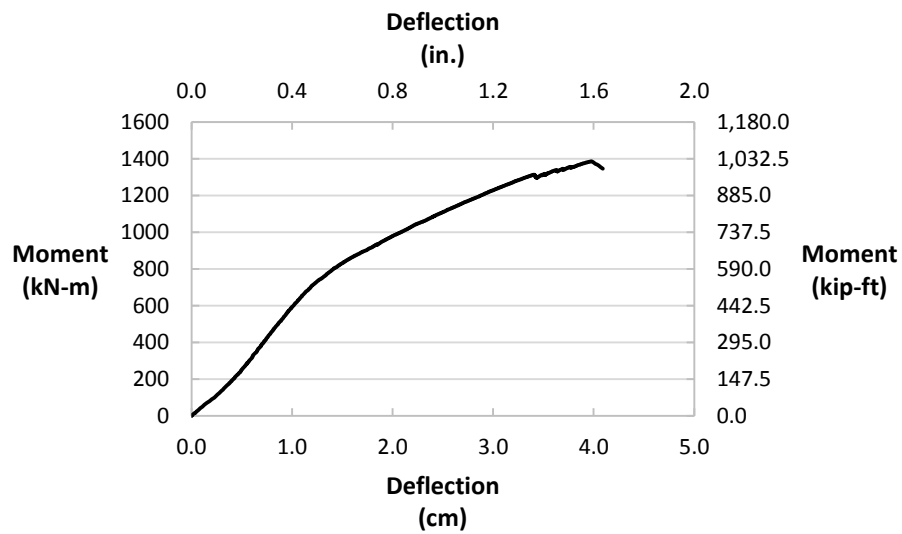


Figure 3.28 Girder #1 $2d_v$ moment vs. deflection plot

initial elastic region, followed by a reduction of the stiffness of the girders after initial cracking of the concrete. Moment vs. deflection plots for the Girder #1 $2d_v$ and Girder #3 $4d_v$ tests are shown in Figures 3.28 and 3.29, respectively. The shear vs. deflection plots and moment vs. deflection plots for all other tests are included in Appendix B.

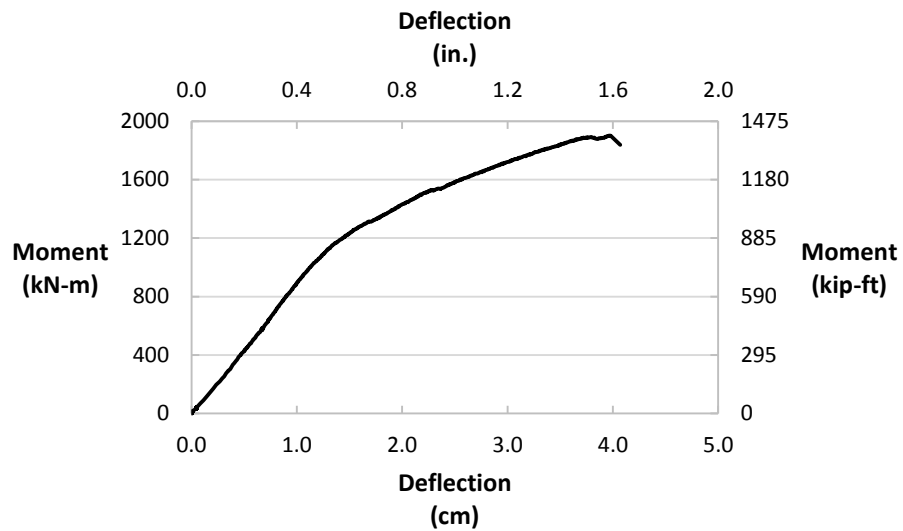


Figure 3.29 Girder #3 $4d_v$ moment vs. deflection plot

During the shear testing for Girders #2 and #3 it was observed that one web of the girder would fail prior to the other web. Figure 3.30 shows the results of this type of failure. Girders #2 and #3 had a wider flange on one side and the shear test loading was uniformly distributed across the entire flange. Using tributary areas to calculate the total force being experienced by each web

Table 3.5 Shear capacity test results

it is clear more of the distributed load was resisted by the side of the girder with the wider flange. Also shown in Figure 3.30 is a de-bonding failure in the south web demonstrated by the vertical crack in the concrete through the prestressing strands.

Table 3.5 shows the sequence of the shear testing, the girder number, the side of the girder the test was performed, and the maximum loads applied with the resulting maximum shear



Figure 3.30 Girder #3 $2d_v$ failure

Sequence	Shear Test	Girder # & Side	Max. Applied Load (kN/kips)	Max. Shear Force (kN/kips)	Average Max. Shear Force (kN/kips)
1	$2d_v$	1E	1591.6 / 357.8	1298.9 / 292.0	1401.4 / 315.1
6	$2d_v$	3W	1894 / 425.8	1503.9 / 338.1	
2	$3d_v$	1W	878.1 / 197.4	635.6 / 142.9	836.3 / 188.0
4	$3d_v$	2W	1432.3 / 322.0	1036.9 / 233.1	
3	$4d_v$	2E	1156.5 / 260.0	731.3 / 164.4	811.4 / 182.4
5	$4d_v$	3E	1410.1 / 317.0	891.4 / 200.4	

forces experienced by the girders during each test. The maximum shear forces for the two 2d_v and two 4d_v tests compared fairly well with each other. However, the two 3d_v tests varied by approximately 401 kN (91 kips). This discrepancy could be a result of severe deterioration of the deck on the west side Girder #1 while the girders were in-place over the Weber River (see Figure



3.31). The difference could also be a result of the wider flange of Girder #2 compared with the

Figure 3.31 Girder #1 west side deck deterioration
narrower flange of Girder #1.

3.4.4 Punching Shear Capacity Testing

The east half of Girder #1 and the west half of Girder #2 were stored in the lab while the



Figure 3.32 Typical punching shear test setup

flexural and shear capacity testing of Girder #3 was completed. Following the last shear capacity

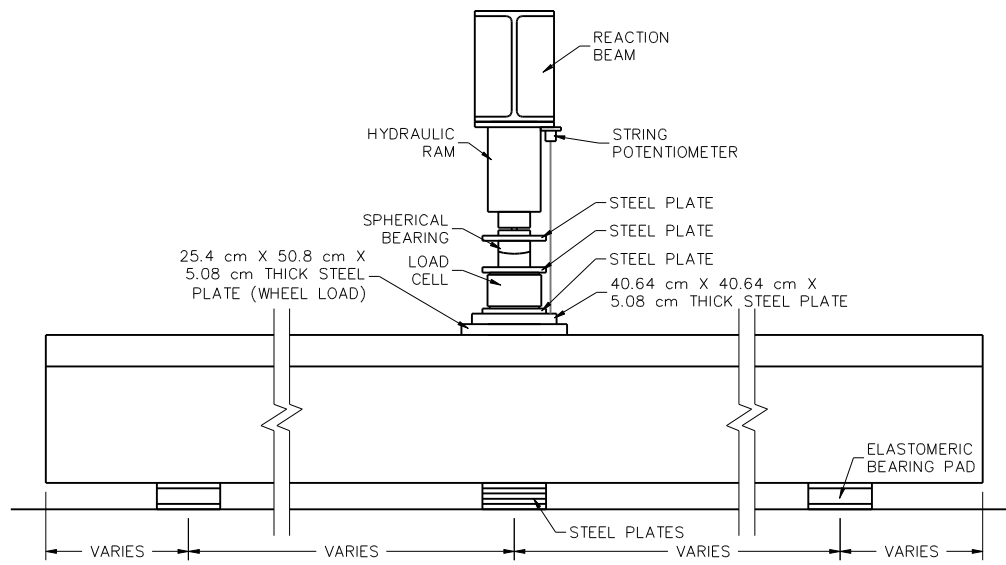


Figure 3.33 Punching shear instrumentation side view

test on Girder #3, punching shear tests were performed on the remaining halves of Girders #1 and

#2 and both halves of Girder #3. Locations for the punching shear tests on the girder decks were

chosen to avoid the other tests and were based on the visible damage to the deck from the flexural

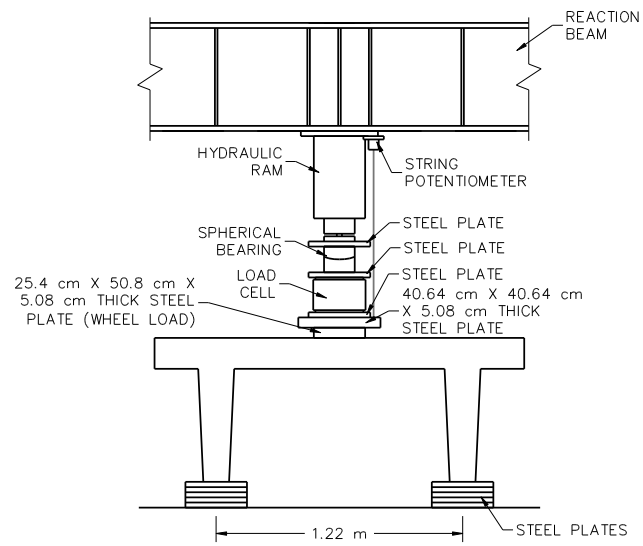


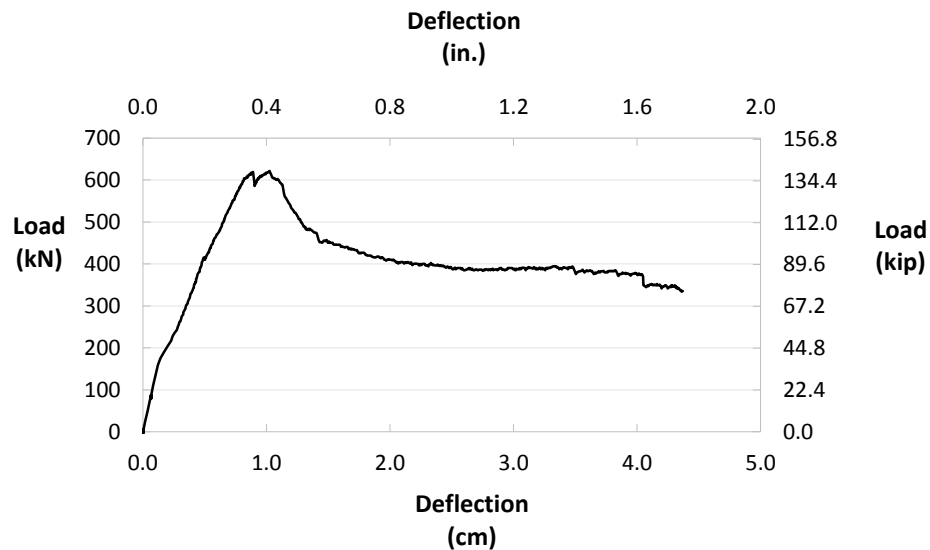
Figure 3.34 Punching shear instrumentation end view

and shear capacity testing. The tests were centered evenly between the webs of the girders and were spaced such that the failure of the bottom of the flange was not impacted by adjacent punching shear tests. Estimates were made of the deck thickness at each test location to the nearest 2.54 cm (1 in.). A 25.4 cm wide x 50.8 cm long x 5.08 cm thick (10 in. wide x 20 in. long x 2 in. thick) steel plate was placed directly on the deck at the test locations and used to apply the load to the deck. The plate dimensions were meant to mimic the tire contact area required by Article 3.6.1.2.5 of the AASHTO LRFD Bridge Design Specification. Figures 3.32 through 3.34 show the typical punching shear test setup. A 40.6 cm x 40.6 cm x 5.1 cm thick (16 in. x 16 in. x 2 in. thick) plate was placed on top of the tire contact area plate, then the load cell and spherical bearing. 30.5 cm x 30.5 cm x 2.5 cm (12 in. x 12 in. x 1 in. thick) steel plates were placed as



Figure 3.36 Tire contact area plate embedded in deck

spacers between the load cell and the spherical bearing and on top of the spherical bearing to ensure the load could be applied without reaching the maximum stroke of the hydraulic ram. Steel plates were placed on the strong floor in line with the load below each web to prevent the girder from bending longitudinally during the test. A string potentiometer was attached to the underside of the reaction beam and to the steel plate below the load cell for punching shear tests #7 through #13 to measure the deflection of the tire contact area as the load was applied. The load was applied monotonically through failure of the concrete in the deck and to where the loading began to yield the transverse and longitudinal steel. The yielding of the steel was indicated by the drop in the load following the long flat section in the load vs. deflection plot as shown in Figure 3.35. The cracking of the concrete is apparent in the plot at the peak load of 605



kN (136 kips) and a deflection of approximately 1.0 cm (0.392 in.). The load vs. deflection plots for punching shear tests #7 through #13 are included in Appendix B. Figure 3.36 shows a punching shear test after the loading has been applied and Figure 3.37 shows the typical punching shear failure of the concrete.

The results of the punching shear capacity testing are shown in Table 3.6 and are fairly consistent when the maximum loads applied are compared with the estimated deck thicknesses. Tests #2 and #4 were located where an asphalt overlay of approximately 2.54 cm (1 in.) and 7.62 cm (3 in.), respectively, were placed over the 15.24 cm (6 in.) concrete deck. The tire contact

Table 3.6 Punching shear capacity results

Test #	Girder # & Side	Estimated Deck Thickness (cm/in)	Max. Load (kN/kips)	Load per Thickness (kN/cm - kips/in)
1	3W	15.2 / 6.0	565.8 / 127.2	37.1 - 21.2
2	3W	17.8 / 7.0	619.2 / 139.2	34.8 - 19.9
3	3W	15.2 / 6.0	549.4 / 123.5	36 - 20.6
4	3E	22.9 / 9.0	988.8 / 222.3	43.2 - 24.7
5	3E	15.2 / 6.0	671.2 / 150.9	44 - 25.2
6	3E	15.2 / 6.0	646.8 / 145.4	42.4 - 24.2
7	2W	12.7 / 5.0	505.3 / 113.6	39.8 - 22.7
8	2W	15.2 / 6.0	700.1 / 157.4	45.9 - 26.2
9	2W	12.7 / 5.0	500 / 112.4	39.3 - 22.5
10	1E	10.2 / 4.0	338.1 / 76.0	33.3 - 19.0
11	1E	15.2 / 6.0	648.1 / 145.7	42.5 - 24.3
12	1E	15.2 / 6.0	854.5 / 192.1	56 - 32.0
13	1E	15.2 / 6.0	621.9 / 139.8	40.8 - 23.3

area plate was placed directly on the concrete deck in the other eleven tests.

CHAPTER 4

ANALYSIS OF THE ICY SPRINGS BRIDGE GIRDERS

During the testing of the girders, samples of the concrete, prestressing steel, and mild steel reinforcement in the girders were obtained and laboratory tested as described in Section 4.1. The material properties determined from testing were used in the theoretical calculations based on recommended procedures in the 2012 AASHTO LRFD Bridge Design Specifications (AASHTO 2012) as outlined in Section 4.2. For the purposes of this document, the 2012 AASHTO LRFD Bridge Design Specifications will be abbreviated “ALBDS”. The tested values were then compared with the theoretical values.

4.1 Material Properties

4.1.1 Concrete

A total of five concrete core samples that were 10 cm (4 in.) in diameter were obtained to determine the unit weight, w_c , of the concrete in the girders, as well as the maximum compressive strength, f'_c , using ASTM C39 testing standards. Three samples were removed from the web of Girder #1 and two samples were taken from the web of Girder #2. One sample from each girder included a partial length of rebar running across the sample perpendicular to the cylinder. The rebar was cut from the samples and the ends of all five specimens were squared using a concrete table saw. Measurements of the diameter, height, and weight of each sample were recorded.

After all measurements were completed, the samples were compressed to failure and the

maximum sustained load was recorded. Figure 4.1 shows Sample #5 in the testing apparatus

prior to testing. Figure 4.2 shows the sample after the completed test. The maximum

compressive stress in each sample was calculated by dividing the maximum applied load to each



Figure 4.1 Concrete cylinder test setup



Figure 4.2 Concrete cylinder after failure

sample by the cross-sectional area of the sample. The average maximum compressive stress was



Figure 4.3 Concrete aggregate

calculated to be 38.61 MPa (5.6 ksi). The unit weight of the concrete was calculated using the dimensional measurements and weights obtained prior to testing the cylinders and was determined to be 17 kN/m³ (110 lb/ft³). As a result of these calculations, it was concluded lightweight concrete was used in the construction of the girders. The bridge was constructed next to a lightweight aggregate source and it is believed that this source was used for the construction of this bridge. Figure 4.3 shows the porous aggregate used in the concrete mix for the girders. Tabulated calculations for the concrete compressive strength and unit weight are included in Appendix B.

The modulus of elasticity, E_c , was estimated at 19.65 GPa (2,850 ksi) using the following equation from Section 5.4.2.4 of the ALBDS;

$$E_c = 33,000 K_1 w_c^{1.5} \sqrt{f'_c} \quad (4.1)$$

where,

K_1 = correction factor for source of aggregate to be taken as 1.0 unless determined by physical test, and as approved by the authority of jurisdiction

w_c = unit weight of concrete (kcf)

f'_c = compressive strength of concrete (ksi)

The modulus of rupture, f_r , was determined to be approximately 2.77 MPa (0.402 ksi) based on the following equation for lightweight concrete from Section C5.4.2.6 of the ALBDS and the average measured compressive strength;

$$f_r = 0.17\sqrt{f'_c} \quad (4.2)$$

4.1.2 *Prestressing Strands*

Fifteen prestressing strands approximately 0.9144 m (3 ft 0 in.) long were obtained from Girder #2 following the flexural test. The strands were tested in tension to failure with the maximum load being recorded. Figure 4.4 shows the typical test setup for the prestressing strands. The average ultimate stress in the strands was determined to be 1917 MPa (278 ksi). The average unit weight of the strands was calculated to be 5751 N/1,000 m (394 lb/1,000 ft). Calculations for the measured material properties of the prestressing strands are included in Appendix B.



Figure 4.4 Prestressing strand test setup

Based on the specifications for prestressing strands and the tested data, it was determined that the strands used for the original Icy Springs Bridge over the Weber River were Grade 1860 (270) seven-wire 1.11 cm (7/16 in.) diameter strands. Also, the prestressing strands are assumed to be stress relieved based on the age of the bridge and the available materials at the time of its construction.

From Article 5.4.4 of the ALBDS, the tensile strength of the prestressing strands, f_{pu} , was 1862 MPa (270 ksi), the yield strength, f_{py} , was $0.85f_{pu} = 1583$ MPa (229.5 ksi), and the modulus of elasticity, E_p , was 196.5 GPa (28,500 ksi).

4.1.3 Mild Steel

One 76 cm (30 in.) length of rebar taken from the deck of Girder #1 was tested in tension to determine the grade of mild steel used in the construction of the bridge. The strain and load relationship for the specimen was recorded as part of the test. The results of the test are shown in Figure 4.5. Figure 4.6 shows the specimen following the test. Based on the measured yield

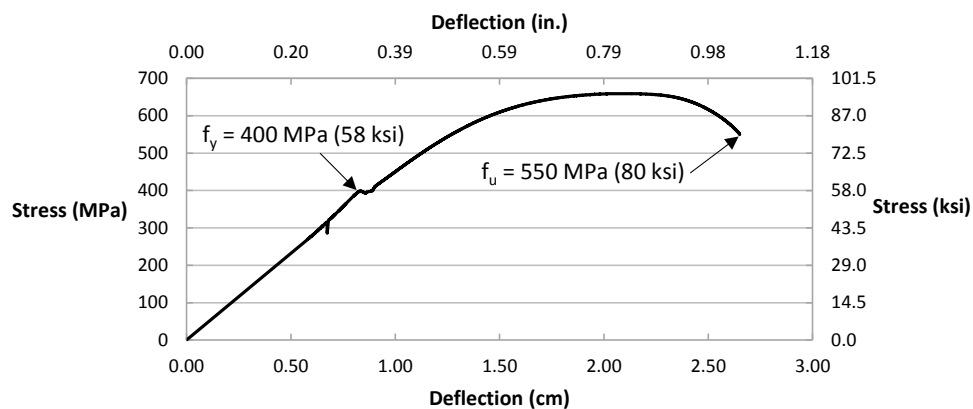


Figure 4.5 Mild steel stress vs. deflection curve

strength of the steel, it was determined that Grade 50 steel was used for the construction of the girders. The yield strength, f_y , of the steel for calculations was taken as 400 MPa (58 ksi) and the modulus of elasticity, E_s , of the mild steel was 200 GPa (29,000 ksi) from Article 5.4.3.2 of the ALBDS.

4.2 AASHTO LRFD Bridge Design Specifications Analysis and Comparison

The tested results from Chapter 3 were compared with calculated values from the 2012 AASHTO LRFD Bridge Design Specifications (AASHTO 2012). The AASHTO LRFD Bridge Design Specifications (ALBDS) is the current code used by the majority of state Departments of Transportation and local transportation agencies for the design of new bridges. Methods for calculating camber, prestressing losses, nominal moment capacity, deflection, shear capacities, and punching shear capacities are part of the design specifications. This section presents the comparisons between the values measured in the lab (experimental) and the predicted values (theoretical) using the ALBDS.

4.2.1 *Prestressing Losses*

Article 5.9.5.1 of the ALBDS states, “Values of prestress losses specified herein shall be applicable to normal weight concrete only and for specified concrete strengths up to 15.0 ksi, unless stated otherwise.” In addition, Article C5.9.5.1 regarding instantaneous losses states, “For segmental construction, lightweight concrete construction, multi-stage prestressing, and bridges where more exact evaluation of prestress losses is desired, calculations for loss of prestress should be made in accordance with a time-step method supported by proven research data. See references cited in Article C5.4.2.3.2.” Since the Icy Springs Bridge girders were fabricated using lightweight concrete, the refined method of estimating time-dependent losses outlined in Article 5.9.5.4 of the ALBDS and the recommendations for shrinkage and creep specified in Article 5.4.2.3 of the ALBDS were applied. Also, the recommendations for material properties

and strength analyses of lightweight concrete described in the NCHRP Report 733 High-Performance/High-Strength Lightweight Concrete for Bridge Girders and Decks (Section 2.9) were applied.

The total prestress losses (Δf_{pT}) are a combination of the short-term losses (Δf_{pEs}) and long-term losses (Δf_{pLT}) as shown in Equation 4.3 (AASHTO 2012).

$$\Delta f_{pT} = \Delta f_{pEs} + \Delta f_{pLT} \quad (4.3)$$

Two methods are recommended according to the procedures in the ALBDS to calculate the total prestress losses; the general method and the refined method. Both methods use the same elastic loss equation as defined in Equation 4.4 to calculate short-term losses. For long-term losses, the general method uses an approximate estimate, where individual components are grouped together, of time-dependent losses that requires the members be made of normal weight concrete. Therefore, the refined method, which uses a refined estimate of time-dependent losses as defined in Equation 4.5, has been used in this research.

$$\Delta f_{pEs} = \frac{A_{ps} f_{pbt} (I_g + e_m^2 A_g) - e_m M_g A_g}{A_{ps} (I_g + e_m^2 A_g) + \frac{A_g I_g E_{ci}}{E_p}} \quad (4.4)$$

where,

A_{ps} = area of prestressing steel (in.²)

f_{pbt} = stress in prestressing steel immediately prior to transfer (in.⁴)

I_g = moment of inertia of the gross concrete section (in.⁴)

e_m = average prestressing steel eccentricity at midspan (in.)

A_g = gross area of section (in.²)

M_g = midspan moment due to member self-weight (kip-in.)

E_{ci} = modulus of elasticity of concrete at transfer (ksi)

E_p = modulus of elasticity of prestressing tendons (ksi)

$$\Delta f_{pLT} = (\Delta f_{pSR} + \Delta f_{pCR} + \Delta f_{pR1})_{id} + (\Delta f_{pSD} + \Delta f_{pCD} + \Delta f_{pR2} - \Delta f_{pSS})_{af} \quad (4.5)$$

where,

Δf_{pSR} = prestress loss due to shrinkage of girder concrete between transfer and deck placement (ksi)

Δf_{pCR} = prestress loss due to creep of girder concrete between transfer and deck placement (ksi)

Δf_{pR1} = prestress loss due to relaxation of prestressing strands between time of transfer and deck placement (ksi)

Δf_{pSD} = prestress loss due to shrinkage of girder concrete between deck placement and final time (ksi)

Δf_{pCD} = prestress loss due to creep of girder concrete between deck placement and final time (ksi)

Δf_{pR2} = prestress loss due to relaxation of prestressing strands in composite section between time of deck placement and final time (ksi)

Δf_{pSS} = prestress gain due to shrinkage of deck in composite section (ksi)

Since the deck of the double-tee girders was cast monolithically with the webs, the latter half of Equation 4.5 was not applied and the time dependent variables were calculated based on the 48 year service life of the bridge. The NCHRP Report concluded, “The current AASHTO refined method for calculating prestress losses is appropriate for lightweight girders with lightweight decks.” Equations 4.6 through 4.15 are required to complete the calculation of the long-term prestressing losses. No adjustments to the equations were made for the use of

lightweight concrete. However, the material properties f'_c and E_c of the lightweight concrete were used, which differ from the material properties of normal weight concrete.

$$\Delta f_{pSR} = \varepsilon_{bid} E_p K_{id} \quad (4.6)$$

$$\varepsilon_{bid} = k_s k_{hs} k_f k_{td} 0.48 \times 10^{-3} \quad (4.7)$$

where,

$$k_s = 1.45 - 0.13 \left(\frac{V}{S} \right) \geq 1.0 \quad (4.8)$$

$$k_{hs} = 1.56 - 0.008H \quad (4.9)$$

$$k_f = \frac{5}{(1 + f'_{ci})} \quad (4.10)$$

$$k_{td} = \frac{t}{(61 - f'_c + t)} \quad (4.11)$$

$$K_{id} = \frac{1}{1 + \frac{E_p A_{ps}}{E_{ci} A_g} \left(1 + \frac{A_g e_{pg}^2}{I_g} \right) [1 + 0.7\psi_b(t_f, t_i)]} \quad (4.12)$$

where,

$$\psi_b(t_f, t_i) = 1.9 k_s k_{hc} k_f k_{td} t_i^{-0.118} \quad (4.13)$$

$$\Delta f_{pCR} = \frac{E_p}{E_{ci}} f_{cgp} \psi_b(t_d, t_i) K_{id} \quad (4.14)$$

$$\Delta f_{pR1} = \left[\frac{f_{pt}}{K'_L} \frac{\log(24t)}{\log(24t_i)} \left(\frac{f_{pt}}{f_{py}} - 0.55 \right) \right] \left[1 - \frac{3(\Delta f_{pSR} + \Delta f_{pCR})}{f_{pt}} \right] K_{id} \quad (4.15)$$

where,

f_{pt} is taken not less than $0.55f_{py}$.

The initial jacking stresses for the Icy Springs Bridge girders was unknown, therefore, the actual prestressing losses could not be calculated. However, the prestressing in the girders at the time of testing was measured as outlined in Section 3.4.1. Using the measured prestressing, the material properties from Section 4.1, and the equations relating to prestress losses from the ALBDS, the original jacking stresses for the girders can be estimated. Calculations of the estimated original jacking stresses for the three girders are provided in Appendix C with a

Table 4.1 Calculated prestressing loss summary

Girder #	Prestress % of f_{pu}	Initial Prestress, f_{pj} (MPa/ksi)	Prestress Loss, Δf_{pT} (MPa/ksi)	Remaining Prestress, f_{pe} (MPa/ksi)	% Loss
1	44%	819.1 / 118.80	212.1 / 30.76	607 / 88.04	25.9%
2	46%	856.33 / 124.20	217.01 / 31.47	639.32 / 92.73	25.3%
3	46%	856.33 / 124.20	217.01 / 31.47	639.32 / 92.73	25.3%

summary of the results included in Table 4.1.

It is evident from the prestressing loss summary that the jacking stress applied to the girders, $\approx 0.5f_{pu}$, was less than the usual jacking stress for girders made of normal weight concrete, $0.75f_{pu}$. There is not much difference in the calculated jacking stress and the effective prestress between the full deck analysis and the half deck analysis. One explanation for the lower jacking stress is the girder designers may have been concerned with the prestressing strands de-bonding from the lightweight concrete following release.

4.2.2 Moment Design

Two methods were used to calculate the nominal moment capacity (M_n) based on the ALBDS; the AASHTO approximate method and the strain compatibility method. The nominal moment capacity (M_n) of a concrete member for the AASHTO approximate method can be determined using the Equation 4.16. The resistance factor (ϕ) was not used for these calculations so a direct comparison with the measured results could be performed. The NCHRP report does not suggest modifying the ALBDS calculations for determining the flexural capacity of girders constructed of lightweight concrete. Also, the ALBDS allows the approximate method and strain compatibility methods to be used unmodified for determining the flexural capacities of lightweight concrete girders. Therefore, the ALBDS approximate method and strain compatibility method were used in this study unmodified.

$$M_n = A_{ps}f_{ps} \left(d_p - \frac{a}{2} \right) + A_s f_s \left(d_s - \frac{a}{2} \right) - A'_s f'_s \left(d'_s - \frac{a}{2} \right) + 0.85f'_c (b - b_w) h_f \left(\frac{a}{2} - \frac{h_f}{2} \right) \quad (4.16)$$

where,

A_{ps} = area of prestressing steel (in.²)

f_{ps} = specified tensile strength of prestressing steel (ksi)

d_p = distance from extreme compression fiber to the centroid of the prestressing tendons (in.)

a = depth of effective concrete compressive stress from top of compression block (in.)

A_s = area of mild steel tension reinforcement (in.²)

f_s = stress in mild tension steel at nominal flexural resistance (ksi)

d_s = distance from top of compression block to centroid of mild tensile steel (in.)

A'_s = area of compression reinforcement (in.²)

f'_s = stress in mild compression steel at nominal flexural resistance (ksi)

d'_s = distance from top of compression block to centroid of mild compression steel
(in.)

f'_c = specified compressive strength of concrete at 28 days (ksi)

b = width of the compression face of the member (in.)

b_w = width of web (in.)

h_f = depth of compression flange (in.)

A few of the variables used in Equation 4.16 require additional calculations. Equations 4.17 through 4.21 are used for these calculations.

$$a = \beta_1 c \quad (4.17)$$

where,

$$\beta_1 = 0.85 - 0.05(f'_c - 4) \geq 0.65, \text{ for all } f'_c > 4 \text{ ksi}$$

For rectangular section behavior:

$$c = \frac{A_{ps}f_{pu} + A_s f_s - A'_s f'_s}{0.85 f'_c \beta_1 b + K A_{ps} \frac{f_{pu}}{d_p}} \quad (4.18)$$

where,

f_{pu} = specified tensile strength of prestressing steel (ksi)

For T-section behavior:

$$c = \frac{A_{ps}f_{pu} + A_s f_s - A'_s f'_s - 0.85 f'_c (b - b_w) h_f}{0.85 f'_c \beta_1 b_w + K A_{ps} \frac{f_{pu}}{d_p}} \quad (4.19)$$

where,

$$K = 2(1.04 - \frac{f_{py}}{f_{pu}}) \quad (4.20)$$

$$f_{ps} = f_{pu}(1 - K \frac{c}{d_p}) \quad (4.21)$$

where,

f_{ps} = the average stress in prestressing steel (ksi)

The strain compatibility method is explained in Article 5.7.2 of the ALBDS with the calculations for this method being provided in Appendix C. During the ultimate moment capacity analysis, it became apparent the values being calculated were not conservative when compared with the tested values. Therefore, additional calculations were made using half the thickness of the flange to account for deck deterioration and to evaluate the effect of a reduced section. Complete calculations for the moment capacities of all girders based on full deck and half deck flange thicknesses are included in Appendix C. The results of the flexural analysis are shown in

Table 4.2 Calculated moment capacity summary

Table 4.2.

The approximate method and strain compatibility method yielded similar result for the

Full Deck				
Girder #	Approximate Method (kN-m/kip-ft)	Strain Compatibility (kN-m/kip-ft)	Measured Values (kN-m/kip-ft)	Difference (AM/SC)
1	2241 / 1,653	2182 / 1,609	1538 / 1,135	45.7% /41.8%
2	2261 / 1,667	2200 / 1,623	1681 / 1,240	34.5% /30.9%
3	2261 / 1,667	2200 / 1,623	1777 / 1,311	27.2% /23.8%
Half Deck				
Girder #	Approximate Method (kN-m/kip-ft)	Strain Compatibility (kN-m/kip-ft)	Measured Values (kN-m/kip-ft)	Difference (AM/SC)
1	1853 / 1,367	1873 / 1,381	1538 / 1,135	20.4% /21.7%
2	1927 / 1,421	1889 / 1,393	1681 / 1,240	14.6% /12.3%
3	1927 / 1,421	1889 / 1,393	1777 / 1,311	8.4% /6.3%

three girders. However, the calculated values for both the full deck thickness and half deck thickness are *not* conservative when compared with the measured values. This can be attributed to possible imperfections in the lightweight aggregate that could reduce the capacity of the concrete and the deterioration of the concrete deck, which would reduce the effective moment of inertia of the girders. Also, the use of sixteen prestressing strands with an initial prestress of $0.5f_{pu}$ in the fabrication of the girders increases the calculated capacity of the girders. Calculating the capacity of the girders using ten prestressing strands with an initial prestress of $0.75f_{pu}$ results in a flexural capacity of approximately 1,401 kN-m (1,033 kip-ft), which more closely matches the measured values.

Deflections at the ultimate loads for each girder were calculated based on the effective moment of inertia, I_e , (Equation 4.22) from Article 5.7.3.6 of the ALBDS and the simple beam deflection equation of two equal concentrated loads symmetrically placed from the AISC Steel Manual (Equation 4.24).

$$I_e = \left(\frac{M_{cr}}{M_a}\right)^3 I_g + \left[1 - \left(\frac{M_{cr}}{M_a}\right)^3\right] I_{cr} \leq I_g \quad (4.22)$$

in which,

$$M_{cr} = \left[\frac{P_e}{A_g} + \frac{P_e e y_t}{I_g} - f_r \right] \frac{I_g}{y_t} \quad (4.23)$$

where,

M_{cr} = cracking moment (kip-in.)

P_e = effective prestressing force (kips)

A_g = gross area of girder (in.²)

e = distance from neutral axis to centroid of prestressing steel (in.)

y_t = distance from the neutral axis to the extreme tension fiber (in.)

I_g = gross moment of inertia (in.⁴)

f_r = modulus of rupture of concrete (ksi)

M_a = maximum moment in a component at the stage for which deformation is computed (kip-in.)

I_{cr} = cracked moment of inertia (in.⁴)

$$\Delta_{max} = \frac{Pa}{24EI_e}(3L^2 - 4a^2) \quad (4.24)$$

where,

Δ_{max} = maximum deflection at midspan (in.)

P = half of the total applied load (kips)

a = distance from reaction to load (in.)

L = simply supported span (in.)

E = modulus of elasticity of the concrete (ksi)

I_e = effective moment of inertia (in.⁴)

The results of the deflection analysis and a comparison to the measured values are

Table 4.3 Calculated maximum deflection summary
included in Table 4.3.

The calculated deflections for Girders #2 and #3 were within approximately 5% of the

Girder #	Load (kN/kips)	Calculated Deflection (cm/in.)	Measured Deflection (cm/in.)	Difference (%)
1	403.45 / 90.7	21.24 / 8.36	25.58 / 10.07	-17.0%
2	443.93 / 99.8	23.31 / 9.18	24.31 / 9.57	-4.1%
3	484.41 / 108.9	25.74 / 10.13	27.05 / 10.65	-4.9%

measured deflections. However, the calculated deflection for Girder #1 was 17.0% less than the measured deflection. This could be a result of the more deteriorated deck of Girder #1 that caused a reduction in the effective moment of inertia. Also, the estimated modulus of elasticity of 19.65 GPa (2,850 ksi) used for the analysis could be high.

4.2.3 *Shear Design*

The shear analysis was calculated for the $2d_v$, $3d_v$, and $4d_v$ load spacing by following the simplified procedure for prestressed and non-prestressed sections outlined in Article 5.8.3.4.3 of the ALBDS. Also, the strut and tie procedure was applied for the $2d_v$ analysis as outlined in Article 5.6.3. According to the ALBDS, the strut and tie procedures are applicable when a point load is located within a distance of $2d$, where d is the depth from the top of the compression block to the centroid of the prestressing steel, from a support or discontinuity which will cause a nonlinear strain distribution (AASHTO 2012). When using lightweight aggregates, according to Article 5.8.2.2, the term $V(f'_c)$ shall be substituted with $0.75V(f'_c)$ in all calculations.

Equations 4.25 through 4.36 were used to calculate the nominal shear resistance using the simplified procedure. The nominal shear resistance (V_n) is the lesser value of Equations 4.25 and 4.26 and is a combination of the capacity due to tensile stresses in the concrete (V_c), tensile stresses in the transverse reinforcement (V_s), and the vertical component of the prestressing force (V_p). As with the moment design, no resistance factor (ϕ) was used for the shear calculations.

$$V_n = 0.25f'_c b_v d_v + V_p \quad (4.25)$$

$$V_n = V_c + V_s + V_p \quad (4.26)$$

where,

$$V_c = \text{lesser value of } V_{ci} \text{ and } V_{cw}$$

$$V_{ci} = 0.02(0.75\sqrt{f'_c})b_v d_v + V_d + \frac{V_i M_{cre}}{M_{max}} \geq 0.06(0.75\sqrt{f'_c})b_v d_v \quad (4.27)$$

where,

f'_c = specified compressive strength of concrete at 28 days (ksi)

b_v = effective web width taken as the minimum web width within the depth d_v (in.)

d_v = effective shear depth as determined in Article 5.8.2.9 and $> 0.9d_e$ or $0.72h$ (in.)

V_d = shear force at section due to unfactored dead load and includes both DC and DW
(kip)

V_i = factored shear force at section due to externally applied loads occurring
simultaneously with M_{max} (kip)

M_{cre} = moment causing flexural cracking at section due to externally applied loads
(kip-in)

M_{max} = maximum factored moment at section due to externally applied loads (kip-in)

$$M_{cre} = S_c(f_r + f_{cpe} - \frac{M_{dnc}}{S_{nc}}) \quad (4.28)$$

where,

S_c = section modulus for the extreme fiber of the composite section where tensile
stress is caused by externally applied loads (in.³)

f_r = modulus of rupture of concrete (ksi)

f_{cpe} = compressive stress in concrete due to effective prestress forces only (after
allowance for all prestress losses) at extreme fiber of section where tensile stress
is caused by externally applied loads (ksi)

M_{dnc} = total unfactored dead load moment acting on the monolithic or noncomposite section (kip-in)

S_{nc} = section modulus for the extreme fiber of the monolithic or noncomposite section where tensile stress is caused by externally applied loads (in.³)

$$S_c = \frac{I_c}{c_c} \quad (4.29)$$

where,

I_c = moment of inertia of composite section (in.⁴)

c_c = distance from bottom of girder to non-composite or girder neutral axis (in.)

$$f_{cpe} = \frac{P_e}{A_g} + \frac{P_e c_2 c_g}{I_g} \quad (4.30)$$

where,

P_e = effective prestressing force (kips)

A_g = gross area of section (in.²)

c_2 = distance between centroid of prestressing steel and girder neutral axis (in.)

c_g = distance between extreme tension fiber and girder neutral axis (in.)

I_g = moment of inertia of the gross concrete section about the centroidal axis (in.⁴)

$$M_{dnc} = \frac{W_d x}{2} (L - x) \quad (4.31)$$

where,

W_d = uniform distributed load due to dead weight of the girder (kip/in.)

x = distance from center of support to center of applied load (in.)

L = distance between center of supports (in.)

$$S_{nc} = \frac{I_g}{c_g} \quad (4.32)$$

$$V_{cw} = \left[0.06 \left(0.75\sqrt{f'_c} \right) + 0.30f_{pc} \right] b_v d_v + V_p \quad (4.33)$$

where,

f_{pc} = compressive stress in concrete (after allowance for all prestress losses) at centroid of cross section resisting externally applied loads or at junction of web and flange when the centroid lies within the flange (ksi)

$$f_{pc} = \frac{P_e}{A_g} + \frac{P_e e (c_c - c_g)}{I_g} + \frac{M_d (c_c - c_g)}{I_g} \quad (4.34)$$

$$V_s = \frac{A_v f_y d_v (\cot \theta + \cot \alpha) \sin \alpha}{s} \quad (4.35)$$

where,

A_v = area of transverse reinforcement within distance s (in.²)

f_y = specified minimum yield strength of reinforcing bars (ksi)

$\cot \theta = 1.0$ where $V_{ci} < V_{cw}$ or $1.0 + 3 \{ f_{pc} / [0.75\sqrt{f'_c}] \} \leq 1.8$ where $V_{ci} > V_{cw}$

α = angle of inclination of transverse reinforcement to longitudinal axis (degrees)

s = spacing of transverse reinforcement measured in a direction parallel to the longitudinal reinforcement (in.)

$$V_p = P_e \sin(\psi) \quad (4.36)$$

where,

ψ = angle of the harped prestressing strands from horizontal (degrees)

Table 4.4 summarizes the results of the simplified method analysis for both the full deck

Table 4.4 Simplified method analysis results

Full Deck						
Load-Sup. Spacing	V_p (kN/kips)	V_c (lesser of V_{ci} & V_{cw})		V_s (kN/kips)	V_n (lesser of V_{n1} & V_{n2})	
		V_{ci} (kN/kips)	V_{cw} (kN/kips)		V_{n1} ($0.25f_c b_v d_v + V_p$) (kN/kips)	V_{n2} ($V_c + V_s + V_p$) (kN/kips)
$2d_v$	42.68 / 9.59	644.98 / 145.00	313.33 / 70.44	168.85 / 37.96	1534.86 / 345.05	524.86 / 117.99
$3d_v$	42.68 / 9.59	510.59 / 114.79	310.85 / 69.88	168.85 / 37.96	1520.8 / 341.89	522.38 / 117.44
$4d_v$	42.68 / 9.59	457.82 / 102.92	308.37 / 69.32	168.85 / 37.96	1506.74 / 338.73	519.9 / 116.88
Half Deck						
Load-Sup. Spacing	V_p (kN/kips)	V_c (lesser of V_{ci} & V_{cw})		V_s (kN/kips)	V_n (lesser of V_{n1} & V_{n2})	
		V_{ci} (kN/kips)	V_{cw} (kN/kips)		V_{n1} ($0.25f_c b_v d_v + V_p$) (kN/kips)	V_{n2} ($V_c + V_s + V_p$) (kN/kips)
$2d_v$	44.96 / 10.11	531.89 / 119.57	360.2 / 80.98	162.48 / 36.53	1375.2 / 309.16	567.64 / 127.61
$3d_v$	44.96 / 10.11	426.66 / 95.92	357.34 / 80.33	162.48 / 36.53	1362.7 / 306.35	564.78 / 126.97
$4d_v$	44.96 / 10.11	386.98 / 87.00	354.47 / 79.69	162.48 / 36.53	1350.2 / 303.54	561.91 / 126.32

thickness and half deck thickness. In all cases, V_{cw} was less than V_{ci} and V_{n2} was less than V_{n1} .

The strut and tie procedure uses a nodal analysis as shown in Figure 4.7, which shows the supports, R1 and R2, at Nodes A and C and the location of the load being applied at Node B. The

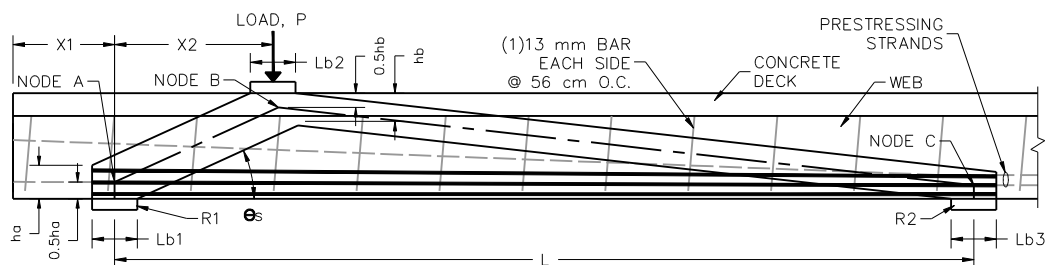


Figure 4.7 Strut and tie model

tie AC is at the centroid of the straight prestressing strands. The nodes are assigned a region type to determine the limits for the concrete compressive stress in each region. Node B is surrounded by two compressive struts and a bearing area, therefore, it is known as a (c-c-c) region. Nodes A and C are surrounded by one compressive strut, one bearing area, and one tension tie, therefore, they are known as (c-c-t) regions. Many different trusses may be used in a strut and tie analysis, which requires an iterative process to determine the most accurate model. In this analysis, the cracking of the concrete between Nodes A and B is the area of interest, so a simple truss, ABC, will accurately model the shear strength of the girder. The equations used in the strut and tie analysis are listed as Equations 4.37 through 4.47.

$$f_{ce} = \begin{cases} 0.75f'_c & \text{for } c - c - t \\ 0.85f'_c & \text{for } c - c - c \end{cases} \quad (4.37)$$

where,

f'_c = concrete compressive strength at each node (ksi)

f_{ce} = limiting concrete compressive stress for each nodal region type (ksi)

$$M_B = f_{ce} h_b t \left[h - c_p - \left(\frac{h_b}{2} \right) \right] \quad (4.38)$$

where,

M_B = moment applied to girder from point load P (kip-in.)

h_b = depth of nodal influence (in.)

t = width of node region (in.)

h = total height of girder (in.)

c_p = distance from bottom of girder to centroid of prestressing strands (in.)

$$\theta = \theta_1 + \theta_2 \quad (4.39)$$

where,

θ_1 = angle of Strut AB from horizontal (degrees)

θ_2 = angle of the harped prestressing strands from horizontal (degrees)

θ = total angle between Strut AB and the harped prestressing strands (degrees)

$$F_{AB} = \frac{R_A}{(\sin\theta_1 + \cos\theta_1 \tan\theta_2)} \quad (4.40)$$

where,

F_{AB} = force along Strut AB resulting from load P (kips)

R_A = upward force at Reaction A resulting from load P (kips)

$$F_{AC} = \frac{F_{AB}(\cos\theta_1)}{\cos\theta_2} \quad (4.41)$$

where,

F_{AC} = force along Tie AC resulting from load P (kips)

$$\epsilon_s = \frac{(F_{AC}/A_{ps})}{E_{ps}} - \epsilon_{ps} \quad (4.42)$$

where,

ϵ_s = tensile strain due to tension force in tie AC minus the prestressing strain

A_{ps} = area of the prestressing steel (in.²)

E_{ps} = modulus of elasticity of the prestressing steel (ksi)

ϵ_{ps} = effective prestressing strain

$$\varepsilon_1 = \varepsilon_s + (\varepsilon_s + 0.002)\cot^2\theta \quad (4.43)$$

where,

ε_1 = principal tensile strain in cracked concrete due to applied loads

$$f_{cu} = \frac{f'_c}{0.8 + 170\varepsilon_1} \leq 0.85f'_c \quad (4.44)$$

where,

f_{cu} = limiting concrete compressive stress (ksi)

$$P_n = f_{cu}A_{cs} \quad (4.45)$$

$$A_{cs} = [L_{b1}\sin\theta_1 + h_a\cos\theta_1]t \quad (4.46)$$

where,

P_n = limiting compressive force in strut AB (kips)

A_{cs} = cross-sectional area of strut AB perpendicular to the strut (in.²)

L_{b1} = width of bearing at Reaction 1 (in.)

$$V = P_n\sin\theta \quad (4.47)$$

where,

V = shear capacity or vertical component of P_n (kips)

Complete calculations of the simplified method and the strut and tie method of calculating shear capacity for full and half deck thicknesses are included in Appendix C with Table 4.5 showing a summary of the results.

Table 4.5 Calculated shear capacity summary

Full Deck					
Load-Sup. Spacing	Simplified Method (kN/kips)	Strut & Tie (kN/kips)	Measured Values (kN/kips)	Difference SM (%)	Difference S&T (%)
2d _v	524.86 / 117.99	1252.49 / 281.57	1401.41 / 315.05	-62.5%	-10.6%
3d _v	522.38 / 117.44	N/A	836.26 / 188.00	-37.5%	N/A
4d _v	519.9 / 116.88	N/A	811.35 / 182.40	-35.9%	N/A
Half Deck					
Load-Sup. Spacing	Simplified Method (kN/kips)	Strut & Tie (kN/kips)	Measured Values (kN/kips)	Difference SM (%)	Difference S&T (%)
2d _v	567.64 / 127.61	1227.97 / 276.06	1401.41 / 315.05	-59.5%	-12.4%
3d _v	564.78 / 126.97	N/A	836.26 / 188.00	-32.5%	N/A
4d _v	561.91 / 126.32	N/A	811.35 / 182.40	-30.7%	N/A

The simplified method underestimated the measured shear capacity of all three load spacings with the 2d_v capacity being underestimated by 62.5% for the full deck thickness and 59.5% for the half deck thickness. The 3d_v and 4d_v capacities were underestimated by 37.5% and 35.9% for the full deck thicknesses and 32.5% and 30.7% for the half deck thicknesses, respectively. The strut and tie method conservatively estimated the capacity of the 2d_v test very closely with a difference of only 10.6% for the full deck thickness and 12.4% for the half deck thickness.

When using the simplified method for calculating the shear capacity of a girder, the effective web width, b_v, is applied along the effective shear depth, d_v. The concrete available to resist shear is taken only as the area of concrete covered by b_v and d_v. The thickness of the deck, therefore, has minimal impact on the shear capacity of the girder, as shown in Table 4.4. In fact, the shear capacity of the half deck was calculated as being slightly greater than the shear capacity of the full deck due to the higher measured effective prestressing force used to calculate V_p in the half deck analysis and the lighter self-weight of the half deck girder.

4.2.4 Punching Shear Design

The double-tee girder webs of the Icy Springs Bridge were spaced 1.22 m (4 ft 0 in.) apart center-to-center. When a load is applied to the deck (flange) of the girders between the webs using the typical AASHTO tire contact area, the mode of failure of the deck is primarily punching shear, as witnessed in the experimental testing. The ALBDS equation for two-way action design, also known as punching shear, is shown as Equation 4.48. Three primary parameters used in this equation are; the concrete compressive strength, the depth of the concrete section, and the width of the concrete section. The width is based on an assumed failure plane at an angle of 45 degrees and is averaged from the top of the concrete to the bottom rebar centroid, d . The modification of the $\sqrt{f'_c}$ term to $0.75\sqrt{f'_c}$ used in Section 4.2.3 for lightweight concrete only applies to Articles 5.8.2 and 5.8.3 of the ALBDS, which cover beam shear. Therefore, no modification was made to the $\sqrt{f'_c}$ term for punching shear.

$$V_n = \left(0.063 + \frac{0.126}{\beta_c} \right) \sqrt{f'_c} b_o d_v \leq 0.126 \sqrt{f'_c} b_o d_v \quad (4.48)$$

where,

β_c = ratio of long side to short side of the rectangle through which the concentrated load or reaction force is transmitted.

f'_c = compressive strength of concrete (ksi)

b_o = perimeter of critical section (in.)

d_v = effective shear depth (in.)

V_n = nominal punching shear (kips)

To better compare the tested results with calculated results, an analysis was performed for the overall deck thicknesses of 10.2 cm (4 in.), 12.7 cm (5 in.), and 15.2 cm (6 in.). A summary

Deck Thickness, d (cm/in.)	Effective Shear Depth, d_v (cm/in.)	Punching Shear Capacity, V_n (kN/kips)	Avg. Measured Punch. Shear, V_u (kN/kips)	Difference (%)
15.24 / 6.0	12.7 / 5.0	663.16 / 149.09	657.22 / 147.75	0.90%
12.7 / 5.0	10.16 / 4.0	488.09 / 109.73	502.65 / 113.00	-2.90%
10.16 / 4.0	Table 4.6.3	Table 4.6.3	338.06 / 76.00	-1.13%

of the punching shear values calculated at these differing deck thicknesses is included as Table 4.6 with complete calculations included in Appendix C.

Using an effective shear depth equal to the deck thickness minus 2.56 cm (1 in.), the measured punching shear capacity is within 3% of the calculated shear capacity for the three deck thicknesses explored.

4.2.5 *Camber*

The final camber is a combination of the initial camber from prestress and the self-weight of the girder and the long-term, time-dependent prestress losses; creep and shrinkage. The initial theoretical camber was calculated using the material properties determined in Section 4.1 and the prestressing forces from the crack testing in Section 3.4.1. The improved multiplier method from the Precast/Prestressed Concrete Institute Bridge Design Manual (PCI 2011) was then applied to the initial camber to determine the time-dependent prestress losses. According to the NCHRP report regarding lightweight concrete girders, “The PCI improved multiplier method, used with the AASHTO creep and shrinkage model, provides reasonable estimates of camber at the time of erection, but not of camber growth after the composite deck is placed.” Since the Icy Springs Bridge girders were not fabricated using composite decks, the PCI multiplier method applies. Table 8.7.1-1 of the PCI Bridge Design Manual includes the multipliers applied to the elastic deflection due to member weight and prestress. For this study, the multipliers for the final time and girders fabricated without a composite topping were used. The multipliers used for elastic deflection due to member weight and prestress were 2.70 and 2.45, respectively. Complete calculations for theoretical camber are included in Appendix B with Table 4.7 showing a comparison of the calculated and measured camber values.

The differences between the measured camber and the calculated camber could be

Girder #	Measured Average Camber (cm/in.)	Calculated Camber (cm/in.)	Difference (%)
1	13.83 / 5.45	12.97 / 5.11	-6.2%
2	10.13 / 3.99	13.53 / 5.33	33.5%
3	10.97 / 4.32	13.53 / 5.33	23.3%

attributed to the deterioration of the deck, which reduced the amount of concrete and, therefore, the dead load acting on the section. Also, the actual relaxation of the strands and creep of the concrete throughout the life of the bridge may not be accurately estimated in the multipliers used to calculate long-term camber.

CHAPTER 5

FINITE ELEMENT MODELING

The finite element modeling of the Icy Springs Bridge girders was performed using the software program ANSYS, which was selected for its ability to model nonlinear behavior including the cracking and crushing of concrete. To replicate the span lengths and loadings used in the laboratory testing, a model depicting the 14.94 m (49 ft) span of the girders and a load spacing of 1.83 m (6 ft) was created in the finite element software to investigate the theoretical cracking and flexural capacities. The shear finite element analyses used half span models of the girders and the punching shear analyses was performed by modeling only the flange. The loads were applied to the half span models at the same $2d_v$, $3d_v$, and $4d_v$ locations as were tested. The load was positioned between the supports depicting the girder webs for the punching shear models. Appendix D contains the ANSYS input used for one of the full span model, one of the half span models, and one of the flange models. The input was created as a text file, then copied to ANSYS where the model was executed and output created for comparison to the tested data. Adjustments to the input were made to match the tested data as discussed further in this chapter.

5.1 Volumes

To initiate the modeling process in ANSYS, volumes were established. Volumes delineate the different portions of the prototype. For this research, the volumes consisted of the concrete girder (both the web and the flange), the steel reaction bearing pads, and the steel load bearing pads. To create a volume, the keypoints of the corners of the volumes are defined using an XYZ coordinate system. Eight keypoints must be defined for each volume. Adjacent volumes can share keypoints, if desired. Volumes are defined by selecting the eight keypoints that constitute an acceptable shape, which is defined for each element (ANSYS, Inc. 2009). Volumes may also be defined using the BLOCK command, where the XYZ coordinates of one corner and

the XYZ coordinates of the diagonal corner are input. The volumes used for this research were modeled as being connected with one another using a command in ANSYS known as gluing.

5.2 Materials

Once the volumes of the model are defined, a material type is defined for each volume. Material types have assigned properties and a material number for each individual application.

Table 5.1 ANSYS material numbers

Material #	Material
1	Concrete w/low modulus of rupture
2	Concrete w/high modulus of rupture
3	Prestressed strands
4	Mild reinforcing and steel plates

The material numbers and material used for this research are listed in Table 5.1.

The material properties used for the finite-element model were initially based on the measured values. To create a model that accurately reflected the data collected in the lab, the material properties were increased or decreased until the finite-element model output was similar to the measured values. The material properties for each material type are defined using tables and real constants.

5.3 Tables

Tables were used to ensure a certain material behaves as intended and are predefined in the software. Two different types of tables were used in this research; a concrete table and a biso table. The concrete table contains user defined material properties, such as compressive and tensile strengths. The biso table is used for materials with two separate slopes (bilinear) in a stress-strain diagram, such as steel. Prior to yielding, steel behaves in a linear elastic manor and

after yielding it becomes nonlinear. The biso table allows the material to yield, then continue to the ultimate strength of the material.

5.4 Real Constants

Real constants are used for defining properties that are not defined in the material tables and are specific to the element type. For example, real constants can be used to define the percentage of smeared bars oriented with respect to the girder longitudinal axis, cross sectional areas of prestressing strands, and the initial strain in a prestressing strand. The real constants used for the steel plates in this research do not contain information used in the model, but are needed to complete the analysis. A series of real constants were used to define the prestressing strands. One real constant was used at the ends of the girders to define a low initial strain. Subsequent real constants were used to increase the initial strain along 41 cm (16 in.) increments until the full initial strain was reached approximately 163 cm (64 in.) from the ends of the girders. This was done to model a gradual increase in strand stress over the transfer length and to prevent failure of the concrete at the ends of the girders due to the full initial prestress being greater than the compressive strength of the modeled concrete.

5.5 Element Types

ANSYS supplies many different types of elements that are used to model various structural elements. For this research, the SOLID65 element was used to model concrete, the LINK8 element was used for the prestressing strands, and the SOLID45 element was used for the steel plates.

Figure 5.1 shows the geometry of the SOLID65 element, which has the ability to replicate cracking in tension, crushing in compression, and nonlinear behavior through failure. Also, the SOLID65 element can model internal discrete pieces of rebar as a smeared mesh. These attributes make the SOLID65 element ideal for modeling nonlinear, reinforced concrete.

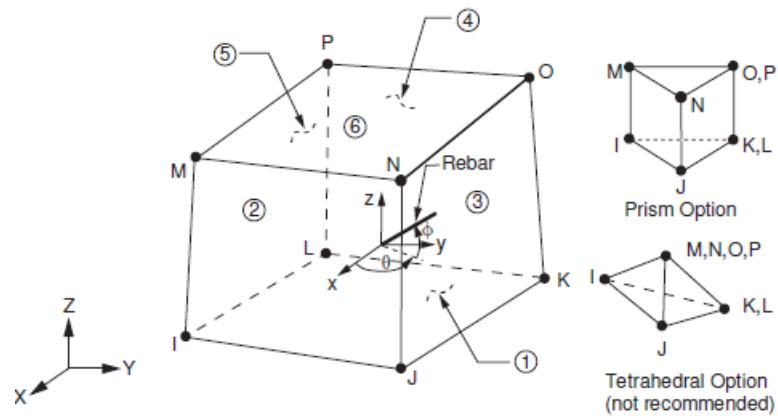
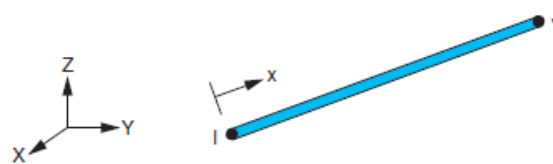


Figure 5.1 SOLID45 & SOLID65 geometric shapes (ANSYS, Inc. 2009)

The LINK8 element is used to model tension and compressive forces and can be assigned an initial strain and cross sectional area, which makes it ideal for modeling prestressing strands. Figure 5.2 shows the LINK8 element geometry. The keypoints for the LINK8 element are defined by cutting the volumes along the alignments of the prestressing strands and assigning the element to the resulting line.



element to the resulting line.

The SOLID45 element is capable of modeling plastic behavior, stress stiffening, and large strains, which makes it a great candidate for modeling solid steel sections. The geometry of the SOLID45 element is defined similarly to the SOLID65 element.

Figure 5.2 LINK8 geometric shape (ANSYS, Inc. 2009)

5.6 Element Size and Boundary Conditions

The next step in the modeling process is to mesh all volumes and the lines used for the prestressing strands and assign a material, real constant, and element type to each volume and line. Meshing is the process by which ANSYS generates finite elements from the volumes and lines. The size of a finite element cube is defined using one number, the dimension of one side of the cube. Since irregular shapes occur during the meshing process, not all finite elements will have the exact same size. If the resulting element sizes are too large or too small, errors will be formulated by ANSYS during meshing. Therefore, different models will not always have the same element size. For this research, a finite element size of 51 mm (2 in.) was used.

Once the model is meshed, the boundary conditions of the model can be assigned. Boundary conditions define the support conditions and the applied loads. A roller was assigned to support one side of the girders and a pin and roller were assigned to the other side. The load bearing plates were used to distribute the load on the girder.

5.7 Executing an Analysis

After the elements are discretized and the boundary conditions are applied, the model can be analyzed. The load is applied to the model using incremental time steps by user-defined or program default values. The time steps used for this research are single integers, where the number 1 is the first full time step, 2 is the second, and 3 is the third. Each integer indicates the full load defined for that particular time step is applied to the model. For example, if the first time step is associated with a load of 100 kips, time step 0.5 means 50 kips is applied to the model. In addition, if the first time step is 100 kips and the second time step is associated with a decrease in load to 20 kips, time step 1.5 means 60 kips is applied to the model. ANSYS increases or decreases the load based on the convergence of the previous time step and will terminate prior to the full load being applied if any member in the structure fails. Predefined

loads higher than the tested maximum loads were applied to each model to ensure the girders failed in the model.

5.8 ANSYS Models

Finite-element models were created for each of the laboratory test configurations. The models used for the flexural finite element analysis consisted of the full span of the girders, while the shear models used the half span of the girders and the punching shear models used only the flange of the girders. The ANSYS codes used for the flexural, shear, and punching shear models are included in Appendix D. The location and magnitude of the loading and the bearing locations were altered to match the experimental setup of each test. Changes to the concrete material properties were then applied until a match between the results of the finite element modeling and the experimental results of the laboratory testing was made. The material properties for the prestressing strands and mild steel were in all cases kept constant.

Three criteria checks for the flexural and shear modeling were performed to confirm the results of the model matched those of the testing. First, the cracking scheme and mode of failure had to be similar. Secondly, the ultimate capacities must be close. And lastly, the deflection plots had to match. For each deflection plot, the R^2 value and the mean difference value were determined using Equations 5.1 and 5.2, respectively. An R^2 value close to 1.0 indicates a close correlation between the two separate sets of data at intervals of deflection. The mean difference is an indication of how closely related the two sets of data are overall.

$$R^2 = \frac{cov(M_{Model}M_{Experimental})}{\sigma(M_{Model})\sigma(M_{Experimental})} \quad (5.1)$$

where,

cov = covariance of two lists of data

M_{model} = moment or shear values from the finite element model

$M_{\text{Experimental}}$ = moment or shear values from experimental data

σ = standard deviation of selected data

$$\text{Mean Diff.} = \frac{\Sigma(M_{\text{Experimental}} - M_{\text{Model}})}{n} \quad (5.2)$$

where,

n = number of data points

The ultimate capacities from the punching shear models were compared directly to the ultimate capacities measured in the lab. The following sections describe each finite element model used and the results of each analysis.

5.8.1 Flexural Models

Three flexural models were created, one for each of the three flexural tests. The flexural model for Girder #1 was used to calibrate the geometry and prestressing properties for the subsequent models. In order to match the experimental results and the deteriorated deck for

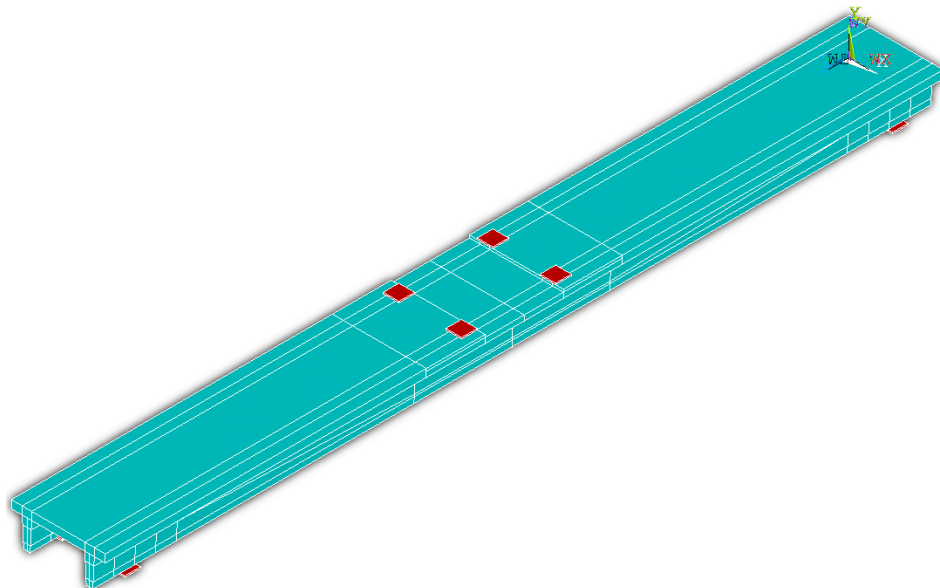


Figure 5.3 Girder #1 flexural finite element model

Girder #1 the flange thickness between the point loads above the webs was reduced to 10.2 cm (4 in.), as shown in Figure 5.3. The remainder of the flange for Girder #1 was modeled as 15.2 cm (6 in.) thick. Since the decks of Girders #2 and #3 were not as deteriorated as Girder #1, the entire flanges for Girders #2 and #3 were modeled as 15.2 cm (6 in.) thick. Figure 5.3 also shows the loading and support configurations used in the models. A roller was assigned to the left support and a pin was assigned to the right support. The support spacing was consistent for the three models, but the load spacing for Girders #1 and #2 was 1.83 m (6 ft.) and for Girder #3 the load spacing was 2.13 m (7 ft.). From previous analyses it is apparent the girders had been cracked prior to the ultimate capacity testing being performed. Therefore, the flexural models included a load-unload-load cycle to initially crack the modeled girders using a 133.4 kN (30 kip) initial load. The load was fully removed, then the load to failure applied. The results of the Girder #1 model are shown in Figure 5.4, where the cracked area is indicated by the reduction in stiffness of the girder on the reload portion of the load vs. deflection plot. The measured cracking load was 114.6 kN (25.76 kips), which compares quite well with the modeled cracking load in

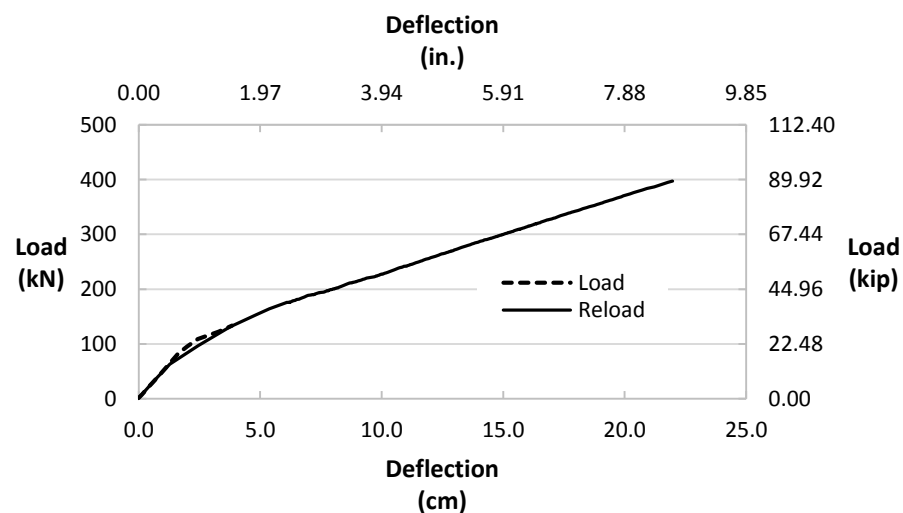


Figure 5.4 Girder #1 flexural model load vs. deflection

Figure 5.4. The load vs. deflection plots for Girders #2 and #3 are included in Appendix D. To match the stiffness of the tested girders, two regions of concrete were modeled where the modulus of rupture, f_{rc} , was different. The first region of concrete is directly below the straight prestressing strands between the load points along the girder and was assigned an f_{rc} equal to 2.8 MPa (0.4 ksi). This region was used to match the pre-cracked stiffness of the girders. The

second region covered the remainder of the concrete and was assigned an f_{rc} equal to 5.5 MPa (0.8 ksi). This region was used to match the post-cracked stiffness of the girders. Using an f_{rc} equal to 2.8 MPa (0.4 ksi) for the entire girder resulted in a post-cracked stiffness significantly less than was experienced in the lab. Figure 5.5 shows the comparison of the experimental cracking and the modeled cracking for Girder #1. In general, the predicted analytical cracking

matches experimental behavior well. Figure 5.6 shows the moment vs. deflection relationships for the measured and modeled data for the Girder #1 flexural test. The overall shapes of the lines correspond well and the ultimate capacities are within 2.0% of each other. Moment vs. deflection comparison plots for Girders #2 and #3 are included in Appendix D. Table 5.2 summarizes the results of the flexural finite element modeling for each girder and compares them with the

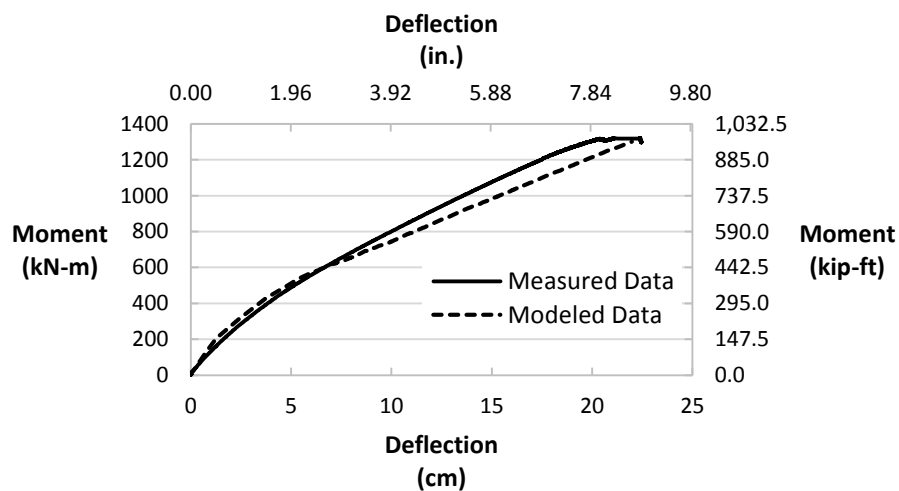


Figure 5.5 Girder #1 tested vs. modeled flexural cracking

experimental testing data using the percent difference in the ultimate capacity, the R^2 value, and the mean difference. The f_{rc2}

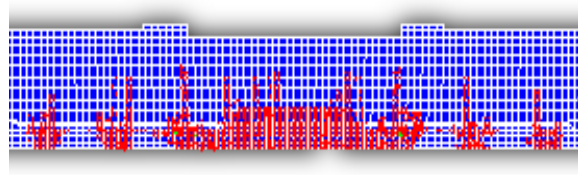


Figure 5.6 Girder #1 flexural moment vs. deflection comparison

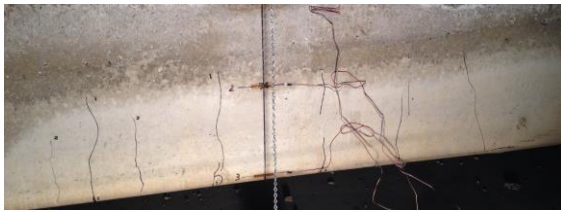


Table 5.2 Flexural modeling summary

value for Girder #3 was required to be 11.0 MPa (1.6 ksi) to match the measured stiffness of the girder.

Gir. #	f'_c (MPa/ksi)	f_{rc2} (MPa/ksi)	E_c (GPa/ksi)	Modeled Ultimate Capacity (kN-m/kip-ft)	Measured Ultimate Capacity (kN-m/kip-ft)	Diff. (%)	Statistical Analysis	
	Measured	Measured	Measured				R^2	Mean Diff. (kN-m/kip-ft)
1 ¹	34.5 / 5.0	5.5 / 0.8	16.5 / 2,400	1300.9 / 959.5	1321.9 / 975.0	-1.6%	0.97	41.5 / 30.6
2 ²	34.5 / 5.0	5.5 / 0.8	16.5 / 2,400	1476.5 / 1089.0	1454.6 / 1072.9	1.5%	0.96	60.6 / 44.7
3 ²	34.5 / 5.0	11 / 1.6	16.5 / 2,400	1581.6 / 1166.5	1550.3 / 1143.5	2.0%	0.97	73.9 / 54.5

- Notes:
- Girder #1 deck was modeled as 10.2 cm (4 in.) thick between load points to match deck deterioration.
 - Girders #2 and #3 decks were modeled as 15.2 cm (6 in.) thick throughout.
 - f_{rc1} is 2.8 MPa (0.4 ksi) for measured and modeled.

5.8.2 Shear Models

Finite-element models of the three shear test configurations ($2d_v$, $3d_v$, and $4d_v$) were created based on the tested material properties. Modifications were made to the concrete material properties in the analytical models to match the experimental data. The $2d_v$ test from Girder #1,

the $3d_v$ test from Girder #2, and the $4d_v$ test from Girder #3 were used to make the comparisons.

Figure 5.7 shows the model used for the $2d_v$ setup. The uniform load, indicated by the strip

across the deck in the isometric view and the downward facing arrows in the side view, was

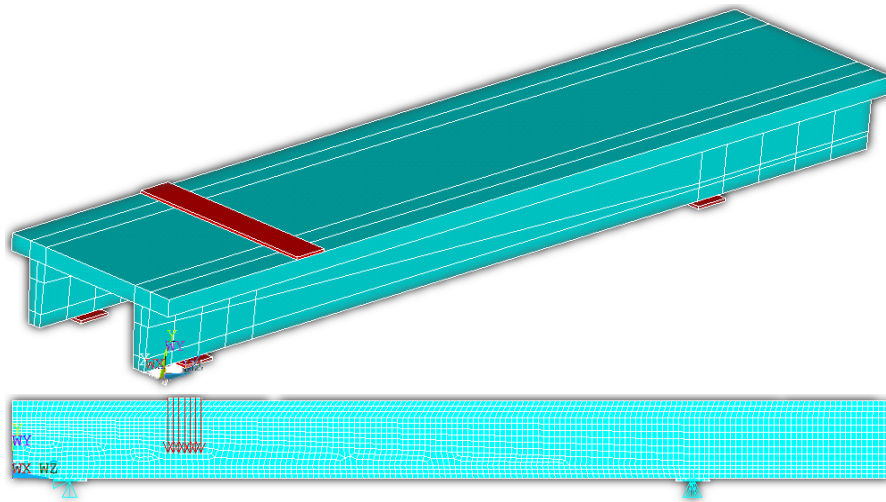


Figure 5.7 Girder #1 2d_v finite element model

positioned away from the near support in 53.3 cm (21 in.) increments from the 2d_v model for the

3d_v and 4d_v models. A pin was assigned to the support nearest the uniform load and a roller was assigned to the other support. As with the flexural models, a load-unload-load cycle was incorporated to mimic the forcing experienced by the girders throughout their life. The shear vs. deflection comparison plot for the Girder #1 2d_v model using the same material properties as the flexural analyses is shown in Figure 5.8. The modeled data did not correlate well with the measured data using the flexural model material properties. Therefore, the compressive strength, f'_c , and the modulus of rupture, f_{rc} , of the concrete was modified in the models to better match the experimental results. Figure 5.9 shows the modeled data resulting from modifying the material

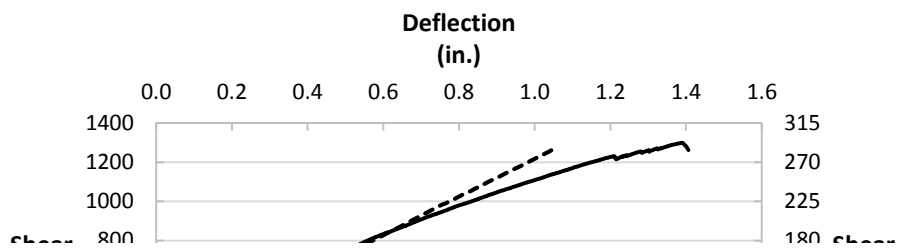
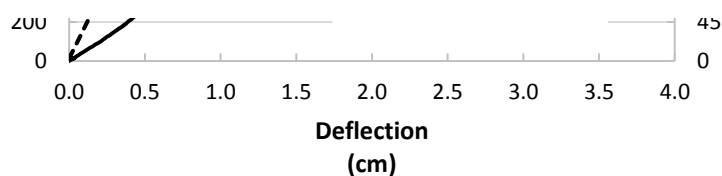


Figure 5.8 Girder #1 2d_v shear vs. deflection comparison (flexural concrete properties)



properties of the concrete. The shear vs. deflection comparison plots using modified material properties to match the experimental values for the 3d_v and 4d_v models are included in Appendix D. The results of the 2d_v model match closely against the tested values with the ultimate capacities within 2.2% of each other. Figure 5.10 shows the crack behavior post-testing compared well with the cracks in the predicted finite-element model for the Girder #1 2d_v configuration. A summary of the three shear models is included as Table 5.3. The properties of f'_c needed to be adjusted for each model to match the tested capacities of each test. Keeping f'_c at

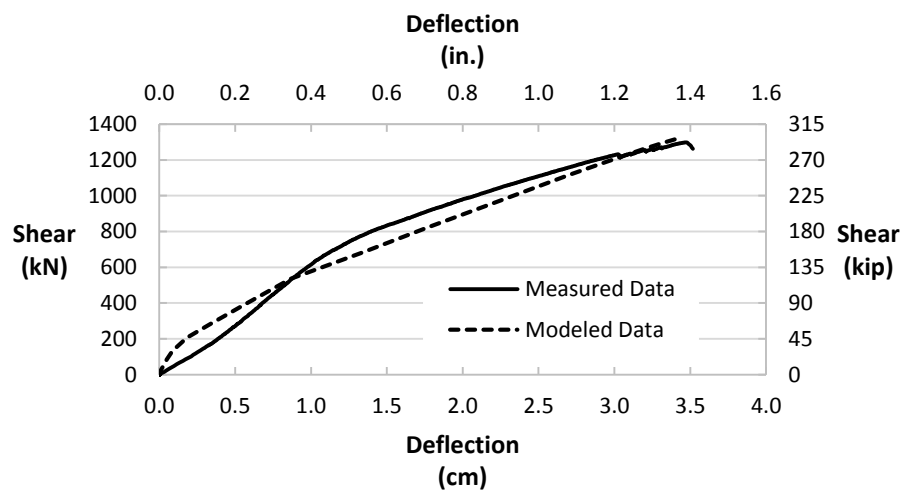


Figure 5.9 Girder #1 2d_v shear vs. deflection comparison (modified concrete properties)

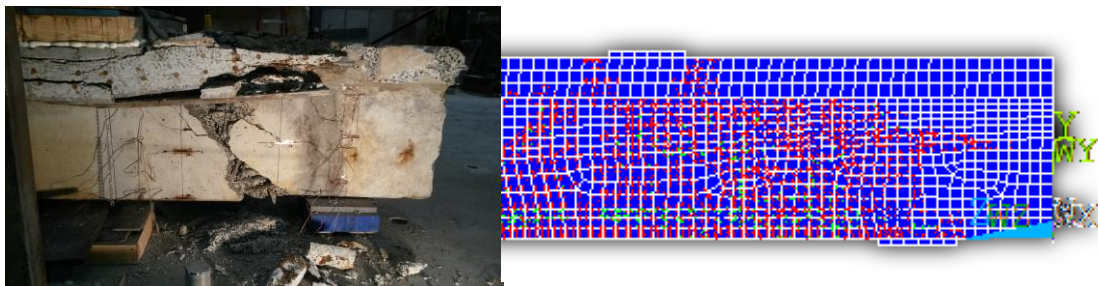


Figure 5.10 Girder #1 2d_v crack comparison

38.6 MPa (5.6 ksi), the value measured, resulted in a much lower modeled capacity when compared with the tested capacities. Also, f_{rc} was adjusted to match the overall shape (stiffness) of the shear vs. deflection plot.

The samples of concrete used for material properties testing were taken from the midspan portion of the girders near the top of the web. This was done since some prestressing strands were harped and prevented a sample from being taken at the ends of the girders. In addition, as a result of the girders being cracked near their mid-spans prior to removal from the bridge, the

Table 5.3 Shear modeling summary

Gir. #	Model Type	f'_c	f_{rc2}	E_c	Modeled Ultimate Capacity (kN/kips)	Measured Ultimate Capacity (kN/kips)	Diff. (%)	Statistical Analysis	
		(MPa/ksi) Measured	(MPa/ksi) Measured	(GPa/ksi) Measured				R^2	Mean Diff. (kN/kips)
1 ²	2d _v	74.5 / 10.8	5.5 / 0.8	16.5 / 2,400	1319.8 / 296.7	1298.9 / 292.0	1.6%	0.97	20.77 / 4.67
2 ²	3d _v	67.6 / 9.8	11 / 1.6	16.5 / 2,400	1013.7 / 227.9	1036.9 / 233.1	-2.2%	0.98	36.34 / 8.17
3 ¹	4d _v	62.1 / 9.0	21.4 / 3.1	16.5 / 2,400	884.3 / 198.8	891.4 / 200.4	-0.8%	0.98	43.9 / 9.87

Notes: 1. A 20.3 cm (8 in.) thick deck was used between near support and load to match test specimen.

2. A 15.2 cm (6 in.) thick deck was used throughout for Girders #1 & #2.

3. f_{rc1} is 2.8 MPa (0.4 ksi) for measured and modeled.

concrete at the ends could have had slightly different material properties than the concrete closer to the mid-spans of the girders. These observations may explain the discrepancies in the material properties. Also, it has been observed that ANSYS may not accurately model the compressive strut between the applied load and the support nearest the node. Therefore, the modeled results using the tested material properties could be slightly inaccurate.

Another observation to note is the 3d_v and 4d_v shear models exhibited differential deflection between the two webs of the girders resulting from the uniform loading as discussed in Section 3.4.3. The modeled deflection from the webs with the higher deflection were compared to the tested deflections of the corresponding webs for both test configurations. These are the values reported in Table 5.3.

5.8.3 *Punching Shear Models*

Three finite element models, using the tested material capacities for concrete and mild steel, were created to compare with the experimental punching shear testing results. Deck thicknesses of 10.2 cm (4 in.), 12.7 cm (5 in.), and 15.2 cm (6 in.) were modeled using an effective deck thickness of 2.53 cm (1 in.) less than the actual deck thicknesses to account for the ineffective thickness below the bottom layer of reinforcement. The steel reinforcement in the deck was smeared in the element used for concrete, rather than being discretely modeled. Figure 5.11 shows a three-dimensional view of a typical punching shear model result and the associated



Figure 5.11 Punching shear 3D view

cracking of the concrete in the model.

Table 5.4 summarizes the results of the punching shear modeling and compares the

Table 5.4 Punching shear modeling summary

modeled results with the tested data. The modeled ultimate capacities for all three deck thicknesses match within 8.4% of the ultimate capacities determined by the lab testing. A value of 16.5 MPa (2,400 ksi) was used for the modulus of elasticity of the concrete, E_c , for each punching shear model to match the E_c values used in the flexural and shear models.

Deck	f'_c (Mpa/ksi)	f_{rc} (Mpa/ksi)	E_c (GPa/ksi)	f_y (MPa/ksi)	Modeled Ultimate Capacity (kN/kips)	Measured Ultimate Capacity (kN/kips)	Diff. (%)
Thickness (cm/in)	Measured	Measured	Measured	Measured			
15.2 / 6.0	38.6 / 5.6	2.8 / 0.4	16.5 / 2,400	399.9 / 58.0	693.2 / 155.8	657.2 / 147.8	5.47%
12.7 / 5.0	38.6 / 5.6	2.8 / 0.4	16.5 / 2,400	399.9 / 58.0	460.5 / 103.5	502.6 / 113.0	-8.38%
10.2 / 4.0	38.6 / 5.6	2.8 / 0.4	16.5 / 2,400	399.9 / 58.0	350.7 / 78.9	338.1 / 76.0	3.75%

CHAPTER 6

CONCLUSIONS

Three prestressed concrete double-tee girders were salvaged from the replacement of the Icy Springs Bridge located on 2nd South Street west of Interstate 80 in Coalville, Utah and were experimentally tested for failure in flexure, shear, and punching shear. The results of the testing were compared with the theoretical values based on procedures recommended in the 2012 AASHTO LRFD Bridge Design Specifications (ALBDS) and predicted behavior using finite-element models. A bulleted summary of the results is provided below:

1. Material Properties

a. Concrete

- i. The concrete used in the construction of the girders was made of lightweight aggregate with a total unit weight, w_c , of 17 kN/m³ (110 lb/ft³) and a tested compressive strength, f'_c , of 38.6 MPa (5.6 ksi). A value of 38.6 MPa (5.6 ksi) for f'_c was used for all ALBDS calculations, with f'_c ranging from 34.5 MPa (5.0 ksi) to 74.5 MPa (10.8 ksi) for the finite-element modeling.
- ii. A modulus of elasticity, E_c , of 19.65 GPa (2,850 ksi) was used for the ALBDS calculations and 16.5 GPa (2,400 ksi) for the finite element modeling. A lower E_c was used for the finite element model to account for the likely higher moment of inertia, I , of the model when compared with the test specimens for the deflection comparisons.
- iii. A modulus of rupture, f_{rc} , of 2.77 MPa (0.40 ksi) was used in the ALBDS calculations. The value of f_{rc} ranged from 2.77 MPa (0.40 ksi) to 21.4 MPa (3.1 ksi) in the finite-element models to match the experimental cracking and deflection results.

b. Prestressing Strands

- i. The prestressing strands in the girders were experimentally determined to be Grade 270K seven-wire 1.11 cm (7/16 in.) diameter stress relieved strands with a modulus of elasticity, E_p , of 196.5 GPa (28,500 ksi).

c. Mild Steel

- i. The yield strength, f_y , of the mild steel was experimentally determined to be 400 MPa (58 ksi) with a modulus of elasticity, E_s , of 200 GPa (29,000 ksi).

2. Prestressing Losses

- a. It is believed that the initial prestressing used in the lightweight concrete girders was approximately 50% of the ultimate strength of the prestressing strands, $0.5f_{pu}$, which is 33% less than the $0.75f_{pu}$ usually used to prestress normal weight concrete.
- b. The refined method of estimating time-dependent losses was used with no modifications for lightweight concrete.
- c. The ALBDS refined method for estimating prestressing losses calculated the total prestressing losses in the girders to be approximately 25% using a jacking stress equal to $0.5f_{pu}$.

3. Flexural Results

- a. The ALBDS does not specify modifications to the methods used for flexural capacity and deflection in the use of lightweight concrete, therefore, no modifications to the equations used were made.
- b. The ALBDS approximate method estimated the flexural capacity to be between 27.2% and 45.7% more than the measured values for a full deck thickness and between 8.4% and 20.4% for a half deck thickness, all non-conservative.

- c. The ALBDS strain compatibility method estimated the flexural capacity to be between 23.8% and 41.8% more than the measured values for a full deck thickness and between 6.3% and 21.7% for a half deck thickness, all non-conservative.
 - d. The calculated deflection for Girder #1 was 17.0% less than the measured deflection and was 4.1% and 4.9% less for Girders #2 and #3, respectively.
4. Shear-Flexure Results (3d_v & 4d_v)
- a. To follow the recommendations of the ALBDS, the term $\sqrt{f'_c}$ was replaced by $0.75\sqrt{f'_c}$ in all equations for shear capacity.
 - b. The ALBDS simplified method for full-decked 3d_v and 4d_v configurations conservatively estimated the shear capacities to be 37.5% and 35.9% lower than the tested capacities, respectively.
 - c. The ALBDS simplified method for half-decked 3d_v and 4d_v configurations conservatively estimated the shear capacities to be 30.7% and 32.5% lower than the tested capacities, respectively.
5. Shear Results (2d_v)
- a. To follow the recommendations of the ALBDS, the term $\sqrt{f'_c}$ was replaced by $0.75\sqrt{f'_c}$ in all equations for shear capacity.
 - b. The ALBDS simplified method for full-decked and half-decked 2d_v configurations conservatively estimated the shear capacities to be 62.5% and 59.5% lower than the tested capacities, respectively.
 - c. The strut and tie method for full-decked and half-decked 2d_v configurations conservatively estimated the shear capacities to be 10.6% and 12.4% lower than the tested capacities, respectively.
6. Punching Shear Results

- a. The punching shear calculations were performed with no modifications to the equations for lightweight concrete.
- b. The calculated ALBDS two-way (punching shear) capacities for the following deck thicknesses; 15.24 cm (6.0 in.), 12.7 cm (5.0 in.), and 10.16 cm (4.0 in.), differed from the measured punching shear capacities by 0.9%, -2.9%, and -1.1%, respectively.

REFERENCES

- AASHTO. (2012). *LRFD Bridge Design Specifications*. 6th ed. American Association of State Highway and Transportation Officials, Washington, D.C.
- AISC. (1998). *Load & resistance factor design: Manual of steel construction*. 2nd ed. American Institute of Steel Construction, Chicago.
- ANSYS, Inc. (2009). *Element reference*. ANSYS, Canonsburg, Pa.
- Cousins, T., Roberts-Wollmann, C., and Brown, M. (2013). *High-Performance/High-Strength Lightweight Concrete for Bridge Girders and Decks*. NCHRP Report 733. Transportation Research Board, Washington, D.C.
- Eder, R., Miller, R., Baseheart, T., and Swanson, J. (2005). "Testing of two 50-year-old precast post-tensioned concrete bridge girders." *PCI J.*, 50(3), 90-95.
- Grace, N., Abdel-Sayed, G., Navarre, F., Nacey, R., Bonus, W., and Collavino, L. (2003). "Full-scale test of prestressed double-tee beam." *Concrete Intl.*, 25(4), 52-58.
- Kahn, L., and Lopez, M. (2005). "Prestress losses in high performance lightweight concrete pretensioned bridge girders." *PCI J.*, 50(5), 84-94.
- Lundqvist, P., and Riihimäki, J. (2010). "Testing of five 30-year-old prestressed concrete beams." *PCI Journal*, 46-58.
- Maguire, M., Morcous, G., and Tadros, M. (2012). "Structural performance of precast/prestressed bridge double-tee girders made of high-strength concrete, welded wire reinforcement, and 18-mm-diameter strands." *J. of Bridge Engrg.*, 18(10), 1053-1061.
- Meyer, K., and Kahn, L. (2002). "Lightweight concrete reduces weight and increases span length of pretensioned concrete bridge girders." *PCI J.*, 47(1), 68-75.
- Nawy, E. (2006). *Prestressed concrete*. 5th ed. Prentice Hall, Upper Saddle River, N.J.
- Nilson, A. (1987). *Design of prestressed concrete*. 2nd ed. Wiley, New York.
- Pessiki, S., Kaczinski, M., and Wescott, H. (1996). "Evaluation of effective prestress force in 28-year-old prestressed concrete bridge beams." *PCI J.*, 41(6), 78-89.
- PCI. (2011). "Precast prestressed concrete bridge design manual." 3rd ed. Precast Prestressed Concrete Institute, Chicago.
- Rosenboom, O., Carneiro, R., Hassan, T., Mirmiran, A., and Rizkalla, S. (2006). "Static behavior of 40 year-old prestressed concrete bridge girders strengthened with various FRP systems." North Carolina State University, Raleigh, N.C.

Svirsky, A. (2014). "The national bridge inventory database." <<http://nationalbridges.com>> (July 29, 2014).

Wilden, H. (2010). *PCI design handbook: Precast and prestressed concrete*. 7th ed. Precast/Prestressed Concrete Institute, Chicago.

APPENDICES

APPENDIX A. GIRDER PHYSICAL PROPERTIES

Icy Springs Bridge Girders - Preliminary Cross Sectional Beam Properties Calculations

Note: Shaded cells input by user.

$f'_c = 4$ ksi	$K = 0.28$ (low relaxation strands)	$A_{ps} = 0.085$ in. ² (single strand)
$E_c = 3,000$ ksi	$\bar{y} = 19.92$ in. (from bottom of girder)	# of top strands = 12
$f_{pu} = 270$ ksi	$I_g = 20,609.85$ in. ⁴	# of bottom strands = 4
$E_{ps} = 28,500$ ksi	$A'_s = 0.31$ in. ² (single #5 bar)	$A_{pst} = 1.020$ in. ² (top strands)
$f'_y = 60$ ksi	bar spacing = 12 in.	$A_{psb} = 0.340$ in. ² (bottom strands)
$E_s = 29,000$ ksi	$A'_s = 0.31$ in. ² (area of steel in deck)	$\beta_1 = 0.85 - 0.05[f'_c - 4] = 0.85 \geq 0.65$

Flange Dimensions	Web Dimensions
$b = 36.00$ in.	$b_{w1} = 7.00$ in.
$h_f = 6.00$ in.	$b_{w2} = 5.00$ in.
	$h_w = 22.00$ in.

AT END OF GIRDER

$$d_{pt} = 12.375 \text{ in. (top of girder to middle of top strands)}$$

$$d_{pb} = 23.375 \text{ in. (top of girder to middle of bottom strands)}$$

$$d_e = [A_{pst}d_{et} + A_{psb}d_{eb}]/[A_{pst} + A_{psb}]$$

$$d_p = 15.125 \text{ in.}$$

AT CENTER OF GIRDER

$$d_{pt} = 21.6875$$

$$d_{pb} = 24.4375$$

$$d_p = 22.375 \text{ in.}$$

Assume Neutral Axis (N.A.) is in flange:

$$c = [A_{ps}f_{pu} + A_s f_y - A'_s f'_y] / [0.85 f'_c \beta_1 b + K A_{ps} (f_{pu} / d_p)]$$

AT END OF GIRDER

$$c = 3.15 \text{ in.}$$

c < hf, N.A. is in top flange, use this 'c' value

AT CENTER OF GIRDER

$$c = 3.21 \text{ in.}$$

c < hf, N.A. is in top flange, use this 'c' value

Consider as T-beam, N.A. is in web:

$$c = [A_{ps}f_{pu} + A_s f_y - A'_s f'_y - 0.85 f'_c \beta_1 (b - b_w) h_f] / [0.85 f'_c \beta_1 b_w + K A_{ps} (f_{pu} / d_p)]$$

AT END OF GIRDER

$$c = -7.59$$

c < hf, N.A. is in flange, use above 'c' value

AT CENTER OF GIRDER

$$c = -7.78 \text{ in.}$$

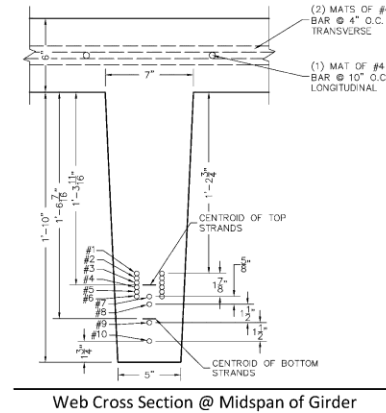
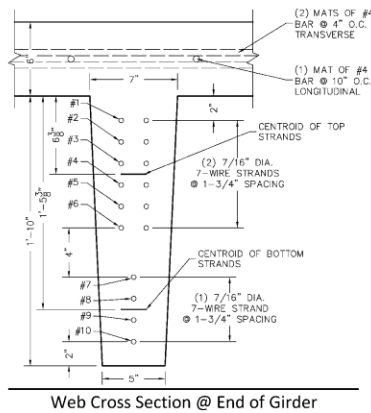
c < hf, N.A. is in flange, use above 'c' value

$$a = \beta_1 c = 2.67 \text{ in.}$$

$$d_v = d_p - a/2 = 13.79 \text{ in.}$$

$$a = \beta_1 c = 2.73 \text{ in.}$$

$$d_v = d_p - a/2 = 21.01 \text{ in.}$$



Full Deck Thickness Cross Sectional Properties Calculations (Girder #1)

Note: Shaded cells input by user.

$f'_c = 5.6$ ksi	$K = 0.38$ (0.28 for low relaxation, 0.38 for stress relieved strands)	$A_{ps} = 0.115$ in. ² (single strand)
$E_c = 2,850$ ksi	$\bar{y} = 19.92$ in. (from bottom of girder)	# of top strands = 24
$f_{pu} = 270$ ksi	$I_g = 41,219.71$ in. ⁴	# of bottom strands = 8
$E_{ps} = 28,500$ ksi	$A'_s = 0.20$ in. ² (single #4 bar)	$A_{pst} = 2.760$ in. ² (top strands)
$f'_y = 58$ ksi	bar spacing = 10 in.	$A_{psb} = 0.920$ in. ² (bottom strands)
$E_s = 29,000$ ksi	$A'_s = 1.44$ in. ² (area of steel in deck)	$A_{ps} = 3.680$ in. ² (all strands)
		$\beta_1 = 0.85 - 0.05[f'_c - 4] = 0.77 \geq 0.65$

Flange Dimensions	Web Dimensions	x 2 webs
$b = 72.00$ in.	$b_{w1} = 7.00$	14.00 in.
$h_f = 6.00$ in.	$b_{w2} = 5.00$	10.00 in.
	$h_w = 22.00$	in.
$A_g = 696.00$ in. ² (cross-sectional area of girder)		

AT END OF GIRDER

$d_{bte} = 15.625$ in. (bottom of girder to middle of top strands)
$d_{bbe} = 4.625$ in. (bottom of girder to middle of bottom strands)
$d_{pte} = 12.375$ in. (top of girder to middle of top strands)
$d_{pbe} = 23.375$ in. (top of girder to middle of bottom strands)

$$d_p = [A_{pst}d_{pt} + A_{psb}d_{pb}]/[A_{pst} + A_{psb}]$$

$$d_{pe} = 15.125 \text{ in.}$$

AT MIDSPAN OF GIRDER

$d_{btm} = 6.312$ in.
$d_{bbm} = 3.562$ in.
$d_{ptm} = 21.688$ in.
$d_{pbm} = 24.438$ in.

$$d_{pm} = 22.376 \text{ in.}$$

Assume Neutral Axis (N.A.) is in flange (AASHTO 5.7.3.1.1-4):

$$c = [A_{ps}f_{pu} + A_s f_y - A'_s f'_y] / [0.85 f'_c \beta_1 b + K A_{ps} (f_{pu} / d_p)]$$

AT END OF GIRDER

$$c = 3.15 \text{ in.}$$

$c < h_f$, N.A. is in top flange, use this 'c' value

AT MIDSPAN OF GIRDER

$$c = 3.24 \text{ in.}$$

$c < h_f$, N.A. is in top flange, use this 'c' value

Consider as T-beam, N.A. is in web (AASHTO 5.7.3.1.1-3):

$$c = [A_{ps}f_{pu} + A_s f_y - A'_s f'_y - 0.85 f'_c \beta_1 (b - b_w) h_f] / [0.85 f'_c \beta_1 b_w + K A_{ps} (f_{pu} / d_p)]$$

AT END OF GIRDER

$$c = -6.47$$

$c < h_f$, N.A. is in flange, use above 'c' value

AT MIDSPAN OF GIRDER

$$c = -6.68 \text{ in.}$$

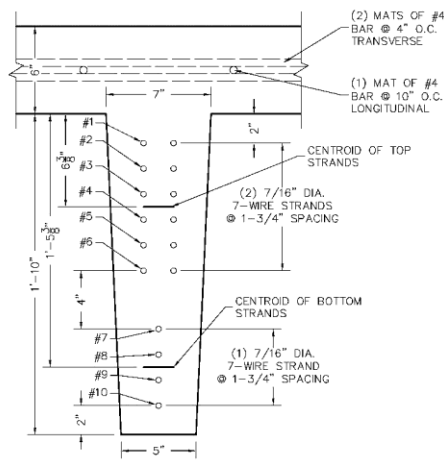
$c < h_f$, N.A. is in flange, use above 'c' value

$$a = \beta_1 c = 2.43 \text{ in.}$$

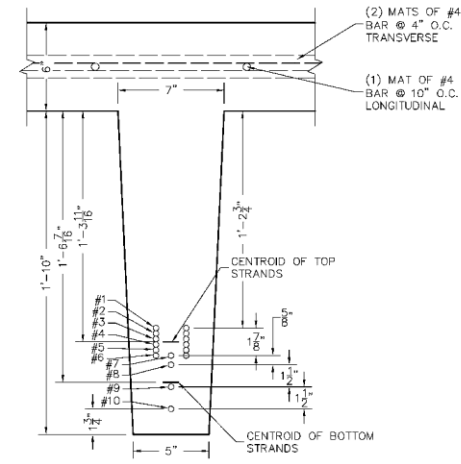
$$d_v = d_{pe} - a/2 = 13.91 \text{ in.}$$

$$a = \beta_1 c = 2.50 \text{ in.}$$

$$d_v = d_{pm} - a/2 = 21.13 \text{ in.}$$



Web Cross Section @ End of Girder



Web Cross Section @ Midspan of Girder

Full Deck Thickness Cross Sectional Properties Calculations (Girders #2 & #3)

Note: Shaded cells input by user.

$f'_c = 5.6$ ksi	$K = 0.38$ (0.28 for low relaxation, 0.38 for stress relieved strands)	$A_{ps} = 0.115$ in. ² (single strand)
$E_c = 2,850$ ksi	$\bar{y} = 20.15$ in. (from bottom of girder)	# of top strands = 24
$f_{pu} = 270$ ksi	$I_g = 42,131.30$ in. ⁴	# of bottom strands = 8
$E_{ps} = 28,500$ ksi	$A'_s = 0.20$ in. ² (single #4 bar)	$A_{pst} = 2.760$ in. ² (top strands)
$f'_y = 58$ ksi	bar spacing = 10 in.	$A_{psb} = 0.920$ in. ² (bottom strands)
$E_s = 29,000$ ksi	$A'_s = 1.55$ in. ² (area of steel in deck)	$A_{ps} = 3.680$ in. ² (all strands)
		$\beta_1 = 0.85 - 0.05[f'_c - 4] = 0.77 \geq 0.65$

Flange Dimensions	Web Dimensions	x 2 webs
$b = 77.50$ in.	$b_{w1} = 7.00$	14.00 in.
$h_f = 6.00$ in.	$b_{w2} = 5.00$	10.00 in.
	$h_w = 22.00$	in.
$A_g = 729.00$ in. ² (cross-sectional area of girder)		

AT END OF GIRDER

$d_{bte} = 15.625$ in. (bottom of girder to middle of top strands)
 $d_{bbe} = 4.625$ in. (bottom of girder to middle of bottom strands)
 $d_{pte} = 12.375$ in. (top of girder to middle of top strands)
 $d_{pbe} = 23.375$ in. (top of girder to middle of bottom strands)
 $d_p = [A_{pst}d_{pt} + A_{psb}d_{pb}]/[A_{pst} + A_{psb}]$
 $d_{pe} = 15.125$ in.

AT MIDSPAN OF GIRDER

$d_{btm} = 6.312$ in.
 $d_{bbm} = 3.562$ in.
 $d_{ptm} = 21.688$ in.
 $d_{pbm} = 24.438$ in.
 $d_{pm} = 22.376$ in.

Assume Neutral Axis (N.A.) is in flange (AASHTO 5.7.3.1.1-4):

$$c = [A_{ps}f_{pu} + A_s f_y - A'_s f'_y] / [0.85f'_c \beta_1 b + K A_{ps}(f_{pu}/d_p)]$$

AT END OF GIRDER

$c = 2.92$ in.

$c < h_f$, N.A. is in top flange, use this 'c' value

AT MIDSPAN OF GIRDER

$c = 3.00$ in.

$c < h_f$, N.A. is in top flange, use this 'c' value

Consider as T-beam, N.A. is in web (AASHTO 5.7.3.1.1-3):

$$c = [A_{ps}f_{pu} + A_s f_y - A'_s f'_y - 0.85f'_c \beta_1 (b - b_w) h_f] / [0.85f'_c \beta_1 b_w + K A_{ps}(f_{pu}/d_p)]$$

AT END OF GIRDER

$c = -8.48$

$c < h_f$, N.A. is in flange, use above 'c' value

AT MIDSPAN OF GIRDER

$c = -8.76$ in.

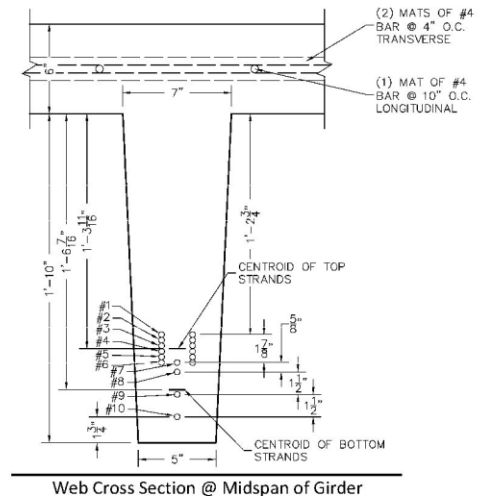
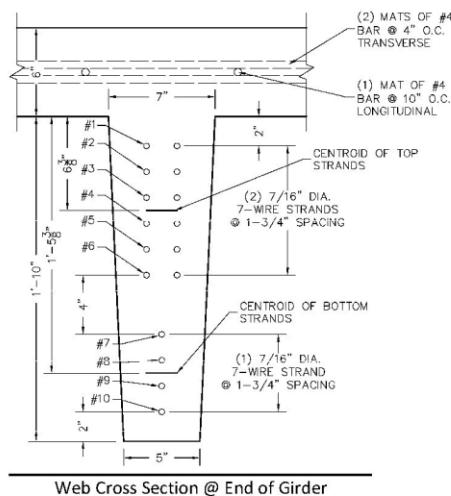
$c < h_f$, N.A. is in flange, use above 'c' value

$a = \beta_1 c = 2.25$ in.

$d_v = d_p - a/2 = 14.00$ in.

$a = \beta_1 c = 2.31$ in.

$d_v = d_p - a/2 = 21.22$ in.



Half Deck Thickness Cross Sectional Properties Calculations (Girder #1)

Note: Shaded cells input by user.

$f'_c = 5.6$ ksi	$K = 0.38$ (0.28 for low relaxation, 0.38 for stress relieved strands)	$A_{ps} = 0.115$ in. ² (single strand)
$E_c = 2,850$ ksi	$\bar{y} = 16.96$ in. (from bottom of girder)	# of top strands = 24
$f_{pu} = 270$ ksi	$I_g = 27,503.27$ in. ⁴	# of bottom strands = 8
$E_{ps} = 28,500$ ksi	$A'_s = 0.20$ in. ² (single #4 bar)	$A_{pst} = 2.760$ in. ² (top strands)
$f'_y = 58$ ksi	bar spacing = 10 in.	$A_{psb} = 0.920$ in. ² (bottom strands)
$E_s = 29,000$ ksi	$A'_s = 1.44$ in. ² (area of steel in deck)	$A_{ps} = 3.680$ in. ² (all strands)
		$\beta_1 = 0.85 - 0.05[f'_c - 4] = 0.77 \geq 0.65$

Flange Dimensions	Web Dimensions	x 2 webs
$b = 72.00$ in.	$b_{w1} = 7.00$	14.00 in.
$h_f = 3.00$ in.	$b_{w2} = 5.00$	10.00 in.
	$h_w = 22.00$	in.
$A_g = 480.00$ in. ² (cross-sectional area of girder)		

AT END OF GIRDER

$d_{bte} = 15.625$ in. (bottom of girder to middle of top strands)
 $d_{bbe} = 4.625$ in. (bottom of girder to middle of bottom strands)
 $d_{pte} = 9.375$ in. (top of girder to middle of top strands)
 $d_{pbe} = 20.375$ in. (top of girder to middle of bottom strands)
 $d_p = [A_{pst}d_{pt} + A_{psb}d_{pb}]/[A_{pst} + A_{psb}]$
 $d_{pe} = 12.125$ in.

AT MIDSPAN OF GIRDER

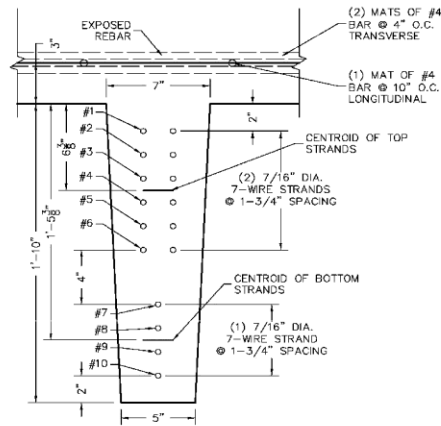
$d_{btm} = 6.312$ in.
 $d_{bbm} = 3.562$ in.
 $d_{ptm} = 18.688$ in.
 $d_{pbm} = 21.438$ in.
 $d_{pm} = 19.376$ in.

Assume Neutral Axis (N.A.) is in flange (AASHTO 5.7.3.1.1-4):

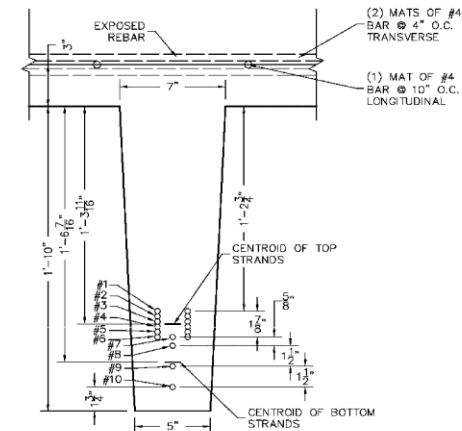
$c = [A_{ps}f_{pu} + A_s f_y - A'_s f'_y] / [0.85f'_c \beta_1 b + K A_{ps} (f_{pu} / d_p)]$
AT END OF GIRDER **AT MIDSPAN OF GIRDER**
 $c = 3.08$ in. $c = 3.21$ in.
 $c > h_f$, N.A. is in web, use 'c' value below **$c > h_f$, N.A. is in web, use 'c' value below**

Consider as T-beam, N.A. is in web (AASHTO 5.7.3.1.1-3):

$c = [A_{ps}f_{pu} + A_s f_y - A'_s f'_y - 0.85f'_c \beta_1 (b - b_w) h_f] / [0.85f'_c \beta_1 b_w + K A_{ps} (f_{pu} / d_p)]$
AT END OF GIRDER **AT MIDSPAN OF GIRDER**
 $c = 3.74$ $c = 3.91$ in.
 $c > h_f$, N.A. is in web, use this 'c' value **$c > h_f$, N.A. is in web, use this 'c' value**
 $a = \beta_1 c = 2.88$ in. $a = \beta_1 c = 3.01$ in.
 $d_v = d_{pe} - a/2 = 10.68$ in. $d_v = d_{pm} - a/2 = 17.87$ in.



Web Cross Section @ End of Girder



Web Cross Section @ Midspan of Girder

Half Deck Thickness Cross Sectional Properties Calculations (Girders #2 & #3)

Note: Shaded cells input by user.

$f'_c = 5.6$ ksi	$K = 0.38$ (0.28 for low relaxation, 0.38 for stress relieved strands)	$A_{ps} = 0.115$ in. ² (single strand)
$E_c = 2,850$ ksi	$\bar{y} = 17.18$ in. (from bottom of girder)	# of top strands = 24
$f_{pu} = 270$ ksi	$I_g = 28,197.70$ in. ⁴	# of bottom strands = 8
$E_{ps} = 28,500$ ksi	$A'_s = 0.20$ in. ² (single #4 bar)	$A_{pst} = 2.760$ in. ² (top strands)
$f_y = 58$ ksi	bar spacing = 10 in.	$A_{psb} = 0.920$ in. ² (bottom strands)
$E_s = 29,000$ ksi	$A'_s = 1.55$ in. ² (area of steel in deck)	$A_{ps} = 3.680$ in. ² (all strands)
		$\beta_1 = 0.85 - 0.05[f'_c - 4] = 0.77 \geq 0.65$

Flange Dimensions	Web Dimensions	x 2 webs
$b = 77.50$ in.	$b_{w1} = 7.00$	14.00 in.
$h_f = 3.00$ in.	$b_{w2} = 5.00$	10.00 in.
	$h_w = 22.00$	in.
$A_g = 496.50$ in. ² (cross-sectional area of girder)		

AT END OF GIRDER

$d_{bte} = 15.625$ in. (bottom of girder to middle of top strands)	
$d_{bbe} = 4.625$ in. (bottom of girder to middle of bottom strands)	
$d_{pte} = 9.375$ in. (top of girder to middle of top strands)	
$d_{pbe} = 20.375$ in. (top of girder to middle of bottom strands)	
$d_p = [A_{pst}d_{pt} + A_{psb}d_{pb}]/[A_{pst} + A_{psb}]$	
$d_{pe} = 12.125$ in.	

AT MIDSPAN OF GIRDER

$d_{btm} = 6.312$ in.	
$d_{bbm} = 3.562$ in.	
$d_{ptm} = 18.688$ in.	
$d_{pbm} = 21.438$ in.	
$d_{pm} = 19.376$ in.	

Assume Neutral Axis (N.A.) is in flange (AASHTO 5.7.3.1.1-4):

$$c = [A_{ps}f_{pu} + A_s f_y - A'_s f'_y] / [0.85f'_c \beta_1 b + K A_{ps}(f_{pu}/d_p)]$$

AT END OF GIRDER

$$c = 2.87 \text{ in.}$$

$c < hf$, N.A. is in top flange, use this 'c' value

AT MIDSPAN OF GIRDER

$$c = 2.98 \text{ in.}$$

$c < hf$, N.A. is in top flange, use this 'c' value

Consider as T-beam, N.A. is in web (AASHTO 5.7.3.1.1-3):

$$c = [A_{ps}f_{pu} + A_s f_y - A'_s f'_y - 0.85f'_c \beta_1 (b - b_w) h_f] / [0.85f'_c \beta_1 b_w + K A_{ps}(f_{pu}/d_p)]$$

AT END OF GIRDER

$$c = 2.74$$

$c < hf$, N.A. is in flange, use above 'c' value

$$a = \beta_1 c = 2.21 \text{ in.}$$

$$d_v = d_p - a/2 = 11.02 \text{ in.}$$

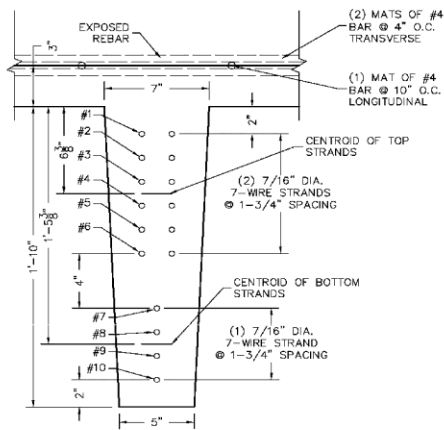
AT MIDSPAN OF GIRDER

$$c = 2.87 \text{ in.}$$

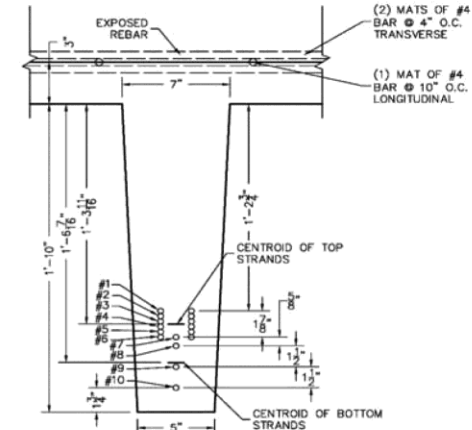
$c < hf$, N.A. is in flange, use above 'c' value

$$a = \beta_1 c = 2.29 \text{ in.}$$

$$d_v = d_p - a/2 = 18.23 \text{ in.}$$



Web Cross Section @ End of Girder



Web Cross Section @ Midspan of Girder

APPENDIX B. TESTED DATA

Cracking Test Data

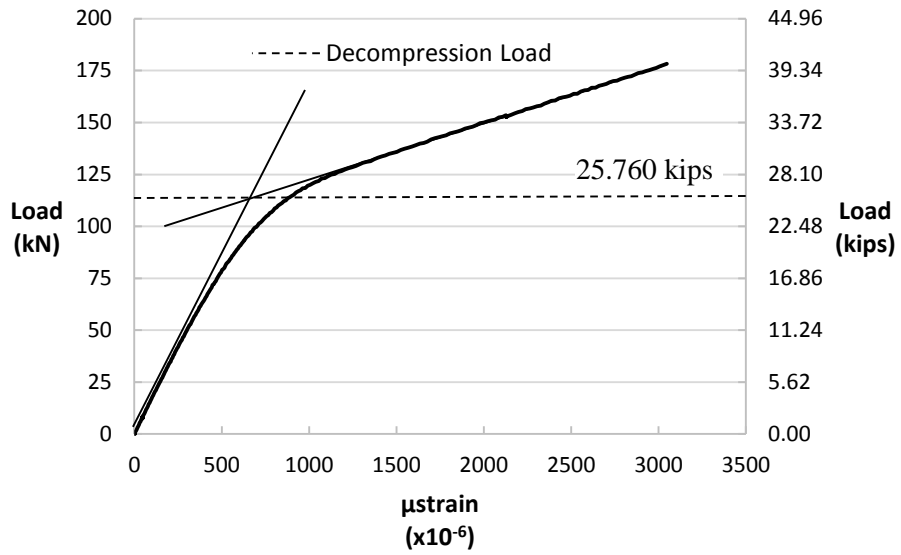


Figure B.1 Girder #1 cracking load test data

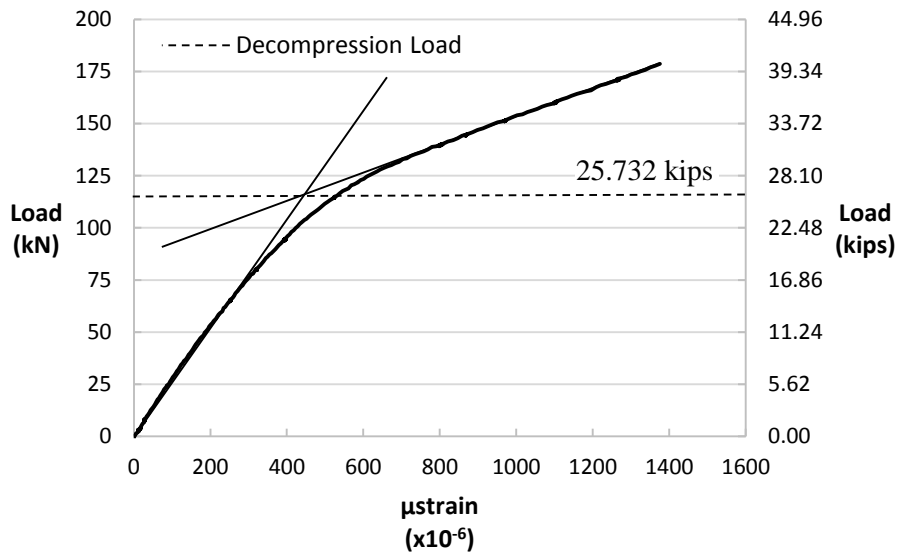


Figure B.2 Girder #2 cracking load test data

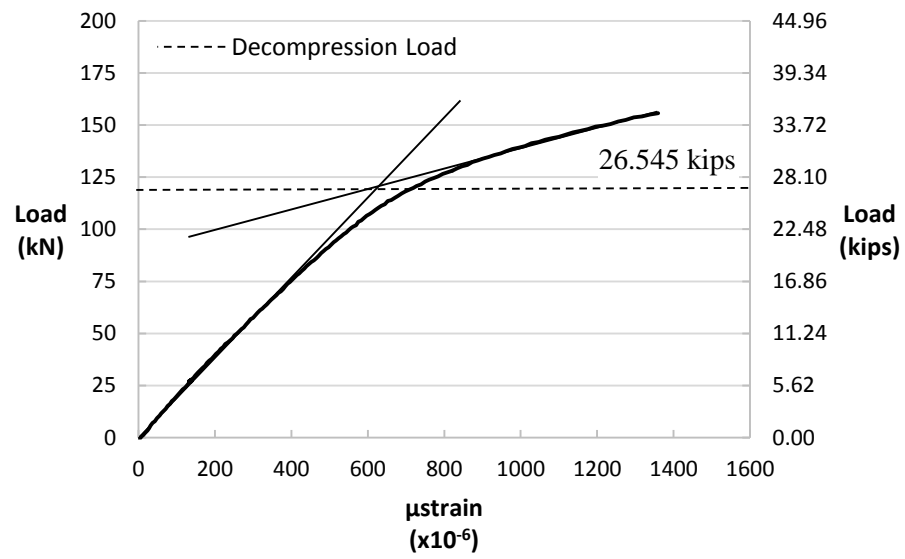
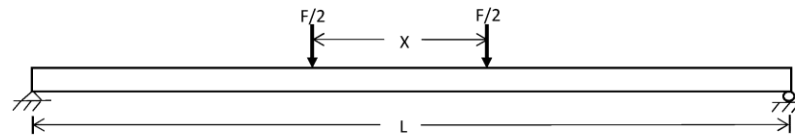


Figure B.3 Girder #3 cracking load test data

Full Deck Thickness Effective Prestressing Calculations

Note: Outlined values obtained from previous calculations, shaded cells input by user.



$$P = \frac{\frac{M_{sw} C_g}{I_g} + \frac{M_{xt} C}{I}}{\frac{1}{A_g} + \frac{e_{pg} C_g}{I_g}}$$

$$w_c = 110 \text{ lb/ft}^3 \text{ (unit weight of concrete from testing)}$$

$$L = 49.0 \text{ ft (span length of girder)}$$

Girder #1

$$A_g = 4.83 \text{ ft}^2 \text{ (cross-sectional area of girder)}$$

$$q = w_c(A_g) = 531.67 \text{ lb/ft (uniform load from self-weight)}$$

$$M_{sw} = (qL^2)/8 = 159,566 \text{ lb-ft (self-weight moment at midspan)}$$

$$C = C_g = \bar{y} = 19.92 \text{ in. (from bottom of girder)}$$

$$e_{pg} = C - (h - d_{pm}) = 14.30 \text{ in.}$$

$$I = I_g = 41,219.71 \text{ in.}^4$$

$$X = 6.0 \text{ ft (distance between point loads)}$$

$$F = 25,760 \text{ lbs (total cracking force from load vs. strain plot)}$$

$$M_{xt} = (F/2)(L/2 - X/2) = 276,920 \text{ lb-ft (cracking moment)}$$

$$P = 325,679 \text{ lb (effective prestressing force)}$$

$$A_{ps} = 3.680 \text{ in.}^2 \text{ (cross sectional area of all strands)}$$

$$\sigma_{ps} = P/A_{ps} = 88,500 \text{ psi (effective prestress stress)}$$

$$\epsilon_{ps} = \sigma_{ps}/E_{ps} = 0.003105 \text{ (effective prestress strain)}$$

Girder #2

$$A_g = 5.06 \text{ ft}^2 \text{ (cross-sectional area of girder)}$$

$$q = w_c(A_g) = 556.88 \text{ lb/ft (uniform load from self-weight)}$$

$$M_{sw} = (qL^2)/8 = 167,132 \text{ lb-ft (self-weight moment at midspan)}$$

$$C = C_g = \bar{y} = 20.15 \text{ in. (from bottom of girder)}$$

$$e_{pg} = C - (h - d_{pm}) = 13.37 \text{ in.}$$

$$I = I_g = 42,131.30 \text{ in.}^4$$

$$X = 6.0 \text{ ft (distance between point loads)}$$

$$F = 25,732 \text{ lbs (total cracking force from load vs. strain plot)}$$

$$M_{xt} = (F/2)(L/2 - X/2) = 276,619 \text{ lb-ft (cracking moment)}$$

$$P = 342,550 \text{ lb (effective prestressing force)}$$

$$A_{ps} = 3.680 \text{ in.}^2 \text{ (cross sectional area of all strands)}$$

$$\sigma_{ps} = P/A_{ps} = 93,084 \text{ psi (effective prestress stress)}$$

$$\epsilon_{ps} = \sigma_{ps}/E_{ps} = 0.003266 \text{ (effective prestress strain)}$$

Girder #3

$$A_g = 5.06 \text{ ft}^2 \text{ (cross-sectional area of girder)}$$

$$q = w_c(A_g) = 556.88 \text{ lb/ft (uniform load from self-weight)}$$

$$M_{sw} = (qL^2)/8 = 167,132 \text{ lb-ft (self-weight moment at midspan)}$$

$$C = C_g = \bar{y} = 20.15 \text{ in. (from bottom of girder)}$$

$$e_{pg} = C - (h - d_{pm}) = 13.37 \text{ in.}$$

$$I = I_g = 42,131.30 \text{ in.}^4$$

$$X = 7.0 \text{ ft (distance between point loads)}$$

$$F = 26,545 \text{ lbs (total cracking force from load vs. strain plot)}$$

$$M_{xt} = (F/2)(L/2 - X/2) = 278,723 \text{ lb-ft (cracking moment)}$$

$$P = 344,105 \text{ lb (effective prestressing force)}$$

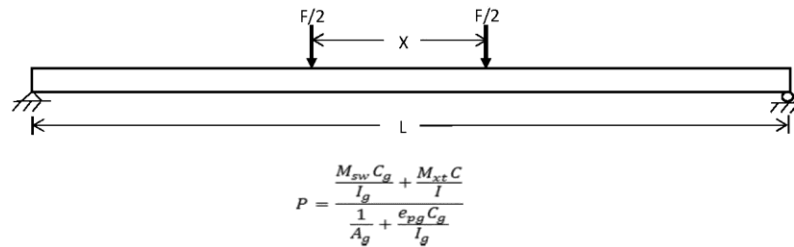
$$A_{ps} = 3.680 \text{ in.}^2 \text{ (cross sectional area of all strands)}$$

$$\sigma_{ps} = P/A_{ps} = 93,507 \text{ psi (effective prestress stress)}$$

$$\epsilon_{ps} = \sigma_{ps}/E_{ps} = 0.003281 \text{ (effective prestress strain)}$$

Half Deck Thickness Effective Prestressing Calculations

Note: Outlined values obtained from previous calculations, shaded cells input by user.



$$w_c = 110 \text{ lb/ft}^3 \text{ (unit weight of concrete from testing)}$$

$$L = 49.0 \text{ ft (span length of girder)}$$

Girder #1

$$A_g = 3.33 \text{ ft}^2 \text{ (cross-sectional area of girder)}$$

$$q = w_c(A_g) = 366.67 \text{ lb/ft (uniform load from self-weight)}$$

$$M_{sw} = (qL^2)/8 = 110,046 \text{ lb-ft (self-weight moment at midspan)}$$

$$C = C_g = \bar{y} = 16.96 \text{ in. (from bottom of girder)}$$

$$e_{pg} = C - (h - d_{pn}) = 11.34 \text{ in.}$$

$$I = I_g = 27,503.27 \text{ in.}^4$$

$$X = 6.0 \text{ ft (distance between point loads)}$$

$$F = 25,760 \text{ lbs (total cracking force from load vs. strain plot)}$$

$$M_{xt} = (F/2)(L/2 - X/2) = 276,920 \text{ lb-ft (cracking moment)}$$

$$P = 343,099 \text{ lb (effective prestressing force)}$$

$$A_{ps} = 3.680 \text{ in.}^2 \text{ (cross sectional area of all strands)}$$

$$\sigma_{ps} = P/A_{ps} = 93,233 \text{ psi (effective prestress stress)}$$

$$\epsilon_{ps} = \sigma_{ps}/E_{ps} = 0.003271 \text{ (effective prestress strain)}$$

Girder #2

$$A_g = 3.45 \text{ ft}^2 \text{ (cross-sectional area of girder)}$$

$$q = w_c(A_g) = 379.27 \text{ lb/ft (uniform load from self-weight)}$$

$$M_{sw} = (qL^2)/8 = 113,829 \text{ lb-ft (self-weight moment at midspan)}$$

$$C = C_g = \bar{y} = 17.18 \text{ in. (from bottom of girder)}$$

$$e_{pg} = C - (h - d_{pn}) = 10.41 \text{ in.}$$

$$I = I_g = 28,197.70 \text{ in.}^4$$

$$X = 6.0 \text{ ft (distance between point loads)}$$

$$F = 25,732 \text{ lbs (total cracking force from load vs. strain plot)}$$

$$M_{xt} = (F/2)(L/2 - X/2) = 276,619 \text{ lb-ft (cracking moment)}$$

$$P = 361,881 \text{ lb (effective prestressing force)}$$

$$A_{ps} = 3.680 \text{ in.}^2 \text{ (cross sectional area of all strands)}$$

$$\sigma_{ps} = P/A_{ps} = 98,337 \text{ psi (effective prestress stress)}$$

$$\epsilon_{ps} = \sigma_{ps}/E_{ps} = 0.003450 \text{ (effective prestress strain)}$$

Girder #3

$$A_g = 3.45 \text{ ft}^2 \text{ (cross-sectional area of girder)}$$

$$q = w_c(A_g) = 379.27 \text{ lb/ft (uniform load from self-weight)}$$

$$M_{sw} = (qL^2)/8 = 113,829 \text{ lb-ft (self-weight moment at midspan)}$$

$$C = C_g = \bar{y} = 17.18 \text{ in. (from bottom of girder)}$$

$$e_{pg} = C - (h - d_{pn}) = 10.41 \text{ in.}$$

$$I = I_g = 28,197.70 \text{ in.}^4$$

$$X = 7.0 \text{ ft (distance between point loads)}$$

$$F = 26,545 \text{ lbs (total cracking force from load vs. strain plot)}$$

$$M_{xt} = (F/2)(L/2 - X/2) = 278,723 \text{ lb-ft (cracking moment)}$$

$$P = 363,721 \text{ lb (effective prestressing force)}$$

$$A_{ps} = 3.680 \text{ in.}^2 \text{ (cross sectional area of all strands)}$$

$$\sigma_{ps} = P/A_{ps} = 98,837 \text{ psi (effective prestress stress)}$$

$$\epsilon_{ps} = \sigma_{ps}/E_{ps} = 0.003468 \text{ (effective prestress strain)}$$

Flexural Test Data

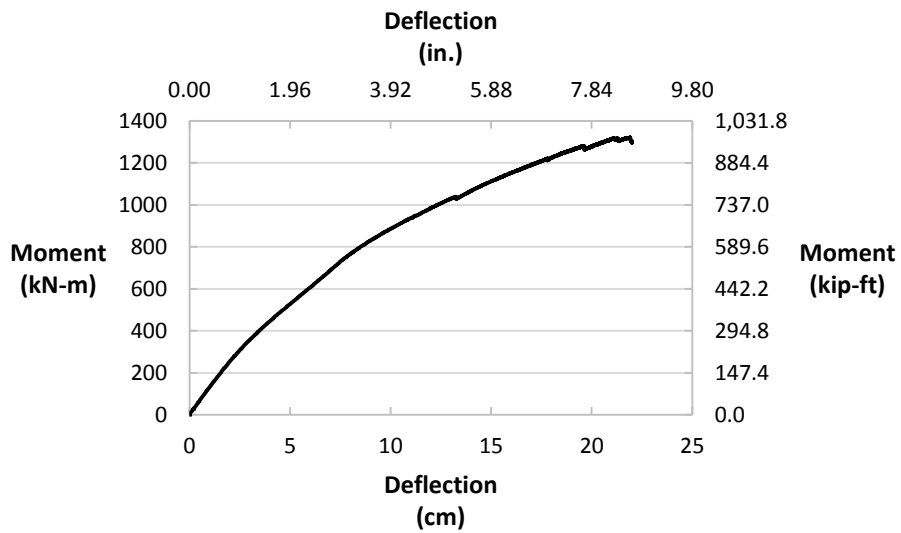


Figure B.4 Girder #1 moment vs. deflection at midspan north side

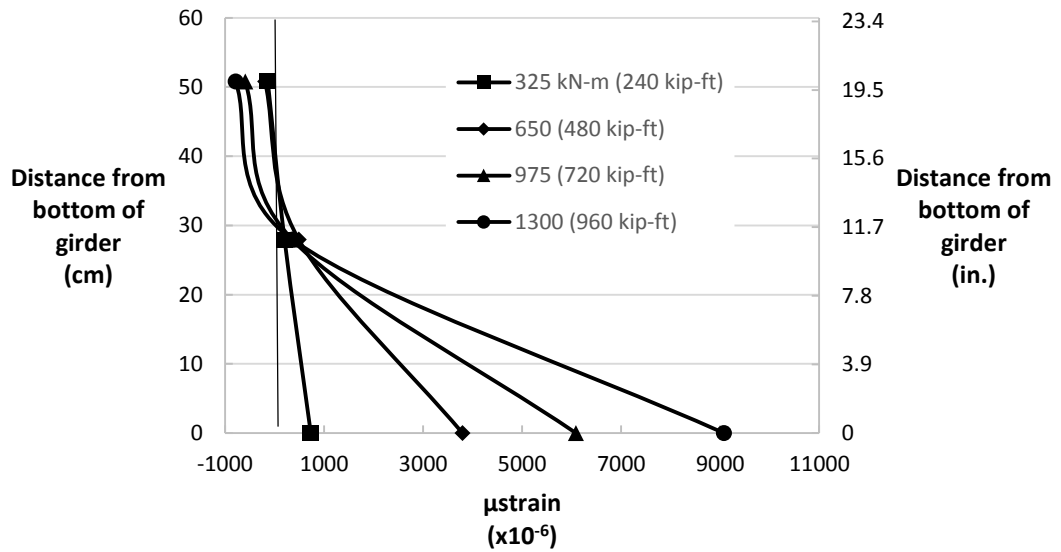


Figure B.5 Girder #1 strain distribution at midspan south side

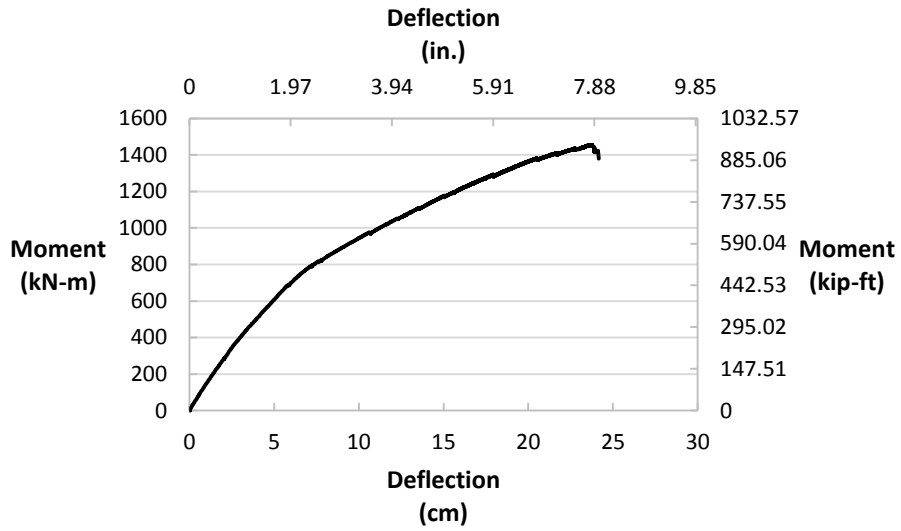


Figure B.6 Girder #2 moment vs. deflection at midspan north side

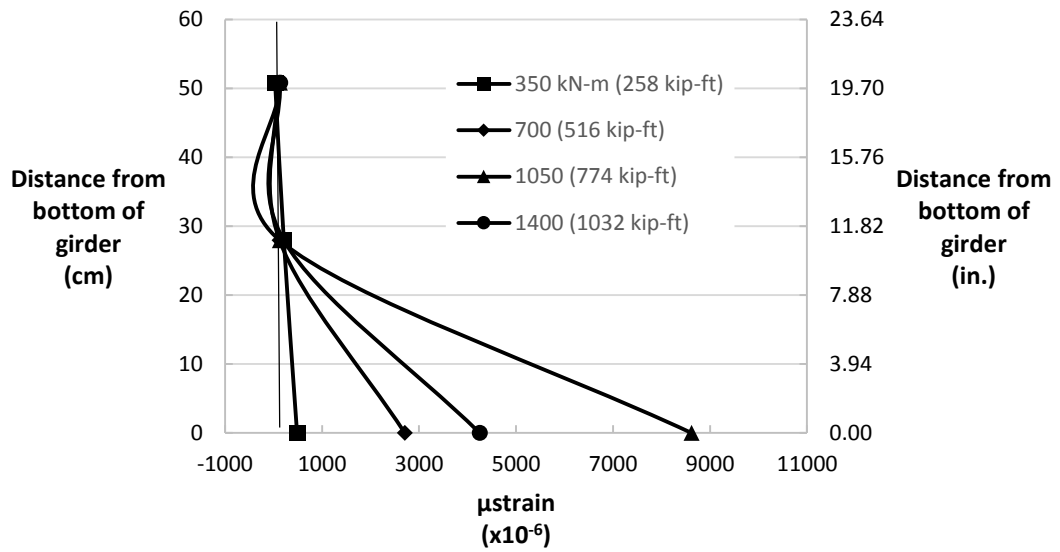


Figure B.7 Girder #2 strain distribution at midspan north side

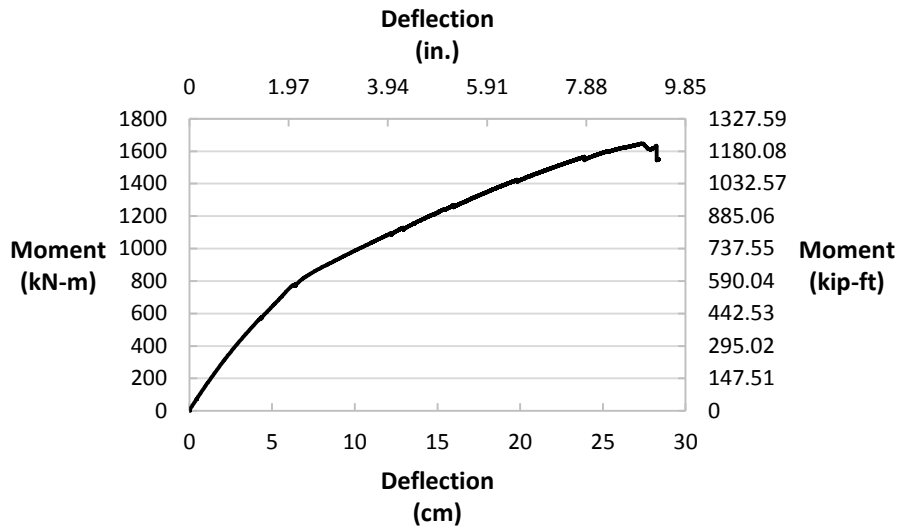


Figure B.8 Girder #3 moment vs. deflection at midspan north side

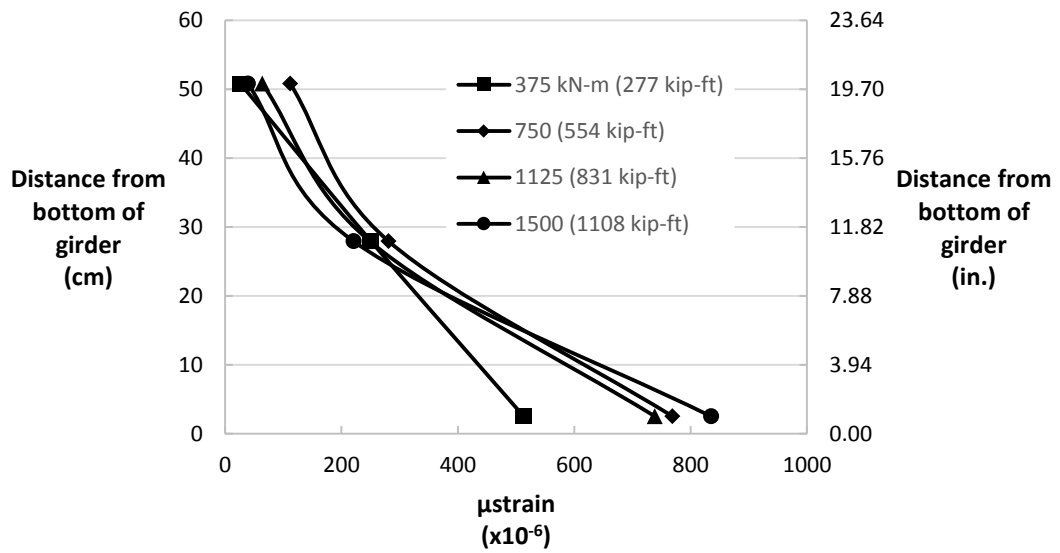


Figure B.9 Girder #3 strain distribution at midspan south side

Shear Test Data

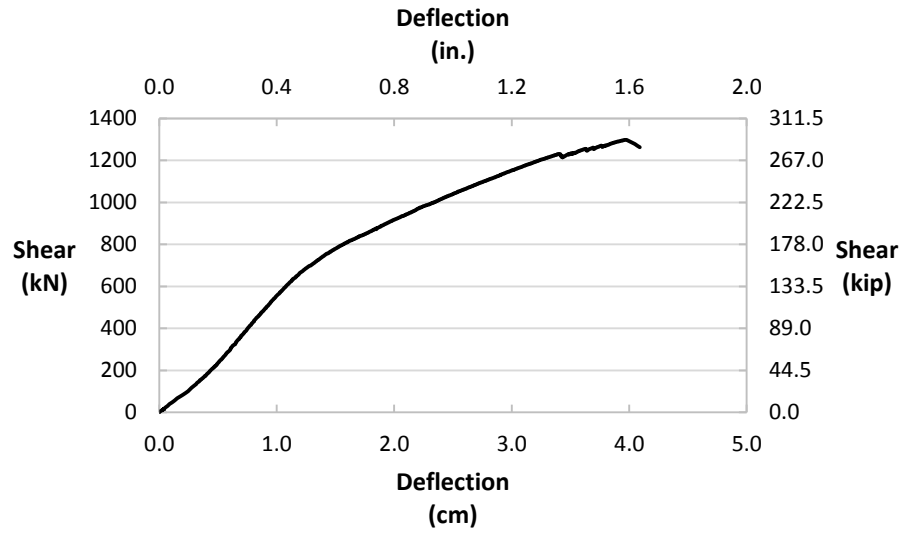


Figure B.10 2d_v test of Girder #1 shear vs. deflection

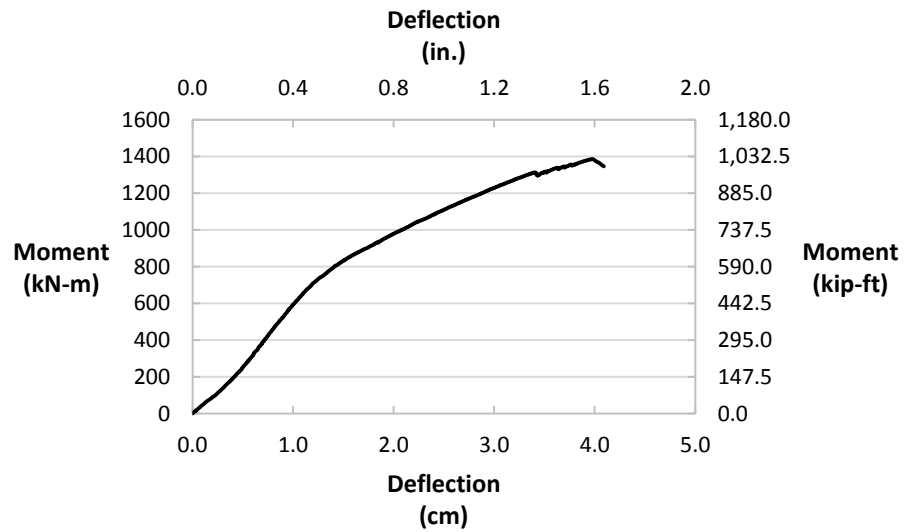


Figure B.11 2d_v test of Girder #1 moment vs. deflection

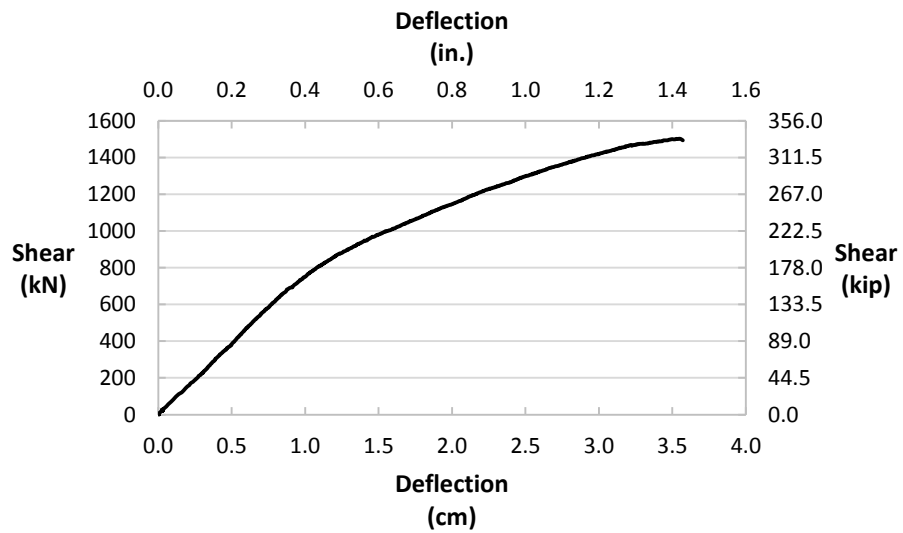
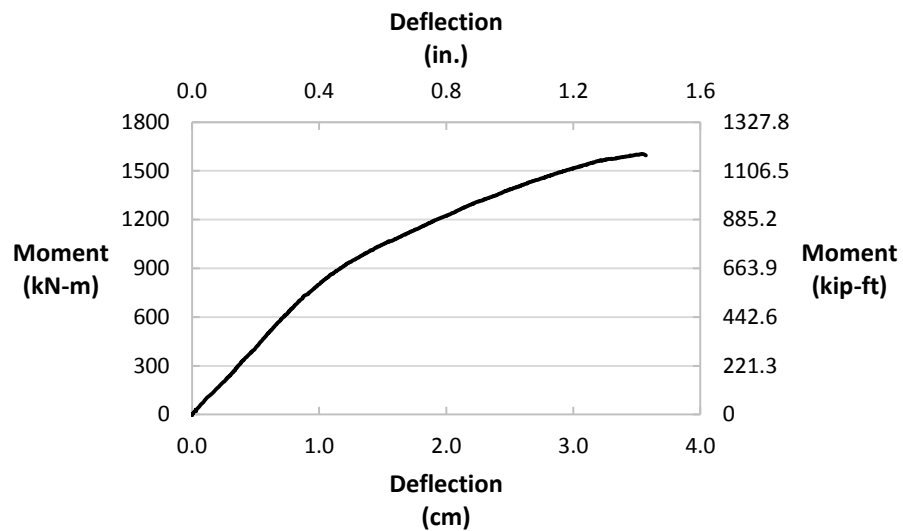


Figure B.12 2d_v test of Girder #3 shear vs. deflection

Figure B.13 2d_v test of Girder #3 moment vs. deflection

Figure B.14 3d_v test of Girder #1 shear vs. deflection



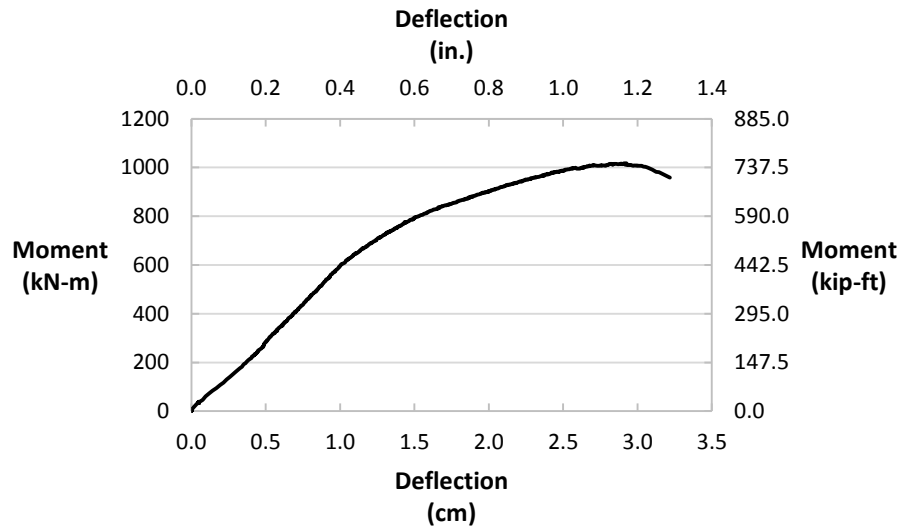


Figure B.15 3d, test of Girder #1 moment vs. deflection

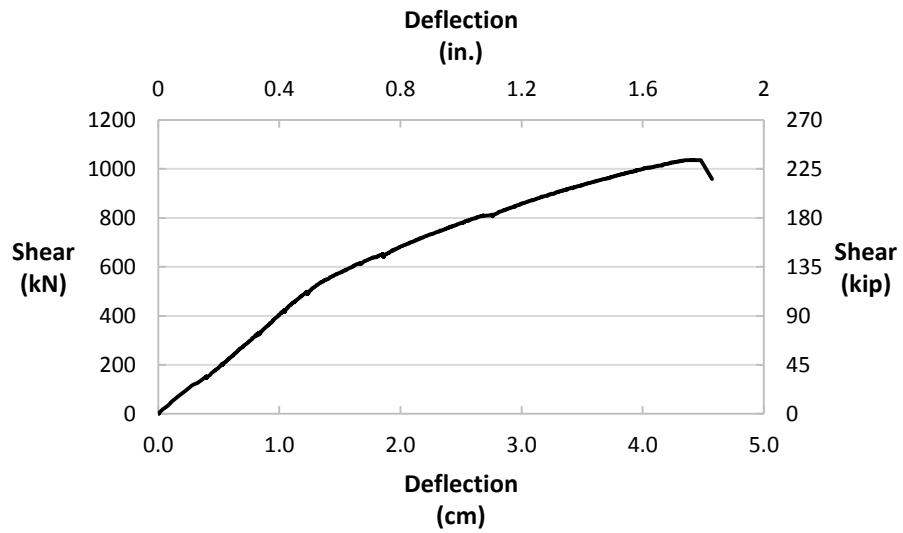


Figure B.16 3d, test of Girder #2 shear vs. deflection

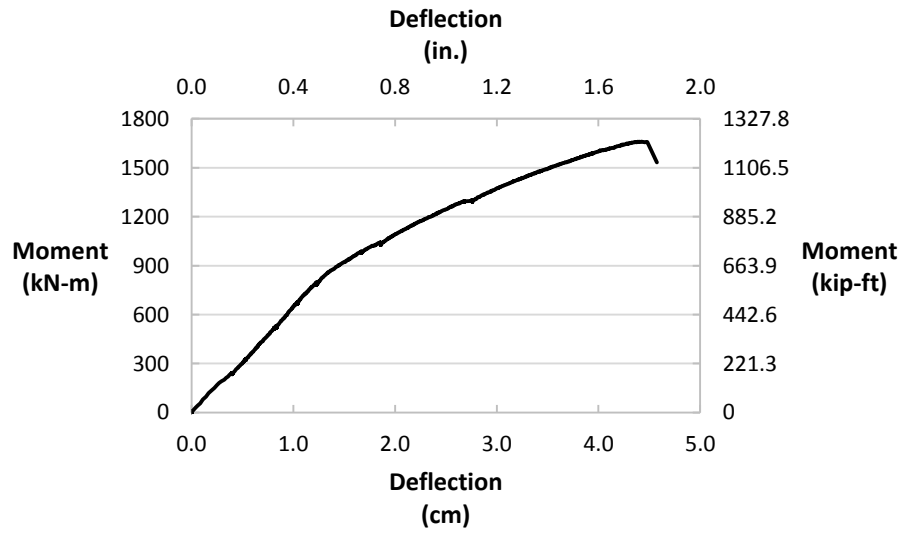


Figure B.17 3d_v test of Girder #2 moment vs. deflection

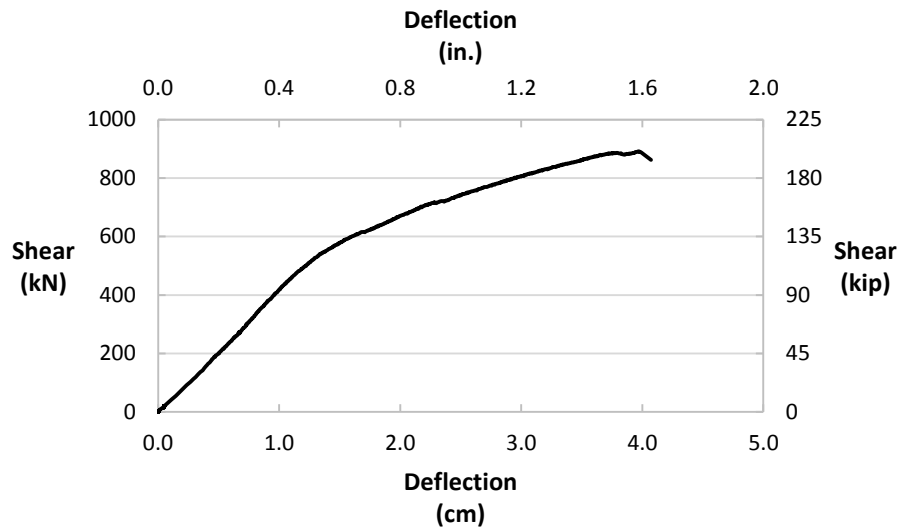


Figure B.18 4d_v test of Girder #3 shear vs. deflection

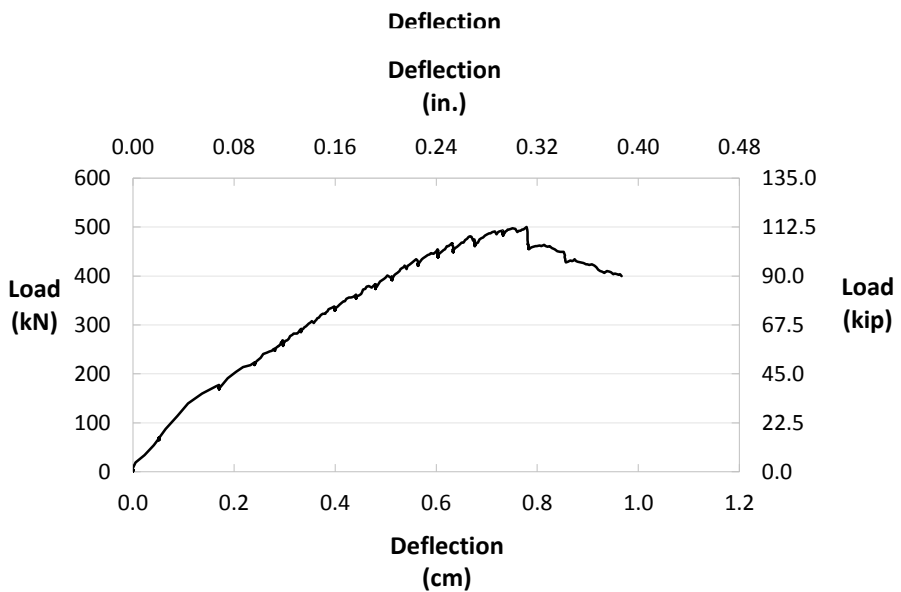
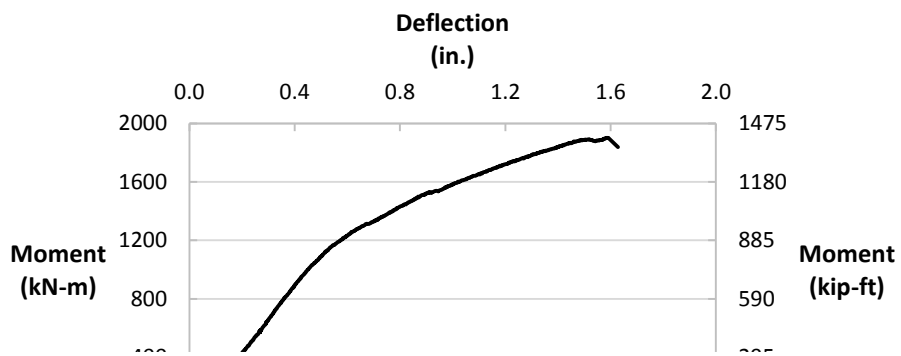
Figure B.19 4d, test of Girder #3 moment vs. deflection

Punching Shear Test Data

Figure B.20 Punching shear test #7 Girder #2 west side load vs. deflection

Figure B.21 Punching shear test #8 Girder #2 west side load vs. deflection

Figure B.22 Punching shear test #9 Girder #2 west side load vs. deflection



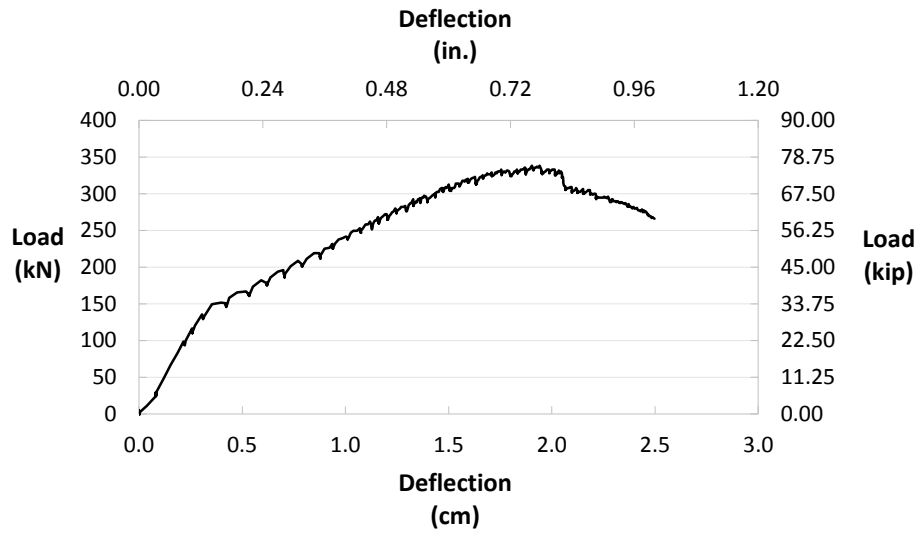


Figure B.23 Punching shear test #10 Girder #1 east side load vs. deflection

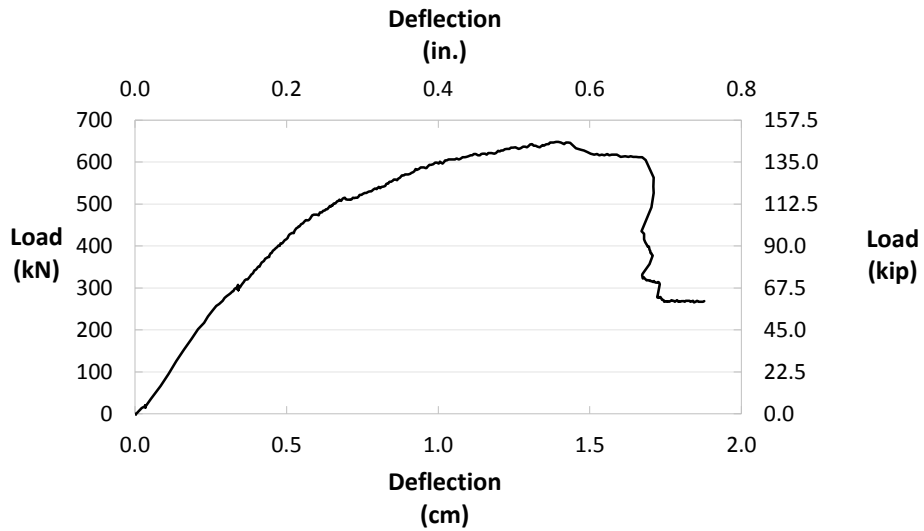


Figure B.24 Punching shear test #11 Girder #1 east side load vs. deflection

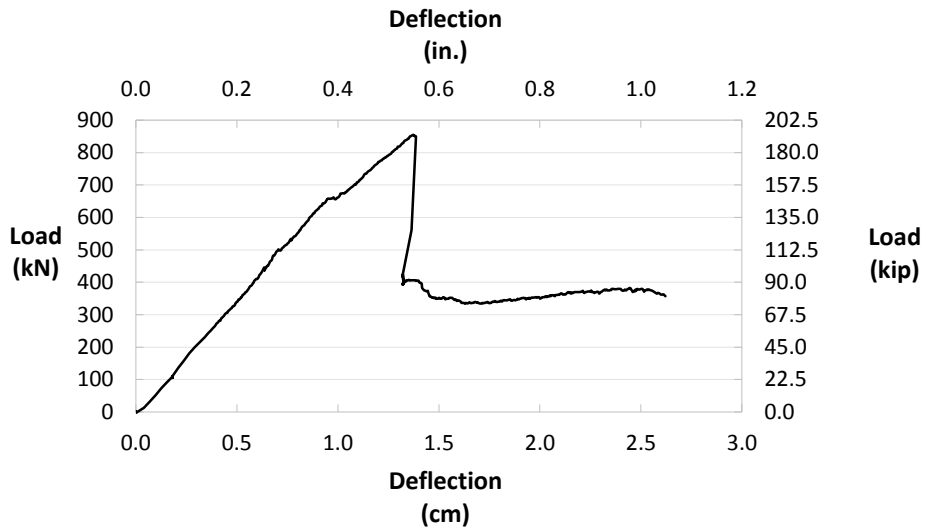


Figure B.25 Punching shear test #12 Girder #1 east side load vs. deflection

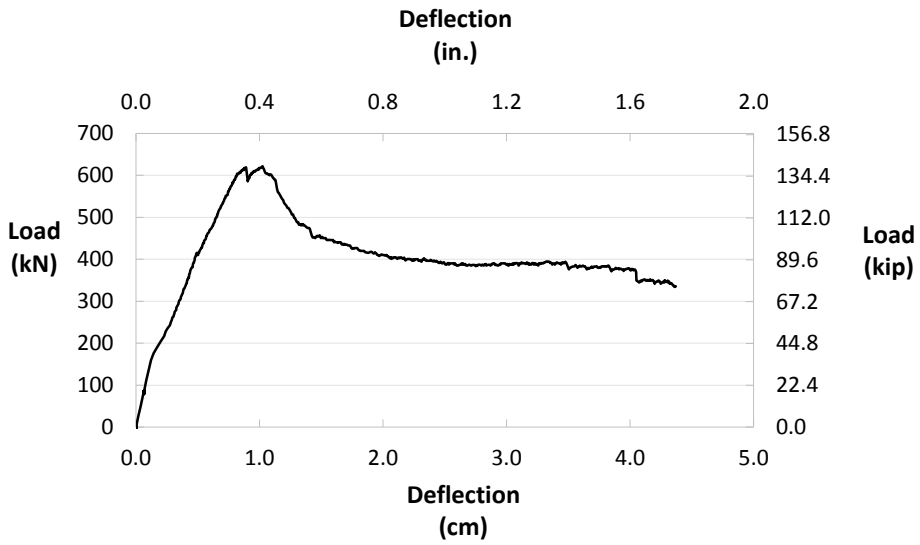


Figure B.26 Punching shear test #13 Girder #1 east side load vs. deflection

Material Properties Data

Table B.1 Tested concrete material properties

Specimen #	Cross Sectional Area (cm ² /in ²)	Measured Ultimate Capacity (kN/kips)	Ultimate Compressive Strength, f _c (MPa/ksi)	Unit Weight, w _c (kN/m ³ - kips/ft ³)
1	69.14 / 10.72	275.14 / 61.86	39.79 / 5.77	17.28 - 0.110
2	69.32 / 10.74	132.31 / 29.75	19.09 / 2.77	17.29 - 0.110
3	69.23 / 10.73	212.2 / 47.71	30.65 / 4.45	17.32 - 0.110
4	69.05 / 10.70	265.38 / 59.66	38.43 / 5.57	17.16 - 0.109
5	69.31 / 10.74	263.13 / 59.16	37.96 / 5.51	16.93 - 0.108
Average =			38.61 / 5.60	17.28 - 0.110

Table B.2 Tested prestressing strand capacity

Specimen #	Strand Diameter (cm/in)	Strand Cross Sectional Area (cm ² /in ²)	Ultimate Load (kN/kips)	Ultimate Stress, f _{pu} (MPa/ksi)
1	1.11 / 0.438	0.74 / 0.115	126.33 / 28.40	1702.72 / 246.96
2	1.11 / 0.438	0.74 / 0.115	129 / 29.00	1738.69 / 252.17
3	1.11 / 0.438	0.74 / 0.115	145.9 / 32.80	1966.52 / 285.22
4	1.11 / 0.438	0.74 / 0.115	137 / 30.80	1846.61 / 267.83
5	1.11 / 0.438	0.74 / 0.115	141.9 / 31.90	1912.56 / 277.39
6	1.11 / 0.438	0.74 / 0.115	150.35 / 33.80	2026.47 / 293.91
7	1.11 / 0.438	0.74 / 0.115	169.03 / 38.00	2278.28 / 330.43
8	1.11 / 0.438	0.74 / 0.115	140.56 / 31.60	1894.57 / 274.78
9	1.11 / 0.438	0.74 / 0.115	145.46 / 32.70	1960.52 / 284.35
10	1.11 / 0.438	0.74 / 0.115	141.45 / 31.80	1906.56 / 276.52
11	1.11 / 0.438	0.74 / 0.115	145.01 / 32.60	1954.53 / 283.48
12	1.11 / 0.438	0.74 / 0.115	138.78 / 31.20	1870.59 / 271.30
13	1.11 / 0.438	0.74 / 0.115	143.23 / 32.20	1930.54 / 280.00
14	1.11 / 0.438	0.74 / 0.115	143.23 / 32.20	1930.54 / 280.00
15	1.11 / 0.438	0.74 / 0.115	135.23 / 30.40	1822.63 / 264.35

Average = 1890.29 / 274.16

APPENDIX C. AASHTO CALCULATIONS

Full Deck Thickness Prestressing Loss Calculations based on AASHTO LRFD Bridge Design Specifications (Girder #1)

Note: Outlined values obtained from previous calculations, shaded cells input by user.

$f'_y =$ <input type="text" value="58"/> ksi	Deck Dimensions	# of strands = <input type="text" value="32"/>
$E_s =$ <input type="text" value="29,000"/> ksi	$b_f =$ <input type="text" value="72.00"/> in.	Single strand $A_{ps} =$ <input type="text" value="0.115"/> in ²
$f_{pu} =$ <input type="text" value="270"/> ksi	$h_f =$ <input type="text" value="6.00"/> in.	Total $A_{ps} =$ <input type="text" value="3.680"/> in ²
$f_{py} = 0.85f_{pu} =$ <input type="text" value="229.50"/> ksi	Web Dimensions	Jacking Stress (% f_{pu}) = <input type="text" value="44%"/>
$E_p = E_{ps} =$ <input type="text" value="28,500"/> ksi	$b_{w1} =$ <input type="text" value="7.00"/> in.	$f_{pbt} = f_{pj} = \%f_{pu} =$ <input type="text" value="118.80"/> ksi
$f'_c =$ <input type="text" value="5,600"/> ksi	$b_{w2} =$ <input type="text" value="5.00"/> in.	$f_{cgp} = f_{pj} \times A_{ps}/A_g =$ <input type="text" value="0.63"/> ksi
$E_{ci} = E_{ct} =$ <input type="text" value="2,850"/> ksi	$h_w =$ <input type="text" value="22.00"/> in.	
$w_c =$ <input type="text" value="110"/> lb/ft ³	$A_g =$ <input type="text" value="696.00"/> in ²	$d_{pm} =$ <input type="text" value="22.3755"/> in.
$q = w_c A_g =$ <input type="text" value="531.67"/> lb/ft	$I_g =$ <input type="text" value="41,219.71"/> in ⁴	$\bar{y} =$ <input type="text" value="19.92"/> in.
$L =$ <input type="text" value="53.5"/> ft		$e_m = d_{pm} - [(h_f + h_w) - \bar{y}] =$ <input type="text" value="14.30"/> in.
$M_g = qL^2/8 =$ <input type="text" value="2,283"/> kip-in.		

Total Loss of Prestress

$$\Delta f_{pT} = \Delta f_{pES} + \Delta f_{pLT}$$

$$\Delta f_{pES} = \frac{A_{ps} f_{pbt} (I_g + e_m^2 A_g) - e_m M_g A_g}{A_{ps} (I_g + e_m^2 A_g) + \frac{A_g I_g E_{ci}}{E_p}} \quad (C5.9.5.2.3a-1)$$

$$\Delta f_{pES} = \underline{16.22} \text{ ksi}$$

$$\Delta f_{pLT} = (\Delta f_{pSR} + \Delta f_{pCR} + \Delta f_{pR1})_{id} + (\Delta f_{pSD} + \Delta f_{pCD} + \Delta f_{pR2} - \Delta f_{pSS})_{df} \quad (5.9.5.4.1-1)$$

$$(\Delta f_{pSR})_{df} = 0 \quad (\text{no deck placement following girder construction})$$

$$\Delta f_{pSR} = \epsilon_{bid} E_p K_{id} \quad (5.9.5.4.2a-1)$$

$$\epsilon_{bid} = \epsilon_{sh} = k_s k_{hs} k_f k_{td} 0.48 \times 10^{-3} \quad (5.4.2.3.3-1)$$

$$k_s = \underline{1.07} \quad (5.4.2.3.2-2)$$

$$k_{hs} = 2.00 - 0.014H \quad (5.4.2.3.3-2)$$

$$H = \underline{60} \quad (\text{Figure 5.4.2.3.3-1})$$

$$k_{hs} = \underline{1.16}$$

$$k_f = \underline{0.912} \quad (5.4.2.3.2-4)$$

$$k_{td} = \underline{0.998} \quad (5.4.2.3.2-5)$$

$$\epsilon_{bid} = \underline{0.000544}$$

$$K_{id} = \frac{1}{1 + \frac{E_p A_{ps}}{E_{ci} A_g} \left(1 + \frac{A_g e_p^2}{I_g} \right) [1 + 0.7 \psi_b(t_r, t_i)]} \quad (5.9.5.4.2a-2)$$

$$e_{pg} = e_m = \underline{14.30} \text{ in.}$$

$$\psi(t_r, t_i) = 1.9 k_s k_{hc} k_f k_{td} t_i^{-0.118} \quad (5.4.2.3.2-1)$$

$$k_s = 1.45 - 0.13(V/S) \geq 1.0 \quad (5.4.2.3.2-2)$$

$$V = (h_f \times b_f) + 2[(b_{w1} + b_{w2})/2 \times h_w] = \underline{696.00} \text{ in}^3/\text{in}$$

Full Deck Thickness Prestressing Loss Calculations based on AASHTO LRFD Bridge Design Specifications (Girder #1)

$$S = 2h_f + b_f + (b_f - 2b_{w1}) + 4(\sqrt{h_w^2 + \{(b_{w1} - b_{w2})/2\}^2}) + 2b_{w2} = 240.09 \text{ in}^2/\text{in}$$

$$V/S = 2.90 \text{ in.}$$

$$k_s = \underline{1.07} \geq 1.0, \text{ OK}$$

$$k_{inc} = 1.56 - 0.008H \quad (5.4.2.3.2-3)$$

$$H = \boxed{60}$$

(Figure 5.4.2.3.3-1)

$$k_{inc} = \underline{1.08}$$

$$k_f = 5/(1+f'_{ci}) \quad (5.4.2.3.2-4)$$

$$f'_{ci} = 0.80f'_c$$

$$f'_{ci} = 4.480 \text{ ksi}$$

$$k_f = \underline{0.912}$$

$$k_{td} = t/(61 - 4f'_c + t) \quad (5.4.2.3.2-5)$$

$$t = \boxed{48} \text{ yrs}$$

$$t = 17,520 \text{ days}$$

$$k_{td} = \underline{0.998}$$

$$t_i = \boxed{48} \text{ yrs}$$

$$t_i = 17,520 \text{ days}$$

$$\psi(t_i, t_i) = \underline{0.633}$$

$$K_{id} = \underline{0.746}$$

$$\Delta f_{pSR} = \underline{11.57} \text{ ksi}$$

$$\Delta f_{pCR} = \frac{E_p}{E_{ci}} f_{cgp} \psi_b(t_d, t_i) K_{id} \quad (5.9.5.4.2b-1)$$

$$\psi(t_d, t_i) = \psi(t_i, t_i) = 0.633$$

$$K_{id} = K_{id} \text{ from above} = 0.746$$

$$\Delta f_{pCR} = \underline{2.97} \text{ ksi}$$

$$\Delta f_{pR1} = \left[\frac{f_{pt}}{K'_L} \frac{\log(24t)}{\log(24t_i)} \left(\frac{f_{pt}}{f_{py}} - 0.55 \right) \right] \left[1 - \frac{3(\Delta f_{pSR} + \Delta f_{pCR})}{f_{pt}} \right] K_{id} \quad (C5.9.5.4.2c-1)$$

$$f_{pt} = \underline{126.23} \text{ ksi (} f_{pj} < 0.55f_{py}, \text{ Use } 0.55f_{py} \text{)}$$

$$K'_L = \boxed{10} \text{ (45 for low relaxation steel, 10 for stress relieved steel)}$$

$$t_i = \boxed{0.75} \text{ days}$$

$$t = \boxed{48} \text{ yrs}$$

$$t = 17,520 \text{ days}$$

$$\Delta f_{pR1} = \underline{0.00} \text{ ksi}$$

$$\Delta f_{pLT} = \underline{14.54} \text{ ksi}$$

$$\Delta f_{pT} = \underline{30.76} \text{ ksi} \quad \leftarrow \text{Total loss of prestress}$$

$$f_{pe} = f_{pj} - \Delta f_{pT} = \boxed{88.04} \text{ ksi} \quad \leftarrow \text{Remaining prestress}$$

Full Deck Thickness Prestressing Loss Calculations based on AASHTO LRFD Bridge Design Specifications (Girder #2 & Girder #3)

Note: Outlined values obtained from previous calculations, shaded cells input by user.

$f'_y =$ <input type="text" value="58"/> ksi	Deck Dimensions	# of strands = <input type="text" value="32"/>
$E_s =$ <input type="text" value="29,000"/> ksi	$b_f =$ <input type="text" value="77.50"/> in.	Single strand $A_{ps} =$ <input type="text" value="0.115"/> in ²
$f_{pu} =$ <input type="text" value="270"/> ksi	$h_f =$ <input type="text" value="6.00"/> in.	Total $A_{ps} =$ <input type="text" value="3.680"/> in ²
$f_{py} = 0.85f_{pu} =$ <input type="text" value="229.50"/> ksi	Web Dimensions	Jacking Stress (% f_{pu}) = <input type="text" value="46%"/>
$E_p = E_{ps} =$ <input type="text" value="28,500"/> ksi	$b_{w1} =$ <input type="text" value="7.00"/> in.	$f_{pbt} = f_{pj} = \%f_{pu} =$ <input type="text" value="124.20"/> ksi
$f'_c =$ <input type="text" value="5.600"/> ksi	$b_{w2} =$ <input type="text" value="5.00"/> in.	$f_{cgp} = f_{pj} \times A_{ps}/A_g =$ <input type="text" value="0.63"/> ksi
$E_{ci} = E_{ct} =$ <input type="text" value="2,850"/> ksi	$h_w =$ <input type="text" value="22.00"/> in.	$d_{pm} =$ <input type="text" value="22.3755"/> in.
$w_c =$ <input type="text" value="110"/> lb/ft ³	$A_g =$ <input type="text" value="729.00"/> in ²	$\bar{y} =$ <input type="text" value="20.15"/> in.
$q = w_c A_g =$ <input type="text" value="556.88"/> lb/ft	$I_g =$ <input type="text" value="42,131.30"/> in ⁴	$e_m = d_{pm} - [(h_f + h_w) - \bar{y}] =$ <input type="text" value="14.53"/> in.
$L =$ <input type="text" value="53.5"/> ft		
$M_g = qL^2/8 =$ <input type="text" value="2,391"/> kip-in.		

Total Loss of Prestress

$$\Delta f_{pT} = \Delta f_{pES} + \Delta f_{pLT}$$

$$\Delta f_{pES} = \frac{A_{ps} f_{pbt} (I_g + e_m^2 A_g) - e_m M_g A_g}{A_{ps} (I_g + e_m^2 A_g) + \frac{A_g I_g E_{ci}}{E_p}} \quad (C5.9.5.2.3a-1)$$

$$\Delta f_{pES} = \underline{16.94} \text{ ksi}$$

$$\Delta f_{pLT} = (\Delta f_{pSR} + \Delta f_{pCR} + \Delta f_{pR1})_{id} + (\Delta f_{pSD} + \Delta f_{pCD} + \Delta f_{pR2} - \Delta f_{pSS})_{df} \quad (5.9.5.4.1-1)$$

$$(\Delta f_{pSR})_{df} = 0 \quad (\text{no deck placement following girder construction})$$

$$\Delta f_{pSR} = \epsilon_{bid} E_p K_{id} \quad (5.9.5.4.2a-1)$$

$$\epsilon_{bid} = \epsilon_{sh} = k_s k_{hs} k_f k_{td} 0.48 \times 10^{-3} \quad (5.4.2.3.3-1)$$

$$k_s = \underline{1.07} \quad (5.4.2.3.2-2)$$

$$k_{hs} = 2.00 - 0.014H \quad (5.4.2.3.3-2)$$

$$H = \underline{60} \quad (\text{Figure 5.4.2.3.3-1})$$

$$k_{hs} = \underline{1.16}$$

$$k_f = \underline{0.912} \quad (5.4.2.3.2-4)$$

$$k_{td} = \underline{0.998} \quad (5.4.2.3.2-5)$$

$$\epsilon_{bid} = \underline{0.000544}$$

$$K_{id} = \frac{1}{1 + \frac{E_p A_{ps}}{E_{ci} A_g} \left(1 + \frac{A_g e_{pg}^2}{I_g} \right) [1 + 0.7 \psi_b(t_f, t_i)]} \quad (5.9.5.4.2a-2)$$

$$e_{pg} = e_m = \underline{14.53} \text{ in.}$$

$$\psi(t_f, t_i) = 1.9 k_s k_{hc} k_f k_{td} t_i^{-0.118} \quad (5.4.2.3.2-1)$$

$$k_s = 1.45 - 0.13(V/S) \geq 1.0 \quad (5.4.2.3.2-2)$$

$$V = (h_f \times b_f) + 2[(b_{w1} + b_{w2})/2 \times h_w] = 729.00 \text{ in}^3/\text{in}$$

Full Deck Thickness Prestressing Loss Calculations based on AASHTO LRFD Bridge Design Specifications (Girder #2 & Girder #3)

$$S = 2h_f + b_f + (b_f - 2b_{w1}) + 4(\sqrt{h_w^2 + ((b_{w1} - b_{w2})/2)^2}) + 2b_{w2} = 251.09 \text{ in}^2/\text{in}$$

$$V/S = 2.90 \text{ in.}$$

$$k_s = \underline{1.07} \geq 1.0, \text{ OK}$$

$$k_{hc} = 1.56 - 0.008H \quad (5.4.2.3.2-3)$$

$$H = \boxed{60}$$

(Figure 5.4.2.3.3-1)

$$k_{hc} = \underline{1.08}$$

$$k_f = 5/(1+f'_{ci}) \quad (5.4.2.3.2-4)$$

$$f'_{ci} = 0.80f'_c$$

$$f'_{ci} = 4.480 \text{ ksi}$$

$$k_f = \underline{0.912}$$

$$k_{td} = t/(61 - 4f'_c + t) \quad (5.4.2.3.2-5)$$

$$t = \boxed{48} \text{ yrs}$$

$$t = 17,520 \text{ days}$$

$$k_{td} = \underline{0.998}$$

$$t_i = \boxed{48} \text{ yrs}$$

$$t_i = 17,520 \text{ days}$$

$$\psi(t_i, t) = \underline{0.632}$$

$$K_{id} = \underline{0.747}$$

$$\Delta f_{pSR} = \underline{11.57} \text{ ksi}$$

$$\Delta f_{pCR} = \frac{E_p}{E_{ci}} f_{cgp} \psi_b(t_d, t_i) K_{id} \quad (5.9.5.4.2b-1)$$

$$\psi(t_d, t_i) = \psi(t_i, t) = 0.632$$

$$K_{id} = K_{id} \text{ from above} = 0.747$$

$$\Delta f_{pCR} = \underline{2.96} \text{ ksi}$$

$$\Delta f_{pR1} = \left[\frac{f_{pt}}{K'_L} \frac{\log(24t)}{\log(24t_i)} \left(\frac{f_{pt}}{f_{py}} - 0.55 \right) \right] \left[1 - \frac{3(\Delta f_{pSR} + \Delta f_{pCR})}{f_{pt}} \right] K_{id} \quad (C5.9.5.4.2c-1)$$

$$f_{pt} = \underline{126.23} \text{ ksi (} f_{pj} < 0.55f_{py}, \text{ Use } 0.55f_{py} \text{)}$$

$$K'_L = \boxed{10} \text{ (45 for low relaxation steel, 10 for stress relieved steel)}$$

$$t_i = \boxed{0.75} \text{ days}$$

$$t = \boxed{48} \text{ yrs}$$

$$t = 17,520 \text{ days}$$

$$\Delta f_{pR1} = \underline{0.00} \text{ ksi}$$

$$\Delta f_{pLT} = \underline{14.53} \text{ ksi}$$

$$\Delta f_{pT} = \underline{31.47} \text{ ksi} \quad \leftarrow \text{Total loss of prestress}$$

$$f_{pe} = f_{pj} - \Delta f_{pT} = \boxed{92.73} \text{ ksi} \quad \leftarrow \text{Remaining prestress}$$

Full Deck Thickness Moment Capacity Calculations based on AASHTO Approximate Method (Girders #1, 2, & 3)

Note: Outlined values obtained from previous calculations, shaded cells input by user.

$$M_n = A_{ps}f_{ps}\left(d_p - \frac{a}{2}\right) + A_s f_s \left(d_s - \frac{a}{2}\right) - A'_s f'_s \left(d'_s - \frac{a}{2}\right) + 0.85 f'_c (b - b_w) h_f \left(\frac{a}{2} - \frac{h_f}{2}\right)$$

Girder #1

Prestressing Steel	Mild Steel (Tension)	Mild Steel (Compression)	Concrete
$A_{ps} = 3.68 \text{ in}^2$	$A_s = 0 \text{ in}^2$	$A'_s = 1.44 \text{ in}^2$	$f'_c = 5.600 \text{ ksi}$
$f_{ps} = 255.14 \text{ ksi}$	$f_s = 0 \text{ ksi}$	$f'_s = 0 \text{ ksi}$	$b = 72.00 \text{ in.}$
$d_p = 22.376 \text{ in.}$	$d_s = 0 \text{ in.}$	$d'_s = 3.00 \text{ in.}$	$b_w = 72.00 \text{ in.}$
$K = 0.38$		↑	$h_f = 6.00 \text{ in.}$
$f_{pu} = 270 \text{ ksi}$		Can be ignored (Article 5.7.2.1)	$c = 3.24 \text{ in.}$
$f_{pe} = 88.04 \text{ ksi}$			$a = 2.50 \text{ in.}$
$f_{pe}/f_{pu} = 0.326$			
$f_{ps} = f_{pu}[1-K(c/d_p)] = 255.14 \text{ ksi}$	$(f_{pe} < 0.5f_{pu})$		

$$M_n = 19,836.76 \text{ kip-in} = \underline{1,653} \text{ kip-ft}$$

Girders #2 & #3

Prestressing Steel	Mild Steel (Tension)	Mild Steel (Compression)	Concrete
$A_{ps} = 3.68 \text{ in}^2$	$A_s = 0 \text{ in}^2$	$A'_s = 1.55 \text{ in}^2$	$f'_c = 5.600 \text{ ksi}$
$f_{ps} = 256.23 \text{ ksi}$	$f_s = 0 \text{ ksi}$	$f'_s = 0 \text{ ksi}$	$b = 77.50 \text{ in.}$
$d_p = 22.376 \text{ in.}$	$d_s = 0 \text{ in.}$	$d'_s = 3.00 \text{ in.}$	$b_w = 77.50 \text{ in.}$
$K = 0.38$		↑	$h_f = 6.00 \text{ in.}$
$f_{pu} = 270 \text{ ksi}$		Can be ignored (Article 5.7.2.1)	$c = 3.00 \text{ in.}$
$f_{pe} = 92.73 \text{ ksi}$			$a = 2.31 \text{ in.}$
$f_{pe}/f_{pu} = 0.343$			
$f_{ps} = f_{pu}[1-K(c/d_p)] = 256.23 \text{ ksi}$	$(f_{pe} < 0.5f_{pu})$		

$$M_n = 20,008.25 \text{ kip-in} = \underline{1,667} \text{ kip-ft}$$

Full Deck Thickness Moment Capacity Calculations based on Strain Compatibility Method (Girders #1, 2, & 3)

Note: Outlined values obtained from previous calculations, shaded cells input by user.

Girder #1

Concrete		Prestressing Steel		Mild Steel (Compression)	
$f'_c =$	5.6 ksi	$A_{ps} =$	3.68 in ²	$A'_s =$	1.44 in ²
$h_f =$	6.00 in.	$d_{pm} =$	22.3755 in.	$d_s = h_f/2 =$	3.00 in.
$b =$	72.00 in.	$f_{pe} =$	88.04 ksi	$E_s =$	29,000 ksi
$b_w =$	14.00 in.	$E_{ps} =$	28,500 ksi	$f'_y =$	58 ksi
		$f_{pu} =$	270 ksi		

$$\text{Ultimate Strain Capacity (USC)} = 0.003 \leftarrow \text{Leave 0.003}$$

Step 1: Assume a N.A. Depth

$$c = 3.421 \text{ in}$$

$$\epsilon_{ps} = \text{USC}[(d_{pm}/c)-1] + f_{pe}/E_{ps} = 0.01971$$

$$\epsilon_s = \text{USC}[(d_s/c)-1] = -0.00037$$

Step 2 : Calculate Stress in Each Layer

$$f_{ps} = E_{ps} * \epsilon_{ps} \{0.025 + (0.975/[1 + (118 * \epsilon_{ps})^{10}])^{0.1}\} = 249.53 \text{ ksi} \quad (< 270 \text{ ksi, OK})$$

$$f_s = E_s * \epsilon_s \{0.025 + (0.975/[1 + (118 * \epsilon_s)^{10}])^{0.1}\} = -10.71 \text{ ksi} \quad (< 58 \text{ ksi, OK})$$

Step 3 : Check for Equilibrium of Forces

$$A_{ps}f_{ps} + A'_sf_s = 902.8 \text{ kips} \leftarrow$$

$$\beta_1 = 0.85 - 0.05(f'_c - 4) = 0.77 \quad (> 0.65, \text{OK})$$

$$a = \beta_1 c = 2.63 \text{ in}$$

If $a > h_f$: $\Sigma(-0.85f'_c A_c) = -[0.85f'_c b h_f + 0.85f'_c b_w(a - h_f)] = \text{See Below kips} \leftarrow$

If $a < h_f$: $\Sigma(-0.85f'_c A_c) = -0.85f'_c b a = -902.8 \text{ kips} \leftarrow$

These need to be equal and opposite, change "c" until they are.

Step 4: Calculate Nominal Moment Capacity

$$M_n = A_{ps}f_{ps}d_{pm} + A'_sf_s d_s + 0.85f'_c b a(a/2) = 19,311 \text{ kip-in.} = \underline{1,609 \text{ kip-ft}}$$

Girders #2 & #3

Concrete		Prestressing Steel		Mild Steel (Compression)	
$f'_c =$	5.6 ksi	$A_{ps} =$	3.68 in ²	$A'_s =$	1.55 in ²
$h_f =$	6.00 in.	$d_{pm} =$	22.3755 in.	$d_s = h_f/2 =$	3.00 in.
$b =$	77.50 in.	$f_{pe} =$	92.73 ksi	$E_s =$	29,000 ksi
$b_w =$	14.00 in.	$E_{ps} =$	28,500 ksi	$f'_y =$	58 ksi
		$f_{pu} =$	270 ksi		

$$\text{Ultimate Strain Capacity (USC)} = 0.003 \leftarrow \text{Leave 0.003}$$

Step 1: Assume a N.A. Depth

$$c = 3.214 \text{ in}$$

$$\epsilon_{ps} = \text{USC}[(d_{pm}/c)-1] + f_{pe}/E_{ps} = 0.02114$$

$$\epsilon_s = \text{USC}[(d_s/c)-1] = -0.00020$$

Step 2 : Calculate Stress in Each Layer

$$f_{ps} = E_{ps} * \epsilon_{ps} \{0.025 + (0.975/[1 + (118 * \epsilon_{ps})^{10}])^{0.1}\} = 250.55 \text{ ksi} \quad (< 270 \text{ ksi, OK})$$

$$f_s = E_s * \epsilon_s \{0.025 + (0.975/[1 + (118 * \epsilon_s)^{10}])^{0.1}\} = -5.79 \text{ ksi} \quad (< 58 \text{ ksi, OK})$$

 Full Deck Thickness Moment Capacity Calculations based on Strain Compatibility Method (Girders #1, 2, & 3)

Step 3 : Check for Equilibrium of Forces

$$\begin{aligned}
 A_{ps}f_{ps} + A'_s f'_s &= 913.0 \text{ kips} \leftarrow \\
 \beta_1 = 0.85 - 0.05(f'_c - 4) &= 0.77 \text{ } (> 0.65, \text{ OK}) \\
 a = \beta_1 c &= 2.47 \text{ in} \\
 \text{If } a > h_f : \Sigma(-0.85f'_c A_c) &= -[0.85f'_c b h_f + 0.85f'_c b_w(a - h_f)] = \text{See Below kips} \leftarrow \\
 \text{If } a < h_f : \Sigma(-0.85f'_c A_c) &= -0.85f'_c b a = -912.9 \text{ kips} \leftarrow
 \end{aligned}$$

These need to be equal and opposite, change "c" until they are.

Step 4: Calculate Nominal Moment Capacity

$$M_n = A_{ps}f_{ps}d_{pm} + A'_s f'_s d_s + 0.85f'_c b a(a/2) = 19,474 \text{ kip-in.} = \underline{1,623} \text{ kip-ft}$$

Full Deck Thickness Maximum Deflection Calculations based on AASHTO Section 5.7.3.6 (Girder #1)

Note: Outlined values obtained from previous calculations, shaded cells input by user.

Concrete		Prestressing Steel		Mild Steel (Compression)	
$f'_c =$	5.6 ksi	$A_{ps} =$	3.68 in ²	$A'_s =$	1.44 in ²
$E_c =$	2,850 ksi	$d = d_{pm} =$	22.3755 in.	$d_s = h_f/2 =$	3.00 in.
$h_f =$	6.00 in.	$f_{pe} =$	88.04 ksi	$E_s =$	29,000 ksi
$b =$	72.00 in.	$E_{ps} =$	28,500 ksi	$f'_y =$	58 ksi
$b_w =$	14.00 in.	$f_{pu} =$	270 ksi		
$h_w =$	22.00 in.	$P_e =$	323.98 kips		
$h =$	28.00 in.	$e =$	14.30 in.		
$I_g =$	41,219.71 in. ⁴				
$A_g =$	696.00 in ²				
$f_r = 0.17V(f'_c) =$	0.402 ksi				
$\gamma_t = \bar{\gamma} =$	19.921 in.				

$$M_{cr} = [(P_e/A_g) + (P_e e \gamma_t / I_g) - f_r] \times (I_g / \gamma_t)$$

$$M_{cr} = 4,762.68 \text{ kip-in.}$$

$$F = 90.7 \text{ kips}$$

$$P = F/2 = 45.35 \text{ kips}$$

$$L = 49 \text{ ft}$$

$$X = 6 \text{ ft}$$

$$M_a = P(L/2 - X/2) = 11,700 \text{ kip-in.}$$

$$n = E_{ps} / E_c = 10.00$$

$$nA_{ps} = 36.80 \text{ in}^2$$

$$\text{Trial } k_d = 4.299 \text{ in.} \quad \leftarrow \text{kd is in flange}$$

$$b(k_d^2/2) = nA_{ps}(d - k_d)$$

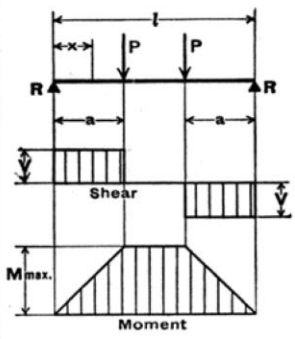
$$b(k_d^2/2) - nA_{ps}(d - k_d) = 0.011 \quad \leftarrow \text{should be approximately equal to zero}$$

$$I_{cr} = (1/3)bk_d^3 + nA_{ps}(d - k_d)^2 = 13,931.60 \text{ in.}^4$$

$$I_e = \left(\frac{M_{cr}}{M_a}\right)^3 I_g + \left[1 - \left(\frac{M_{cr}}{M_a}\right)^3\right] I_{cr} \leq I_g \quad (5.7.3.6.2-1)$$

$$I_e = 15,772.10 \text{ in.}^4$$

9. SIMPLE BEAM—TWO EQUAL CONCENTRATED LOADS SYMMETRICALLY PLACED



Total Equiv. Uniform Load	$= \frac{8 Pa}{l}$
R = V	$= P$
M max. (between loads)	$= Pa$
M_x (when x < a)	$= Px$
Δ_{max.} (at center)	$= \frac{Pa}{24EI} (3l^2 - 4a^2)$
Δ_x (when x < a)	$= \frac{Px}{6EI} (3la - 3a^2 - x^2)$
Δ_x (when x > a and < (l - a))	$= \frac{Pa}{6EI} (3lx - 3x^2 - a^2)$

(AISC. 1998)

$$\Delta_{max} = 8.36 \text{ in.}$$

Full Deck Thickness Maximum Deflection Calculations based on AASHTO Section 5.7.3.6 (Girder #2)

Note: Outlined values obtained from previous calculations, shaded cells input by user.

Concrete		Prestressing Steel		Mild Steel (Compression)	
$f'_c =$	5.6 ksi	$A_{ps} =$	3.68 in ²	$A'_s =$	1.55 in ²
$E_c =$	2,850 ksi	$d = d_{pm} =$	22.3755 in.	$d_s = h_f/2 =$	3.00 in.
$h_f =$	6.00 in.	$f_{pe} =$	92.73 ksi	$E_s =$	29,000 ksi
$b =$	77.50 in.	$E_{ps} =$	28,500 ksi	$f'_y =$	58 ksi
$b_w =$	14.00 in.	$f_{pu} =$	270 ksi		
$h_w =$	22.00 in.	$P_e =$	341.23 kips		
$h =$	28.00 in.	$e =$	14.53 in.		
$I_g =$	42,131.30 in. ⁴				
$A_g =$	729.00 in ²				
$f_r = 0.17V(f'_c) =$	0.402 ksi				
$y_t = \bar{y} =$	20.151 in.				

$$M_{cr} = [(P_e/A_g) + (P_e e y_t / I_g) - f_r] \times (I_g / y_t)$$

$$M_{cr} = 5,094.54 \text{ kip-in.}$$

$$F = 99.8 \text{ kips}$$

$$P = F/2 = 49.9 \text{ kips}$$

$$L = 49 \text{ ft}$$

$$X = 6 \text{ ft}$$

$$M_a = P(L/2 - X/2) = 12,874 \text{ kip-in.}$$

$$n = E_{ps}/E_c = 10.00$$

$$nA_{ps} = 36.80 \text{ in}^2$$

$$\text{Trial } k_d = 4.159 \text{ in.} \quad \leftarrow \text{kd is in flange}$$

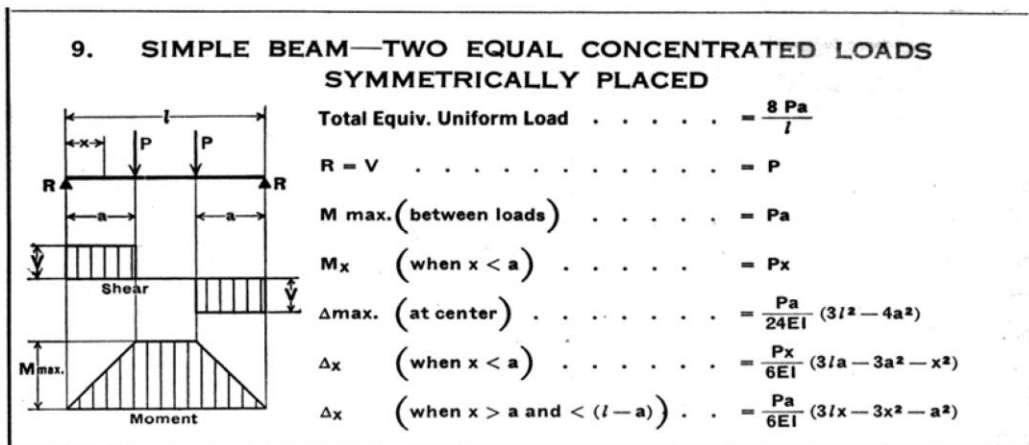
$$b(k_d^2/2) = nA_{ps}(d - k_d)$$

$$b(k_d^2/2) - nA_{ps}(d - k_d) = 0.010 \quad \leftarrow \text{should be approximately equal to zero}$$

$$I_{cr} = (1/3)bk_d^3 + nA_{ps}(d - k_d)^2 = 14,070.18 \text{ in.}^4$$

$$I_e = \left(\frac{M_{cr}}{M_a} \right)^3 I_g + \left[1 - \left(\frac{M_{cr}}{M_a} \right)^3 \right] I_{cr} \leq I_g \quad (5.7.3.6.2-1)$$

$$I_e = 15,809.02 \text{ in.}^4$$



(AISC. 1998)

$$\Delta_{max} = 9.18 \text{ in.}$$

Full Deck Thickness Maximum Deflection Calculations based on AASHTO Section 5.7.3.6 (Girder #3)

Note: Outlined values obtained from previous calculations, shaded cells input by user.

Concrete		Prestressing Steel		Mild Steel (Compression)	
f'_c =	5.6 ksi	A_{ps} =	3.68 in ²	A'_s =	1.55 in ²
E_c =	2,850 ksi	$d = d_{pm}$ =	22.3755 in.	$d_s = h_f/2$ =	3.00 in.
h_f =	6.00 in.	f_{pe} =	92.73 ksi	E_s =	29,000 ksi
b =	77.50 in.	E_{ps} =	28,500 ksi	f'_y =	58 ksi
b_w =	14.00 in.	f_{pu} =	270 ksi		
h_w =	22.00 in.	P_e =	341.23 kips		
h =	28.00 in.	e =	14.53 in.		
I_g =	42,131.30 in. ⁴				
A_g =	729.00 in ²				
$f_r = 0.17V(f'_c)$ =	0.402 ksi				
$y_t = \bar{y}$ =	20.151 in.				

$$M_{cr} = [(P_e/A_g) + (P_e e y_t / I_g) - f_r] \times (I_g / y_t)$$

$$M_{cr} = 5,094.54 \text{ kip-in.}$$

$$F = 108.9 \text{ kips}$$

$$P = F/2 = 54.45 \text{ kips}$$

$$L = 49 \text{ ft}$$

$$X = 7 \text{ ft}$$

$$M_a = P(L/2 - X/2) = 13,721 \text{ kip-in.}$$

$$n = E_{ps}/E_c = 10.00$$

$$nA_{ps} = 36.80 \text{ in}^2$$

$$\text{Trial } k_d = 4.159 \text{ in.} \quad \leftarrow \text{kd is in flange}$$

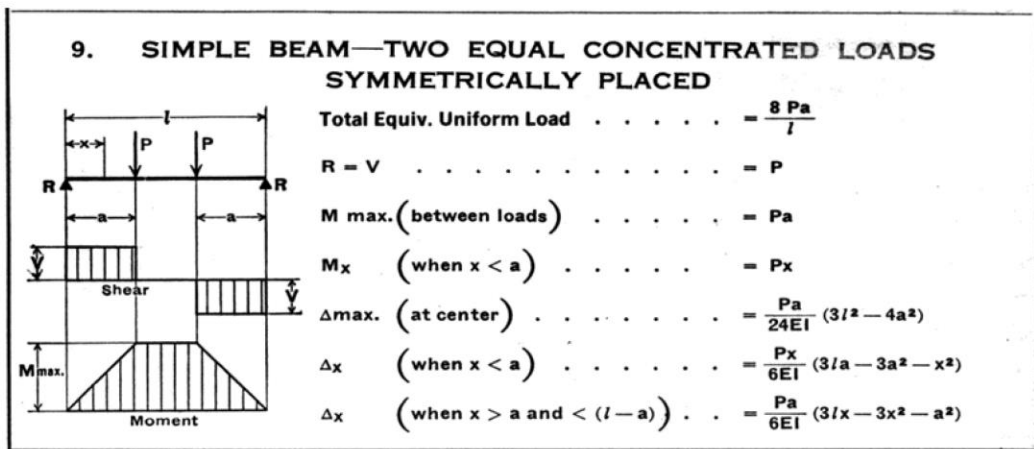
$$b(k_d^2/2) = nA_{ps}(d - k_d)$$

$$b(k_d^2/2) - nA_{ps}(d - k_d) = 0.010 \quad \leftarrow \text{should be approximately equal to zero}$$

$$I_{cr} = (1/3)bk_d^3 + nA_{ps}(d - k_d)^2 = 14,070.18 \text{ in.}^4$$

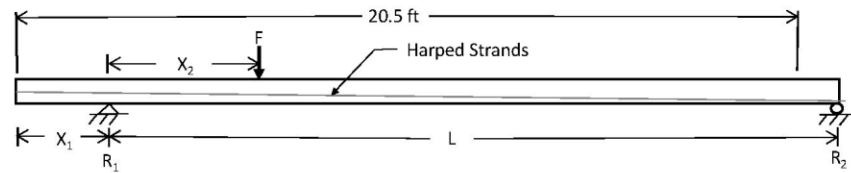
$$I_e = \left(\frac{M_{cr}}{M_a}\right)^3 I_g + \left[1 - \left(\frac{M_{cr}}{M_a}\right)^3\right] I_{cr} \leq I_g \quad (5.7.3.6.2-1)$$

$$I_e = 15,506.41 \text{ in.}^4$$



(AISC. 1998)

$$\Delta_{max} = 10.13 \text{ in.}$$

Full Deck Thickness Shear Capacity Calculations based on AASHTO Simplified Method (2d_v)

Note: Outlined values obtained from previous calculations, shaded cells input by user.

$X_1 =$ <input type="text" value="21"/> in.	$f'_c =$ <input type="text" value="5.6"/> ksi	$d_v =$ <input type="text" value="15.76"/> in.
$X_2 =$ <input type="text" value="42"/> in.	$b_v =$ <input type="text" value="12.23"/> in.	$0.9d_e =$ <input type="text" value="15.28"/> in.
$L =$ <input type="text" value="19"/> ft = 228 in.	$d_v =$ <input type="text" value="20.16"/> in.	$0.72h =$ <input type="text" value="20.16"/> in. (USE for d_v)
$w_c =$ <input type="text" value="110"/> lb/ft ³	$d_e =$ <input type="text" value="16.98"/> in.	
	$h =$ <input type="text" value="28.00"/> in.	
	$f_r = 0.17\sqrt{f'_c} =$ <input type="text" value="0.402"/> ksi	$d_{pm} =$ <input type="text" value="22.38"/> in.
	$I_g = I_c =$ <input type="text" value="41,219.71"/> in. ⁴	$d_{pe} =$ <input type="text" value="15.13"/> in.
	$\bar{y} = c_c = c_g =$ <input type="text" value="19.92"/> in.	$L_h =$ <input type="text" value="20.50"/> ft (length of harp)
	$e = c_2 = (h - \bar{y}) - d_e =$ <input type="text" value="8.90"/> in.	$\psi =$ <input type="text" value="1.69"/> ° ($\tan[(d_{pm} - d_{pe})/L_h]$)
	$A_g =$ <input type="text" value="696.00"/> in. ²	
	$W_d = w_c(A_g) =$ <input type="text" value="0.0443"/> kip/in	
	$V_i =$ <input type="text" value="315.1"/> kips	
	$M_{max} = [V_i(L - X_2)/L](X_2) =$ <input type="text" value="10,794.61"/> kip-in.	
	$P_e =$ <input type="text" value="325.68"/> kips	

Shear Steel	
$f_y =$ <input type="text" value="58"/> ksi	
# <input type="text" value="4"/> bars	
# of bars <input type="text" value="2"/>	
$A_v =$ <input type="text" value="0.39"/> in. ²	
$s =$ <input type="text" value="22"/> in.	
$\alpha =$ <input type="text" value="95"/> degrees	

$$V_n = \text{the lesser of}; \quad V_n = 0.25f'_c b_v d_v + V_p \quad \text{and} \quad V_n = V_c + V_s + V_p$$

$$V_p = P_e \sin \psi$$

$$V_p = \underline{9.59} \text{ kips}$$

$$V_{n1} = 0.25f'_c b_v d_v + V_p = \underline{345.1} \text{ kips} \quad (5.8.3.3-2)$$

$$V_{n2} = V_c + V_s + V_p \quad (5.8.3.3-1)$$

$$V_c = \text{the lesser of } V_{ci} \text{ and } V_{cw}$$

$$V_{ci} = 0.02(0.75\sqrt{f'_c})b_v d_v + V_d + \frac{V_i M_{cre}}{M_{max}} \geq 0.06(0.75\sqrt{f'_c})b_v d_v \quad (5.8.3.4.3-1)$$

$$0.06(0.75\sqrt{f'_c})b_v d_v = \underline{26.25} \text{ kips}$$

$$V_d = (W_d/2)(L - X_2) = \underline{4.12} \text{ kips}$$

$$M_{cre} = S_c (f_r + f_{cpe} - \frac{M_{dnc}}{S_{nc}}) \quad (5.8.3.4.3-2)$$

$$S_c = I_c / c_c = \underline{2069.11} \text{ in.}^3$$

$$f_{cpe} = (P_e / A_g) + (P_e c_2 c_g / I_g) = \underline{1.869} \text{ ksi}$$

$$M_{dnc} = (W_d X_2 / 2)(L - X_2) = \underline{173.06} \text{ kip-in.}$$

$$S_{nc} = I_g / c_g = \underline{2069.11} \text{ in.}^3$$

$$M_{cre} = \underline{4,527.15} \text{ kip-in.}$$

$$V_{ci} = \underline{145.00} \text{ kips}$$

$$V_{cw} = [0.06(0.75\sqrt{f'_c}) + 0.30f_{pc}]b_v d_v + V_p \quad (5.8.3.4.3-3)$$

$$f_{pc} = \frac{P_e}{A_g} + \frac{P_e e(c_c - c_g)}{I_g} + \frac{M_d(c_c - c_g)}{I_g}$$

$$M_d = M_{dnc} = \underline{173.06} \text{ kip-in.}$$

$$f_{pc} = \underline{0.468} \text{ ksi}$$

$$V_{cw} = \underline{70.44} \text{ kips}$$

$$V_c = \underline{70.44} \text{ kips}$$

$$V_s = \frac{A_v f_y d_v (\cot \theta + \cot \alpha) \sin \alpha}{s} \quad (5.8.3.3-4)$$

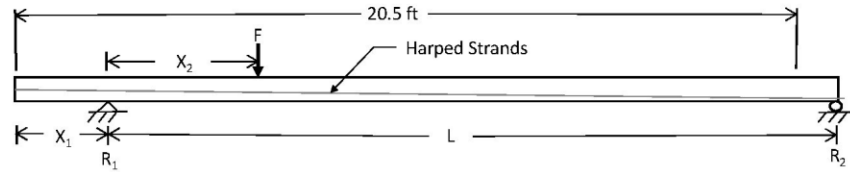
$$\cot \theta = 1.593 \quad V_c > V_{cw}$$

$$V_s = \underline{37.96} \text{ kips}$$

$$V_{n2} = \underline{117.99} \text{ kips}$$

$$V_n = \boxed{117.99} \text{ kips}$$

Full Deck Thickness Shear Capacity Calculations based on AASHTO Simplified Method (3d_v)



Note: Outlined values obtained from previous calculations, shaded cells input by user.

X ₁ = 21 in.	f' _c = 5.6 ksi	d _v = 16.38 in.
X ₂ = 63 in.	b _v = 12.11 in.	0.9d _e = 15.84 in.
L = 19 ft = 228 in.	d _v = 20.16 in.	0.72h = 20.16 in. (USE for d _v)
w _c = 110 lb/ft ³	d _e = 17.60 in.	d _{pm} = 22.38 in.
	h = 28.00 in.	d _{pe} = 15.13 in.
	f _r = 0.17V(f' _c) = 0.402 ksi	L _h = 20.50 ft (length of harp)
	l _g = l _c = 41,219.71 in. ⁴	ψ = 1.69 ° (tan[(d _{pm} -d _{pe})/L _h])
	ȳ = c _c = c _g = 19.92 in.	
	e = c ₂ = (h-ȳ)-d _e = 9.52 in.	
	A _g = 696.00 in. ²	
	W _d = w _c (A _g) = 0.0443 kip/in	
	V _i = 188.0 kips	
	M _{max} = [V _i (L-x ₂)/L](x ₂) = 8,571.32 kip-in.	
	P _e = 325.68 kips	

Shear Steel	
f _y = 58 ksi	
# = 4 bars	
# of bars = 2	
A _v = 0.39 in. ²	
s = 22 in.	
α = 95 degrees	

V_n = the lesser of; $V_n = 0.25f'_c b_v d_v + V_p$ and $V_n = V_c + V_s + V_p$

$V_p = P_e \sin \psi$

$V_p = 9.59$ kips

$V_{n1} = 0.25f'_c b_v d_v + V_p = 341.9$ kips (5.8.3.3-2)

$V_{n2} = V_c + V_s + V_p$ (5.8.3.3-1)

V_c = the lesser of V_{ci} and V_{cw}

$V_{ci} = 0.02(0.75\sqrt{f'_c})b_v d_v + V_d + \frac{V_i M_{cre}}{M_{max}} \geq 0.06(0.75\sqrt{f'_c})b_v d_v$ (5.8.3.4.3-1)

$0.06(0.75\sqrt{f'_c})b_v d_v = 26.01$ kips

$V_d = (W_d/2)(L-x_2) = 3.66$ kips

$M_{cre} = S_c (f_r + f_{cpe} - \frac{M_{dnc}}{S_{nc}})$ (5.8.3.4.3-2)

$S_c = I_g/c_c = 2069.11$ in.³

$f_{cpe} = (P_e/A_g) + (P_e c_2 c_g / I_g) = 1.967$ ksi

$M_{dnc} = (W_d x_2 / 2)(L-x_2) = 230.28$ kip-in.

$S_{nc} = I_g/c_g = 2069.11$ in.³

$M_{cre} = 4,671.51$ kip-in.

$V_{ci} = 114.79$ kips

Full Deck Thickness Shear Capacity Calculations based on AASHTO Simplified Method (3d_v)

$$V_{cw} = [0.06(0.75\sqrt{f'_c}) + 0.30f_{pc}]b_v d_v + V_p \quad (5.8.3.4.3-3)$$

$$f_{pc} = \frac{P_e}{A_g} + \frac{P_e e(c_c - c_g)}{I_g} + \frac{M_d(c_c - c_g)}{I_g}$$

$$M_d = M_{dnc} = \underline{230.28} \text{ kip-in.}$$

$$f_{pc} = \underline{0.468} \text{ ksi}$$

$$V_{cw} = \underline{69.88} \text{ kips}$$

$$V_c = \underline{69.88} \text{ kips}$$

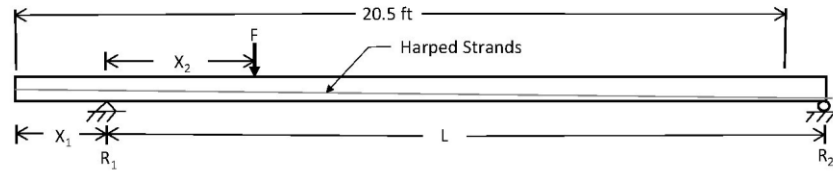
$$V_s = \frac{A_v f_y d_v (\cot \theta + \cot \alpha) \sin \alpha}{s} \quad (5.8.3.3-4)$$

$$\cot \theta = 1.593 \quad V_c > V_{cw}$$

$$V_s = \underline{37.96} \text{ kips}$$

$$V_{n2} = \underline{117.44} \text{ kips}$$

$$V_n = \boxed{117.44} \text{ kips}$$

Full Deck Thickness Shear Capacity Calculations based on AASHTO Simplified Method (4d_v)

Note: Outlined values obtained from previous calculations, shaded cells input by user.

$X_1 =$ <input type="text" value="21"/> in.	$f'_c =$ <input type="text" value="5.6"/> ksi	$d_v =$ <input type="text" value="16.99"/> in.
$X_2 =$ <input type="text" value="84"/> in.	$b_v =$ <input type="text" value="12.00"/> in.	$0.9d_e =$ <input type="text" value="16.40"/> in.
$L =$ <input type="text" value="19"/> ft = 228 in.	$d_v =$ <input type="text" value="20.16"/> in.	$0.72h =$ <input type="text" value="20.16"/> in. (USE for d_v)
$w_c =$ <input type="text" value="110"/> lb/ft ³	$d_e =$ <input type="text" value="18.22"/> in.	
	$h =$ <input type="text" value="28.00"/> in.	
	$f_r = 0.17\sqrt{f'_c} =$ <input type="text" value="0.402"/> ksi	$d_{pm} =$ <input type="text" value="22.38"/> in.
	$I_g = I_c =$ <input type="text" value="41,219.71"/> in. ⁴	$d_{pe} =$ <input type="text" value="15.13"/> in.
	$\bar{y} = c_c = c_g =$ <input type="text" value="19.92"/> in.	$L_h =$ <input type="text" value="20.50"/> ft (length of harp)
	$e = c_2 = (h - \bar{y}) - d_e =$ <input type="text" value="10.14"/> in.	$\psi =$ <input type="text" value="1.69"/> ° ($\tan^{-1}[(d_{pm} - d_{pe})/L_h]$)
	$A_g =$ <input type="text" value="696.00"/> in. ²	
	$W_d = w_c(A_g) =$ <input type="text" value="0.0443"/> kip/in	
	$V_i =$ <input type="text" value="182.4"/> kips	
	$M_{max} = [V_i(L - X_2)]/L =$ <input type="text" value="9,676.80"/> kip-in.	
	$P_e =$ <input type="text" value="325.68"/> kips	

$$V_n = \text{the lesser of; } V_n = 0.25f'_c b_v d_v + V_p \quad \text{and} \quad V_n = V_c + V_s + V_p$$

$$V_p = P_e \sin \psi$$

$$V_p = \underline{9.59} \text{ kips}$$

$$V_{n1} = 0.25f'_c b_v d_v + V_p = \underline{338.7} \text{ kips} \quad (5.8.3.3-2)$$

$$V_{n2} = V_c + V_s + V_p \quad (5.8.3.3-1)$$

$$V_c = \text{the lesser of } V_{ci} \text{ and } V_{cw}$$

$$V_{ci} = 0.02(0.75\sqrt{f'_c})b_v d_v + V_d + \frac{V_i M_{cre}}{M_{max}} \geq 0.06(0.75\sqrt{f'_c})b_v d_v \quad (5.8.3.4.3-1)$$

$$0.06(0.75\sqrt{f'_c})b_v d_v = \underline{25.77} \text{ kips}$$

$$V_d = (W_d/2)(L - X_2) = \underline{3.19} \text{ kips}$$

$$M_{cre} = S_c(f_r + f_{cpe} - \frac{M_{dnc}}{S_{nc}}) \quad (5.8.3.4.3-2)$$

$$S_c = I_g/c_c = \underline{2069.11} \text{ in.}^3$$

$$f_{cpe} = (P_e/A_g) + (P_e c_2 c_g / I_g) = \underline{2.064} \text{ ksi}$$

$$M_{dnc} = (W_d X_2 / 2)(L - X_2) = \underline{267.96} \text{ kip-in.}$$

$$S_{nc} = I_g/c_g = \underline{2069.11} \text{ in.}^3$$

$$M_{cre} = \underline{4,835.40} \text{ kip-in.}$$

Full Deck Thickness Shear Capacity Calculations based on AASHTO Simplified Method (4d_v)

$$V_d = \underline{102.92} \text{ kips}$$

$$V_{cw} = [0.06(0.75\sqrt{f'_c}) + 0.30f_{pc}] b_v d_v + V_p \quad (5.8.3.4.3-3)$$

$$f_{pc} = \frac{P_e}{A_g} + \frac{P_e e(c_c - c_g)}{I_g} + \frac{M_d(c_c - c_g)}{I_g}$$

$$M_d = M_{dnc} = \underline{267.96} \text{ kip-in.}$$

$$f_{pc} = \underline{0.468} \text{ ksi}$$

$$V_{cw} = \underline{69.32} \text{ kips}$$

$$V_c = \underline{69.32} \text{ kips}$$

$$V_s = \frac{A_v f_y d_v (\cot \theta + \cot \alpha) \sin \alpha}{s} \quad (5.8.3.4-4)$$

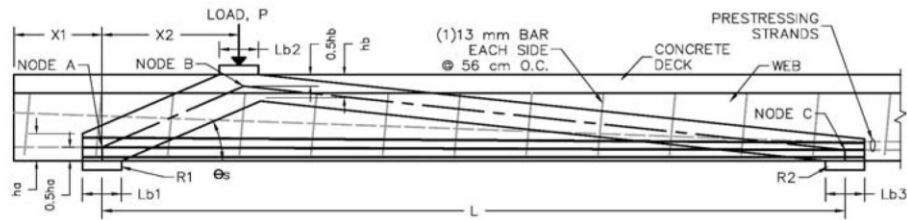
$$\cot \theta = 1.593 \quad V_c > V_{cw}$$

$$V_s = \underline{37.96} \text{ kips}$$

$$V_{n2} = \underline{116.88} \text{ kips}$$

$$V_n = \boxed{116.88} \text{ kips}$$

Full Deck Thickness Shear Capacity Calculations based on AASHTO Strut & Tie Method (2d_v)



Note: Outlined values obtained from previous calculations, shaded cells input by user.

X ₁ = 27 in.	f' _c = 5.600 ksi	h _r = 6.00 in.
X ₂ = 42 in.	f' _{ce} = 4.200 ksi (0.75f' _c for c-c-t)	h _w = 22.00 in.
L = 19 ft = 228 in.	f' _{ce} = 4.760 ksi (0.85f' _c for c-c-c)	h = h _r + h _w = 28.00 in.
L _{b1} = 12 in.	E _c = 2,850 ksi	d _{pm} = 22.376 in.
L _{b2} = 12 in.	E _{ps} = 28,500 ksi	d _{pe} = 15.125 in.
L _{b3} = 12 in.	A _{ps} = 3.68 in. ²	L _n = 20.50 ft
b _{w1} = 14.00 in.	P _e = 325.68 kips	d _p = 15.921 in.
b _{w2} = 10.00 in.	ε _{ps} = 0.003105	c _p = 0.5h _s = h - d _p = 12.079 in.
t _r = b = 72.00 in.		t _w = 13.10 in.

$$M_B = f_{ce} h_b t [h - c_p - (h_b/2)]$$

Trial P = 281.57 kips
 Trial h_b = 1.88 in. hb < hf, hb is in flange

$$R_1 = R_A = P[(L - X_2)/L] = 229.70 \text{ kips}$$

$$M_B = R_A X_2 = 9,647.48 \text{ kip-in}$$

$$0 = f_{ce} h_b t [h - c_p - (h_b/2)] - M_B$$

0.00 ← change P until zero

Solve for h_b

Solving for h_b above = 1.88 in.

$$\theta_1 = \tan^{-1}[(h - h_b/2 - c_p)/X_2] = 15.86 \text{ degrees}$$

$$\theta_2 = \tan^{-1}[(d_{pm} - d_{pe})/L_n] = 1.69 \text{ degrees}$$

$$\theta = \theta_1 + \theta_2 = 17.55 \text{ degrees}$$

$$F_{AB} = R_A / (\sin\theta_1 + \cos\theta_1 \tan\theta_2) = 761.34 \text{ kips}$$

$$F_{AC} = F_{AB} \cos(\theta_1) / \cos(\theta_2) = 732.66 \text{ kips}$$

$$\epsilon_s = (F_{AC}/A_{ps})/E_{ps} - \epsilon_{ps} = 0.00388$$

$$\epsilon_1 = \epsilon_s + (\epsilon_s + 0.002) \cot^2 \theta = 0.062658$$

$$f_{cu} = f'_c / (0.8 + 170\epsilon_1) \leq 0.85f'_c$$

$$0.85f'_c = 4.76 \text{ ksi}$$

$$f'_c / (0.8 + 170\epsilon_1) = 0.489 \text{ ksi}$$

$$f_{cu} = 0.489 \text{ ksi}$$

$$P_n = f_{cu} A_{cs}$$

$$A_{cs} = [L_{b1} \sin(\theta_1) + h_b \cos(\theta_1)]t = 1909.34 \text{ in.}^2$$

$$P_n = 933.68 \text{ kips}$$

$$V = P_n \sin(\theta) = 281.57 \text{ kips}$$

Full Deck Thickness Theoretical Deflection and Camber Calculations (Girder #1)

Note: Outlined values obtained from previous calculations, shaded cells input by user.

Deflection due to prestressing

$L = 53.5$ ft. = 642.0 in.
 $a = 20.5$ ft. = 246.0 in.
 $E_c = 2,850,000$ psi
 $I_g = 41,219.71$ in.⁴

$e_{e1} = \bar{y} - (h - d_{pte}) = 4.30$ in. (eccentricity of harped strands at end of girder)
 $e_{c1} = \bar{y} - (h - d_{ptm}) = 13.61$ in. (eccentricity of harped strands at midspan of girder)
 $e_{c2} = \bar{y} - (h - d_{pbm}) = 16.36$ in. (eccentricity of straight strands)

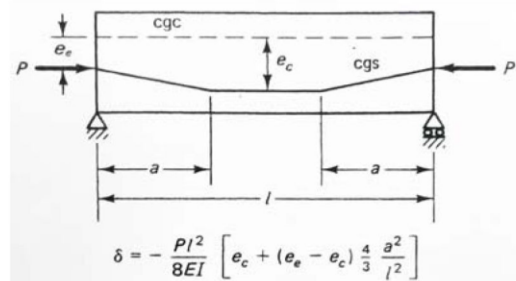
Initial Prestressing, $P = 437,184$ lbs

P of Harped Strands = $3/4P = 327,888$ lbs

$\Delta_1 = 2.22$ in.

Time-dependent multiplier = 2.45 (PCI Table 8.7.1-1)

$\Delta_{1T} = 5.44$ in.

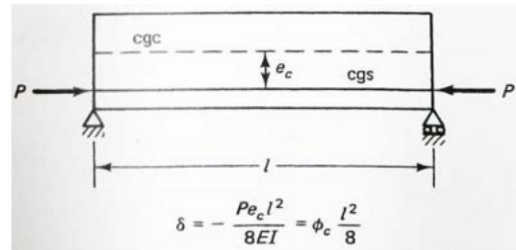


P of Straight Strands = $1/4P = 109,296$ lbs

$\Delta_2 = 0.78$ in.

Time-dependent multiplier = 2.45 (PCI Table 8.7.1-1)

$\Delta_{2T} = 1.92$ in.



(Nawy 2006)

Deflection due to self-weight

$w_c = 110$ lb/ft³

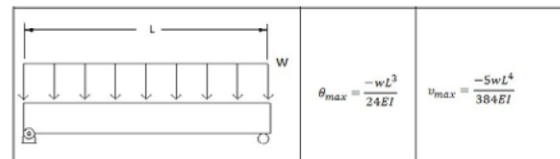
$A = 4.833$ ft²

$w = w_c \times A = 531.667$ lb/ft

$\Delta_3 = -5wL^4 / (384E_cI) = -0.83$ in.

Time-dependent multiplier = 2.70 (PCI Table 8.7.1-1)

$\Delta_{3T} = -2.25$ in.



(Nilson 1987)

$\Delta_{Total} = \Delta_{1T} + \Delta_{2T} + \Delta_{3T} = 5.11$ in.

Full Deck Thickness Theoretical Deflection and Camber Calculations (Girder #2)

Note: Outlined values obtained from previous calculations, shaded cells input by user.

Deflection due to prestressing

$L = 53.5$ ft. = 642.0 in.
 $a = 20.5$ ft. = 246.0 in.
 $E_c = 2,850,000$ psi
 $I_g = 42,131.30$ in.⁴

$e_{e1} = \bar{y} - (h - d_{pte}) = 4.53$ in. (eccentricity of harped strands at end of girder)
 $e_{c1} = \bar{y} - (h - d_{ptm}) = 13.84$ in. (eccentricity of harped strands at midspan of girder)
 $e_{c2} = \bar{y} - (h - d_{pbm}) = 16.59$ in. (eccentricity of straight strands)

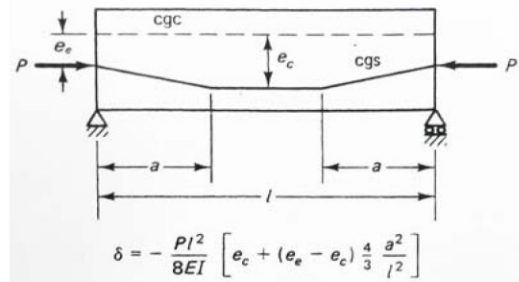
Initial Prestressing, $P = 457,056$ lbs

P of Harped Strands = $3/4P = 342,792$ lbs

$\Delta_1 = 2.30$ in.

Time-dependent multiplier = 2.45 (PCI Table 8.7.1-1)

$\Delta_{1T} = 5.64$ in.

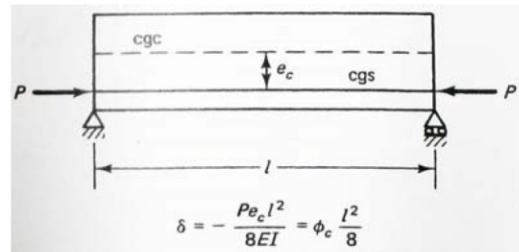


P of Straight Strands = $1/4P = 114,264$ lbs

$\Delta_2 = 0.81$ in.

Time-dependent multiplier = 2.45 (PCI Table 8.7.1-1)

$\Delta_{2T} = 1.99$ in.



(Nawy 2006)

Deflection due to self-weight

$w_c = 110$ lb/ft³

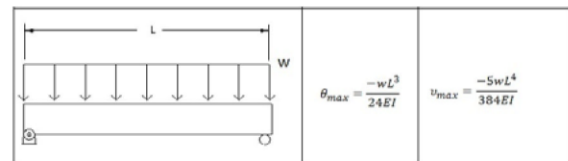
$A = 5.063$ ft²

$w = w_c \times A = 556.875$ lb/ft

$\Delta_3 = -5wL^4 / (384E_cI) = -0.85$ in.

Time-dependent multiplier = 2.70 (PCI Table 8.7.1-1)

$\Delta_{3T} = -2.31$ in.



(Nilson 1987)

$\Delta_{Total} = \Delta_{1T} + \Delta_{2T} + \Delta_{3T} = 5.33$ in.

Full Deck Thickness Theoretical Deflection and Camber Calculations (Girder #3)

Note: Outlined values obtained from previous calculations, shaded cells input by user.

Deflection due to prestressing

$L = 53.5$ ft. = 642.0 in.
 $a = 20.5$ ft. = 246.0 in.
 $E_c = 2,850,000$ psi
 $I_g = 42,131.30$ in.⁴

$e_{e1} = \bar{y} - (h - d_{pte}) = 4.53$ in. (eccentricity of harped strands at end of girder)
 $e_{c1} = \bar{y} - (h - d_{ptm}) = 13.84$ in. (eccentricity of harped strands at midspan of girder)
 $e_{c2} = \bar{y} - (h - d_{pbm}) = 16.59$ in. (eccentricity of straight strands)

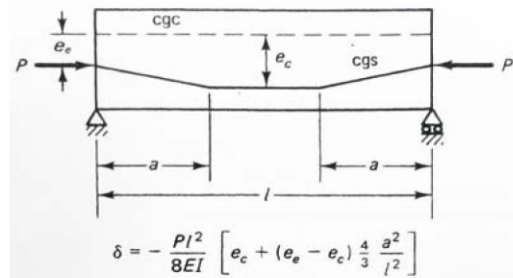
Initial Prestressing, $P = 457,056$ lbs

P of Harped Strands = $3/4P = 342,792$ lbs

$\Delta_1 = 2.30$ in.

Time-dependent multiplier = 2.45 (PCI Table 8.7.1-1)

$\Delta_{1T} = 5.64$ in.

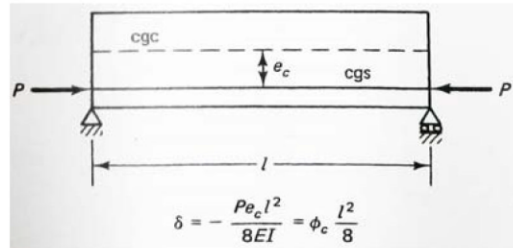


P of Straight Strands = $1/4P = 114,264$ lbs

$\Delta_2 = 0.81$ in.

Time-dependent multiplier = 2.45 (PCI Table 8.7.1-1)

$\Delta_{2T} = 1.99$ in.



(Nawy 2006)

Deflection due to self-weight

$w_c = 110$ lb/ft³

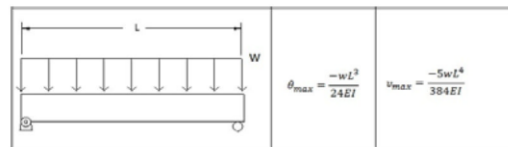
$A = 5.063$ ft²

$w = w_c \times A = 556.875$ lb/ft

$\Delta_3 = -5wL^4 / (384E_cI) = -0.85$ in.

Time-dependent multiplier = 2.70 (PCI Table 8.7.1-1)

$\Delta_{3T} = -2.31$ in.



(Nilson 1987)

$\Delta_{Total} = \Delta_{1T} + \Delta_{2T} + \Delta_{3T} = 5.33$ in.

Half Deck Thickness Prestressing Loss Calculations based on AASHTO LRFD Bridge Design Specifications (Girder #1)

Note: Outlined values obtained from previous calculations, shaded cells input by user.

$f'_y = 58$ ksi	Deck Dimensions	# of strands = 32
$E_s = 29,000$ ksi	$b_f = 72.00$ in.	Single strand $A_{ps} = 0.115$ in ²
$f_{pu} = 270$ ksi	$h_f = 3.00$ in.	Total $A_{ps} = 3.680$ in ²
$f_{py} = 0.85f_{pu} = 229.50$ ksi	Web Dimensions	Jacking Stress (% f_{pu}) = 50%
$E_p = E_{ps} = 28,500$ ksi	$b_{w1} = 7.00$ in.	$f_{pbt} = f_{pj} = \%f_{pu} = 135.00$ ksi
$f'_c = 5,600$ ksi	$b_{w2} = 5.00$ in.	$f_{cgp} = f_{pj} \times A_{ps}/A_g = 1.04$ ksi
$E_{ci} = E_{ct} = 2,850$ ksi	$h_w = 22.00$ in.	$d_{pm} = 19.3755$ in.
$w_c = 110$ lb/ft ³	$A_g = 480.00$ in ²	$\bar{y} = 16.96$ in.
$q = w_c A_g = 366.67$ lb/ft	$I_g = 27,503.27$ in ⁴	$e_m = d_{pm} - [(h_f + h_w) - \bar{y}] = 11.34$ in.
$L = 53.5$ ft		
$M_g = qL^2/8 = 1,574$ kip-in.		

Total Loss of Prestress

$$\Delta f_{pT} = \Delta f_{pES} + \Delta f_{pLT}$$

$$\Delta f_{pES} = \frac{A_{ps} f_{pbt} (I_g + e_m^2 A_g) - e_m M_g A_g}{A_{ps} (I_g + e_m^2 A_g) + \frac{A_g I_g E_{ci}}{E_p}} \quad (C5.9.5.2.3a-1)$$

$$\Delta f_{pES} = 21.68 \text{ ksi}$$

$$\Delta f_{pLT} = (\Delta f_{pSR} + \Delta f_{pCR} + \Delta f_{pR1})_{id} + (\Delta f_{pSD} + \Delta f_{pCD} + \Delta f_{pR2} - \Delta f_{pSS})_{df} \quad (5.9.5.4.1-1)$$

$$(\Delta f_{pCR})_{df} = 0 \quad (\text{no deck placement following girder construction})$$

$$\Delta f_{pSR} = \epsilon_{bid} E_p K_{id} \quad (5.9.5.4.2a-1)$$

$$\epsilon_{bid} = \epsilon_{sh} = k_s k_{hs} k_f k_{td} 0.48 \times 10^{-3} \quad (5.4.2.3.3-1)$$

$$k_s = 1.18 \quad (5.4.2.3.2-2)$$

$$k_{hs} = 2.00 - 0.014H \quad (5.4.2.3.3-2)$$

$$H = 60 \quad (\text{Figure 5.4.2.3.3-1})$$

$$k_{hs} = 1.16$$

$$k_f = 0.912 \quad (5.4.2.3.2-4)$$

$$k_{td} = 0.998 \quad (5.4.2.3.2-5)$$

$$\epsilon_{bid} = 0.0006$$

$$K_{id} = \frac{1}{1 + \frac{E_p A_{ps}}{E_{ci} A_g} \left(1 + \frac{A_g e_{pg}^2}{I_g} \right) [1 + 0.7 \psi_b(t_r, t_i)]} \quad (5.9.5.4.2a-2)$$

$$e_{pg} = e_m = 11.34 \text{ in.}$$

$$\psi(t_r, t_i) = 1.9 k_s k_{ic} k_f k_{td} t_i^{-0.118} \quad (5.4.2.3.2-1)$$

$$k_s = 1.45 - 0.13(V/S) \geq 1.0 \quad (5.4.2.3.2-2)$$

$$V = (h_f \times b_f) + 2[(b_{w1} + b_{w2})/2 \times h_w] = 480.00 \text{ in}^3/\text{in}$$

Half Deck Thickness Prestressing Loss Calculations based on AASHTO LRFD Bridge Design Specifications (Girder #1)

$$S = 2h_1 + b_f + (b_f - 2b_{w1}) + 4\sqrt{h_w^2 + ((b_{w1} - b_{w2})/2)^2} + 2b_{w2} = 234.09 \text{ in}^2/\text{in}$$

$$V/S = 2.05 \text{ in.}$$

$$k_s = 1.18 \geq 1.0, \text{ OK}$$

$$k_{hc} = 1.56 - 0.008H \quad (5.4.2.3.2-3)$$

$$H = 60 \quad (\text{Figure 5.4.2.3.3-1})$$

$$k_{hc} = 1.08$$

$$k_f = 5/(1+f'_{ci}) \quad (5.4.2.3.2-4)$$

$$f'_{ci} = 0.80f'_c$$

$$f'_{ci} = 4.480 \text{ ksi}$$

$$k_f = 0.912$$

$$k_{td} = t/(61 - 4f'_{ci} + t) \quad (5.4.2.3.2-5)$$

$$t = 48 \text{ yrs}$$

$$t = 17,520 \text{ days}$$

$$k_{td} = 0.998$$

$$t_i = 48 \text{ yrs}$$

$$t_i = 17,520 \text{ days}$$

$$\psi(t_i, t) = 0.698$$

$$K_{id} = 0.730$$

$$\Delta f_{pSR} = 12.48 \text{ ksi}$$

$$\Delta f_{pCR} = \frac{E_p}{E_{ci}} f_{cgp} \psi_b(t_d, t_i) K_{id} \quad (5.9.5.4.2b-1)$$

$$\psi(t_d, t_i) = \psi(t_i, t) = 0.698$$

$$K_{id} = K_{id} \text{ from above} = 0.730$$

$$\Delta f_{pCR} = 5.27 \text{ ksi}$$

$$\Delta f_{pR1} = \left[\frac{f_{pt}}{K'_L} \frac{\log(24t)}{\log(24t_i)} \left(\frac{f_{pt}}{f_{py}} - 0.55 \right) \right] \left[1 - \frac{3(\Delta f_{pSR} + \Delta f_{pCR})}{f_{pt}} \right] K_{id} \quad (C5.9.5.4.2c-1)$$

$$f_{pt} = 135.00 \text{ ksi (fpj} > 0.55f_{py} \text{, Use fpj)}$$

$$K'_L = 10 \text{ (45 for low relaxation steel, 10 for stress relieved steel)}$$

$$t_i = 0.75 \text{ days}$$

$$t = 48 \text{ yrs}$$

$$t = 17,520 \text{ days}$$

$$\Delta f_{pR1} = 1.02 \text{ ksi}$$

$$\Delta f_{pLT} = 18.77 \text{ ksi}$$

$$\Delta f_{pT} = 40.45 \text{ ksi} \quad \leftarrow \text{Total loss of prestress}$$

$$f_{pe} = f_{pj} - \Delta f_{pT} = 94.55 \text{ ksi} \quad \leftarrow \text{Remaining prestress}$$

Half Deck Thickness Prestressing Loss Calculations based on AASHTO LRFD Bridge Design Specifications (Girder #2 & Girder #3)

Note: Outlined values obtained from previous calculations, shaded cells input by user.

$f'_y =$ <input type="text" value="58"/> ksi	Deck Dimensions	# of strands = <input type="text" value="32"/>
$E_s =$ <input type="text" value="29,000"/> ksi	$b_f =$ <input type="text" value="77.50"/> in.	Single strand $A_{ps} =$ <input type="text" value="0.115"/> in ²
$f_{pu} =$ <input type="text" value="270"/> ksi	$h_f =$ <input type="text" value="3.00"/> in.	Total $A_{ps} =$ <input type="text" value="3.680"/> in ²
$f_{py} = 0.85f_{pu} =$ <input type="text" value="229.50"/> ksi	Web Dimensions	Jacking Stress (% f_{pu}) = <input type="text" value="52%"/>
$E_p = E_{ps} =$ <input type="text" value="28,500"/> ksi	$b_{w1} =$ <input type="text" value="7.00"/> in.	$f_{pbt} = f_{pj} = \%f_{pu} =$ <input type="text" value="140.40"/> ksi
$f'_c =$ <input type="text" value="5.600"/> ksi	$b_{w2} =$ <input type="text" value="5.00"/> in.	$f_{cgp} = f_{pj} \times A_{ps}/A_g =$ <input type="text" value="1.04"/> ksi
$E_{ci} = E_{ct} =$ <input type="text" value="2,850"/> ksi	$h_w =$ <input type="text" value="22.00"/> in.	$d_{pm} =$ <input type="text" value="19.3755"/> in.
$w_c =$ <input type="text" value="110"/> lb/ft ³	$A_g =$ <input type="text" value="496.50"/> in ²	$\bar{y} =$ <input type="text" value="17.18"/> in.
$q = w_c A_g =$ <input type="text" value="379.27"/> lb/ft	$I_g =$ <input type="text" value="28,197.70"/> in ⁴	$e_m = d_{pm} - [(h_f + h_w) - \bar{y}] =$ <input type="text" value="11.55"/> in.
$L =$ <input type="text" value="53.5"/> ft		
$M_g = qL^2/8 =$ <input type="text" value="1,628"/> kip-in.		

Total Loss of Prestress

$$\Delta f_{pT} = \Delta f_{pES} + \Delta f_{pLT}$$

$$\Delta f_{pES} = \frac{A_{ps} f_{pbt} (I_g + e_m^2 A_g) - e_m M_g A_g}{A_{ps} (I_g + e_m^2 A_g) + \frac{A_g I_g E_{ci}}{E_p}} \quad (C5.9.5.2.3a-1)$$

$$\Delta f_{pES} = \underline{22.59} \text{ ksi}$$

$$\Delta f_{pLT} = (\Delta f_{pSR} + \Delta f_{pCR} + \Delta f_{pR1})_{id} + (\Delta f_{pSD} + \Delta f_{pCD} + \Delta f_{pR2} - \Delta f_{pSS})_{df} \quad (5.9.5.4.1-1)$$

$$(\Delta f_{pCR})_{df} = 0 \quad (\text{no deck placement following girder construction})$$

$$\Delta f_{pSR} = \epsilon_{bid} E_p K_{id} \quad (5.9.5.4.2a-1)$$

$$\epsilon_{bid} = \epsilon_{sh} = k_s k_{hs} k_f k_{td} 0.48 \times 10^{-3} \quad (5.4.2.3.3-1)$$

$$k_s = \underline{1.19} \quad (5.4.2.3.2-2)$$

$$k_{hs} = 2.00 - 0.014H \quad (5.4.2.3.3-2)$$

$$H = \underline{60} \quad (\text{Figure 5.4.2.3.3-1})$$

$$k_{hs} = \underline{1.16}$$

$$k_f = \underline{0.912} \quad (5.4.2.3.2-4)$$

$$k_{td} = \underline{0.998} \quad (5.4.2.3.2-5)$$

$$\epsilon_{bid} = \underline{0.000601}$$

$$K_{id} = \frac{1}{1 + \frac{E_p A_{ps}}{E_{ci} A_g} \left(1 + \frac{A_g e_m^2}{I_g} \right) [1 + 0.7 \psi_b(t_r, t_i)]} \quad (5.9.5.4.2a-2)$$

$$e_{pg} = e_m = \underline{11.55} \text{ in.}$$

$$\psi(t_r, t_i) = 1.9 k_s k_{hc} k_f k_{td} t_i^{-0.118} \quad (5.4.2.3.2-1)$$

$$k_s = 1.45 - 0.13(V/S) \geq 1.0 \quad (5.4.2.3.2-2)$$

$$V = (h_f \times b_f) + 2[(b_{w1} + b_{w2})/2 \times h_w] = \underline{496.50} \text{ in}^3/\text{in}$$

Half Deck Thickness Prestressing Loss Calculations based on AASHTO LRFD Bridge Design Specifications (Girder #2 & Girder #3)

$$S = 2h_f + b_f + (b_f - 2b_{w1}) + 4(\sqrt{h_w^2 + ((b_{w1} - b_{w2})/2)^2}) + 2b_{w2} = 245.09 \text{ in}^2/\text{in}$$

$$V/S = 2.03 \text{ in.}$$

$$k_s = 1.19 \geq 1.0, \text{ OK}$$

$$k_{hc} = 1.56 - 0.008H \quad (5.4.2.3.2-3)$$

H = 60

(Figure 5.4.2.3.3-1)

$$k_{hc} = 1.08$$

$$k_f = 5/(1+f'_{ci}) \quad (5.4.2.3.2-4)$$

$$f'_{ci} = 0.80f'_c$$

$$f'_{ci} = 4.480 \text{ ksi}$$

$$k_f = 0.912$$

$$k_{td} = t/(61 - 4f'_c + t) \quad (5.4.2.3.2-5)$$

$$t = 48 \text{ yrs}$$

$$t = 17,520 \text{ days}$$

$$k_{td} = 0.998$$

$$t_i = 48 \text{ yrs}$$

$$t_i = 17,520 \text{ days}$$

$$\psi(t_i, t) = 0.700$$

$$K_{id} = 0.730$$

$$\Delta f_{pSR} = 12.51 \text{ ksi}$$

$$\Delta f_{pCR} = \frac{E_p}{E_{ci}} f_{cgp} \psi_b(t_d, t_i) K_{id} \quad (5.9.5.4.2b-1)$$

$$\psi(t_d, t_i) = \psi(t_i, t) = 0.700$$

$$K_{id} = K_{id} \text{ from above} = 0.730$$

$$\Delta f_{pCR} = 5.31 \text{ ksi}$$

$$\Delta f_{pR1} = \left[\frac{f_{pt}}{K'_L} \frac{\log(24t)}{\log(24t_i)} \left(\frac{f_{pt}}{f_{py}} - 0.55 \right) \right] \left[1 - \frac{3(\Delta f_{pSR} + \Delta f_{pCR})}{f_{pt}} \right] K_{id} \quad (C5.9.5.4.2c-1)$$

$$f_{pt} = 140.40 \text{ ksi (fpj} > 0.55f_{py} \text{, Use fpj)}$$

$$K'_L = 10 \text{ (45 for low relaxation steel, 10 for stress relieved steel)}$$

$$t_i = 0.75 \text{ days}$$

$$t = 48 \text{ yrs}$$

$$t = 17,520 \text{ days}$$

$$\Delta f_{pR1} = 1.76 \text{ ksi}$$

$$\Delta f_{pLT} = 19.58 \text{ ksi}$$

$$\Delta f_{pT} = 42.17 \text{ ksi} \quad \leftarrow \text{Total loss of prestress}$$

$$f_{pe} = f_{pj} - \Delta f_{pT} = 98.23 \text{ ksi} \quad \leftarrow \text{Remaining prestress}$$

 Half Deck Thickness Moment Capacity Calculations based on AASHTO Approximate Method (Girders #1, 2, & 3)

Note: Outlined values obtained from previous calculations, shaded cells input by user.

$$M_n = A_{ps}f_{ps}\left(d_p - \frac{a}{2}\right) + A_s f_s \left(d_s - \frac{a}{2}\right) - A'_s f'_s \left(d'_s - \frac{a}{2}\right) + 0.85 f'_c (b - b_w) h_f \left(\frac{a}{2} - \frac{h_f}{2}\right)$$

Girder #1

Prestressing Steel	Mild Steel (Tension)	Mild Steel (Compression)	Concrete
$A_{ps} = $ <input type="text" value="3.68"/> $ \text{in}^2$	$A_s = $ <input type="text" value="0"/> $ \text{in}^2$	$A'_s = $ <input type="text" value="1.44"/> $ \text{in}^2$	$f'_c = $ <input type="text" value="5.600"/> $ \text{ksi}$
$f_{ps} = $ <input type="text" value="249.29"/> $ \text{ksi}$	$f_s = $ <input type="text" value="0"/> $ \text{ksi}$	$f'_s = $ <input type="text" value="0"/> $ \text{ksi}$	$b = $ <input type="text" value="72.00"/> $ \text{in.}$
$d_p = $ <input type="text" value="19.376"/> $ \text{in.}$	$d_s = $ <input type="text" value="0"/> $ \text{in.}$	$d'_s = $ <input type="text" value="1.50"/> $ \text{in.}$	$b_w = $ <input type="text" value="14.00"/> $ \text{in.}$
$K = $ <input type="text" value="0.38"/>		↑	$h_f = $ <input type="text" value="3.00"/> $ \text{in.}$
$f_{pu} = $ <input type="text" value="270"/> $ \text{ksi}$		Can be ignored (Article 5.7.2.1)	$c = $ <input type="text" value="3.91"/> $ \text{in.}$
$f_{pe} = $ <input type="text" value="94.55"/> $ \text{ksi}$			$a = $ <input type="text" value="3.01"/> $ \text{in.}$
$f_{pe}/f_{pu} = $ <input type="text" value="0.350"/>			
$f_{ps} = f_{pu}[1-K(c/d_p)] = $ <input type="text" value="249.29"/> $ \text{ksi}$	$(f_{pe} < 0.5f_{pu})$		

$$M_n = 16,398.16 \text{ kip-in} = \underline{1,367} \text{ kip-ft}$$

Girders #2 & #3

Prestressing Steel	Mild Steel (Tension)	Mild Steel (Compression)	Concrete
$A_{ps} = $ <input type="text" value="3.68"/> $ \text{in}^2$	$A_s = $ <input type="text" value="0"/> $ \text{in}^2$	$A'_s = $ <input type="text" value="1.55"/> $ \text{in}^2$	$f'_c = $ <input type="text" value="5.600"/> $ \text{ksi}$
$f_{ps} = $ <input type="text" value="254.23"/> $ \text{ksi}$	$f_s = $ <input type="text" value="0"/> $ \text{ksi}$	$f'_s = $ <input type="text" value="0"/> $ \text{ksi}$	$b = $ <input type="text" value="77.50"/> $ \text{in.}$
$d_p = $ <input type="text" value="19.376"/> $ \text{in.}$	$d_s = $ <input type="text" value="0"/> $ \text{in.}$	$d'_s = $ <input type="text" value="1.50"/> $ \text{in.}$	$b_w = $ <input type="text" value="77.50"/> $ \text{in.}$
$K = $ <input type="text" value="0.38"/>		↑	$h_f = $ <input type="text" value="3.00"/> $ \text{in.}$
$f_{pu} = $ <input type="text" value="270"/> $ \text{ksi}$		Can be ignored (Article 5.7.2.1)	$c = $ <input type="text" value="2.98"/> $ \text{in.}$
$f_{pe} = $ <input type="text" value="98.23"/> $ \text{ksi}$			$a = $ <input type="text" value="2.29"/> $ \text{in.}$
$f_{pe}/f_{pu} = $ <input type="text" value="0.364"/>			
$f_{ps} = f_{pu}[1-K(c/d_p)] = $ <input type="text" value="254.23"/> $ \text{ksi}$	$(f_{pe} < 0.5f_{pu})$		

$$M_n = 17,055.01 \text{ kip-in} = \underline{1,421} \text{ kip-ft}$$

 Half Deck Thickness Moment Capacity Calculations based on Strain Compatibility Method (Girders #1, 2, & 3)

Note: Outlined values obtained from previous calculations, shaded cells input by user.

Girder #1

Concrete		Prestressing Steel		Mild Steel (Compression)	
$f'_c =$	5.6 ksi	$A_{ps} =$	3.68 in ²	$A'_s =$	1.44 in ²
$h_f =$	3.00 in.	$d_{pm} =$	19.3755 in.	$d_s = h_f/2 =$	1.50 in.
$b =$	72.00 in.	$f_{pe} =$	94.55 ksi	$E_s =$	29,000 ksi
$b_w =$	14.00 in.	$E_{ps} =$	28,500 ksi	$f'_y =$	58 ksi
		$f_{pu} =$	270 ksi		

$$\text{Ultimate Strain Capacity (USC)} = 0.003 \leftarrow \text{Leave 0.003}$$

Step 1: Assume a N.A. Depth

$$c = 3.213 \text{ in}$$

$$\epsilon_{ps} = \text{USC}[(d_{pm}/c)-1] + f_{pe}/E_{ps} = 0.01841$$

$$\epsilon_s = \text{USC}[(d_s/c)-1] = -0.00160$$

Step 2 : Calculate Stress in Each Layer

$$f_{ps} = E_{ps} * \epsilon_{ps} \{0.025 + (0.975/[1 + (118 * \epsilon_{ps})^{10,0.1}])\} = 248.59 \text{ ksi} \quad (< 270 \text{ ksi, OK})$$

$$f_s = E_s * \epsilon_s \{0.025 + (0.975/[1 + (118 * \epsilon_s)^{10,0.1}])\} = -46.38 \text{ ksi} \quad (< 58 \text{ ksi, OK})$$

Step 3 : Check for Equilibrium of Forces

$$A_{ps}f_{ps} + A'_sf_s = 848.0 \text{ kips} \leftarrow$$

$$\beta_1 = 0.85 - 0.05(f'_c - 4) = 0.77 \quad (> 0.65, \text{OK})$$

$$a = \beta_1 c = 2.47 \text{ in}$$

If $a > h_f$: $\Sigma(-0.85f'_cA_c) = -[0.85f'_cbh_f + 0.85f'_cb_w(a-h_f)] = \text{See Below kips} \leftarrow$

If $a < h_f$: $\Sigma(-0.85f'_cA_c) = -0.85f'_cba = -847.9 \text{ kips} \leftarrow$

These need to be equal and opposite, change "c" until they are.

Step 4: Calculate Nominal Moment Capacity

$$M_n = A_{ps}f_{ps}d_{pm} + A'_sf_s d_s + 0.85f'_c b a (a/2) = 16,576 \text{ kip-in.} = \underline{1,381 \text{ kip-ft}}$$

Girders #2 & #3

Concrete		Prestressing Steel		Mild Steel (Compression)	
$f'_c =$	5.6 ksi	$A_{ps} =$	3.68 in ²	$A'_s =$	1.55 in ²
$h_f =$	3.00 in.	$d_{pm} =$	19.3755 in.	$d_s = h_f/2 =$	1.50 in.
$b =$	77.50 in.	$f_{pe} =$	98.23 ksi	$E_s =$	29,000 ksi
$b_w =$	14.00 in.	$E_{ps} =$	28,500 ksi	$f'_y =$	58 ksi
		$f_{pu} =$	270 ksi		

$$\text{Ultimate Strain Capacity (USC)} = 0.003 \leftarrow \text{Leave 0.003}$$

Step 1: Assume a N.A. Depth

$$c = 2.997 \text{ in}$$

$$\epsilon_{ps} = \text{USC}[(d_{pm}/c)-1] + f_{pe}/E_{ps} = 0.01984$$

$$\epsilon_s = \text{USC}[(d_s/c)-1] = -0.00150$$

Step 2 : Calculate Stress in Each Layer

$$f_{ps} = E_{ps} * \epsilon_{ps} \{0.025 + (0.975/[1 + (118 * \epsilon_{ps})^{10,0.1}])\} = 249.62 \text{ ksi} \quad (< 270 \text{ ksi, OK})$$

$$f_s = E_s * \epsilon_s \{0.025 + (0.975/[1 + (118 * \epsilon_s)^{10,0.1}])\} = -43.46 \text{ ksi} \quad (< 58 \text{ ksi, OK})$$

 Half Deck Thickness Moment Capacity Calculations based on Strain Compatibility Method (Girders #1, 2, & 3)

Step 3 : Check for Equilibrium of Forces

$$\begin{array}{rcl}
 A_{ps}f_{ps} + A'_s f'_s & = & 851.2 \text{ kips} \leftarrow \\
 \beta_1 = 0.85 - 0.05(f'_c - 4) & = & 0.77 \text{ (> 0.65, OK)} \\
 a = \beta_1 c & = & 2.31 \text{ in} \\
 \text{If } a > h_f : \Sigma(-0.85f'_c A_c) = -[0.85f'_c b h_f + 0.85f'_c b_w(a - h_f)] & = & \text{See Below kips} \leftarrow \\
 \text{If } a < h_f : \Sigma(-0.85f'_c A_c) = -0.85f'_c b a & = & -851.3 \text{ kips} \leftarrow
 \end{array}$$

These need to be equal and opposite, change "c" until they are.

Step 4: Calculate Nominal Moment Capacity

$$M_n = A_{ps}f_{ps}d_{pm} + A'_s f'_c d_s + 0.85f'_c b a(a/2) = 16,715 \text{ kip-in.} = \underline{1,393} \text{ kip-ft}$$

Half Deck Thickness Maximum Deflection Calculations based on AASHTO Section 5.7.3.6 (Girder #1)

Note: Outlined values obtained from previous calculations, shaded cells input by user.

Concrete		Prestressing Steel		Mild Steel (Compression)	
f'_c	5.6 ksi	A_{ps}	3.68 in ²	A'_s	1.44 in ²
E_c	2,850 ksi	$d = d_{pm}$	19.3755 in.	$d_s = h_f/2$	1.50 in.
h_f	3.00 in.	f_{pe}	94.55 ksi	E_s	29,000 ksi
b	72.00 in.	E_{ps}	28,500 ksi	f'_y	58 ksi
b_w	14.00 in.	f_{pu}	270 ksi		
h_w	22.00 in.	P_e	347.93 kips		
h	25.00 in.	e	11.34 in.		
I_g	27,503.27 in. ⁴				
A_g	480.00 in ²				
$f_r = 0.17V(f'_c)$	0.402 ksi				
$y_t = \bar{y}$	16.961 in.				

$$M_{cr} = [(P_e/A_g) + (P_e e y_t / I_g) - f_r] \times (I_g / y_t)$$

$$M_{cr} = 4,467.40 \text{ kip-in.}$$

$$F = 90.7 \text{ kips}$$

$$P = F/2 = 45.35 \text{ kips}$$

$$L = 49 \text{ ft}$$

$$X = 6 \text{ ft}$$

$$M_a = P(L/2 - X/2) = 11,700 \text{ kip-in.}$$

$$n = E_{ps}/E_c = 10.00$$

$$nA_{ps} = 36.80 \text{ in}^2$$

$$\text{Trial } k_d = 3.969 \text{ in.} \quad \leftarrow kd \text{ is in web}$$

$$b(k_d^2/2) = nA_{ps}(d - k_d)$$

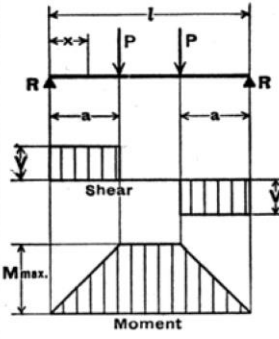
$$b(k_d^2/2) - nA_{ps}(d - k_d) = 0.018 \quad \leftarrow \text{should be approximately equal to zero}$$

$$I_{cr} = (1/3)bk_d^3 + nA_{ps}(d - k_d)^2 = 10,235.42 \text{ in.}^4$$

$$I_e = \left(\frac{M_{cr}}{M_a} \right)^3 I_g + \left[1 - \left(\frac{M_{cr}}{M_a} \right)^3 \right] I_{cr} \leq I_g \tag{5.7.3.6.2-1}$$

$$I_e = 11,196.62 \text{ in.}^4$$

9. SIMPLE BEAM—TWO EQUAL CONCENTRATED LOADS SYMMETRICALLY PLACED



Total Equiv. Uniform Load	$= \frac{8 Pa}{l}$
R = V	$= P$
M max. (between loads)	$= Pa$
M_x (when x < a)	$= Px$
Δ max. (at center)	$= \frac{Pa}{24EI} (3l^2 - 4a^2)$
Δ_x (when x < a)	$= \frac{Px}{6EI} (3la - 3a^2 - x^2)$
Δ_x (when x > a and < (l-a))	$= \frac{Pa}{6EI} (3lx - 3x^2 - a^2)$

(AISC. 1998)

$$\Delta_{max} = 11.78 \text{ in.}$$

Half Deck Thickness Maximum Deflection Calculations based on AASHTO Section 5.7.3.6 (Girder #2)

Note: Outlined values obtained from previous calculations, shaded cells input by user.

Concrete		Prestressing Steel		Mild Steel (Compression)	
$f'_c =$	5.6 ksi	$A_{ps} =$	3.68 in ²	$A'_s =$	1.55 in ²
$E_c =$	2,850 ksi	$d = d_{pm} =$	19.3755 in.	$d_s = h_f/2 =$	1.50 in.
$h_f =$	3.00 in.	$f_{pe} =$	98.23 ksi	$E_s =$	29,000 ksi
$b =$	77.50 in.	$E_{ps} =$	28,500 ksi	$f'_y =$	58 ksi
$b_w =$	14.00 in.	$f_{pu} =$	270 ksi		
$h_w =$	22.00 in.	$P_e =$	361.50 kips		
$h =$	25.00 in.	$e =$	11.55 in.		
$I_g =$	28,197.70 in. ⁴				
$A_g =$	496.50 in ²				
$f_r = 0.17V(f'_c) =$	0.402 ksi				
$y_t = \bar{y} =$	17.178 in.				

$$M_{cr} = [(P_e/A_g) + (P_e e y_t / I_g) - f_r] \times (I_g / y_t)$$

$$M_{cr} = 4,711.52 \text{ kip-in.}$$

$$F = 99.8 \text{ kips}$$

$$P = F/2 = 49.9 \text{ kips}$$

$$L = 49 \text{ ft}$$

$$X = 6 \text{ ft}$$

$$M_g = P(L/2 - X/2) = 12,874 \text{ kip-in.}$$

$$n = E_{ps} / E_c = 10.00$$

$$nA_{ps} = 36.80 \text{ in}^2$$

$$\text{Trial } k_d = 3.841 \text{ in.} \quad \leftarrow \text{kd is in web}$$

$$b(k_d^2/2) = nA_{ps}(d - k_d)$$

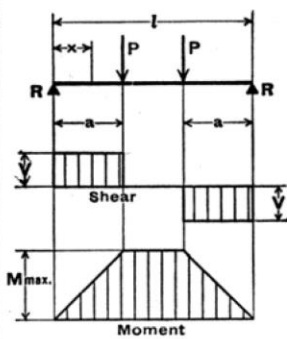
$$b(k_d^2/2) - nA_{ps}(d - k_d) = -0.013 \quad \leftarrow \text{should be approximately equal to zero}$$

$$I_{cr} = (1/3)bk_d^3 + nA_{ps}(d - k_d)^2 = 10,344.51 \text{ in.}^4$$

$$I_e = \left(\frac{M_{cr}}{M_a} \right)^3 I_g + \left[1 - \left(\frac{M_{cr}}{M_a} \right)^3 \right] I_{cr} \leq I_g \quad (5.7.3.6.2-1)$$

$$I_e = 11,219.57 \text{ in.}^4$$

9. SIMPLE BEAM—TWO EQUAL CONCENTRATED LOADS SYMMETRICALLY PLACED



Total Equiv. Uniform Load	$= \frac{8 Pa}{l}$
R = V	$= P$
M max. (between loads)	$= Pa$
M_x (when x < a)	$= Px$
Δ_{max.} (at center)	$= \frac{Pa}{24EI} (3l^2 - 4a^2)$
Δ_x (when x < a)	$= \frac{Px}{6EI} (3/a - 3a^2 - x^2)$
Δ_x (when x > a and < (l - a))	$= \frac{Pa}{6EI} (3lx - 3x^2 - a^2)$

(AISC. 1998)

$$\Delta_{max} = 12.93 \text{ in.}$$

Half Deck Thickness Maximum Deflection Calculations based on AASHTO Section 5.7.3.6 (Girder #3)

Note: Outlined values obtained from previous calculations, shaded cells input by user.

Concrete		Prestressing Steel		Mild Steel (Compression)	
$f'_c =$	5.6 ksi	$A_{ps} =$	3.68 in ²	$A'_s =$	1.55 in ²
$E_c =$	2,850 ksi	$d = d_{pm} =$	19.3755 in.	$d_s = h_f/2 =$	1.50 in.
$h_f =$	3.00 in.	$f_{pe} =$	98.23 ksi	$E_s =$	29,000 ksi
$b =$	77.50 in.	$E_{ps} =$	28,500 ksi	$f'_y =$	58 ksi
$b_w =$	14.00 in.	$f_{pu} =$	270 ksi		
$h_w =$	22.00 in.	$P_e =$	361.50 kips		
$h =$	25.00 in.	$e =$	11.55 in.		
$I_g =$	28,197.70 in. ⁴				
$A_g =$	496.50 in ²				
$f_r = 0.17V(f'_c) =$	0.402 ksi				
$y_t = \bar{y} =$	17.178 in.				

$$M_{cr} = [(P_e/A_g) + (P_e e y_t / I_g) - f_r] \times (I_g / y_t)$$

$$M_{cr} = 4,711.52 \text{ kip-in.}$$

$$F = 108.9 \text{ kips}$$

$$P = F/2 = 54.45 \text{ kips}$$

$$L = 49 \text{ ft}$$

$$X = 7 \text{ ft}$$

$$M_3 = P(L/2 - X/2) = 13,721 \text{ kip-in.}$$

$$n = E_{ps} / E_c = 10.00$$

$$n A_{ps} = 36.80 \text{ in}^2$$

$$\text{Trial } k_d = 3.841 \text{ in.} \quad \leftarrow \text{kd is in web}$$

$$b(k_d^2/2) = n A_{ps}(d - k_d)$$

$$b(k_d^2/2) - n A_{ps}(d - k_d) = -0.013 \quad \leftarrow \text{should be approximately equal to zero}$$

$$I_{cr} = (1/3) b k_d^3 + n A_{ps} (d - k_d)^2 = 10,344.51 \text{ in.}^4$$

$$I_e = \left(\frac{M_{cr}}{M_a} \right)^3 I_g + \left[1 - \left(\frac{M_{cr}}{M_a} \right)^3 \right] I_{cr} \leq I_g \tag{5.7.3.6.2-1}$$

$$I_e = 11,067.28 \text{ in.}^4$$

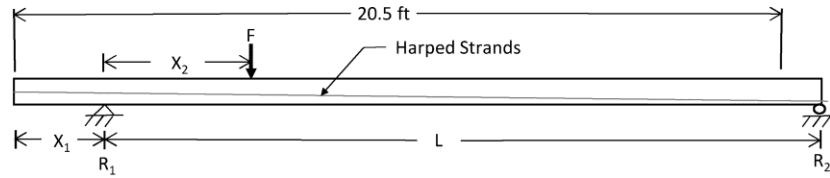
9. SIMPLE BEAM—TWO EQUAL CONCENTRATED LOADS SYMMETRICALLY PLACED

Total Equiv. Uniform Load	$= \frac{8 Pa}{l}$
R = V	$= P$
M max. (between loads)	$= Pa$
M_x (when x < a)	$= Px$
Δ max. (at center)	$= \frac{Pa}{24EI} (3l^2 - 4a^2)$
Δ_x (when x < a)	$= \frac{Px}{6EI} (3la - 3a^2 - x^2)$
Δ_x (when x > a and < (l - a))	$= \frac{Pa}{6EI} (3lx - 3x^2 - a^2)$

(AISC. 1998)

$$\Delta_{max} = 14.20 \text{ in.}$$

Half Deck Thickness Shear Capacity Calculations based on AASHTO Simplified Method (2dv)



Note: Outlined values obtained from previous calculations, shaded cells input by user.

$X_1 =$ <input type="text" value="21"/> in.	$f'_c =$ <input type="text" value="5.6"/> ksi	$d_v =$ <input type="text" value="12.52"/> in.
$X_2 =$ <input type="text" value="42"/> in.	$b_v =$ <input type="text" value="12.27"/> in.	$0.9d_e =$ <input type="text" value="12.58"/> in.
$L =$ <input type="text" value="19"/> ft = 228 in.	$d_v =$ <input type="text" value="18"/> in.	$0.72h =$ <input type="text" value="18"/> in. (USE for dv)
$w_c =$ <input type="text" value="110"/> lb/ft ³	$d_e =$ <input type="text" value="13.98"/> in.	
	$h =$ <input type="text" value="25.00"/> in.	
	$f_r = 0.17\sqrt{f'_c} =$ <input type="text" value="0.402"/> ksi	$d_{pm} =$ <input type="text" value="19.38"/> in.
	$I_g = I_c =$ <input type="text" value="27,503.27"/> in. ⁴	$d_{pe} =$ <input type="text" value="12.13"/> in.
	$\bar{y} = c_c = c_g =$ <input type="text" value="16.96"/> in.	$L_h =$ <input type="text" value="20.50"/> ft (length of harp)
	$e = c_2 = (h - \bar{y}) - d_e =$ <input type="text" value="5.94"/> in.	$\psi =$ <input type="text" value="1.69"/> ° ($\tan[(d_{pm} - d_{pe})/L_h]$)
	$A_g =$ <input type="text" value="480.00"/> in. ²	
	$W_d = w_c(A_g) =$ <input type="text" value="0.0306"/> kip/in	
	$V_i =$ <input type="text" value="315.1"/> kips	
	$M_{max} = [V_i(L - X_2)/L](X_2) =$ <input type="text" value="10,794.61"/> kip-in.	
	$P_e =$ <input type="text" value="343.10"/> kips	

$V_n =$ the lesser of; $V_{n1} = 0.25f'_c b_v d_v + V_p$ and $V_{n2} = V_c + V_s + V_p$

$V_p = P_e \sin \psi$

$V_p =$ kips

$V_{n1} = 0.25f'_c b_v d_v + V_p =$ kips (5.8.3.3-2)

$V_{n2} = V_c + V_s + V_p$ (5.8.3.3-1)

$V_c =$ the lesser of V_{ci} and V_{cw}

$V_{ci} = 0.02(0.75\sqrt{f'_c})b_v d_v + V_d + \frac{V_i M_{cre}}{M_{max}} \geq 0.06(0.75\sqrt{f'_c})b_v d_v$ (5.8.3.4.3-1)

$0.06(0.75\sqrt{f'_c})b_v d_v =$ kips

$V_d = (W_d/2)(L - X_2) =$ kips

$M_{cre} = S_c (f_r + f_{cpe} - \frac{M_{dnc}}{S_{nc}})$ (5.8.3.4.3-2)

$S_c = I_g / c_c =$ in.³

$f_{cpe} = (P_e / A_g) + (P_e c_2 c_g / I_g) =$ ksi

$M_{dnc} = (W_d X_2 / 2)(L - X_2) =$ kip-in.

$S_{nc} = I_g / c_g =$ in.³

$M_{cre} =$ kip-in.

$V_{ci} =$ kips

 Half Deck Thickness Shear Capacity Calculations based on AASHTO Simplified Method (2dv)

$$V_{cw} = [0.06(0.75\sqrt{f'_c}) + 0.30f_{pc}] b_v d_v + V_p \quad (5.8.3.4.3-3)$$

$$f_{pc} = \frac{P_e}{A_g} + \frac{P_e e (c_c - c_g)}{I_g} + \frac{M_d (c_c - c_g)}{I_g}$$

$$M_d = M_{dnc} = \underline{119.35} \text{ kip-in.}$$

$$f_{pc} = \underline{0.715} \text{ ksi}$$

$$V_{cw} = \underline{80.98} \text{ kips}$$

$$V_c = \underline{80.98} \text{ kips}$$

$$V_s = \frac{A_v f_y d_v (\cot \theta + \cot \alpha) \sin \alpha}{s} \quad (5.8.3.3-4)$$

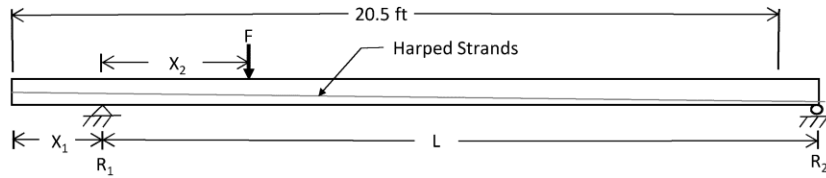
$$\cot \theta = 1.800 \quad V_{ci} > V_{cw}$$

$$V_s = \underline{36.53} \text{ kips}$$

$$V_{n2} = \underline{127.61} \text{ kips}$$

$$V_n = \boxed{127.61} \text{ kips}$$

Half Deck Thickness Shear Capacity Calculations based on AASHTO Simplified Method (3dv)



Note: Outlined values obtained from previous calculations, shaded cells input by user.

$X_1 = 21$ in.	$f'_c = 5.6$ ksi	$d_v = 13.14$ in.
$X_2 = 63$ in.	$b_v = 12.16$ in.	$0.9d_e = 13.14$ in.
$L = 19$ ft = 228 in.	$d_v = 18$ in.	$0.72h = 18$ in. (USE for dv)
$w_c = 110$ lb/ft ³	$d_c = 14.60$ in.	
	$h = 25.00$ in.	
	$f_r = 0.17\sqrt{f'_c} = 0.402$ ksi	$d_{pm} = 19.38$ in.
	$I_g = I_c = 27,503.27$ in. ⁴	$d_{pe} = 12.13$ in.
	$\bar{y} = c_c = c_g = 16.96$ in.	$L_h = 20.50$ ft (length of harp)
	$e = c_2 = (h - \bar{y}) - d_c = 6.56$ in.	$\psi = 1.69^\circ$ ($\tan[(d_{pm} - d_{pe})/L_h]$)
	$A_g = 480.00$ in. ²	
	$W_d = w_c(A_g) = 0.0306$ kip/in	
	$V_i = 188.0$ kips	
	$M_{max} = [V_i(L - X_2)/L](X_2) = 8,571.32$ kip-in.	
	$P_e = 343.10$ kips	

Shear Steel	
$f_y = 58$ ksi	
# = 4 bars	
# of bars = 2	
$A_v = 0.39$ in. ²	
$s = 22$ in.	
$\alpha = 95$ degrees	

$V_n =$ the lesser of; $V_n = 0.25f'_c b_v d_v + V_p$ and $V_n = V_c + V_s + V_p$

$V_p = P_e \sin \psi$

$V_p = 10.11$ kips

$V_{n1} = 0.25f'_c b_v d_v + V_p = 306.3$ kips (5.8.3.3-2)

$V_{n2} = V_c + V_s + V_p$ (5.8.3.3-1)

$V_c =$ the lesser of V_{ci} and V_{cw}

$V_{ci} = 0.02(0.75\sqrt{f'_c})b_v d_v + V_d + \frac{V_i M_{cre}}{M_{max}} \geq 0.06(0.75\sqrt{f'_c})b_v d_v$ (5.8.3.4.3-1)

$0.06(0.75\sqrt{f'_c})b_v d_v = 23.30$ kips

$V_d = (W_d/2)(L - X_2) = 2.52$ kips

$M_{cre} = S_c (f_r + f_{cpe} - \frac{M_{dnc}}{S_{nc}})$ (5.8.3.4.3-2)

$S_c = I_g/c_c = 1621.55$ in.³

$f_{cpe} = (P_e/A_g) + (P_e c_2 c_g/I_g) = 2.103$ ksi

$M_{dnc} = (W_d X_2/2)(L - X_2) = 158.81$ kip-in.

$S_{nc} = I_g/c_g = 1621.55$ in.³

$M_{cre} = 3,903.97$ kip-in.

$V_{ci} = 95.92$ kips

 Half Deck Thickness Shear Capacity Calculations based on AASHTO Simplified Method (3dv)

$$V_{cw} = [0.06(0.75\sqrt{f'_c}) + 0.30f_{pc}] b_v d_v + V_p \quad (5.8.3.4.3-3)$$

$$f_{pc} = \frac{P_e}{A_g} + \frac{P_e e (c_c - c_g)}{I_g} + \frac{M_d (c_c - c_g)}{I_g}$$

$$M_d = M_{dnc} = \underline{158.81} \text{ kip-in.}$$

$$f_{pc} = \underline{0.715} \text{ ksi}$$

$$V_{cw} = \underline{80.33} \text{ kips}$$

$$V_c = \underline{80.33} \text{ kips}$$

$$V_s = \frac{A_v f_y d_v (\cot \theta + \cot \alpha) \sin \alpha}{s} \quad (5.8.3.3-4)$$

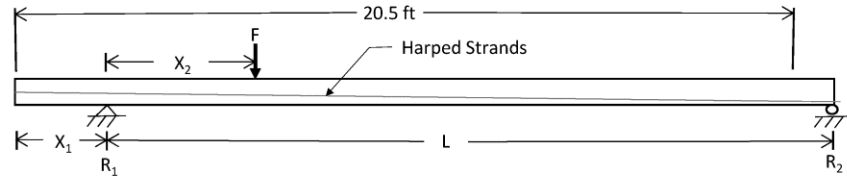
$$\cot \theta = 1.800 \quad V_c > V_{cw}$$

$$V_s = \underline{36.53} \text{ kips}$$

$$V_{n2} = \underline{126.97} \text{ kips}$$

$$V_n = \boxed{126.97} \text{ kips}$$

Half Deck Thickness Shear Capacity Calculations based on AASHTO Simplified Method (4dv)



Note: Outlined values obtained from previous calculations, shaded cells input by user.

$X_1 =$ <input type="text" value="21"/> in.	$f'_c =$ <input type="text" value="5.6"/> ksi	$d_v =$ <input type="text" value="13.75"/> in.
$X_2 =$ <input type="text" value="84"/> in.	$b_v =$ <input type="text" value="12.05"/> in.	$0.9d_e =$ <input type="text" value="13.70"/> in.
$L =$ <input type="text" value="19"/> ft = 228 in.	$d_v =$ <input type="text" value="18"/> in.	$0.72h =$ <input type="text" value="18"/> in. (USE for dv)
$w_c =$ <input type="text" value="110"/> lb/ft ³	$d_e =$ <input type="text" value="15.22"/> in.	$d_{pm} =$ <input type="text" value="19.38"/> in.
	$h =$ <input type="text" value="25.00"/> in.	$d_{pe} =$ <input type="text" value="12.13"/> in.
	$f_r = 0.17v(f'_c) =$ <input type="text" value="0.402"/> ksi	$L_h =$ <input type="text" value="20.50"/> ft (length of harp)
	$I_g = I_c =$ <input type="text" value="27,503.27"/> in. ⁴	$\psi =$ <input type="text" value="1.69"/> ° ($\tan^{-1}[(d_{pm}-d_{pe})/L_h]$)
	$\bar{y} = c_c = c_g =$ <input type="text" value="16.96"/> in.	
	$e = c_2 = (h-\bar{y})-d_e =$ <input type="text" value="7.18"/> in.	
	$A_g =$ <input type="text" value="480.00"/> in. ²	
	$W_d = w_c(A_g) =$ <input type="text" value="0.0306"/> kip/in	
	$V_i =$ <input type="text" value="182.4"/> kips	
	$M_{max} = [V_i(L-X_2)/L](X_2) =$ <input type="text" value="9,676.80"/> kip-in.	
	$P_e =$ <input type="text" value="343.10"/> kips	

$V_n =$ the lesser of; $V_n = 0.25f'_c b_v d_v + V_p$ and $V_n = V_c + V_s + V_p$

$V_p = P_e \sin \psi$

$V_p =$ kips

$V_{n1} = 0.25f'_c b_v d_v + V_p =$ kips (5.8.3.3-2)

$V_{n2} = V_c + V_s + V_p$ (5.8.3.3-1)

$V_c =$ the lesser of V_{ci} and V_{cw}

$V_{ci} = 0.02(0.75\sqrt{f'_c})b_v d_v + V_d + \frac{V_i M_{cre}}{M_{max}} \geq 0.06(0.75\sqrt{f'_c})b_v d_v$ (5.8.3.4.3-1)

$0.06(0.75\sqrt{f'_c})b_v d_v =$ kips

$V_d = (W_d/2)(L-X_2) =$ kips

$M_{cre} = S_c(f_r + f_{cpe} - \frac{M_{dnc}}{S_{nc}})$ (5.8.3.4.3-2)

$S_c = I_c/c_c =$ in.³

$f_{cpe} = (P_e/A_g) + (P_e c_2 c_g / I_g) =$ ksi

$M_{dnc} = (W_d X_2 / 2)(L-X_2) =$ kip-in.

$S_{nc} = I_g/c_g =$ in.³

$M_{cre} =$ kip-in.

$V_{ci} =$ kips

 Half Deck Thickness Shear Capacity Calculations based on AASHTO Simplified Method (4dv)

$$V_{cw} = \left[0.06 \left(0.75 \sqrt{f'_c} \right) + 0.30 f_{pc} \right] b_v d_v + V_p \quad (5.8.3.4.3-3)$$

$$f_{pc} = \frac{P_e}{A_g} + \frac{P_e e (c_c - c_g)}{I_g} + \frac{M_d (c_c - c_g)}{I_g}$$

$$M_d = M_{dnc} = \underline{184.80} \text{ kip-in.}$$

$$f_{pc} = \underline{0.715} \text{ ksi}$$

$$V_{cw} = \underline{79.69} \text{ kips}$$

$$V_c = \underline{79.69} \text{ kips}$$

$$V_s = \frac{A_v f_y d_v (\cot \theta + \cot \alpha) \sin \alpha}{s} \quad (5.8.3.4-4)$$

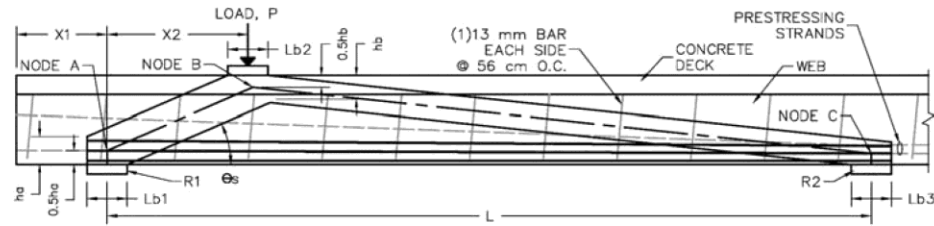
$$\cot \theta = 1.800 \quad V_c > V_{cw}$$

$$V_s = \underline{36.53} \text{ kips}$$

$$V_{n2} = \underline{126.32} \text{ kips}$$

$$V_n = \boxed{126.32} \text{ kips}$$

Half Deck Thickness Shear Capacity Calculations based on AASHTO Strut & Tie Method (2dv)



Note: Outlined values obtained from previous calculations, shaded cells input by user.

$X_1 =$	27	in.	$f'_c =$	5.600	ksi	$h_f =$	3.00	in.
$X_2 =$	42	in.	$f_{ce} =$	4.200	ksi (0.75 f'_c for c-c-t)	$h_w =$	22.00	in.
$L =$	19	ft = 228		4.760	ksi (0.85 f'_c for c-c-c)	$h = h_f + h_w =$	25.00	in.
$L_{b1} =$	12	in.	$E_c =$	2,850	ksi	$d_{pm} =$	19.376	in.
$L_{b2} =$	12	in.	$E_{ps} =$	28,500	ksi	$d_{pe} =$	12.125	in.
$L_{b3} =$	12	in.	$A_{ps} =$	3.68	in. ²	$L_h =$	20.50	ft
$b_{w1} =$	14.00	in.	$P_e =$	343.10	kips	$d_p =$	12.921	in.
$b_{w2} =$	10.00	in.	$\epsilon_{ps} =$	0.003271		$c_p = 0.5h_a = h - d_p =$	12.079	in.
$t_f = b =$	72.00	in.				$t_w =$	13.10	in.

$$M_B = f_{ce} h_b t [h - c_p - (h_b/2)]$$

Trial $P = 276.06$ kips
 Trial $h_b = 2.35$ in. $hb < hf$, hb is in flange
 $R_1 = R_A = P[(L - X_2)/L] = 225.21$ kips
 $M_B = R_A X_2 = 9,458.69$ kip-in
 $0 = f_{ce} h_b t [h - c_p - (h_b/2)] - M_B$
 0.00 ← change P until zero
 Solve for h_b

Solving for h_b above = 2.35 in.

$$\theta_1 = \tan^{-1}[(h - h_b/2 - c_p)/X_2] = 15.57$$
 degrees

$$\theta_2 = \tan^{-1}[(d_{pm} - d_{pe})/L_h] = 1.69$$
 degrees

$$\theta = \theta_1 + \theta_2 = 17.25$$
 degrees

$$F_{AB} = R_A / (\sin\theta_1 + \cos\theta_1 \tan\theta_2) = 758.91$$
 kips

$$F_{AC} = F_{AB} \cos(\theta_1) / \cos(\theta_2) = 731.39$$
 kips

$$\epsilon_s = (F_{AC}/A_{ps})/E_{ps} - \epsilon_{ps} = 0.003702$$

$$\epsilon_1 = \epsilon_s + (\epsilon_s + 0.002) \cot^2 \theta = 0.06281$$

$$f_{cu} = f'_c / (0.8 + 170\epsilon_1) \leq 0.85f'_c$$

$$0.85f'_c = 4.76$$
 ksi

$$f'_c / (0.8 + 170\epsilon_1) = 0.488$$
 ksi

$$f_{cu} = 0.488$$
 ksi

$$P_n = f_{cu} A_{cs}$$

$$A_{cs} = [L_{b1} \sin(\theta_1) + h_a \cos(\theta_1)] t = 1907.47$$
 in.²

$$P_n = 930.66$$
 kips

$$V = P_n \sin(\theta) = 276.05$$
 kips

Half Deck Thickness Theoretical Deflection and Camber Calculations (Girder #1)

Note: Outlined values obtained from previous calculations, shaded cells input by user.

Deflection due to prestressing

$$L = 53.5 \text{ ft.} = 642.0 \text{ in.}$$

$$a = 20.5 \text{ ft.} = 246.0 \text{ in.}$$

$$E_c = 2,850,000 \text{ psi}$$

$$I_g = 27,503.27 \text{ in.}^4$$

$$e_{e1} = \bar{y} - (h - d_{pte}) = 1.34 \text{ in. (eccentricity of harped strands at end of girder)}$$

$$e_{c1} = \bar{y} - (h - d_{ptm}) = 10.65 \text{ in. (eccentricity of harped strands at midspan of girder)}$$

$$e_{c2} = \bar{y} - (h - d_{pbm}) = 13.40 \text{ in. (eccentricity of straight strands)}$$

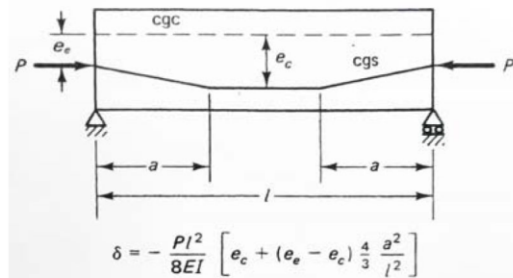
$$\text{Initial Prestressing, } P = 496,800 \text{ lbs}$$

$$P \text{ of Harped Strands} = 3/4P = 372,600 \text{ lbs}$$

$$\Delta_1 = 3.05 \text{ in.}$$

$$\text{Time-dependent multiplier} = 2.45 \text{ (PCI Table 8.7.1-1)}$$

$$\Delta_{1T} = 7.48 \text{ in.}$$

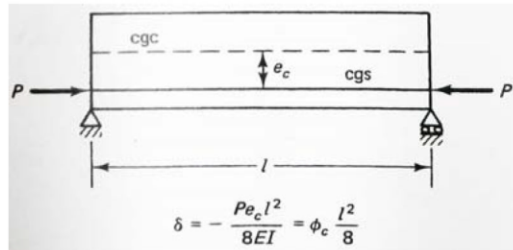


$$P \text{ of Straight Strands} = 1/4P = 124,200 \text{ lbs}$$

$$\Delta_2 = 1.09 \text{ in.}$$

$$\text{Time-dependent multiplier} = 2.45 \text{ (PCI Table 8.7.1-1)}$$

$$\Delta_{2T} = 2.68 \text{ in.}$$



(Nawy 2006)

Deflection due to self-weight

$$w_c = 110 \text{ lb/ft}^3$$

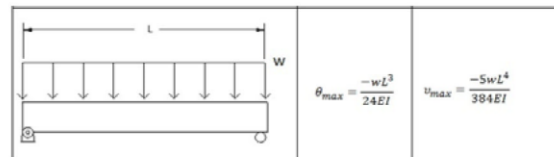
$$A = 3.333 \text{ ft}^2$$

$$w = w_c \times A = 366.667 \text{ lb/ft}$$

$$\Delta_3 = -5wL^4 / (384E_cI) = -0.86 \text{ in.}$$

$$\text{Time-dependent multiplier} = 2.70 \text{ (PCI Table 8.7.1-1)}$$

$$\Delta_{3T} = -2.33 \text{ in.}$$



(Nilson 1987)

$$\Delta_{\text{Total}} = \Delta_1 + \Delta_2 + \Delta_3 = 7.84 \text{ in.}$$

Half Deck Thickness Theoretical Deflection and Camber Calculations (Girder #2)

Note: Outlined values obtained from previous calculations, shaded cells input by user.

Deflection due to prestressing

$$L = 53.5 \text{ ft.} = 642.0 \text{ in.}$$

$$a = 20.5 \text{ ft.} = 246.0 \text{ in.}$$

$$E_c = 2,850,000 \text{ psi}$$

$$I_g = 28,197.70 \text{ in.}^4$$

$$e_{e1} = \bar{y} - (h - d_{pte}) = 1.55 \text{ in. (eccentricity of harped strands at end of girder)}$$

$$e_{c1} = \bar{y} - (h - d_{ptm}) = 10.87 \text{ in. (eccentricity of harped strands at midspan of girder)}$$

$$e_{c2} = \bar{y} - (h - d_{pbm}) = 13.62 \text{ in. (eccentricity of straight strands)}$$

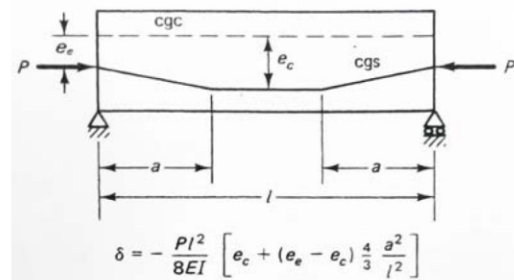
$$\text{Initial Prestressing, } P = 516,672 \text{ lbs}$$

$$P \text{ of Harped Strands} = 3/4P = 387,504 \text{ lbs}$$

$$\Delta_1 = 3.15 \text{ in.}$$

$$\text{Time-dependent multiplier} = 2.45 \text{ (PCI Table 8.7.1-1)}$$

$$\Delta_{1T} = 7.72 \text{ in.}$$

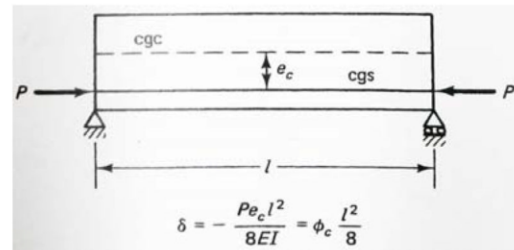


$$P \text{ of Straight Strands} = 1/4P = 129,168 \text{ lbs}$$

$$\Delta_2 = 1.13 \text{ in.}$$

$$\text{Time-dependent multiplier} = 2.45 \text{ (PCI Table 8.7.1-1)}$$

$$\Delta_{2T} = 2.76 \text{ in.}$$



(Nawy 2006)

Deflection due to self-weight

$$w_c = 110 \text{ lb/ft}^3$$

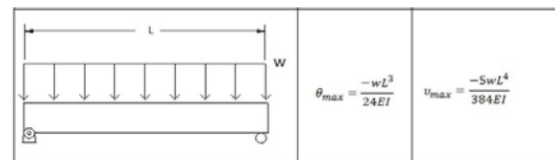
$$A = 3.448 \text{ ft}^2$$

$$w = w_c \times A = 379.271 \text{ lb/ft}$$

$$\Delta_3 = -5wL^4 / (384E_c I) = -0.87 \text{ in.}$$

$$\text{Time-dependent multiplier} = 2.70 \text{ (PCI Table 8.7.1-1)}$$

$$\Delta_{3T} = -2.35 \text{ in.}$$



(Nilson 1987)

$$\Delta_{Total} = \Delta_1 + \Delta_2 + \Delta_3 = 8.14 \text{ in.}$$

Half Deck Thickness Theoretical Deflection and Camber Calculations (Girder #3)

Note: Outlined values obtained from previous calculations, shaded cells input by user.

Deflection due to prestressing

$L = 53.5$ ft. = 642.0 in.
 $a = 20.5$ ft. = 246.0 in.
 $E_c = 2,850,000$ psi
 $I_g = 28,197.70$ in.⁴

$e_{e1} = \bar{y} - (h - d_{pte}) = 1.55$ in. (eccentricity of harped strands at end of girder)
 $e_{c1} = \bar{y} - (h - d_{ptm}) = 10.87$ in. (eccentricity of harped strands at midspan of girder)
 $e_{c2} = \bar{y} - (h - d_{pbm}) = 13.62$ in. (eccentricity of straight strands)

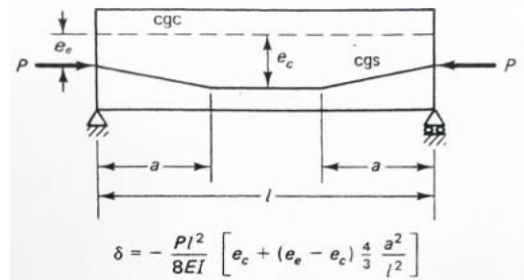
Initial Prestressing, $P = 516,672$ lbs

P of Harped Strands = $3/4P = 387,504$ lbs

$\Delta_1 = 3.15$ in.

Time-dependent multiplier = 2.45 (PCI Table 8.7.1-1)

$\Delta_{1T} = 7.72$ in.

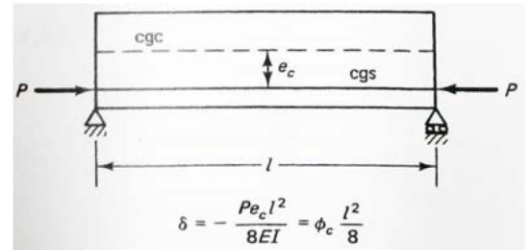


P of Straight Strands = $1/4P = 129,168$ lbs

$\Delta_2 = 1.13$ in.

Time-dependent multiplier = 2.45 (PCI Table 8.7.1-1)

$\Delta_{2T} = 2.76$ in.



(Nawy 2006)

Deflection due to self-weight

$w_c = 110$ lb/ft³

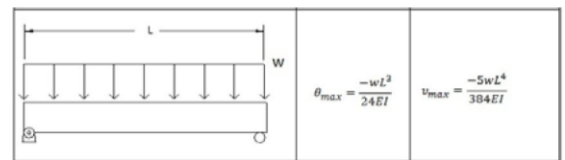
$A = 3.448$ ft²

$w = w_c \times A = 379.271$ lb/ft

$\Delta_3 = -5wL^4 / (384E_cI) = -0.87$ in.

Time-dependent multiplier = 2.70 (PCI Table 8.7.1-1)

$\Delta_{3T} = -2.35$ in.



(Nilson 1987)

$\Delta_{Total} = \Delta_1 + \Delta_2 + \Delta_3 = 8.14$ in.

 Punching Shear Capacity Calculations based on AASHTO Two-Way Action (5.13.3.6.3)

Note: Outlined values obtained from previous calculations, shaded cells input by user.

$$V_n = \left(0.063 + \frac{0.126}{\beta_c}\right) \sqrt{f'_c} b_o d_v \leq 0.126 \sqrt{f'_c} b_o d_v \quad (5.13.3.6.3-1)$$

$$\begin{aligned} f'_c &= 5.600 \text{ ksi} \\ L &= 20 \text{ in. (length of tire contact area)} \\ W &= 10 \text{ in. (width of tire contact area)} \\ \beta_c = L/W &= 2.00 \end{aligned}$$

6-inch deck thickness

$$\begin{aligned} d &= 6 \text{ in. (deck thickness)} \\ d_v &= 5 \text{ in. (effective shear depth)} \\ b_o = 2[(L+2d_v)+(W+2d_v)] &= 100.00 \text{ in. (perimeter at effective shear depth, critical section)} \\ V_{n1} &= 149.09 \text{ kips} \\ V_{n2} &= 149.09 \text{ kips} \\ V_n &= 149.09 \text{ kips} \end{aligned}$$

5-inch deck thickness

$$\begin{aligned} d &= 5 \text{ in. (deck thickness)} \\ d_v &= 4 \text{ in. (effective shear depth)} \\ b_o = 2[(L+2d_v)+(W+2d_v)] &= 92.00 \text{ in. (perimeter at effective shear depth, critical section)} \\ V_{n1} &= 109.73 \text{ kips} \\ V_{n2} &= 109.73 \text{ kips} \\ V_n &= 109.73 \text{ kips} \end{aligned}$$

4-inch deck thickness

$$\begin{aligned} d &= 4 \text{ in. (deck thickness)} \\ d_v &= 3 \text{ in. (effective shear depth)} \\ b_o = 2[(L+2d_v)+(W+2d_v)] &= 84.00 \text{ in. (perimeter at effective shear depth, critical section)} \\ V_{n1} &= 75.14 \text{ kips} \\ V_{n2} &= 75.14 \text{ kips} \\ V_n &= 75.14 \text{ kips} \end{aligned}$$

APPENDIX D. ANSYS INPUT FILES & FIGURES

Flexural ANSYS Code

```

finish
/clear
/title,Girder #1 Flexural Model

/prep7

! Units in kips & inches

! Concrete material properties
fc=5.0      !Compressive strength
frc1=0.4    !Modulus of rupture
frc2=0.8
Emuc=0.2    !Poisson's ratio
Ec=2400     !Modulus of elasticity

! Prestressing steel material properties
fys=243     !Yield strength
Emuys=0.3   !Poisson's ratio
Eps=28500   !Modulus of elasticity

! Reinforcing steel material properties
fy=58       !Yield strength
Emus=0.3    !Poisson's ratio
Es=29000    !Modulus of elasticity

! Defining materials

! Concrete (frc1)
MP,EX,1,Ec      !Material Property, E in the X direction, Material 1, Ec
MP,PRXY,1,Emuc !Material Property, Poisson's Ratio in the X & Y direction, Material 1, Emuc
TB,CONCR,1      !Table, see ans_cmd.pdf
TBDATA,,.2,.8,frc1,fc, !20% open crack shear trans., 80% closed crack shear trans.

! Concrete (frc2)
MP,EX,2,Ec      !Material Property, E in the X direction, Material 2, Ec
MP,PRXY,2,Emuc !Material Property, Poisson's Ratio in the X & Y direction, Material 2, Emuc
TB,CONCR,2      !Table, see ans_cmd.pdf
TBDATA,,.2,.8,frc2,fc, !20% open crack shear trans., 80% closed crack shear trans.

! Prestressing Steel
MP,EX,3,Eps     !Material Property, E in the X direction, Material 3, Eps
MP,PRXY,3,Emuys !Material Property, Poisson's Ratio in the X & Y direction, Material 3,
Emuys
TB,BISO,3       !Table, see ans_cmd.pdf
TBDATA,,fys,2850 !see ans_cmd.pdf & ans_elem.pdf, slope of curve after yielding

! Steel
MP,EX,4,Es      !Material Property, E in the X direction, Material 4, Es

```

MP,PRXY,4,Emus !Material Property, Poisson's Ratio in the X & Y direction, Material 4, Emus
 TB,BISO,4 !Table, see ans_cmd.pdf
 TBDATA,,fy,2900 !see ans_cmd.pdf & ans_elem.pdf, slope of curve after yielding

! Real constants

R,1,3,.00223,90,5 !Concrete Web w/Shear Steel Right Side
 R,2,3,.00223,90,-5 !Concrete Web w/Shear Steel Left Side
 R,3,4,.00370,,90,4,.01672 !6" Concrete Deck w/Rebar, steel properties, volume ratio
 R,4,4,.00555,,90,4,.02508 !4" Concrete Deck w/Rebar, steel properties, volume ratio
 R,5,, !Steel
 R,6,1.380,.00005 !Harped Strands, 0.115 in2/strand (12 strands), 5% initial strain
 R,7,1.380,.00025 !Harped Strands(25% initial strain)
 R,8,1.380,.00050 !Harped Strands(50% initial strain)
 R,9,1.380,.00075 !Harped Strands(75% initial strain)
 R,10,1.380,.00100 !Harped Strands(100% initial strain)
 R,11,0.460,.00005 !Straight Strands, Area Prestressing, (5% initial strain, 4 strands)
 R,12,0.460,.00025 !Straight Strands(25% initial strain)
 R,13,0.460,.00050 !Straight Strands(50% initial strain)
 R,14,0.460,.00075 !Straight Strands(75% initial strain)
 R,15,0.460,.00100 !Straight Strands(100% initial strain)

! Element Types

ET,1,SOLID65 !Concrete
 ET,2,LINK8 !Bar or strands
 ET,3,SOLID45 !Solid Steel Sections

! Key Points of concrete beam (tapered)

K,1,9.5,0,0
 K,2,12,0,0
 K,3,14.5,0,0
 K,4,8.375,22,0
 K,5,12,22,0
 K,6,15.625,22,0
 K,7,8.9375,11,0
 K,8,12,11,0
 K,9,15.0625,11,0

!Generate key points for end of beams

KGEN,2,ALL,,,,,642

!Create beam volume

V,1,3,6,4,10,12,15,13

!Cut beam volume for prestressing strands

WPOFF,,,246
 VSBW,ALL
 WPSTYL,DEFA
 WPOFF,,,396
 VSBW,ALL
 WPSTYL,DEFA

WPROTA,,90 !Rotate working plane

WPOFF,,12

VSBW,ALL

WPSTYL,DEFA

VSEL,S,LOC,Z,0,246

WPOFF,,15.625

WPROTA,,92.1679

VSBW,ALL

WPSTYL,DEFA

VSEL,S,LOC,Z,396,642

WPOFF,,15.625,642

WPROTA,,-92.1679

VSBW,ALL

WPSTYL,DEFA

VSEL,S,LOC,Z,246,396

WPOFF,,6.31266,321

WPROTA,,90

VSBW,ALL

WPSTYL,DEFA

VSEL,ALL

WPOFF,12,4.625

WPROTA,,90

VSBW,ALL

WPSTYL,DEFA

VSEL,ALL

!Generate second beam

VGEN,2,ALL,,48

!Cut ends of beams for prestressing build-up

WPOFF,,16

VSBW,ALL

WPOFF,,16

VSBW,ALL

WPOFF,,16

VSBW,ALL

WPOFF,,16

VSBW,ALL

WPOFF,,257

VSBW,ALL

WPOFF,,257

VSBW,ALL
WPOFF,,,16
VSBW,ALL
WPOFF,,,16
VSBW,ALL
WPOFF,,,16
VSBW,ALL
WPSTYL,DEFA

!Create Deck

BLOCK,0,8.375,22,28,0,246
BLOCK,8.375,15.625,22,28,0,246
BLOCK,15.625,56.375,22,28,0,246
BLOCK,56.375,63.625,22,28,0,246
BLOCK,63.625,72,22,28,0,246

BLOCK,0,8.375,22,26,246,291
BLOCK,8.375,15.625,22,26,246,291
BLOCK,15.625,56.375,22,26,246,291
BLOCK,56.375,63.625,22,26,246,291
BLOCK,63.625,72,22,26,246,291

BLOCK,0,8.375,22,26,291,321
BLOCK,8.375,15.625,22,26,291,321
BLOCK,15.625,56.375,22,26,291,321
BLOCK,56.375,63.625,22,26,291,321
BLOCK,63.625,72,22,26,291,321

BLOCK,0,8.375,26,28,246,291
BLOCK,8.375,15.625,26,28,246,291
BLOCK,15.625,56.375,26,28,246,291
BLOCK,56.375,63.625,26,28,246,291
BLOCK,63.625,72,26,28,246,291

BLOCK,0,8.375,22,26,321,351
BLOCK,8.375,15.625,22,26,321,351
BLOCK,15.625,56.375,22,26,321,351
BLOCK,56.375,63.625,22,26,321,351
BLOCK,63.625,72,22,26,321,351

BLOCK,0,8.375,22,26,351,396
BLOCK,8.375,15.625,22,26,351,396
BLOCK,15.625,56.375,22,26,351,396
BLOCK,56.375,63.625,22,26,351,396
BLOCK,63.625,72,22,26,351,396

BLOCK,0,8.375,26,28,351,396
BLOCK,8.375,15.625,26,28,351,396
BLOCK,15.625,56.375,26,28,351,396
BLOCK,56.375,63.625,26,28,351,396

BLOCK,63.625,72,26,28,351,396

BLOCK,0,8.375,22,28,396,642

BLOCK,8.375,15.625,22,28,396,642

BLOCK,15.625,56.375,22,28,396,642

BLOCK,56.375,63.625,22,28,396,642

BLOCK,63.625,72,22,28,396,642

!Create Support Bearing Pads

BLOCK,6.0,18.0,0,-1,21,33

VSEL,S,LOC,Y,0,-1

VGEN,2,ALL,,,48

VGEN,2,ALL,,,,,588

!Create Load Bearing Pads

BLOCK,6,18,28,29,279,291

BLOCK,54,66,28,29,279,291

BLOCK,6,18,28,29,351,363

BLOCK,54,66,28,29,351,363

VSEL,ALL

VGLUE,ALL

!Loading

finish

/solu

ALLSEL,ALL

WPSTYL,DEFA

! Assigning roller to far supports

NSEL,S,LOC,Y,-1

NSEL,R,LOC,Z,609

D,ALL,UX

D,ALL,UY

! Assigning pin to near supports

NSEL,S,LOC,Y,-1

NSEL,R,LOC,Z,33

D,ALL,UX

D,ALL,UY

D,ALL,UZ

! Assigning initial load (30 kips)

NSEL,S,LOC,29

cm,fnodes,NODE

*Get,Ncount,node,0,count

F=30/Ncount

F,fnodes,Fy,-F

! Run solution

```

ALLSEL,ALL
cnvtol,f,,0.05,2,0.01
nsubst,100
outres,all,all
!autots,1
!ncnv,2
neqit,200
!pred,on
! Loadstep1 (30 kips)
time,1
solve

```

```

! Loadstep2 (0 kips)
F,fnodes,Fy,0
nsubst,10
neqit,200
time,2
solve

```

```

! Loadstep3 (100 kips)
F,fnodes,Fy,-100*F/30
nsubst,100
neqit,200
time,3
solve

```

Shear ANSYS Code

```

finish
/clear
/title,Girder #1 2dv Shear Model
/prep7

! Units in kips & inches

! Concrete material properties
fc=10.8
fr1=0.4
fr2=0.8
Emuc=0.2
Ec=2400

! Prestressing steel material properties
fys=243
Emuys=0.3
Eps=28500

! Reinforcing steel material properties

```

fy=58
 Emus=0.3
 Es=29000

! Defining materials

! Concrete (frc1)
 MP,EX,1,Ec
 MP,PRXY,1,Emuc
 TB,CONCR,1
 TBDATA,,.2,.8,frc1,fc,

! Concrete (frc2)
 MP,EX,2,Ec
 MP,PRXY,2,Emuc
 TB,CONCR,2
 TBDATA,,.2,.8,frc2,fc,

! Prestressing Steel
 MP,EX,3,Eps
 MP,PRXY,3,Emuys
 TB,BISO,3
 TBDATA,,fys,2850

! Steel
 MP,EX,4,Es
 MP,PRXY,4,Emus
 TB,BISO,4
 TBDATA,,fy,2900

! Real constants
 R,1,3,.00223,90,5
 R,2,3,.00223,90,-5
 R,3,4,.00370,,90,4,.01672
 R,4,,
 R,5,1.380,.00005
 R,6,1.380,.00025
 R,7,1.380,.00050
 R,8,1.380,.00075
 R,9,1.380,.00100
 R,10,0.460,.00005
 R,11,0.460,.00025
 R,12,0.460,.00005
 R,13,0.460,.00075
 R,14,0.460,.00100

!Concrete Web w/Shear Steel Right Side
 !Concrete Web w/Shear Steel Left Side
 !6" Concrete Deck w/Rebar
 !Steel
 !Prestressing Steel Harped Strands(5% initial strain)
 !Prestressing Steel Harped Strands(25% initial strain)
 !Prestressing Steel Harped Strands(50% initial strain)
 !Prestressing Steel Harped Strands(75% initial strain)
 !Prestressing Steel Harped Strands(100% initial strain)
 !Prestressing Steel Straight Strands(5% initial strain)
 !Prestressing Steel Straight Strands(25% initial strain)
 !Prestressing Steel Straight Strands(50% initial strain)
 !Prestressing Steel Straight Strands(75% initial strain)
 !Prestressing Steel Straight Strands(100% initial strain)

! Element Types
 ET,1,SOLID65
 ET,2,LINK8
 ET,3,SOLID45

!Concrete
 !Bar or strands
 !Solid Steel Sections

! Key Points of concrete beam (tapered)

K,1,9.5,0,0

K,2,12,0,0

K,3,14.5,0,0

K,4,8.375,22,0

K,5,12,22,0

K,6,15.625,22,0

K,7,8.9375,11,0

K,8,12,11,0

K,9,15.0625,11,0

!Generate key points for end of beams

KGEN,2,ALL,,,,,321

!Create beam volume

V,1,3,6,4,10,12,15,13

!Cut beam volume for prestressing strands

WPOFF,,,246

VSBW,ALL

WPSTYL,DEFA

WPROTA,,,90

!Rotate working plane

WPOFF,,,12

VSBW,ALL

WPSTYL,DEFA

VSEL,S,LOC,Z,0,246

WPOFF,,15.625

WPROTA,,92.1679

VSBW,ALL

WPSTYL,DEFA

VSEL,S,LOC,Z,246,321

WPOFF,,6.31266,321

WPROTA,,90

VSBW,ALL

WPSTYL,DEFA

VSEL,ALL

WPOFF,12,4.625

WPROTA,,90

VSBW,ALL

WPSTYL,DEFA

VSEL,ALL

!Generate second beam
 VGEN,2,ALL,,48

!Cut ends of beams for prestressing build-up

WPOFF,,12
 VSBW,ALL
 WPOFF,,12
 VSBW,ALL
 WPOFF,,12
 VSBW,ALL
 WPOFF,,12
 VSBW,ALL
 WPOFF,,209
 VSBW,ALL
 WPOFF,,16
 VSBW,ALL
 WPOFF,,16
 VSBW,ALL
 WPOFF,,16
 VSBW,ALL
 WPOFF,,16
 VSBW,ALL
 WPSTYL,DEFA

!Create Deck

BLOCK,0,8.375,22,28,0,321
 BLOCK,8.375,15.625,22,28,0,321
 BLOCK,15.625,56.375,22,28,0,321
 BLOCK,56.375,63.625,22,28,0,321
 BLOCK,63.625,72,22,28,0,321

!Create Support and Load Bearing Pads

BLOCK,6.0,18.0,0,-1,15,27
 VSEL,S,LOC,Y,0,-1
 VGEN,2,ALL,,48
 VGEN,2,ALL,,,,228
 BLOCK,0,72,28,29,57,69 !Load Bearing (2dv)

VSEL,ALL
 VGLUE,ALL

! Assigning harped prestressing strand properties to lines

LSEL,S,,17
 LSEL,A,,123
 LSEL,A,,159
 LSEL,A,,164
 LATT,3,5,2 !Material, Real Constant, Element Type
 ESIZE,2
 LMESH,ALL

LSEL,S,,268
 LSEL,A,,272

LSEL,A,,,616
 LSEL,A,,,620
 LATT,3,6,2
 ESIZE,2
 LMESH,ALL

LSEL,S,,,152
 LSEL,A,,,300
 LSEL,A,,,421
 LSEL,A,,,432
 LATT,3,7,2
 ESIZE,2
 LMESH,ALL

LSEL,S,,,384
 LSEL,A,,,392
 LSEL,A,,,500
 LSEL,A,,,508
 LATT,3,8,2
 ESIZE,2
 LMESH,ALL

LSEL,S,,,9
 LSEL,A,,,247
 LSEL,A,,,184
 LSEL,A,,,408
 LATT,3,9,2
 ESIZE,2
 LMESH,ALL

! Assigning straight prestressing strand properties to lines

LSEL,S,,,176
 LSEL,A,,,204
 LSEL,A,,,495
 LSEL,A,,,595
 LATT,3,10,2
 ESIZE,2
 LMESH,ALL

!Material, Real Constant, Element Type

LSEL,S,,,278
 LSEL,A,,,283
 LSEL,A,,,626
 LSEL,A,,,632
 LATT,3,11,2
 ESIZE,2
 LMESH,ALL

LSEL,S,,,227
 LSEL,A,,,341
 LSEL,A,,,536

```
LSEL,A,,,567
LATT,3,12,2
ESIZE,2
LMESH,ALL
```

```
LSEL,S,,,390
LSEL,A,,,400
LSEL,A,,,506
LSEL,A,,,516
LATT,3,13,2
ESIZE,2
LMESH,ALL
```

```
LSEL,S,,,235
LSEL,A,,,305
LSEL,A,,,363
LSEL,A,,,437
LATT,3,14,2
ESIZE,2
LMESH,ALL
```

```
! Assigning concrete and steel properties to volumes
VSEL,S,LOC,Y,0,22 !Concrete for Web
VATT,2,1,1 !Material, Real Constant, Element Type
```

```
VSEL,S,LOC,Y,22,28 !Concrete for Deck
VATT,2,3,1 !Material, Real Constant, Element Type
```

```
VSEL,S,LOC,Y,28,29 !Steel for Bearing & Loading
VSEL,A,LOC,Y,0,-1
VATT,4,4,3 !Material, Real Constant, Element Type
```

```
VSEL,ALL
ESIZE,2
VSWEEP,ALL
ALLSEL,ALL
```

```
!Loading
finish
/solu
Allsel,all
wpstyl,defa
```

```
! Assigning roller to far supports
NSEL,S,LOC,Y,-1
NSEL,R,LOC,Z,249
d,all,ux
d,all,uy
```

```
! Assigning pin to near supports
```

```

NSEL,S,LOC,Y,-1
NSEL,R,LOC,Z,21
d,all,ux
d,all,uy
d,all,uz

! Assigning initial load (150 kips)
Nsel,s,loc,y,29
cm,fnodes,NODE
*Get,Ncount,node,0,count
F=150/Ncount
F,fnodes,Fy,-F

! Run solution
allsel,all
cnvtol,f,,0.05,2,0.01
nsubst,100
outres,all,all
!autots,1
!ncnv,2
neqit,200
!pred,on
! Loadstep1 (150 kips)
time,1
solve

! Loadstep2 (0 kips)
F,fnodes,Fy,0
nsubst,10
neqit,200
time,2
solve

! Loadstep3 (400 kips)
F,fnodes,Fy,-400*F/150
nsubst,100
neqit,200
time,3
solve

```

Punching Shear ANSYS Code

```

finish
/clear
/title,Girder #1 Punching Shear Model (5" Deck)

/prep7

! Units in kips & inches

```

! Concrete material properties

fc=5.6

frc=0.4

Emuc=0.2

Ec=2400

! Reinforcing steel material properties

fy=58

Emus=0.3

Es=29000

! Defining materials

! Concrete

MP,EX,1,Ec

MP,PRXY,1,Emuc

TB,CONCR,1

TBDATA,,.2,.8,frc,fc,

! Steel

MP,EX,2,Es

MP,PRXY,2,Emus

TB,BISO,2

TBDATA,,fy,2900

! Real constants

R,1,2,.00444,,90,2,.02006

!Concrete Deck w/Rebar

R,2,,

!Steel

! Element Types

ET,1,SOLID65

!Concrete

ET,2,SOLID45

!Solid Steel Sections

!Create Deck

BLOCK,0,8.5,0,5,0,120

BLOCK,8.5,15.5,0,5,0,120

BLOCK,15.5,31,0,5,0,120

BLOCK,31,41,0,5,0,120

BLOCK,41,56.5,0,5,0,120

BLOCK,56.5,63.5,0,5,0,120

BLOCK,63.5,72,0,5,0,120

!Create Support Bearing Pads

BLOCK,8.5,15.5,0,-1,0,120

VSEL,S,LOC,Y,0,-1

VGEN,2,ALL,,48

!Create Load Bearing Pad

BLOCK,31,41,5,7,50,70

VSEL,ALL
VGLUE,ALL

! Assigning concrete and steel properties to volumes

VSEL,S,LOC,Y,0,5 !Concrete for Deck
VATT,1,1,1 !Material, Real Constant, Element Type

VSEL,S,LOC,Y,0,-1 !Steel for Bearing & Loading
VSEL,A,LOC,Y,5,7
VATT,2,2,2 !Material, Real Constant, Element Type

VSEL,ALL
ESIZE,2
VSWEEP,ALL
ALLSEL,ALL

!Loading
finish
/solu
Allsel,all
wpstyl,defa

!Assigning pin to left supports

NSEL,S,LOC,Y,-1
NSEL,R,LOC,X,15.5
d,all,ux
d,all,uy
d,all,uz

!Assigning pin to right supports

NSEL,S,LOC,Y,-1
NSEL,R,LOC,X,56.5
d,all,ux
d,all,uy
d,all,uz

!Assigning load (200 kips)

Nsel,s,loc,y,7
cm,fnodes,NODE
*Get,Ncount,node,0,count
F=200/Ncount
F,fnodes,Fy,-F

!Run solution

allsel,all
cnvtol,f,,0.05,2,0.01
nsubst,100
outres,all,all

```

!autots,1
!ncnv,2
neqit,200
!pred,on
time,1
solve
    
```

Load vs. Deflection Figures for Modeled Data

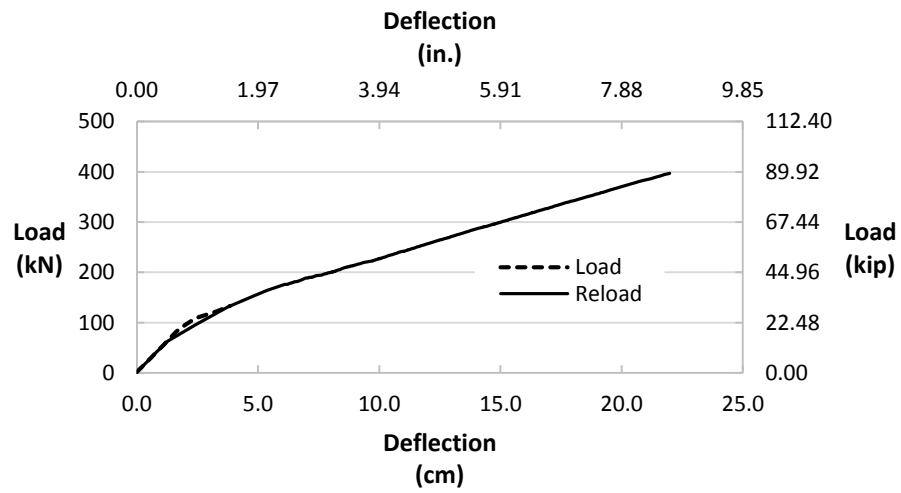


Figure D.1 Girder #1 modeled flexural load vs deflection

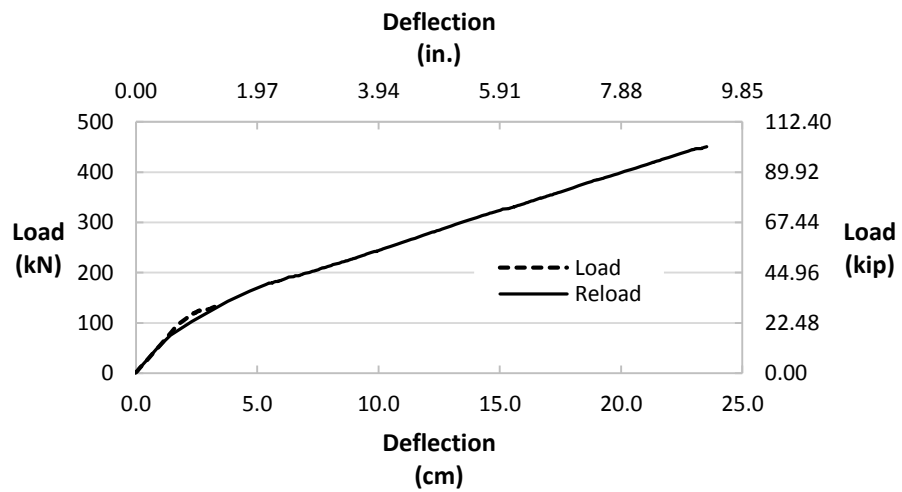


Figure D.2 Girder #2 modeled flexural load vs deflection

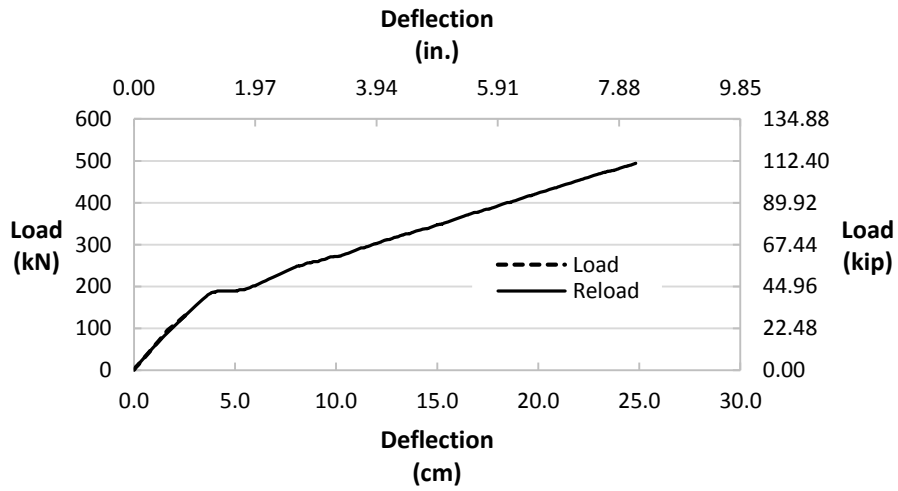


Figure D.3 Girder #3 modeled flexural load vs deflection

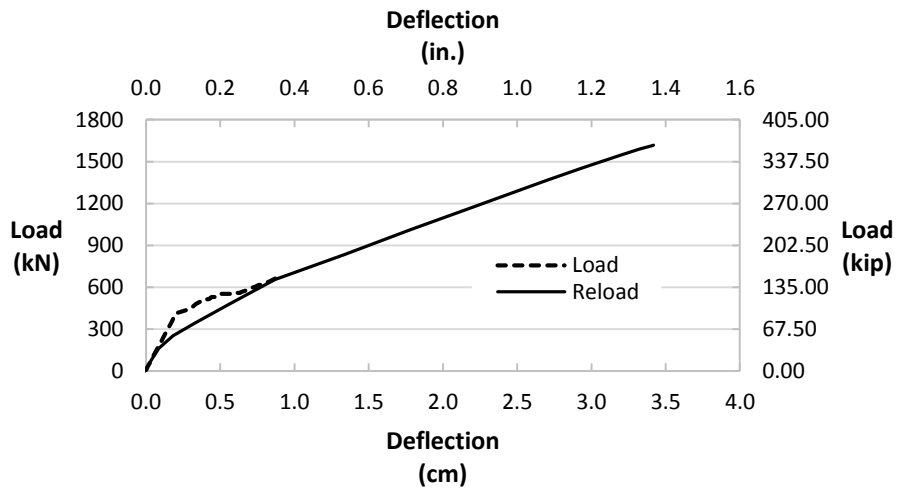


Figure D.4 Girder #1 modeled $2d_v$ load vs deflection

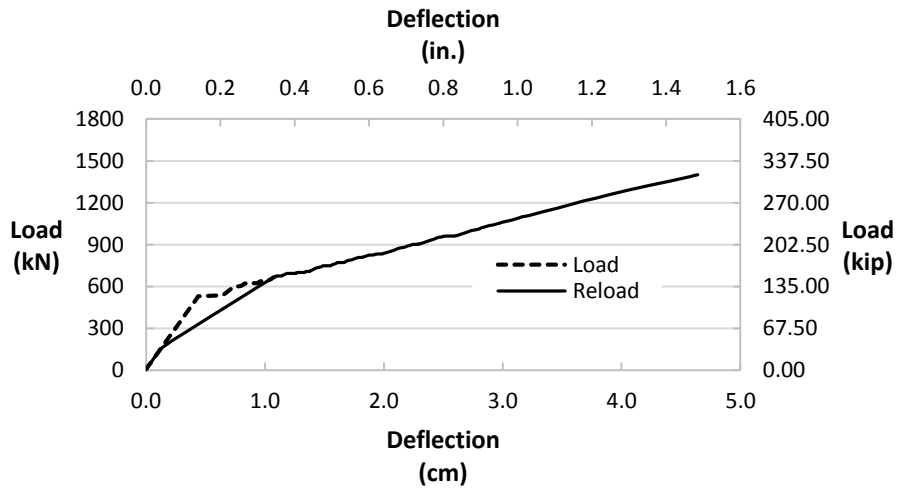


Figure D.5 Girder #2 modeled 3d_v load vs deflection

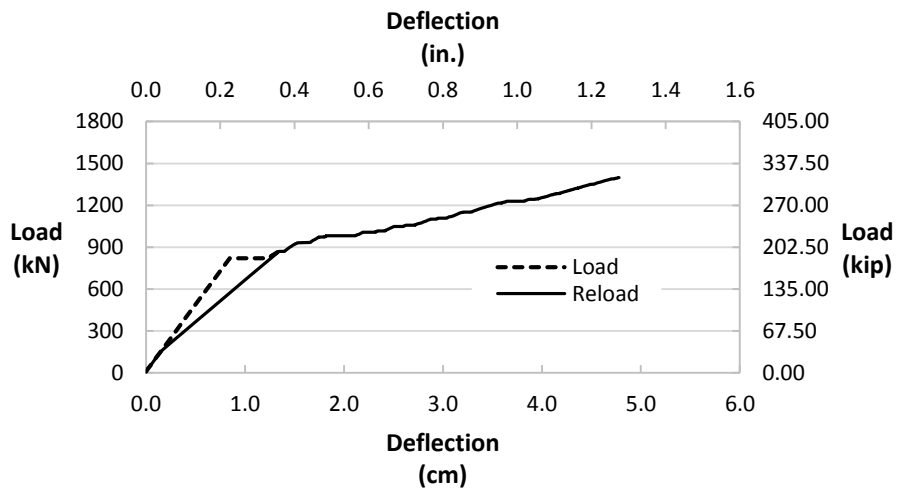


Figure D.6 Girder #3 modeled 4d_v load vs deflection

Comparison Figures to Tested Data

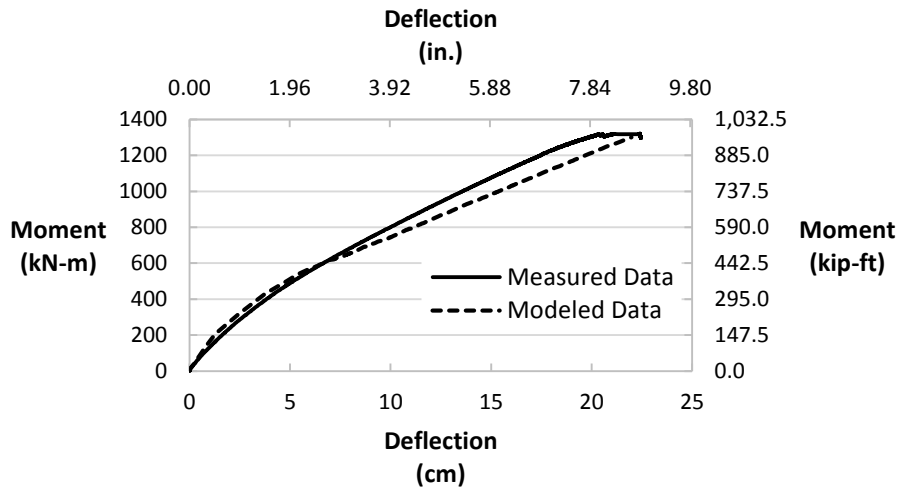


Figure D.7 Girder #1 flexural comparison to FEM

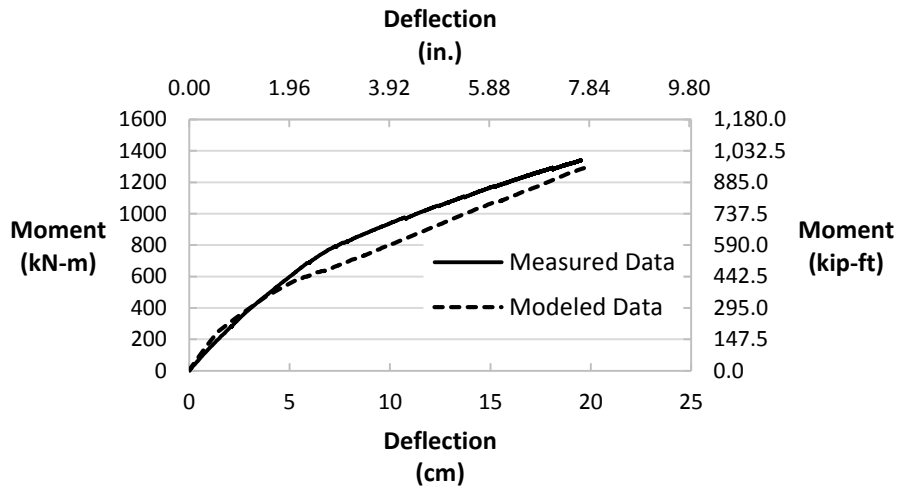


Figure D.8 Girder #2 flexural comparison to FEM

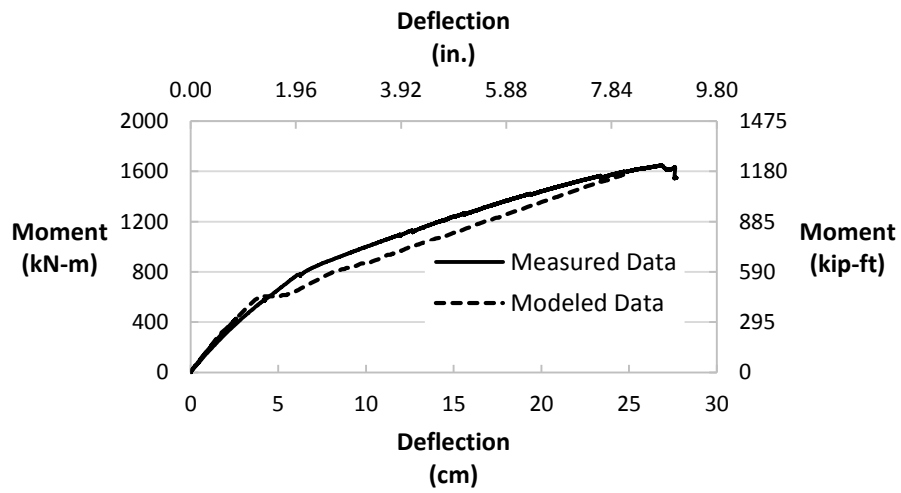


Figure D.9 Girder #3 flexural comparison to FEM

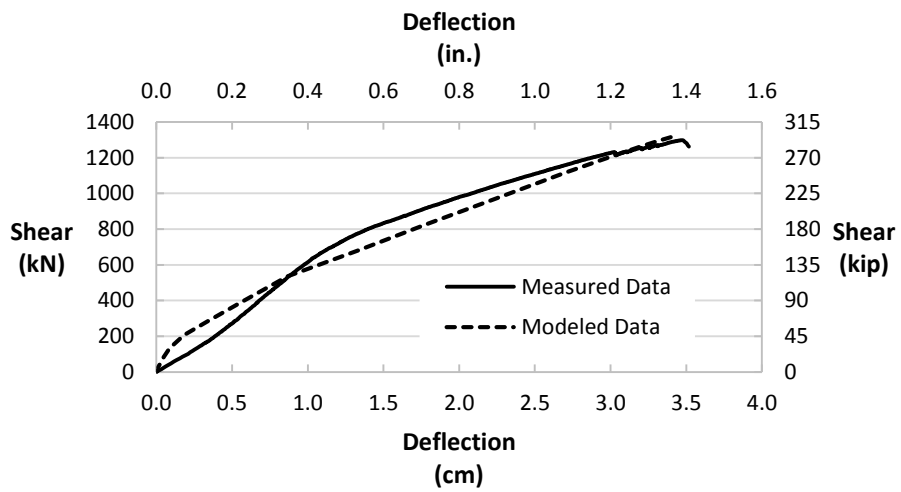


Figure D.10 Girder #1 $2d_v$ comparison to FEM

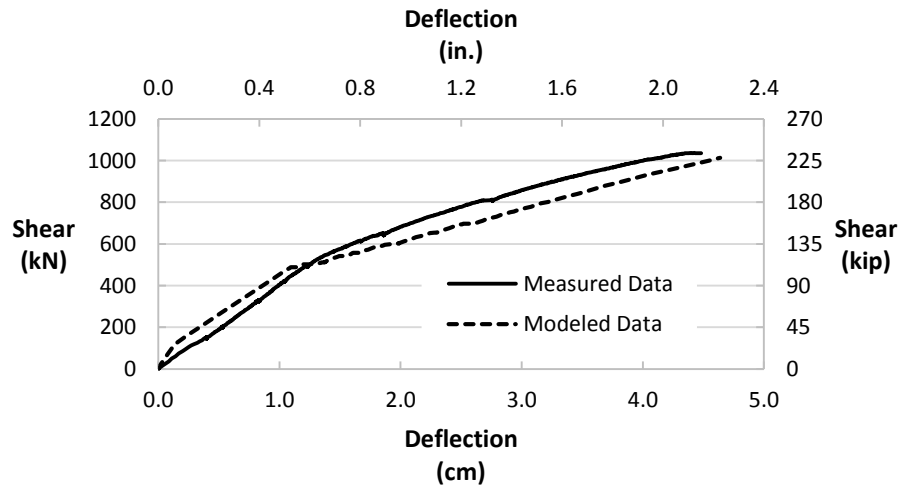


Figure D.11 Girder #2 3d_v comparison to FEM

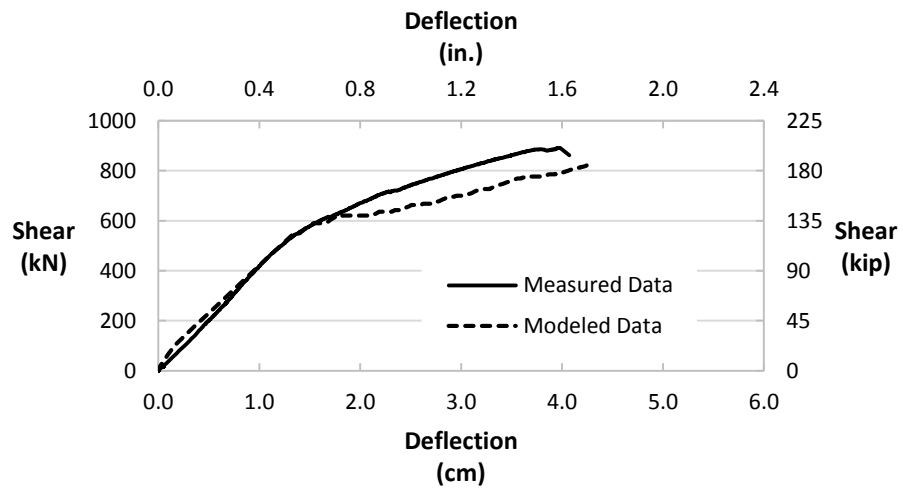


Figure D.12 Girder #3 4d_v comparison to FEM